

Chethan Parthasarathy

**Accurate Battery  
Modelling for  
Control Design  
and Economic  
Analysis of  
Lithium-ion  
Battery Energy  
Storage Systems in  
Smart Grid**



ACTA WASAENSIA 510



Vaasan yliopisto  
UNIVERSITY OF VAASA

Copyright © University of Vaasa and the copyright holders.

ISBN 978-952-395-089-4 (print)  
978-952-395-090-0 (online)

ISSN 0355-2667 (Acta Wasaensia 510, print)  
2323-9123 (Acta Wasaensia 510, online)

URN <http://urn.fi/URN:ISBN:978-952-395-090-0>


Hansaprint Oy, Turenki, 2023.

ACADEMIC DISSERTATION

*To be presented, with the permission of the Board of the School of Technology  
and Innovations of the University of Vaasa, for public examination on  
the 20<sup>th</sup> of June, 2023, at noon.*

Article based dissertation, School of Technology and Innovations, Electrical Engineering.

Author Chethan Parthasarathy

 <https://orcid.org/0000-0002-2926-9367>

Supervisor(s) Professor Hannu Laaksonen  
University of Vaasa. School of Technology and Innovations,  
Electrical Engineering.

Professor Kimmo Kauhaniemi  
University of Vaasa. School of Technology and Innovations,  
Electrical Engineering.

Custos Professor Hannu Laaksonen  
University of Vaasa. School of Technology and Innovations,  
Electrical Engineering.

Reviewers Associate Professor Daniel-Ioan Stroe  
Aalborg University. The Faculty of Engineering and Science,  
Power Electronics System Integration and Materials

Professor Ali Sari  
University Claude Bernard Lyon 1 – Ampère lab. Annuaire du  
Département MIS, Methods for System Engineering.

Opponent Professor Pertti Kauranen  
LUT University. LUT School of Energy Systems, Electrical  
Engineering.

## Tiivistelmä

Aurinkosähköjärjestelmien ja tuulivoiman laajamittainen integrointi sähkövoimajärjestelmän eri jännitetasoille on lisääntynyt nopeasti. Uusiutuva energia on kuitenkin luonteeltaan vaihtelevaa, joka voi aiheuttaa nopeita muutoksia taajuudessa ja jännitteessä. Näiden vaihteluiden hallintaan tarvitaan erilaisia joustavia energiasursseja, kuten energiavarastoja, sekä niiden tehokkaan hyödyntämisen mahdollistavia älykkäitä ja aktiivisia hallinta- ja ohjausjärjestelmiä.

Litiumioniakkuihin pohjautuvien invertteriliitännäisten energian varastointijärjestelmien käyttö joustoresursseina aktiiviseen verkonhallintaan niiden pätö- ja loistehon ohjauksen avulla on lisääntynyt nopeasti johtuen niiden kustannusten laskusta, modulaarisuudesta ja teknisistä ominaisuuksista. Litiumioniakuilla on erittäin epälineaariset ominaisuudet joita kuvaavat parametrit ovat esimerkiksi lataustila, lämpötila, purkaussyvyys, lataus/ purkausnopeus ja akun ikääntyminen. Akkujen ominaisuuksien dynaaminen luonne onkin tärkeää huomioida myös akkujen sähköverkkoratkaisuihin liittyvien säätöjärjestelmien kehittämisessä sekä teknis-taloudellisissa kannattavuusanalyseissa.

Tämä väitöstutkimus keskittyy ensisijaisesti aktiiviseen verkonhallintaan käytettävien litiumioniakkujen säätöratkaisuiden parantamiseen hyödyntämällä tarkkoja, dynaamisia akun suorituskykymalleja, jotka perustuvat toisen asteen ekvivalenttipiirien akkumallinnustekniikkaan, jossa otetaan huomioon lataustila, lataus/purkausnopeus ja lämpötila. Työssä kehitetyn aktiivisen verkonhallintajärjestelmän avulla tehtävät akun pätö- ja loistehon ohjausperiaatteet on validoitu laajamittaisten simulointien avulla, esimerkiksi paikallista älyverkkopilottia Sundom Smart Gridiä simuloimalla. Simuloinnit tehtiin sekä lyhyen aikavälin offline-simulaatio-ohjelmistoilla että pitkän aikavälin simulaatioilla hyödyntäen reaaliaikasilmoiltilaitteistoa.

Pitkän aikavälin simulaatioissa akun ikääntymisen vaikutus otettiin huomioon litiumioniakun ohjauksen suunnittelussa jotta sen vaikutusta sähköjärjestelmän kokonaistoimintaan voitiin analysoida. Tätä tarkoitusta varten luotiin akun ikääntymismalleja, joilla on mahdollista määrittää akun huipputehon muutos sen ikääntyessä. Akun huipputehon muutos taas vaikuttaa sen hyödynnettävyyteen erilaisten pätötehon ohjaukseen perustuvien joustopalveluiden tarjoamiseen liittyen. Lisäksi väitöstutkimuksessa tarkasteltiin akkujen ikääntymisen vaikutusta niiden taloudelliseen kannattavuuteen sisällyttämällä akkujen ikääntymismalleja teknis-taloudellisiin tarkasteluihin.

Avainsanat: Litiumioniakut; aktiivinen verkonhallinta; akun karakterisointi ja testaus; mukautuva ohjaus; akun ikääntyminen

## Abstract

Adoption of lithium-ion battery energy storage systems (Li-ion BESSs) as a flexible energy source (FES) has been rapid, particularly for active network management (ANM) schemes to facilitate better utilisation of inverter based renewable energy sources (RES) in power systems. However, Li-ion BESSs display highly nonlinear performance characteristics, which are based on parameters such as state of charge (SOC), temperature, depth of discharge (DOD), charge/discharge rate (C-rate), and battery-aging conditions. Therefore, it is important to include the dynamic nature of battery characteristics in the process of the design and development of battery system controllers for grid applications and for techno-economic studies analyzing the BESS economic profitability.

This thesis focuses on improving the design and development of Li-ion BESS controllers for ANM applications by utilizing accurate battery performance models based on the second-order equivalent-circuit dynamic battery modelling technique, which considers the SOC, C-rate, temperature, and aging as its performance affecting parameters. The proposed ANM scheme has been designed to control and manage the power system parameters within the limits defined by grid codes by managing the transients introduced due to the intermittence of RESs and increasing the RES penetration at the same time. The validation of the ANM scheme and the effectiveness of controllers that manage the flexibilities in the power system, which are a part of the energy management system (EMS) of ANM, has been validated with the help of simulation studies based on an existing real-life smart grid pilot in Finland, Sundom Smart Grid (SSG). The studies were performed with offline (short-term transient-stability analysis) and real-time (long-term transient analysis) simulations.

In long-term simulation studies, the effect of battery aging has also been considered as part of the Li-ion BESS controller design; thus, its impact on the overall power system operation can be analyzed. For this purpose, aging models that can determine the evolving peak power characteristics associated with aging have been established. Such aging models are included in the control loop of the Li-ion BESS controller design, which can help analyse battery aging impacts on the power system control and stability. These analyses have been validated using various use cases. Finally, the impact of battery aging on economic profitability has been studied by including battery-aging models in techno-economic studies.

**Keywords:** Lithium-ion batteries; active network management; battery characterization and testing; adaptive control; battery aging

## ACKNOWLEDGEMENT

The research work for this doctoral thesis was conducted in School of Technology and Innovations, Flexible Energy Resources, University of Vaasa, Finland, between 2018 and 2022.

I will take this opportunity and privilege to thank my Supervisor, Professor Hannu Laaksonen, for trusting my abilities and being the guiding light for my research progress at the University of Vaasa. He introduced me to the Finnish ways of working, which is based entirely on trust, mutual respect, and openness. Such an environment provided me with the vast freedom to dedicate my time to quality research and development activities. Intriguing and thought-provoking discussions on the topics of power systems and his strong knowledge on the subject helped me improve my technical perspective and develop myself as a better researcher and an engineer.

University of Vaasa will always have a special place in my heart, particularly for being an ideal place for conducting research. I am grateful for the support shown by Dean Raine Hermans for recognizing the importance of the research activities and facilitating much needed support in terms of funding and motivation. Special thanks to the Director of VEBIC Lab, Suvi Karirinne, whose support helped me establish and operate the battery cell testing laboratory.

My journey at University of Vaasa has been blessed with the presence of wonderful and friendly colleagues. I would like to specially thank Hossein Hafezi, previously, Assistant Professor, University of Vaasa (currently, Lecturer at Tampere University), for his valuable contribution as a co-author and a mentor in the topics of power electronic control design and development. I would like to express gratitude to my colleague and friend Hosna Khajeh for collaboration on the topics of battery scheduling and techno-economic analysis. We were able to churn out quality research culminating with interesting research papers. My understanding on real-time simulations and OPAL-RT hardware systems must be attributed to Katja Sirviö. I thank her for being my co-author and a delightful colleague throughout my journey at the University of Vaasa. I also extend my appreciation to Jagdesh Kumar, colleague, co-author, and a good friend. His guidance helped me settle down in Vaasa during my initial days.

My research at University of Vaasa included a plethora of external collaborations, allowing me to observe and learn from various experts, eventually leading to tangible research outcomes in the longer run. My sincere thanks to Serge Pelissier (Director) and Eduardo Redondo Iglesias (Research Engineer), ECO7, LICIT,

Universite Gustav Eiffel, Bron, France, for facilitating our fruitful research collaboration and for hosting me as a visiting researcher for 3 months. I would like to express my gratitude to Ilari Alaperä, Head, Fortum Spring, Finland, for providing the much-needed industry perspective on our research.

I would like to acknowledge the research projects that I worked for at the University of Vaasa. I have actively contributed to Business Finland funded project Solar-X that was led by Professor Kimmo Kauhaniemi. I thank him wholeheartedly for providing me with an opportunity to contribute to the project and for funding conference publications and travel. Fleximar and CLIC Flex e-demo were the other projects that I participated during my time at Vaasa. Professor Hannu Laaksonen led both projects and special thanks for letting me be part of it.

Life in the city of Vaasa and Finland has been a mixed bag of experiences. I am grateful for Pingviini ice swimming sauna club for keeping me sane during extreme Finnish winters, especially during the most challenging COVID times. I was happy being a part of the Wasa Segelförening club during my time at Vaasa to learn and enjoy sailing. I am deeply thankful to my friend and colleague Kendall Rutledge for the weeks' long sailing expedition in the beloved "*Andiamo*." Sailing in the high seas has been one of the most adventurous and peaceful experiences at the same time. Being a part of the staff Football team has been one of the most cherishing moments at the University of Vaasa. I thank Tuukka Järvinen for actively organizing the team and events. I appreciate the role of my friend and mentor Professor Lauri Kumpulainen for organizing Badminton games and helping in maintaining good spirits during his time in University of Vaasa.

Home is where the heart lies. My Indian friends in Vaasa made me feel at home and I am deeply indebted of their presence at Vaasa. I would like to mention Raghu, Kannan, Tania, Raja, Rathan, Thilepan, and Prakash for being there for me always. I will always cherish our long drives to late night fire sessions to summer barbeques. I am also thankful to my Finnish-Indian friend Nirupam, for the good times in Vaasa, especially in their Family's summer cottage.

Finally, I am deeply indebted to my parents Mr. D Parthasarathy and Mrs. P Meenakshi for their unconditional love and care throughout my life. It is their sacrifice in various aspects that has brought me this far. A special thanks to my brother Mr. Naveen Parthasarathy, who has always been my backbone. I would also like to acknowledge the role of my supportive sister-in-law Mrs. Saranya and their little one Samruddhi for putting a smile on my face at the hardest of times.



## Contents

TIIVISTELMÄ.....	V
ABSTRACT .....	VI
ACKNOWLEDGEMENT .....	VII
<b>1 INTRODUCTION.....</b>	<b>1</b>
1.1 Scope and Objective of the Thesis .....	3
1.1.1 SSG .....	7
1.2 Main research questions and methods.....	8
1.3 Summary of Publications .....	11
1.4 Scientific Contributions.....	15
1.5 Outline of the thesis .....	16
<b>2 LITERATURE SURVEY AND STATE OF THE ART - LI-ION BESS MODELING, CONTROL, AND UTILIZATION IN SMART GRIDS FOR ANM APPLICATIONS.....</b>	<b>18</b>
2.1 Power system flexibility and FERs .....	18
2.1.1 ANM.....	21
2.1.2 Battery energy storage systems and ANM.....	22
2.2 Lithium-ion battery energy storage systems and flexibility services .....	25
2.2.1 Lithium-ion BESSs – Technical characteristics and challenges.....	27
2.2.2 Control of Lithium-ion batteries in grid applications – Suitable simulation modes .....	29
2.2.3 Aging-aware Li-ion BESS control design .....	30
2.2.4 Aging aware techno-economic studies of Li-ion BESSs .....	31
2.3 BESS Standards and Grid Codes .....	32
2.3.1 Finnish BESS Grid Code - SJV2019.....	33
<b>3 LI-ION BESS MODELING AND CONTROL FOR SHORT-TERM ANM SIMULATIONS .....</b>	<b>36</b>
3.1 Li-ion BESS modeling.....	37
3.1.1 SOEC-based battery model parameterization process .....	38
3.2 Control design of grid-connected Li-ion BESS .....	42
3.2.1 DC/DC bidirectional converter control.....	43
3.2.2 AC/DC voltage source converter control.....	44
3.3 Case Studies – Coordinated control of Li-ion BESS in ANM applications.....	45
3.3.1 Case 1 – SSG backup feeding .....	46
3.3.2 Case 2: SSG – Li-ion BESS fast charging.....	51

4	LI-ION BESS MODELING AND CONTROL FOR LONG-TERM ANM SIMULATIONS .....	54
4.1	Enhanced Li-ion BESS model.....	56
4.1.1	Enhanced Li-ion BESS model utilization in long-term simulations .....	57
4.2	ANM scheme in long-term simulations.....	58
4.3	Utilization of real-time simulation platform for long-term ANM studies .....	60
4.4	Case Studies - Coordinated control of Li-ion BESS in long-term ANM simulations .....	61
4.4.1	Case 1: Without ANM .....	62
4.4.2	Case 2: With ANM (WTG only).....	63
4.4.3	With ANM (WTG and BESS).....	63
5	EFFECT OF BATTERY-AGING MODELING ON CONTROL AND ECONOMIC PROFITABILITY OF LI-ION BESS .....	67
5.1	Li-ion BESS aging modeling in simulation studies.....	68
5.1.1	Need for aging aware control of Li-ion BESS control.....	69
5.1.2	Need for aging aware techno-economic analysis of Li-ion BESS.....	70
5.2	Case studies considering Li-ion BESS aging .....	71
5.2.1	Case 1: Aging aware Pf- droop control of Li-ion BESSs .....	71
5.2.2	Case 2: Aging aware Li-ion BESS control design for ANM simulations.....	79
5.2.3	Case 3: Aging aware techno-economic analysis of Li-ion BESS providing flexibility services.....	90
5.3	Conclusions.....	102
6	CONCLUSIONS.....	103
6.1	Main contributions .....	105
6.2	Thesis limitations and future research directions.....	106
	REFERENCES .....	109
	APPENDICES.....	124
	Appendix I: Li-ion battery operation and aging mechanisms .....	124
	Appendix I.II: Li-ion BESS aging modes and mechanisms .....	126
	Appendix I.III Li-ion BESS related terminology (Electric & Team, 2008).....	128
	PUBLICATIONS .....	130

## Figures

<b>Figure 1.</b>	Modified SSG Network including Li-ion BESS .....	8
<b>Figure 2.</b>	Summary of publications P1–P9 (P with a number refers to corresponding publication) focus areas .....	12
<b>Figure 3.</b>	(a) Traditional centralized power system; (b) Modern decentralized power systems .....	19
<b>Figure 4.</b>	Basics of ANM operation.....	23
<b>Figure 5.</b>	Classification ANM-related solutions.....	23
<b>Figure 6.</b>	Timescale of operations for different flexibility services ..	26
<b>Figure 7.</b>	Energy Storage Systems Characteristics .....	27
<b>Figure 8.</b>	Cell performance characteristics at different aging intervals .....	28
<b>Figure 9.</b>	Cell performance influencers.....	29
<b>Figure 10.</b>	SOEC battery cell model (NMC type of cell) .....	38
<b>Figure 11.</b>	HPPC current pulse profile.....	39
<b>Figure 12.</b>	HPPC pulse voltage response.....	39
<b>Figure 13.</b>	Simulation model performance with respect to experimental characteristics.....	41
<b>Figure 14.</b>	Battery pack modeling.....	42
<b>Figure 15.</b>	Li-ion BESS grid integration modeling .....	43
<b>Figure 16.</b>	Current Controller.....	44
<b>Figure 17.</b>	VSC controller design .....	45
<b>Figure 18.</b>	SSG one-line diagram during backup feeding case .....	46
<b>Figure 19.</b>	Proposed ANM architecture for SSG .....	48
<b>Figure 20.</b>	a) QU- control (b) BESS PU- control (c) WT PU- control (d) Tap change controller .....	49
<b>Figure 21.</b>	Enhanced Li-ion BESS model utilization in long-term simulations .....	58
<b>Figure 22.</b>	Proposed ANM scheme.....	59
<b>Figure 23.</b>	EMS Controllers: (a) QU- control (b) P- control (c) PU- control .....	60
<b>Figure 24.</b>	SSG real-time simulation setup .....	62
<b>Figure 25.</b>	Results from the SOEC Model; (a) Battery SoC; (b) Battery DC charge/discharge currents; (c) Battery SOC voltage; (d) Battery DC Power characteristics.....	65
<b>Figure 26.</b>	Battery cell operational temperature profile.....	66
<b>Figure 27.</b>	Different Li-ion battery-aging processes .....	69
<b>Figure 28.</b>	Typical active-power-frequency (Pf) -droop curve for BESS participation in FCR-N market.....	73
<b>Figure 29.</b>	Battery cycle aging curve from the manufacturer’s datasheet based on DoD .....	74
<b>Figure 30.</b>	Measured real-life BESS SOC behaviour when utilized for FCR-N frequency control markets .....	76
<b>Figure 31.</b>	Rain-flow counting results on field SOC characteristics ...	76
<b>Figure 32.</b>	Proposed adaptive droop controller.....	76
<b>Figure 33.</b>	Power System Frequency .....	77
<b>Figure 34.</b>	Li-ion BESS power dispatch for FCR-N during BOL .....	78
<b>Figure 35.</b>	Battery cell testing and characterization test bench at University of Vaasa.....	81

<b>Figure 36.</b>	HPPC current pulse profile.....	81
<b>Figure 37.</b>	HPPC voltage response.....	82
<b>Figure 38.</b>	Discharge peak power of Li-ion battery cell at different aging intervals and depending on DOD level .....	83
<b>Figure 39.</b>	Charge peak power of Li-ion battery cell at different aging intervals and depending on SOC level.....	83
<b>Figure 40.</b>	Proposed second order equivalent-circuit model .....	84
<b>Figure 41.</b>	Proposed aging aware P-control scheme.....	85
<b>Figure 42.</b>	Aging aware battery cell model .....	87
<b>Figure 43.</b>	Proposed QU-droop control.....	87
<b>Figure 44.</b>	Li-ion BESS capacity change with cycle aging .....	94
<b>Figure 45.</b>	Flowchart representing cycle counting methodology .....	97
<b>Figure 46.</b>	Frequencies measured for each three minutes in Jan-March 2021 .....	98
<b>Figure 47.</b>	The steps to calculate the outcome of the BESS providing FCR-N.....	98
<b>Figure 48.</b>	Charging/discharging power obtained after scheduling the BESS based on the frequency deviations .....	99
<b>Figure 49.</b>	BESS SOC variations after responding to the frequency changes .....	99
<b>Figure 50.</b>	Upward and downward regulation prices during January to March 2021 .....	100

## Tables

<b>Table 1.</b>	Flexibility/technical ancillary services supported by BESSs.....	25
<b>Table 2.</b>	Classification of grid energy storage based on capacity ..	34
<b>Table 3.</b>	Other grid codes related to energy storage system .....	34
<b>Table 4.</b>	Li-ion BESS characteristics .....	47
<b>Table 5.</b>	PI-controller parameters of grid-side controllers.....	65
<b>Table 6.</b>	Li-ion BESS peak power calculations .....	77
<b>Table 7.</b>	Li-ion BESS peak power dispatch comparison in Case 2 subcases 2 and 3 (- means discharging of BESS and + charging of BESS).....	89
<b>Table 8.</b>	Cell capacity at different cycles .....	94
<b>Table 9.</b>	Results obtained after scheduling BESS based on the proposed method .....	100
<b>Table 10.</b>	TOPC indicator with and without cycle aging effects ....	101
<b>Table 11.</b>	Mapping Battery Parameter Requirement for Controller Development Studies .....	106

## Abbreviations

RES	Renewable Energy Sources
ANM	Active Network Management
FER	Flexible Energy Resources
Li-ion BESS	Lithium-ion Battery Energy Storage Systems
WTG	Wind Turbine Generator
SOC	State of Charge
DOD	Depth of Discharge
C-rate	Current rate
EMS	Energy Management System
SSG	Sundom Smart Grid
BESS	Battery Energy Storage System
ECM	Equivalent-Circuit Model
DER	Distributed Energy Sources
FCR-N	Frequency Containment Reserves – Normal
FCR-D	Frequency Containment Reserves – Disturbances
MV	Medium Voltage
HV	High Voltage
LV	Low Voltage
SOEC	Second Order Equivalent Circuit
PE	Power Electronics
EMT	Electromagnetic Transients
<i>Pf</i> -	Active-Power-Frequency Control
<i>QU</i> -	Reactive Power-Voltage Control
<i>P</i> -	Active-Power Control
<i>PU</i> -	Active-Power-Voltage Control

## XIV

DR	Demand Response
EV	Electric Vehicle
ESS	Energy Storage System
TSO	Transmission Service Operator
DSO	Distribution Service Operator
FRT	Fault Ride Through
FRR	Frequency Restoration and Replacement Reserves
NMC	Nickel Manganese Cobalt
HPPC	Hybrid Pulse Power Characterization
VSC	Voltage Source Converter
OLTC	On-Load Tap Changer
RPW	Reactive Power Window
SOA	State of Age
BOL	Beginning of Life
EOL	End of Life
CCCV	Constant Current Constant Voltage
CC	Constant Current
MSE	Mean Square Error
TOPC	Total Outcome per Cycle

## Publications

This thesis consists of following publications:

**[P1] Parthasarathy, C.** Khajeh, H., Firoozi, H., Laaksonen, H., and Hafezi, H (2022)., Distributed Generation, Storage and Active Network Management. In B. Khan, O. Mahela, S. Padmanaban, H. H. Alhelou (eds.) *Deregulated Electricity Structures and Smart Grids*, pp. 83–111. CRC Press. <https://doi.org/10.1201/9781003278030>. © 2022 Taylor & Francis. Reprinted, with permission.

**[P2] Parthasarathy, C.**, Hafezi, H., Laaksonen, H., Kauhaniemi, K. (2019). Modelling and Simulation of Hybrid PV & BES Systems as Flexible Resources in Smartgrids - Sundom Smart Grid Case. *2019 IEEE Milan PowerTech, Milan, Italy*. <https://doi.org/10.1109/PTC.2019.8810579>. © 2019 IEEE. Reprinted, with permission.

**[P3] Parthasarathy, C.**, Hafezi, H., Laaksonen, H., (2020). Lithium-ion BESS Integration for Smart Grid Applications - ECM Modelling Approach. *2020 IEEE Power & Energy Society Innovative Smart Grid Technologies Conference (ISGT), Washington, DC, USA*. <https://doi.org/10.1109/ISGT45199.2020.9087741>. © 2020 IEEE. Reprinted, with permission.

**[P4] Parthasarathy, C.**, Hafezi, H., Laaksonen, H. (2021). Integration and Control of Lithium-ion BESSs for Active Network Management in Smart Grids – Sundom Smart Grid Back-up Feeding Case. *Electrical Engineering*. 104, 539–553. <https://doi.org/10.1007/s00202-021-01311-8>. © The Author(s) 2021. Published by Springer. CC BY.

**[P5] Parthasarathy, C.**, Laaksonen, H., Hafezi, H. (2021). Control and Co-ordination of Flexibilities for Active Network Management in Smart Grids – Li-ion BESS Fast Charging Case. *2021 IEEE Madrid PowerTech*. <https://doi.org/10.1109/PowerTech46648.2021.9494853>. © 2021 IEEE. Reprinted, with permission.

**[P6] Parthasarathy, C.**, Sirviö, K., Hafezi, H., Laaksonen, H. (2021). Modelling Battery Energy Storage Systems for Active Network Management – Coordinated Control Design and Validation, *IET Renewable Power Generation*, 2021(15), 2426–2437. <https://doi.org/10.1049/rpg2.12174>. © 2021 The Authors. Published by Wiley. CC BY.

**[P7] Parthasarathy, C.,** Laaksonen, H., Redondo-Iglesias, E., Pelissier, S. (2023). Aging aware adaptive control of Li-ion battery energy storage system for flexibility services provision. *Journal of Energy Storage*, 57. 106268, <https://doi.org/10.1016/j.est.2022.106268>. © 2022 The Authors. Published by Elsevier Ltd. CC BY.

**[P8] Parthasarathy, C.,** Laaksonen, H., Alaperä, I. (2022). Aging Characteristics Consideration in Adaptive Control Design of Grid-Scale Lithium-ion battery. *2022 IEEE PES Innovative Smart Grid Technologies Conference Europe (ISGT-Europe)*. <https://doi.org/10.1109/ISGT-Europe54678.2022.9960671>. © 2022 IEEE. Reprinted, with permission.

**[P9] Khajeh, H., Parthasarathy, C.,** Laaksonen, H. (2022) Effects of Battery Aging on BESS Participation in Frequency Service Markets – Finnish Case Study. *2022 18th International Conference on the European Energy Market (EEM)*. <https://doi.org/10.1109/EEM54602.2022.9921139>. © 2022 IEEE. Reprinted, with permission.



## Author's Contribution

Parthasarathy is the first and main author of Publications [P1]–[P8] and second author in Publication [P9]. Specific contributions from each of the publications are presented below.

**Publication [P1]: Chethan Parthasarathy:** Conceptualization, Validation, Formal analysis, Investigation, Writing - Original Draft, Visualization; **Hooman Firoozi:** Formal analysis, Investigation, Writing - Original Draft; **Hosna Khajeh:** Formal analysis, Investigation, Writing - Original Draft; **Hossein Hafezi:** Review & Editing; **Hannu Laaksonen:** Writing - Review & Editing, Supervision, Project administration, Funding acquisition.

**Publication [P2]: Chethan Parthasarathy:** Conceptualization, Methodology, Software, Validation, Formal analysis, Investigation, Writing - Original Draft, Visualization; **Hossein Hafezi:** Software, Validation, Review & Editing; **Hannu Laaksonen:** Writing - Review & Editing, Supervision, Project administration, Funding acquisition; **Kimmo Kauhaniemi:** Review & Editing.

**Publication [P3]: Chethan Parthasarathy:** Conceptualization, Methodology, Software, Validation, Formal analysis, Investigation, Writing - Original Draft, Visualization; **Hossein Hafezi:** Software, Validation, Review & Editing; **Hannu Laaksonen:** Writing - Review & Editing, Supervision, Project administration, Funding acquisition.

**Publication [P4]: Chethan Parthasarathy:** Conceptualization, Methodology, Software, Validation, Formal analysis, Investigation, Writing - Original Draft, Visualization; **Hossein Hafezi:** Software, Validation, Review & Editing; **Hannu Laaksonen:** Writing - Review & Editing, Supervision, Project administration, Funding acquisition.

**Publication [P5]: Chethan Parthasarathy:** Conceptualization, Methodology, Software, Validation, Formal analysis, Investigation, Writing - Original Draft, Visualization; **Hossein Hafezi:** Software, Validation, Review & Editing; **Hannu Laaksonen:** Writing - Review & Editing, Supervision, Project administration, Funding acquisition.

**Publication [P6]: Chethan Parthasarathy:** Conceptualization, Methodology, Software, Validation, Formal analysis, Investigation, Writing - Original Draft, Visualization; **Katja Sirviö:** Software, Validation, Review & Editing; **Hossein Hafezi:** Software, Validation, Review & Editing; **Hannu Laaksonen:** Writing - Review & Editing, Supervision, Project administration, Funding acquisition.

**Publication [P7]: Chethan Parthasarathy:** Conceptualization, Methodology, Software, Validation, Formal analysis, Investigation, Writing - Original Draft, Visualization; **Hannu Laaksonen:** Writing - Review & Editing, Supervision, Project administration, Funding acquisition; **Eduardo Redondo-Iglesias:** Writing - Review & Editing, Methodology, Validation; **Serge Pelissier:** Writing - Review & Editing, Methodology.

**Publication [P8]: Chethan Parthasarathy:** Conceptualization, Methodology, Software, Validation, Formal analysis, Investigation, Writing - Original Draft, Visualization; **Hannu Laaksonen:** Writing - Review & Editing, Supervision, Project administration, Funding acquisition; **Ilari Alaperä:** Data, Review & Editing.

**Publication [P9]: Hosna Khajeh:** Conceptualization, Methodology, Formal analysis, Investigation, Visualization, Writing - Original Draft; **Chethan Parthasarathy:** Conceptualization, Validation, Formal analysis, Investigation, Visualization, Writing - Original Draft; **Hannu Laaksonen:** Writing - Review & Editing, Supervision, Project administration, Funding acquisition.

## Relevant publications (not included in the dissertation)

The following conference and journal publications have also been prepared by the author during the doctoral studies as a co-author or as the main author. However, these publications are not included in the dissertation because they are partially covered by other papers (included in the dissertation) or they are not directly related to the main objectives.

Laaksonen, H., Parthasarathy, C., Khajeh, H., Shafie-khah, M., Hatziargyriou, N. Flexibility Services Provision by Frequency-Dependent Control of On-Load Tap-Changer and Distributed Energy Resources, *IEEE Access*, Vol. 9, March 2021. (<https://doi.org/10.1109/ACCESS.2021.3067297>)

Kumar, J., Parthasarathy, C., Västi, M., Laaksonen, H., Shafie-khah, M., Kauhaniemi, K. Sizing and Allocation of Battery Energy Storage Systems in Åland Islands for Large-scale Integration of Renewables and Electric Ferry Charging Stations, *Energies*, 13 (2), 317, 2020. (doi: <https://doi.org/10.3390/en13020317>)

Laaksonen, H., Khajeh, H., Parthasarathy, C., Shafie-khah, M., Hatziargyriou, N. Towards Flexible Distribution Systems: Future Adaptive Management Schemes, *Applied Sciences*, Vol. 11, Issue 8, 3709, MDPI, April 2021. (<https://www.mdpi.com/2076-3417/11/8/3709>, <https://doi.org/10.3390/app11083709>)

Laaksonen, H., Parthasarathy, C., Hafezi, H., Shafie-khah, M., Khajeh, H., Hatziargyriou, N. Solutions to Increase PV Hosting Capacity and Provision of Services from Flexible Energy Resources, *Applied Sciences*, Vol. 10, Issue 15, July 2020. (doi: <https://doi.org/10.3390/app10155146>)

Laaksonen, H., Parthasarathy C., Hafezi H., Shafie-khah, M., Khajeh, H. Control and Management of Distribution Networks with Flexible Energy Resources, *International Review of Electrical Engineering (IREE)*, Vol. 15 No. 3, June 2020. (doi: <https://doi.org/10.15866/iree.v15i3.18592>)

Parthasarathy, C., Halagi, P., Laaksonen, H. Characterization and modeling Lithium Titanate Oxide battery cell by Equivalent Circuit Modeling Technique. 10th IEEE PES Innovative Smart Grid Technologies Conference (ISGT) – Asia, 5–8 December 2021, Brisbane, Australia, 2021

Laaksonen, H., Parthasarathy, C., Khajeh, H., Shafie-khah, M. Adaptation of DER Control Schemes and Functions during MV Network Back-up Connection. 4th International Conference on Smart Energy Systems and Technologies (SEST), 6–

8 September 2021, Vaasa, Finland,  
(<https://doi.org/10.1109/SEST50973.2021.9543168>)

Laaksonen, H., Parthasarathy C., Hossein H., Shafie-khah, M., Khajeh, H., Flexible Control and Management Methods for Future Distribution Networks. CIRED 2020 Workshop, 22–23 September, Berlin, Germany (online virtual event). (doi: <https://doi.org/10.1049/oap-cired.2021.0024>)

Nemounekhah, B., Faranda, R., Akkala, K., Hafezi, H., Parthasarathy, C., Laaksonen, H., Comparison and Evaluation of State of Charge Estimation Methods for a Verified Battery Model. 3rd International Conference on Smart Energy Systems and Technologies (SEST), 7–9 September 2020, Istanbul, Turkey (doi: <https://doi.org/10.1109/SEST48500.2020.9203121>)

# 1 INTRODUCTION

Electrical energy is considered the backbone for the functioning of modern society, without which life comes to a standstill. The generation, transmission, distribution, and consumption of electrical energy have drastically changed over the years, resulting in modern power systems. There is an emphasis on the reduction of global greenhouse gas emissions in modern power systems, which has resulted in various governments and organizations reducing their utilization of fossil fuel energy sources. Therefore, environmentally friendly renewable energy sources such as solar photovoltaic systems and wind turbine generators have been widely installed all over the world, and their utilization will continue to increase in the future.

However, the energy output of these sources is heavily weather-dependent, resulting in energy security and reliability issues, for example, related to frequency stability and voltage control. Flexible energy resources can provide services that help transmission and distribution system operators to manage the challenges caused by the large-scale integration of intermittent renewable power generation in power systems.

One potential flexible energy resource to manage the challenges and possible network issues is the battery energy storage system (BESS), particularly the lithium-ion (Li-ion)-based battery energy storage system. BESSs can provide different technical flexibility services as part of various applications and functions such as peak shaving, load leveling, voltage and frequency control, power quality improvement, and active network management (ANM) of distribution systems. BESSs are also integrated into power systems via power electronic converter/inverter interfaces, which support the provision of flexibility services requiring active and reactive power control. The scale of power and energy (including the duration of discharge/charge) for each of these applications varies significantly and depends heavily on the case (application, connection point, etc.). Thus, the power requirement for different applications varies from few kW to few hundreds of kW to MWs (based on BESS sizing) and the duration of use could vary from microseconds to few hours.

Excellent power and energy characteristics of the Li-ion battery, along with its modularity, make it a valid choice for multiple technical flexibility service provision in future power systems. Grid-connected BESSs (particularly Li-ion batteries) are generally designed to offer multiple services i.e., single BESS will be designed to provide more than one service to maximize technical and economic

feasibility of the application. This multiuse feature has been facilitated mainly by the advanced characteristics of Li-ion batteries, particularly their fast response characteristics and superior current ramp rates.

However, BESS's real performance to provide flexibility services depends on numerous different parameters such as ambient temperature, charge/discharge current rate (C-rate), depth of discharge (DOD), state of charge (SOC), and their aging characteristics. When developing control and management schemes for stationary, grid-connected Li-ion batteries, it is important to consider their variable performance features as part of the control scheme. Integration of an accurate Li-ion battery model with performance related properties as part of the different management functions enables more realistic knowledge about the capability of BESS to provide flexibility services as well as enables, for example, the development of more accurate flexibility forecasts and enhanced optimization schemes.

The multiuse capability of Li-ion BESS increases challenges in the design and development of battery controllers for ANM schemes, for example, to manage active and reactive power flows in the distribution network or between distribution and transmission systems. The operational power and energy requirement of each application within the multiuse framework (in terms of duration that varies from microseconds to hours) generates challenges in terms of battery controller stability, particularly when dealing with transients in the power systems. Further challenges in the development of Li-ion battery controllers for active-power control related grid applications are mainly due to its own variable performance metrics due to various parameters such as SOC, DOD, C-rate, temperature, and aging. This leads to variable voltage versus SOC and variable power versus SOC curves, which are two important parameters that are generally controlled for ANM applications (or any grid related application) and must be considered while developing battery system controllers.

In addition, battery aging induces various changes in the battery characteristics in terms of reduced energy and power dispatch characteristics. Aging of Li-ion batteries not only causes degradation over its technical characteristics, but also has a direct impact over economic profitability due to reduced power and energy dispatch over a period. To study the impacts of battery aging on its utilization for grid applications, it is necessary to integrate accurate battery-aging models (cycle aging) to cost-based optimization and scheduling algorithms.

## 1.1 Scope and Objective of the Thesis

In this thesis, the role of lithium-ion battery energy storage systems (Li-ion BESSs) for flexible service provision by means of active network management (ANM) is studied. In the developed ANM schemes, a Li-ion BESS was utilized to mitigate network issues arising from the intermittency of DER power generation and to meet the grid-code requirements. For this purpose, modeling of the BESS was developed and improved so that it included the consideration of a more realistic and accurate battery performance model as an integrated part of ANM schemes.

The Li-ion BESS model based on the equivalent-circuit modeling (ECM) technique, which emulates battery performance at different operating conditions such as its SOC, C-rate, temperature, and aging, is developed in the thesis for BESS network integration and ANM studies, both by offline and real-time simulations. The impact of utilizing the proposed Li-ion BESS integration methodologies (including its accurate battery model) on ANM schemes needs to be analyzed, for instance, by means of various use cases.

The timescale of the studied use cases varies from microseconds to hours/days/months, depending on the application and focus of the study case. In real-time and offline simulations of the thesis, the utilization of Li-ion BESS for provision of a system-level frequency control service, through frequency containment reserves for the normal operation (FCR-N) market (Oyj, n.d.), as well as for distribution network ANM-related service provision at different operation time horizons, was studied and analyzed.

Another major focus area in this thesis has been to analyse the role of battery aging in the technical and economic performance of Li-ion BESSs when used for ANM in the distribution network. Battery cycle aging influences the performance characteristics of Li-ion batteries, where its capacity and power dispatch (both charge and discharge) are heavily affected and degraded. Therefore, the proposed battery control schemes for ANM applications include battery cycle aging model, making them adaptive by provisioning BESS energy and power based on its aging characteristics. The motivation to develop such an adaptive BESS control scheme was to maintain battery operation always within safe operating areas.

Similarly, Li-ion battery aging influences the economic performance and outcome of BESS when it is used for stationary grid applications. As mentioned, power and energy dispatch of Li-ion BESS decreases gradually due to aging. These aging related characteristics must be considered when developing cost-based optimization and scheduling algorithms for a Li-ion BESS. Hence, the effect of aging on the economic profitability of Li-ion BESS has been explored in this thesis

by considering its participation on the frequency control service market, particularly the frequency containment reserve (FCR)-N market.

In general, this thesis aims to improve our understanding and knowledge about the role of accurate battery modeling for control design and economic analysis of Li-ion BESS in modern power systems. More detailed scope and objectives of the thesis are presented below.

The main objectives of the thesis are twofold, which are,

1. To address coordinated control related challenges of Li-ion BESS in multiuse ANM applications when connected to a distribution network. The details are mentioned below.
  - i. Design and develop a Li-ion BESS model with independent active and reactive power control features that are suitable for the consideration of multiuse characteristics as part of ANM application related studies
  - ii. Improve the overall battery integration methodology in the medium-voltage (MV) distribution networks, by including a high-accuracy BESS model with performance features for studying ANM schemes
  - iii. Design and develop a coordinated control architecture for grid-side controllers (i.e., the BESS active and reactive power control and other RES flexibility control) which form a part of energy management systems (EMS) of the ANM scheme to effectively utilize the flexibilities available in the MV distribution system
  - iv. Study the impacts of BESS integration to the power system and its role in supporting the power system's stability (both steady-state and transient) by analyzing both short- and long-term perspectives of BESS operation
2. To study the impacts of battery aging on Li-ion BESS control design for ANM schemes and its economic profitability for other technical flexibility/ancillary services like frequency control service through the FCR market.
  - i. Design and develop adaptive controllers for Li-ion BESSs that are part of the EMS in ANM schemes and which depend on battery characteristics, particularly its cycle aging characteristics



as well as study the impact of such adaptive controllers on ANM applications

- ii. Develop local adaptive droop controllers that are dependent on battery cycle aging characteristics for frequency control service-provision-related FCR-N applications
- iii. Develop Li-ion BESS scheduling algorithms based on cost-based optimization studies that consider battery cycle aging as an affecting parameter in FCR-N applications.

The work scope of the thesis for achieving the objectives defined above has been multidisciplinary, including multi-fold research contributions from different fields, such as, a) battery characterization and modeling, b) BESS's MV network integration, c) BESS's operation as part of ANM schemes, and d) techno-economic analysis of BESS utilization for FCR-N service provision. The details include the following:

1. Battery characterization and modeling methodology: two types of battery models were required for the main general objectives of the thesis defined above. They are
  - i. Development of accurate battery models that emulate Li-ion battery performance characteristics at various operating conditions that affect its performance. The battery cell model was based on the second order equivalent-circuit (SOEC) battery modeling technique whose circuit parameters were calculated based on hybrid pulse power characterization tests. This battery cell model was then extended to a battery pack model of required size.
  - ii. To include battery-aging characteristics in both controller development and for studying the economic viability of Li-ion BESSs, accurate aging models were required. The aging model for battery controller development required us to track the battery peak power dispatch capability (both charge and discharge) with respect to various instances of cycle aging. The aging model for techno-economic studies required tracking the nominal power dispatch of Li-ion BESS at different instances of cycle aging. Development of aging models falls within the scope of work in this thesis.

2. Battery integration methodology in MV distribution systems: Two types of battery integration models, offline and real-time, have been explored in the scope of this thesis. They are the following:
  - i. The first one corresponds to detailed model development, which includes integration of battery systems with the aid of power electronic converters (average models), both bidirectional DC/DC Buck–Boost and DC/AC voltage source converters. In this method, the Li-ion BESS was integrated to the MV bus of the distribution network model by means of a coupling transformer. The Li-ion BESS model in the integration method was based on the SOEC model. Detailed battery integration models were utilized in the electromagnetic transient simulation framework that provided a way to analyse the role of Li-ion BESS and its transient/short-term stability when utilized for ANM applications. The models were developed on the Matlab/Simulink platform and simulation studies were performed in offline model.
  - ii. Second, a battery integration modeling method was developed for real-time simulations. It was designed to study steady-state operation and long-term fluctuations when using Li-ion BESSs for ANM applications. Li-ion BESS was represented by a high-accuracy SOEC model, and a simplified average model for power electronic inverters of BESS was utilized. The simulation studies were performed with the OPAL-RT real-time simulator on the ePhasorSim platform.
3. Active network management architecture: The battery integration models were developed to study their role in ANM applications as a flexible energy resource. Therefore, tailored ANM architectures for an existing smartgrid in Finland, in both the study modes mentioned above (i.e., short-term and long-term simulation studies), were designed and developed as part of this thesis. The overall ANM-related scope of the work includes
  - i. Development of ANM architectures that are capable of addressing issues such as managing reactive power flows between HV/MV levels of the power system (i.e., between distribution and transmission networks) to maintain the reactive power flow within the so-called reactive power window, voltage and frequency support issues defined by grid codes, and increasing the overall renewable energy penetration/hosting capacity by means of battery energy storage systems.

- ii. Development of an energy management system (EMS) (which forms the heart of ANM scheme) that is capable of harnessing flexibilities (both active and reactive power related flexibility services).
  - iii. Design and development of grid-side controllers, which are part of the proposed EMS in the ANM schemes. The developed controllers are directly associated with the energy and power management in the MV distribution system as part of the simulation studies, mainly applied on the Sundom Smart Grid (SSG), an existing smartgrid pilot in Vaasa, Finland.
4. Techno-economic studies about BESS utilization for frequency control services provision: To understand the effect of battery cycle aging on the economic profitability when used for FCR-N application, techno-economic studies were undertaken. Therefore, cost-based optimization and battery scheduling algorithms that are aging aware have been proposed in the thesis.

#### 1.1.1 SSG

The smart grid pilot network SSG is a living lab jointly created by ABB, Vaasan Sähköverkko (DSO), Elisa (communications), and University of Vaasa, which is located in Vaasa (Finland). It has been utilized extensively for validation of the designed ANM scheme by means of case studies in Publications [P4] – [P8] of this thesis. Therefore, SSG is also briefly introduced in this section. The SSG network is shown in Fig. 1. It enables utilization of live/streamed measurement data including load demand, wind turbine generation (WTG), voltages, power flows, frequency, and currents. To study future scenarios, particularly with Li-ion BESS, the SSG simulation model (Fig. 1) was modified by adding a Li-ion BESS in the MV distribution network.

Real-time voltage and current measurements (IEC 61850 standard) are recorded from the MV distribution network, from all four feeders at a HV/MV substation and from three MV/LV substations comprising 20 measurement points in total. Measurements are performed at 80 samples/cycle. In addition, active and reactive power, frequency, RMS voltages, and current measurements are received by GOOSE messages. SSG is modeled accurately with available data and grid structure, i.e., distribution network structure, loads, and generation units obtained from the local DSO Vaasan Sähköverkko. Wind power generation is modeled from the measured active power ( $P_{WIND}$ ) and reactive power ( $Q_{WIND}$ ) at bus Tuulivoima

(Jo8), on 30-May-2017.  $P_{WIND}$  and  $Q_{WIND}$  are then converted to system currents, with MV voltage as reference, as explained in Publication 2 [P2]. Loads at the Sulva (Jo6), Sundom (Jo7), and Vaskiluoto (Jo9) feeders are modeled as per the measured data from the MV distribution system.

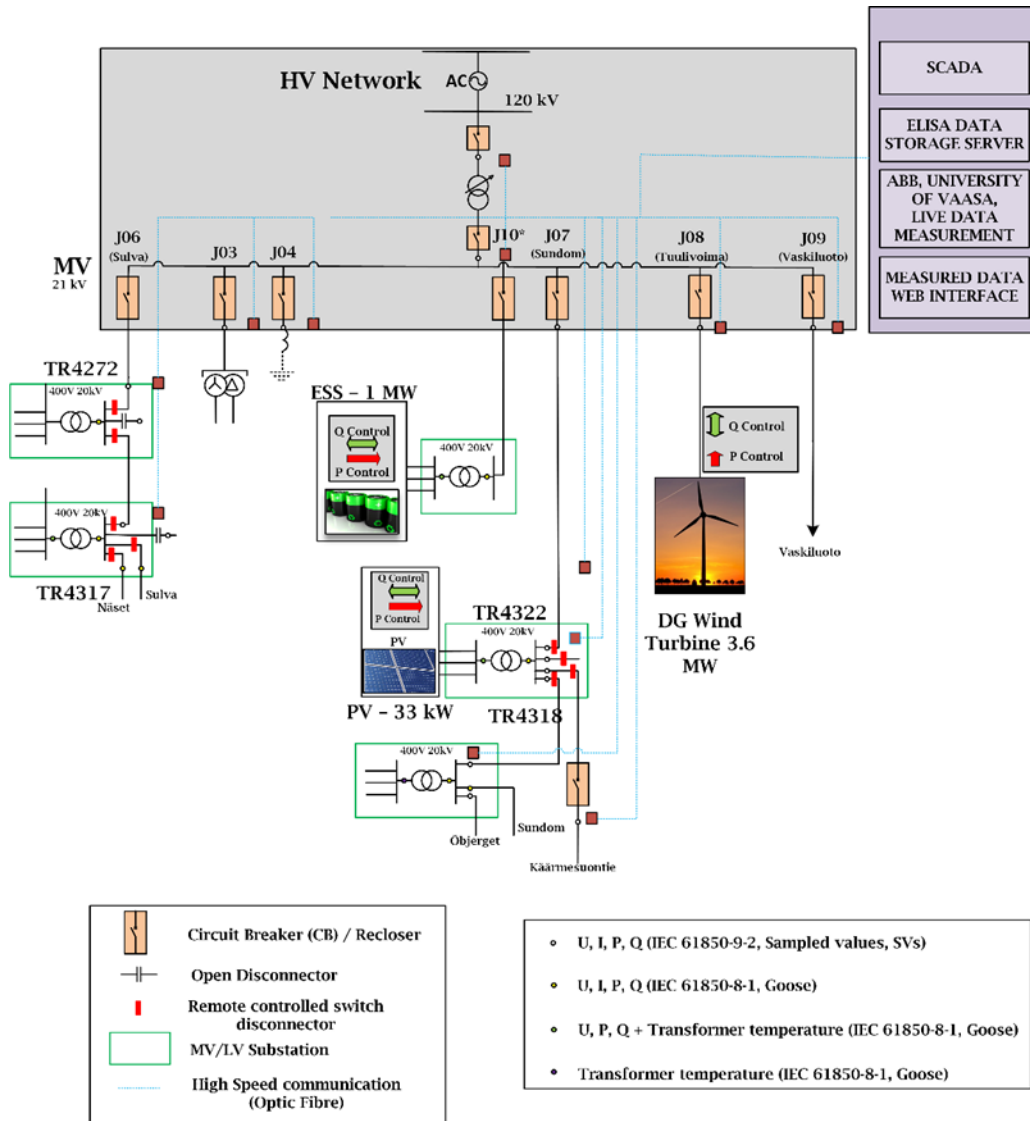


**Figure 1.** Modified SSG Network including Li-ion BESS

## 1.2 Main research questions and methods

This thesis is a compilation dissertation based on nine Publications [P1]–[P9], in which the following main research questions 1–3 have been explored. In the following, the key issues considered, developed and studied in the research related

to these research questions are briefly explained, also covering the main research methods that were used in this thesis.

### **1. What is the benefit of utilizing accurate ECM battery models for grid integration studies of Li-ion BESS?**

Battery integration modeling is related to studying various aspects of connecting BESSs to the power systems through power electronic (PE) converters. The design and development of BESS's converter control methods and principles for power system integration has been extensively studied in the literature. However, when it comes to Li-ion batteries, they are intercalation-based energy storage devices, which operate as a closed system (Lawder et al., 2014) with very few measurable state variables, making it difficult to monitor the states of the battery properly. Therefore, it is required to understand and model the behaviour of Li-ion BESS precisely under various operating conditions, in contrast to recent battery integration related studies (Datta, Kalam, & Shi, 2019, 2020; Iurilli, Brivio, & Merlo, 2019), where generic or the most basic Li-ion battery models are considered.

The advantages of using an ECM-based Li-ion battery model for short-term electromagnetic transient-stability analysis (EMT simulations) is that it enables provision of more accurate battery parameter values, like its voltage and SOC, which are important inputs for the EMS in the ANM scheme. For long-term steady-state studies (ePhasorSim simulations), in addition to voltage and SOC parameter values, it enables the provision of other BESS performance features including highly accurate energy and power values at different operating conditions such as the C-rate, SOC, and temperatures of BESS. This can ensure operation control of the BESS within its allowable characteristics (in terms of their energy, power and SOC) and thereby always secures that the BESS is within its safe operating region. These accurate set-points of the safe operating region can be utilized for PE converter control design as part of battery integration studies. Publications [P2] and [P3] of this thesis focused on the development of battery integration modeling with the help of ECM battery models and validating the overall control design through case studies on the Matlab/Simulink platform.

### **2. How to develop advanced modeling for the control of Li-ion BESS in short- and long-term simulation studies related to flexibility service provision and participation on ANM?**

The first step in advanced modeling of Li-ion BESS's control for grid applications, like ANM, is the development and utilization of accurate battery models, which has been addressed by the previous research question 1. The next step in the advanced

modeling of BESS's control needs to be also aware of both power system and power source characteristics to efficiently manage power system short- and long-term frequency and voltage and power fluctuations due to the intermittency of RESs.

Lithium-ion BESS can provide multiple flexibility services, for example, as part of ANM schemes through its rapid active and reactive power control. For instance, active-power control related flexibility services can be provided by rapidly charging or discharging the BESS. To realize advanced control of BESS in ANM schemes, their performance characteristics and economics must be also considered by an EMS which is integrated to ANM functionality. In the research work related to this thesis, the developed ANM scheme has been utilized to mitigate MV network issues like voltage fluctuations and reactive power flow between voltage levels. The effectiveness of the Li-ion BESS integration methodology, performance of the developed EMS controllers, and the effect ANM on control of Li-ion BESS's grid-side converter (considering operation states and characteristics of the Li-ion BESS) has been validated in this dissertation by means of simulation studies in two different simulation modes, i.e., offline and real-time simulations.

Offline simulations were used to model short-term variations by means of EMT studies. The studied power system model was based on the real-life local distribution network SSG. Publications [P4] and [P5] of this thesis present coordinated control design of various flexibility services for ANM with EMT-based offline simulations. In Publication [P6], OPAL-RT real-time simulations are used to validate the designed ANM scheme in longer-term studies, which meant few days in this case.

### **3. Why BESS aging characteristics should be included in Li-ion BESS control design and how consideration of aging can affect the economic profitability of flexibility services providing Li-ion BESS?**

Lithium-ion battery aging is an irreversible process where power and energy properties of the BESS are degraded over a period due to its utilization including that during cycling and during in rest periods. Therefore, when the BESS's charge and discharge peak powers are analyzed, it can be observed that they reduce with aging. If Li-ion BESS is requested to provide the same peak power at the beginning of life and after aging, it adds mechanical stresses on to the battery cell, which may lead to an even faster rate of aging and potentially to safety risks. Therefore, it is important to operate Li-ion BESS within its safe operating region. Therefore, the control design of Li-ion BESS should take this feature into account. Publications [P7] and [P8] of this dissertation focus on modeling the adaptive Li-ion BESS

control based on its aging, particularly by adapting the peak power charge and discharge characteristics. To calculate the peak power changes of Li-ion batteries, a hybrid pulse power characterization (HPPC) test based method was utilized in Publication P7. In [P8], real-life data from Fortum's (initially with 300 kW peak power) Li-ion BESS participating in Finland FCR-N markets were utilized to determine an adaptive  $Pf$ -droop curve for that BESS which also considers battery aging in terms of its peak power characteristics.

The inclusion of battery-aging characteristics in the control design also has an impact on economic profitability of the BESS. With respect to battery aging, it should be understood that Li-ion BESSs' commitment for nominal or peak power or energy supply provision will vary based on their aging level. Therefore, it is important to understand what difference it makes when aging models are utilized for Li-ion BESS's cost-based optimization and scheduling studies. Publication [P9] of the thesis explores the impact of battery aging on its economic profitability when it is providing frequency control related flexibility services. In [P9], real frequency and market data from January 1st to 31st March, 2021, were extracted from "Fingrid Open Data on the Electricity Market and the Power System" ("Welcome - Fingridin avoin data," n.d.).

### 1.3 Summary of Publications

This section summarizes briefly all nine publications of this compilation dissertation. Fig. 2 provides an overview on how more accurate and advanced Li-ion battery models with performance features included were utilized to improve battery integration modeling, design ANM schemes and their adjoining controllers, and finally understand the effects of battery aging on Li-ion BESS control design and its economic implications.

#### **Publication [P1]:** Distributed Generation, Storage, and ANM

In this Publication 1 [P1], the concepts of distributed generation and utilization of energy storage systems, particularly the battery energy storage systems in the context of ANM schemes have been explored. It provides an understanding on the current state of the art in these aforementioned subjects, with an emphasis on the distribution network management related solutions and their role in modern power systems. It also delves into the understanding of various energy storage systems for stationary grid applications and their control design features highlighting key characteristics based on the literature.

**Publication [P2]:** Modeling and Simulation of Hybrid PV and BES Systems as Flexible Resources in Smartgrids - Sundom Smart Grid Case

The role of hybrid solutions with PV and Li-ion BESS as flexible energy sources to fulfil the increasing short-term flexibility needs was studied in Publication 2 [P2], by means of a simulation case study in the local pilot network SSG. This hybrid PV+BESS solution was connected in the MV distribution network, and simulation studies were performed with Matlab software. The key contribution from this publication has been the design and development of DC/DC converters (both Li-ion BESS and PV with MPPT) and DC/AC voltage source converter controllers for offline simulations, based on average converter models and their validation for flexibility provisioning by means of a case study in SSG.

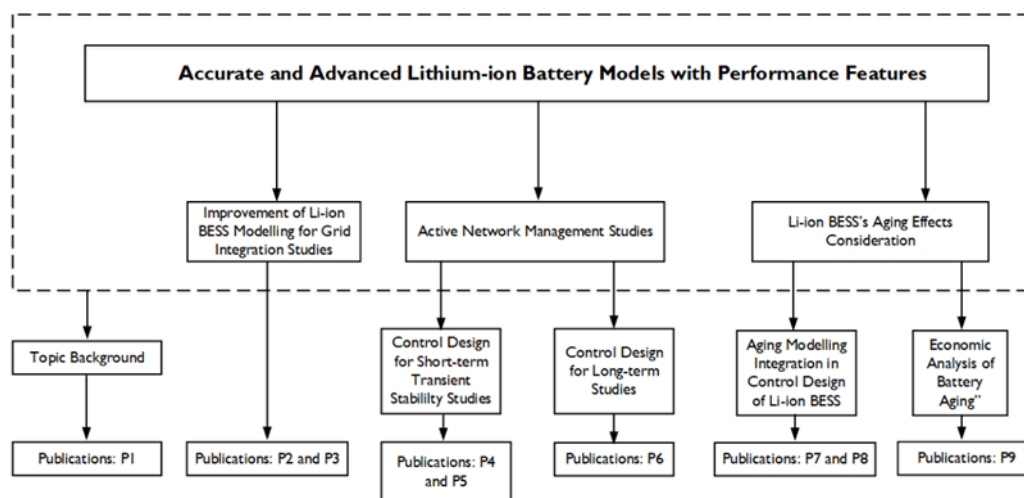


**Figure 2.** Summary of publications P1–P9 (P with a number refers to corresponding publication) focus areas

**Publication [P3]:** Lithium-ion BESS Integration for Smart Grid Applications - ECM Modeling Approach

A generic battery model from the Matlab/Simulink library was used in Publication 2 [P2] for battery grid integration studies. However, these generic battery models lack an understanding of actual battery characteristics such as power, energy and voltage as they are variable and depend on parameters such as DOD, C-rate, temperature, SOC, and aging. Therefore, Publication 3 [P3] developed an equivalent-circuit model, ECM, for Li-ion batteries. A nickel manganese cobalt (NMC) type battery cell was modeled as a SOEC, and the model considered the C-rate, temperature, state of charge, SOC, and aging effects. This battery model has been used for battery integration modeling, i.e., detailed controller design methodology for DC/DC- and DC/AC- converter interfaces to enable advanced



grid integration studies. Overall, Li-ion BESS integration design was validated by simulation studies with the Matlab Simulink Simpowersystems software.

**Publication [P4]:** Integration and Control of Lithium-ion BESSs for ANM in Smart Grids – Sundom Smart Grid Backup Feeding Case

ANM schemes play an important role in solving, for example, increased voltage fluctuations and congestion management issues due to high-RES penetration by effectively managing flexible energy resources, like Li-ion BESS, available in the distribution network. In Publication 4 [P4], first, the ANM architecture for managing available flexibilities in SSG has been developed, followed by the development of an EMS focusing on the integration design of Li-ion BESS and the controllers managing them. The effectiveness of the ANM scheme and its adjoining controllers in the EMS has been validated by means of a case study with EMT-based simulations in the SimPowersystems platform of Matlab/Simulink software, where SSG has been considered in the backup feeding scenario/topology (e.g., due to maintenance).

**Publication [P5]:** Control and Coordination of Flexibilities for ANM in Smart Grids – Li-ion BESS Fast Charging Case

Fast charging of Li-ion BESSs integrated in the MV distribution system of SSG may introduce its own stress and congestions on the network depending on the BESS connection point weakness and simultaneous generation/load situation. Therefore, the role of ANM schemes in mitigating such effects is studied in Publication 5 [P5]. The studies are performed by means of offline simulation with EMT software (SimPowersystems platform), similar to Publication 4 (P4). The effect of such ANM schemes on the integration of Li-ion BESS (Publication P3), i.e., control of its grid-side converter (considering operation states and characteristics of the Li-ion BESS) and their coordination with the grid-side controllers, was analyzed in detail, and particularly, the effect of AC load on the DC characteristics of Li-ion BESSs was analyzed.

**Publication [P6]:** Modeling Battery Energy Storage Systems for ANM – Coordinated Control Design and Validation

In Publication 6 [P6], the control design and validation of Li-ion BESSs has been studied in long-term studies related to ANM. The ANM architecture for managing the available flexibilities in SSG has been developed, followed by the development of EMS to manage different available flexible energy resources (FERs), particularly focusing on the integration design of Li-ion BESS and the controllers managing them. These were designed and implemented in a real-time simulator, OPAL-RT

in its ePhasorSim -platform. A detailed and accurate Li-ion battery model has been used to design BESS controls, which enabled improved overall power system control and management studies by simultaneously considering both component (BESS) and system-level (power system) aspects.

**Publication [P7]:** Aging Aware Adaptive Control of Li-ion Battery Energy Storage System for Flexibility Services Provision

Li-ion BESSs are prone to aging, which results in decreasing performance, particularly in reduced peak power output and capacity of the BESS. Therefore, the BESS controllers in the EMS of the ANM must be aware of changing battery characteristics due to aging, particularly of importance is BESS's peak power change supporting protection, which restricts BESS's operation limits for safety reasons and improves its lifetime in the long run. In Publication 7 [P7], first, an architecture for the ANM scheme is designed considering Li-ion BESSs as one of the FERs in an existing smart grid pilot SSG in Vaasa, Finland. Further, Li-ion BESS controllers are designed to be adaptive in nature to include its aging characteristics, i.e., tracking the changing peak power as the aging parameter. An accurate aging model, tracking peak power changes of Li-ion BESS with aging, has been developed for this purpose. Impact of such aging aware and adaptive Li-ion BESS controllers on the flexibility service provision for power system operator needs was analyzed by means of real-time simulation studies in the OPAL-RT real-time simulator.

**Publication [P8]:** Aging Characteristic Consideration in Adaptive Control Design of Grid-Scale Lithium-ion batteries

Li-ion BESSs are extensively used for frequency control support and service provision through FCR-N and FCR-D markets. This is done by means of active-power-frequency ( $Pf$ )-droop control. However, with aging, the power dispatch (especially its peak-power characteristics) capability of Li-ion BESS reduces considerably, which needs to be considered in the  $Pf$ -droop settings of the BESS. Therefore, an adaptive  $Pf$ -droop curve has been proposed in Publication 8 [P8], which considers battery aging in terms of its peak power characteristics. This will ensure Li-ion BESS to function within its safe operating area. It also provides the possibility to automatically modify Li-ion BESS control settings and the flexibility service provision capability based on battery performance and aging. The effectiveness of the proposed droop curve has been validated by means of case studies with an existing real-life Li-ion BESS, with a beginning of life (BOL) peak power 300 kW, operated in Finland by Fortum company for frequency control service participation through FCR-N markets.

**Publication [P9]:** Effects of Battery Aging on BESS Participation in Frequency Service Markets – a Finnish Case Study

Publication 9 [P9] studies the participation of a Li-ion BESS in providing FCR-N. The Li-ion BESS reacts to the frequency deviations from 0 to 0.1 Hz and  $-0.1$  to 0 Hz in FCR-N operations. Paper P9 presents a method to schedule the charging and discharging power of BESS while considering the effects of BESS cycling aging effects. In simulation studies, a 50 kWh BESS reacts to the frequency changes (real Finnish TSO Fingrid measurement data every three minutes from January 1st to 31st March, 2021 was used), and the corresponding outcome is estimated for three months. Finally, the P9 results demonstrates how cycling aging affects the BESS economic outcome when it provides FCR-N services. Based on the simulation results, aging can decrease the BESS profits by 6.06 Cent in each cycle.

## 1.4 Scientific Contributions

The objectives, scope, and research question addressed by this dissertation has been explained in Sections 1.1 and 1.2 in detail. The research gaps and questions arising from them have been explained in detail in Chapter (2.2) and Chapter 5 (Sections 5.1.1 and 5.1.2). The scientific contributions will be presented briefly in this section, and detailed contributions have been in provided in Chapter 6 (Conclusion). They are as follows:

1. BESS focused Power System Modeling Methods:
  - Defining the type and complexity of Li-ion battery models required for different power system control modeling and simulation studies at different granularities in time steps (i.e., EMT simulation for short-term control stability studies and OPAL-RT platform long-term control stability modeling)
  - Improvement of Li-ion battery integration modeling techniques for power system control and stability studies by utilizing accurate battery performance models (high fidelity equivalent-circuit battery models that are capable of emulating battery performance at different SOC, C-rate, temperature and aging conditions) in both offline and real-time simulation platforms
2. ANM Control Architectures and EMS Design

- Development of grid-specific ANM control architectures and coordinated control of various flexibilities available in the grid to manage power grid stability within specifications defined by grid codes
  - Design and development of EMS for an ANM scheme and their adjoining control design for various DERs in the power system that are better aware of component and network characteristics
3. Battery Aging Aware Adaptive Control Development
- Development of an aging-aware adaptive local droop controller for active-power-frequency droop control settings
  - Development of an aging aware adaptive Li-ion battery controller (EMS of ANM architecture) based on battery peak-power as its aging parameter
4. Techno-economic studies
- Analyzing the effects of Li-ion BESS control, including its aging effects on the economic profitability of Li-ions when used for grid applications (particularly FCR-N application)

## 1.5 Outline of the thesis

This thesis has been organized into six chapters in the following manner.

Chapter 1 introduces the doctoral thesis defining its objectives and scope in detail, followed by the main research questions and methods as well as providing a brief summary regarding the scientific contribution and a summary of the appended Publications P1–P9.

Chapter 2 presents a background on ANM schemes, control modeling of Li-ion BESSs for ANM applications, and the need for developing accurate battery models for this purpose. Further, it focuses on performance characteristics (including its aging effects) of Li-ion batteries that are essential for the design and development of various controllers in the scope of the thesis.

Chapter 3 presents a short-term control-modeling methodology of Li-ion BESSs for ANM schemes to assess its role and contribution in power system support and flexibility service provision for system operators. These studies are developed on

the Matlab/Simulink platform using SimPowerSystems library by means of offline simulations in EMT mode. The proposed ANM scheme and their adjoining controllers are validated by means of various case studies.

Chapter 4 presents long-term control-modeling methodology of Li-ion BESS for ANM scheme simulation studies. These studies are performed with ePhasorSim platform of OPAL-RT real-time simulator. The proposed ANM scheme and their adjoining controllers are validated by means of various case studies.

Chapter 5 explores the effect of Li-ion battery cycle aging on technical and economic performance of Li-ion BESS when it is used for ANM and other technical ancillary/flexibility service provision like system-wide frequency control.

Chapter 6 presents the conclusions and contribution of the research performed in this thesis and discusses future research directions.

## 2 LITERATURE SURVEY AND STATE OF THE ART - LI-ION BESS MODELING, CONTROL, AND UTILIZATION IN SMART GRIDS FOR ANM APPLICATIONS

Modern power systems are undergoing massive changes to reduce greenhouse gas emissions by replacing conventional sources of power generation with renewables. Strict emission control goals have been set in the European Union and elsewhere in the world, with simultaneously supporting integration of RES and improving energy efficiency (Förster et al., 2021; “Growth Opportunities from Decarbonisation in the Global Power Market, 2019–2030,” n.d.). The investments in RES development have been stated to be approximately 3.4 trillion USD worldwide in the coming decade (“\$3.40 Trillion to be Invested Globally in Renewable Energy by 2030, Finds Frost & Sullivan,” n.d.). Such rapid integration of inverter-based, inertia-less and stochastic RESs, such as wind turbine generators and solar photovoltaic systems, introduce various challenges in power systems. These challenges include, fluctuations in voltages (especially in weak distribution networks) and power system frequency, increasingly sensitive power system dynamics due to reduced and variable inertia-level and power quality issues (Anees, 2012; Holjevac et al., 2021). Therefore, controllable and FERs that can help mitigate the challenges faced by the intermittent power generation from RES are increasingly needed in modern power systems.

### 2.1 Power system flexibility and FERs

The power system requires balancing of generation and demand at each point of time. Conventional systems with synchronous generators (SGs) can maintain transient frequency stability after major disturbances, like large generation/load/transmission line disconnection or fault, due to the existing high inertia in the rotating masses of SGs. With higher share of inverter-based intermittent RESs in the power system, stability risks can increase due to a lower and more variable inertia level. Therefore, there is a need for power system stability supporting technical flexibility services (i.e., flexibility) from different energy resources. In addition to frequency stability and control needs, flexibility services are also increasingly needed to manage the line capacity constraint related network congestions (e.g. voltage or thermal/current limit violations) in both distribution and transmission networks (Lund, Lindgren, Mikkola, & Salpakari, 2015).

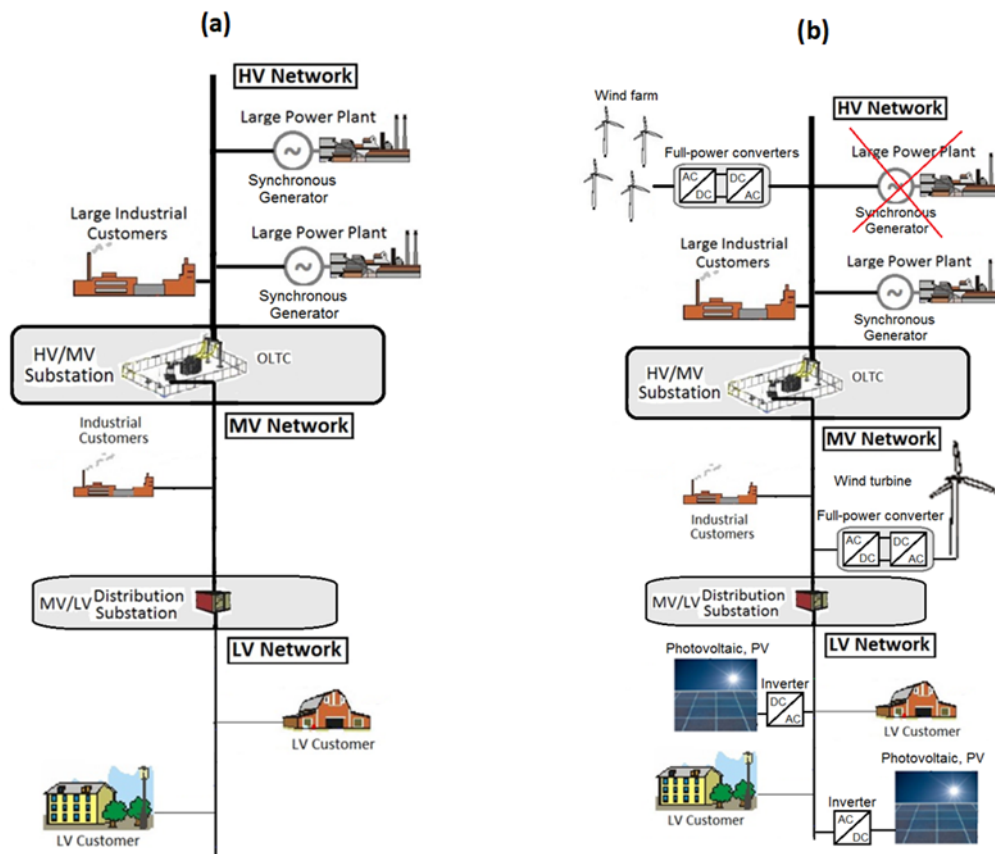


**Figure 3.** (a) Traditional centralized power system; (b) Modern decentralized power systems

A simplified example of a traditional power system is shown in Fig. 3(a), which includes directly connected large-scale centralized SGs with high inertia, as the main power generation sources. The dynamics and transient stability of these traditional power systems are determined largely by dynamics and inertia of the SGs. In the traditional power system, the power flow in the distribution network (MV and LV networks) has been one way, along with very few measurement points with minimal communication with different parts of the network (i.e., between transmission and distribution network). Fig. 3(b) represents an example of modern power systems in which conventional power sources have been replaced by inverter-based RESs, predominantly with wind turbine and solar PV generation. Inverter-based RESs do not have natural inertia like SGs, and their dynamic behaviour is mainly determined by the inverter's control scheme. In addition, their stochastic nature may introduce new challenges to the power systems, such as

- More frequent and larger frequency oscillations.

- Voltage fluctuations and voltage limit violations (congestions) in distribution (MV and LV) and transmission (HV) networks.
- HV, MV, and LV network capacity constraint violations (congestions) related to the current or thermal limits.

In addition, in the future power systems with RES-based distributed generation (DG), power flows are two-way also in the distribution network, which requires new compatible and future-proof protection and islanding detection and management solutions for distribution networks (Sperstad, Degefa, & Kjølle, 2020). To manage the abovementioned challenges, there is a clear need for increased flexibility and flexibility services in both transmission and distribution networks. As defined by IRENA, “Power system flexibility is the ability of a power system to reliably and cost-effectively manage the variability and uncertainty of demand and supply across all relevant timescales” (Renewable Energy Agency, 2018).

The resources that can provide flexibility in the power system are called as FERs. Demand response (DR), electric vehicles (EVs), stationary energy storage systems (ESSs), and controllable inverter-based energy resources (Laaksonen, Parthasarathy, Hafezi, Shafie-Khah, & Khajeh, 2020) can be utilized as FERs providing flexibility services. Active utilization of FERs is of major interest as they are capable of solving network problems locally such as at the LV or MV network level, or system-wide, i.e., whole power system level.

Type of technical ancillary or flexibility services that FERs can provide can be broadly classified as active and reactive power flexibility services for the transmission and distribution system operators (TSOs and DSOs). The possible flexibility services that FERs can provide through corresponding marketplaces, bilateral agreements, technical solutions (e.g., management functionalities), or grid/network codes are

- Frequency control by active-power control (System-wide service);
- Voltage control participation by active/reactive power control (Local/system-wide service);
- Balancing power supply (System-wide service);
- Intentional islanding or microgrid operation (Local service);
- Black-start support (System-wide service);



- Reactive power control in HV point of common coupling according to agreement/need/grid code (Local or System-wide service);
- Network loss minimization (Local service)
- Fault current management and fault ride through capability (Local/system-wide service).

To manage these FERs and their flexibility services efficiently, network management schemes that are capable of controlling all the available flexibilities actively in a coordinated manner will be essential. This can be done, for example, by ANM schemes, which are discussed in the next section.

### 2.1.1 ANM

Power systems have been changing rapidly with the addition of RESs and other DERs at all voltage levels, i.e., the LV, MV, and HV sides (Ghadi et al., 2019; Mishra, Ghadi, Azizivahed, Li, & Zhang, 2021). With recent technological maturity and social acceptance, the integration of RESs and DERs into power systems has increased their utilization in distribution networks (MV and LV). Notably, the RESs and DERs were previously required to be disconnected during faults and disturbances to safeguard the grid and customers. Due to the large-scale integration of DERs, issues such as risk of power system stability and issues caused by the disconnection of a large number of DERs owing to faults or frequency disturbances have emerged. Therefore, in the future, the fault ride through (FRT) capability as well as stability-supporting flexibility services are needed in case of controllable DER units. These flexibility services will be needed not only during emergency situations defined by grid codes but also during steady-state fluctuations (Hu et al., 2022; Kryonidis et al., 2021a).

The ANM schemes provide a way to actively manage the distribution system by controlling their generation, loads, and energy storages. The working definition of ANM is (Douglas, Creighton, Roper, & Ault, 2007) “systems that implement pre-emptive action to maintain networks within their normal operating parameters.” In simple words, ANM provides management of available flexibilities (DERs, EV, DR, demand-side management, or ESSs) in the MV or LV distribution network (either in an isolated or grid-connected microgrid).

- The ANM schemes help to keep the values of voltage, frequency, active-power flow, and reactive power flow within the limits specified by the

system operators typically based on applicable standards and relevant grid codes.

- By managing flexibilities available in the network, ANM schemes help in increasing the network hosting capacity and accommodate a higher number of DER integration, including RESs (Abapour, Nojavan, & Abapour, 2018; Laaksonen, Parthasarathy, Hafezi, Shafie-khah, et al., 2020) as well as EV integration.

Fig. 4 provides an overview on the operation of ANM schemes. Active FERs such as DERs, DRs, and ESSs need to provide information on how much flexibility they can offer at a given period of time, and this information is given as input to the ANM block. Local measurements from the distribution system are given as input to the ANM block. Based on the inputs, the ANM block generates control signals for various FERs in the system by managing their active and reactive powers.

ANM-related solutions in the distribution networks can be broadly classified as techno-economic and technical solutions, as shown in Fig. 5. Techno-economic solutions are related to ANM schemes that are addressed based on respective marketplaces, market/tariff structures, business models/pricing mechanisms, or regulatory frameworks. In contrast, purely technical ANM solutions deal with addressing only technical issues in the distribution system management by the active and reactive power control of FERs without direct economic connection (e.g., related to active and reactive power flow management between HV, MV, and LV networks).

### 2.1.2 Battery energy storage systems and ANM

Because of their fast and controllable dynamics, BESSs have the potential to provide multiple different flexibility services in stationary grid applications, e.g., as part of ANM schemes. The decreasing cost and high degree of flexibility of BESSs has created interest in industrial (system aggregators, OEM manufacturers and network operators) and scientific communities for their use in ANM schemes (“Active Network Management Enables Addition of 8.5 MW of Renewables to Shetland Islands Grid,” n.d.; Carr, Premier, Guwy, Dinsdale, & Maddy, 2014; Das, Bass, Kothapalli, Mahmoud, & Habibi, 2018a; Plé Caš, Xu, & Kockar, n.d.). Increasing technological maturity and reduced capital costs of BESSs have played a considerable role in their adaptation worldwide (Davies et al., 2018). BESS can participate in both active power and reactive power related management solutions due to their inverter-based interface, which is used for the connection to the power system (Carr et al., 2014). Therefore, they can be used for multiuse scenarios,

where one battery system is capable of participating in different ANM applications at different points to time or simultaneously (e.g., active and reactive power related services provision).

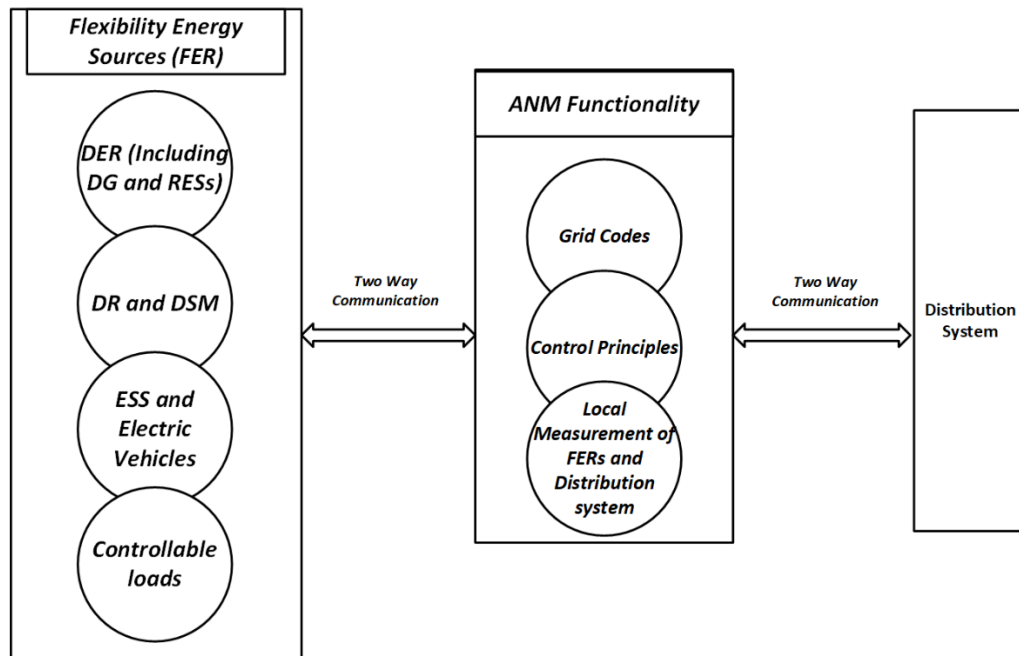


**Figure 4.** Basics of ANM operation

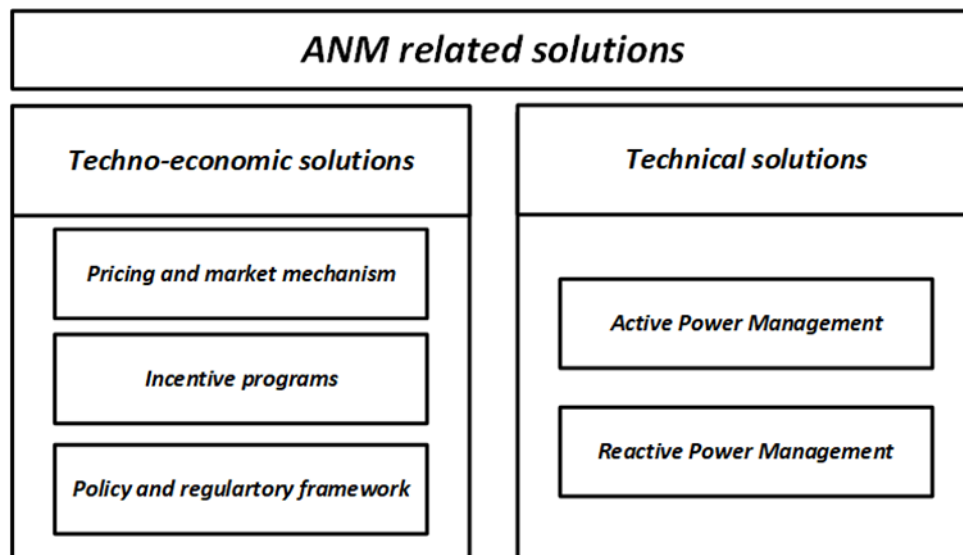


**Figure 5.** Classification ANM-related solutions

From the viewpoint of transmission and distribution system operators (TSO/DSOs), an effective way to utilize BESSs for ANM and local/system-wide

flexibility service provision could be to place them at the HV/MV primary substation or at MV/LV secondary substations. In general, BESSs (Stecca, Ramirez Elizondo, Batista Soeiro, Bauer, & Palensky, 2020) can

1. Increase the capacity to transfer active power by storing the energy at times of higher RES generation, avoiding the cost for additional transfer/line/transformer capacity;
2. Secure reliable LV network distribution to all or the most critical customers in cases of MV network fault by utilizing the intended island operation;
3. Increase the storage capacity of MV/LV substations in a modular way e.g., when customer reliability requirements or RES integration in LV network increase;
4. Locally compensate for the reactive power produced by underground cables by decreasing the reactive power exchange in the MV network, thereby reducing network losses and increasing active-power flow and DER/EV hosting capacity;
5. Continuously control the reactive power flow at the distribution network and possibly adapt reactive power settings to increase network hosting capacity or to minimize frequent tap changes by on load tap changer (OLTC) at the HV/MV substation when the amount of flexibilities is higher in a system (C. Li, Disfani, Pecenak, Mohajeryami, & Kleissl, 2018)

In addition to local flexibility services, BESSs can also provide a variety of system-level technical ancillary/flexibility services (Stecca et al., 2020). Ancillary services in general are designed to improve the grid stability and manage system frequency in the stable region defined by TSOs (e.g. different frequency control markets) and grid codes and mitigate voltage fluctuations in the power system (REISHUS CONSULTING, 2017). Table 1 provides details regarding the type of flexibility/technical ancillary services that the BESSs are capable of providing to support the power system (Kryonidis et al., 2021b; Maeyaert, Vandeveld, & Döring, 2020; Mexis & Todeschini, 2020).

The operation timescale of these ancillary/flexibility services provided by ESSs plays an important role in developing ANM strategies, as shown in Fig. 6. Note that the voltage control application operates by regulating reactive power flows in the network, typically by reactive power control ( $QU$ -) control method and is required to be in active for the whole duration in a day. The operation timescale of applications providing services for inertial support (e.g., very fast active-power

control or virtual inertia control of ESS), frequency control, and load following services etc. varies from cycles of minutes to hours based on the application (Fig. 6). The operation timescale of other frequency control related services like frequency containment reserve (FCR) and frequency restoration and replacement reserves (FRRs) also varies from seconds to hours based on the requirement (Fig. 6).

## 2.2 Lithium-ion battery energy storage systems and flexibility services

Lithium-ion batteries have been gaining prominence as an energy storage technology for various applications such as EVs, mobile phones, laptops, and smart watches and for stationary grid applications. The major reasons behind their adaptation are their considerable technical characteristics such as ability to react fast, high energy and power density, long cycle- and shelf-life, low self-discharge rate, high round-trip efficiency, modularity, and improved safety performance (Yong Li, Song, & Yang, 2014; Román-Ramírez & Marco, 2022; Vennam, Sahoo, & Ahmed, 2022; Xueyuan Wang et al., 2021). The falling prices of Li-ion batteries from about 1200 USD/kW in 2010 to about 132 USD/kW in 2021 (“Battery costs rise as lithium demand outstrips supply - Nikkei Asia,” n.d.; “BloombergNEF: Average battery pack prices to drop below US\$100/kWh by 2024 despite near-term spikes - Energy Storage News,” n.d.) and further expected reduction to about 124 USD/kW in 2024 have been major causes for their utilization worldwide, including power grid applications where high power and energy battery systems are required.

**Table 1.** Flexibility/technical ancillary services supported by BESSs

Technical Terms	Definition
<b>Voltage Control</b>	Mitigates voltage fluctuations due to increased RES integration in distribution systems by controlling ESS active and reactive power.
<b>Frequency Control</b>	A set of control actions that aim to maintain a constant system frequency, where ESS can play a major role in all levels of frequency control such as inertia support, frequency containment reserves (primary control), frequency restoration reserves (secondary control), and replacement reserve or tertiary control.
<b>Congestion Management</b>	To prevent overloading of the distribution system and avoid thermal limits violations at all times.
<b>Power Variations Smoothing</b>	With higher penetration of RESs such as wind and solar PV, variability in power generation is high and the output power may need to be smoothed to improve supply reliability.

Technical Terms	Definition
<b>Voltage Unbalanced Mitigation</b>	To alleviate the voltage unbalance in various feeders, particularly in LV distribution systems.
<b>Losses Compensation</b>	Compensation of losses for the system operators (e.g., DSOs) e.g., line losses.
<b>Reactive Powers Support</b>	The reactive power flow between TSO and DSO networks needs to be regulated according to the agreements/needs/grid codes established in a region.
<b>Black Start</b>	Ability of starting a generating unit of DER without the need for external grid supply and to re-energize the rest of the network (e.g., microgrid).

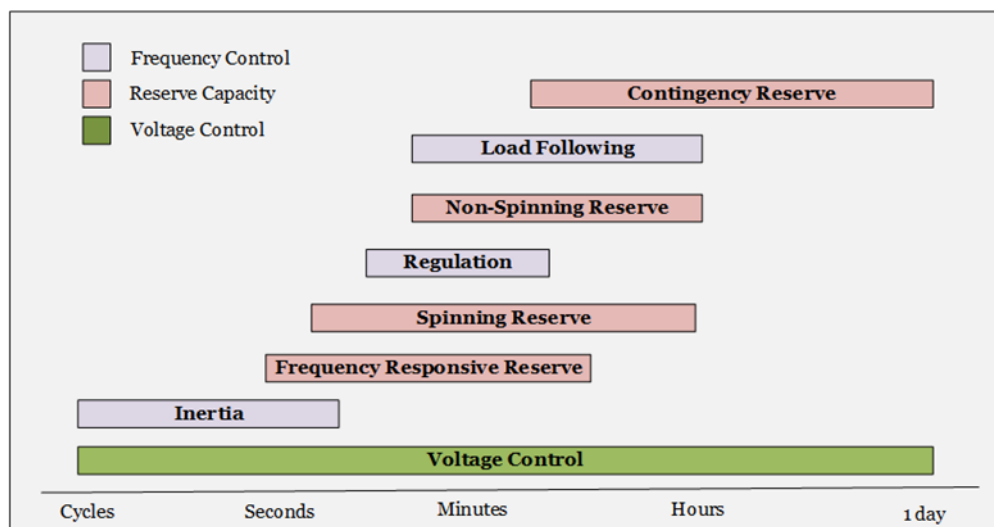


**Figure 6.** Timescale of operations for different flexibility services

Li-ion BESS for power grid applications are important even for transportation applications (EVs, marine applications etc.). Li-ion batteries account for 78% of BESS in operation, with high-temperature sodium and lead-acid batteries taking 11% and 4%, respectively (Inal, Charpentier, & Deniz, 2022). Li-ion BESS have been of enormous interest to the research community, who have been tirelessly working on improving the battery characteristics and design (“Adv. Lithium-Ion Batter.,” 2002; Grey & Hall, 2020), developing better control methods for Li-ion BESS utilization in both real-time and planning phases (Xu & Shen, 2021), and widening their scope of application in land- and ship-based power systems (Choi et al., 2021a; Inal et al., 2022).

Fig. 7 provides a representation of the power ratings and the overall discharge duration required from energy storage technologies for various applications. As mentioned before, Li-ion BESSs are capable of providing multiple technical ancillary/flexibility services (Hesse, Schimpe, Kucevic, & Jossen, 2017; Müller,

2018; Vazquez, Lukic, Galvan, Franquelo, & Carrasco, 2010), whose demand characteristics (power and energy requirements) are represented in Fig 7. Most widely used commercial application for the stationary grid application of Li-ion BESSs tends to be for technical ancillary services (Choi et al., 2021a). It can be assumed that Li-ion BESS are capable of transmission and distribution (T & D) grid support and to some extent in energy management applications, and their utilization has been in the research and pilot phases, especially for transmission related applications (“Battery storage system is connected to transmission grid | E&T Magazine,” n.d.; “Use of Large Scale Energy Storage for Transmission System Support: Energy Storage as Black-Start Resource,” n.d.).

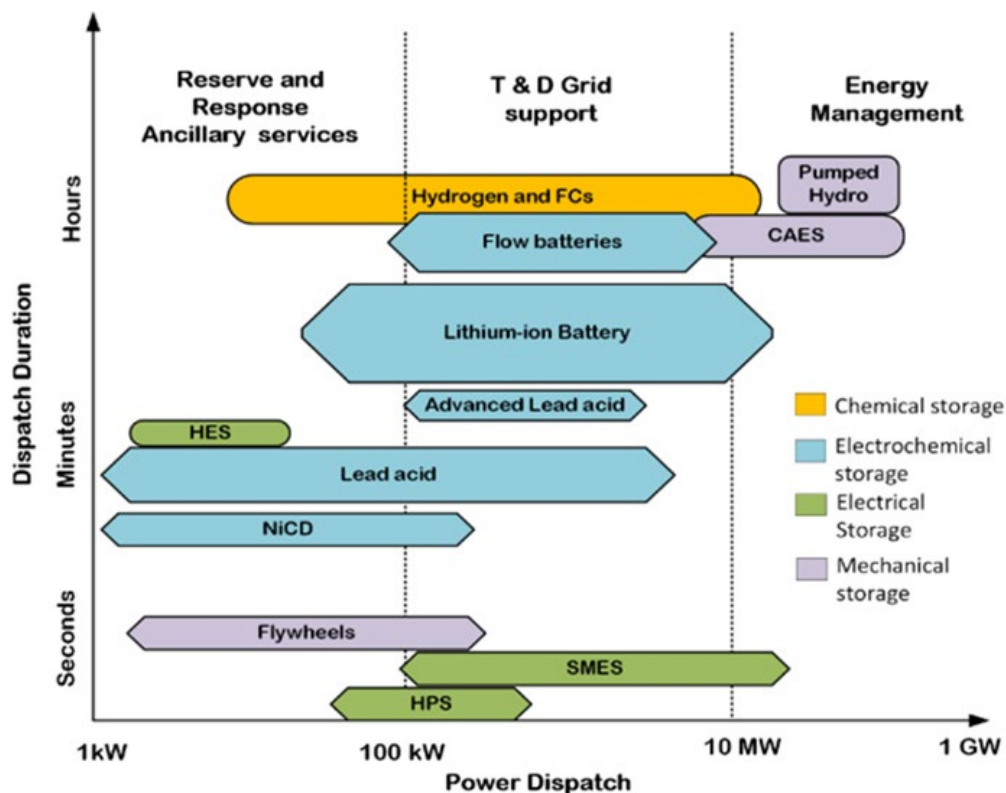


**Figure 7.** Energy Storage Systems Characteristics

### 2.2.1 Lithium-ion BESSs - Technical characteristics and challenges

The application base of Li-ion batteries has been rapidly increasing in recent years. The expected Li-ion BESS performances for these applications are stringent with high life expectations (closer to 8000 cycles or 20 calendar years) (Masias, Marcicki, & Paxton, 2021). However, Li-ion batteries are intercalation-based ESSs, which operate as a closed system (Lawder et al., 2014) with very few measurable

state variables (voltage and current), making it difficult to monitor the states of the battery properly.

The performance characteristics are nonlinear for Li-ion batteries as shown in Fig. 8, which describes the voltage response of a Li-ion battery NMC cell from 100% SOC to 0% SOC at different aging intervals at a 1C rate (check Appendix 1 for definition of C-rate) of discharge. From Fig. 8, it can be observed that the power and energy characteristics of the battery change drastically, with variable amount of nonlinearity introduced in the battery characteristics at different points of aging. The estimation of SOC of the cell becomes challenging due to the nonlinear nature of the Li-ion batteries.

The factors affecting the performance of various Li-ion batteries with different chemistries are shown in Fig. 9. Battery aging brings nonrepairable losses to the cell, thereby affecting their energy and power characteristics, mainly due to two phenomena observed in the cells, their capacity fade and increased resistance, respectively. Therefore, for the development of advanced and feasible Li-ion BESS control schemes, the following challenges/issues need to be considered:

- Determination of accurate voltage reference for control design at various current rates (C-rates);
- Determination of accurate SOC reference, which typically is estimated using voltage and current measurement;
- Determination of correct set-points of varying power and energy reference of the Li-ion batteries due to aging.

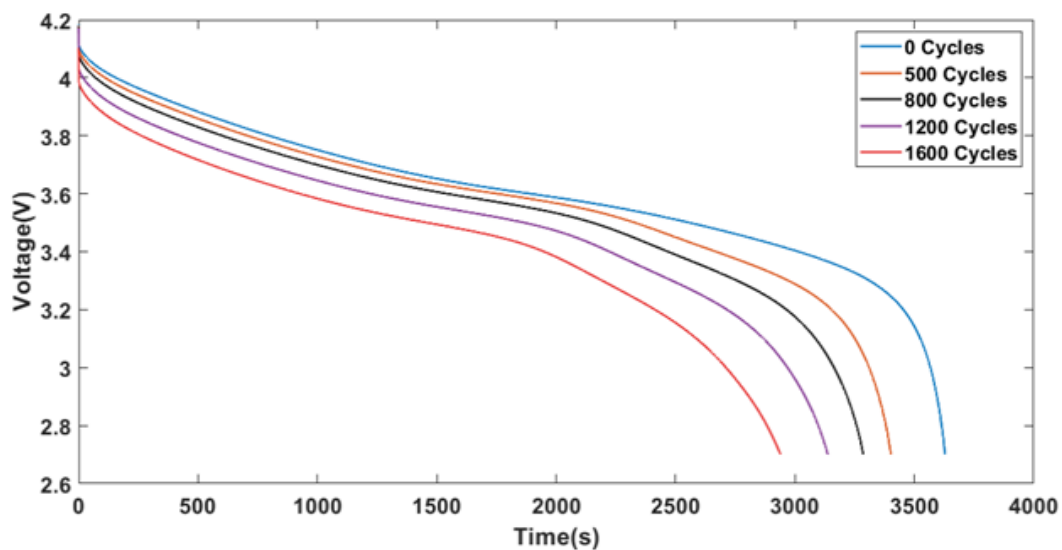


**Figure 8.** Cell performance characteristics at different aging intervals



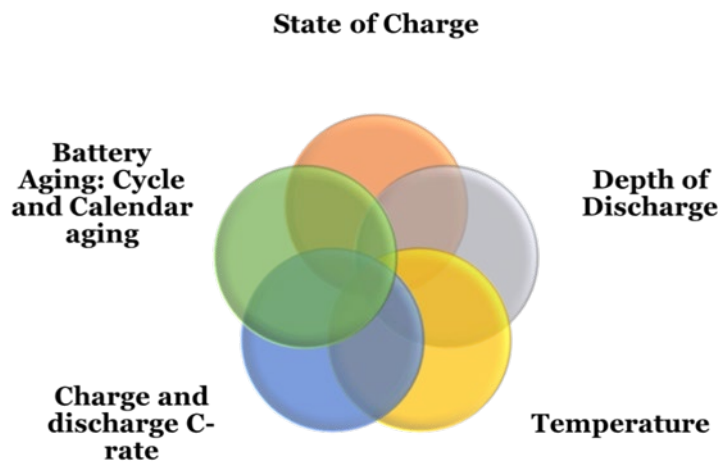


**Figure 9.** Cell performance influencers

### 2.2.2 Control of Lithium-ion batteries in grid applications – Suitable simulation modes

The application and time duration range of Li-ion BESSs for grid applications is wide, with some applications requiring charge/discharge operations in the range of seconds to some applications demanding power dispatch up to few hours. Therefore, control design and validation have to be performed at different timescales and durations for Li-ion BESSs. The simulation types to study multiple timescale power system steady states and dynamic characteristics are classified as (Okubo, Oki, Agematsu, Price, & Wiraau, 1993),

1. Fast transient/short-term simulations: These can be further divided into two parts (a and b):
  - a. **Switching Model Simulations:** This mode simulates the power system in a fixed time-step scale, capturing fast transients associated with events such as faults and switching disturbances (including inverter/converter PE switches). This mode is efficient to study power system transients in short simulations (e.g., order of few seconds). This type of simulations represents EMT type of simulations with switching models, for example, in Matlab/Simulink software platform.
  - b. **Average Model Simulations:** This mode utilizes variable time-step simulations and can also capture slower phenomena in the system, particularly voltage fluctuations or voltage level violations and instability, generation or load unbalance and cascading outages.

This mode of simulation represents the EMT type of simulations with average models, for example, in Matlab/Simulink platform (Cui et al., 2022),(Vinícius A Lacerda, Prieto Araujo, Cheah-Mañe, & Gomis-Bellmunt, n.d.). This mode is efficient for short- to medium-term simulations, typically in the order of a few seconds to minutes.

2. Long-term simulations related to steady-state fluctuations: This mode of simulations helps in capturing slowly evolving scenarios with a slow motion of system variables, where differential equations are replaced by algebraic equations in the power system models. This model helps in scenarios such as studying power imbalances occurring due increasing loads and for aids in long duration simulation studies. This mode of simulations is represented by a phasor type simulation environment, for example, in the Matlab/Simulink platform (“Introducing the Phasor Simulation Method - MATLAB & Simulink - MathWorks Nordic,” n.d.; Vinícius A Lacerda et al., n.d.). This mode is efficient for long-term simulations, typically in the order of hours to days.

To validate the Li-ion BESS controller design and their coordination with other PE converter controls and various other grid-side controllers in the EMS, an extensive simulation-based platform needs to be developed to conduct studies with different timescales and durations. The designed Li-ion BESS controllers’ effectiveness must be studied and analyzed in all time ranges from the short-term to long-term.

### 2.2.3 Aging-aware Li-ion BESS control design

Li-ion BESSs are commercially available for large-scale grid applications with the largest power ratings in the range of hundreds of MWs. The power and energy density, lower self-discharge, slow aging rate, improved safety, and high modularity in their construction are some of the reasons underlying the adoption of Li-ion batteries for grid applications (Choi et al., 2021b). However, Li-ion battery aging is an irreversible process that leads to permanent damages, which can be considered as changes in its ability in terms of reduced capacity and increased resistances leading to reduced current dispatches (de Hoog et al., 2017; J. Wang et al., 2014). In addition, the aging characteristics of Li-ion BESS are highly nonlinear and are also affected by their operating conditions (Schuster et al., 2015).

In the literature, most studies related to battery modeling and control concentrate on long-term optimization with limited discussion about aging effects of Li-ion

BESS (Abogaleela & Kopsidas, 2019; Jin, 2022; Kirli & Kiprakis, 2020; Lee, Kim, & Kim, 2021; K. Liu et al., 2022; Zhang et al., 2022a). In addition, literature focusing on real-time design of BESSs' (e.g. Li-ion BESS) secondary control has not paid attention to their aging characteristics (Allahham, Greenwood, Patsios, & Taylor, 2022; Ryan, Razzaghi, Torresan, Karimi, & Bahrani, 2021; Tian, Fang, & Wang, 2021; Zhao, Lorenz, & Jahns, 2018). While designing controllers for Li-ion BESS, for grid application, particularly in studies involving long-term analysis (e.g., participation to frequency control markets), it is necessary to make sure that the battery system does not charge or discharge with a power value that is more than the value allowed by battery characteristics (including aging effects). Therefore, it is important to include the threshold values of the charge/discharge power (peak power capability) of Li-ion BESS in its control loop. Failure to do so might accelerate the overall aging process and may lead to fatality of BESS due to internal short circuits, especially when the expected peak power can no longer be offered by the Li-ion BESSs, which shall happen particularly when the battery is nearing its end of life.

#### 2.2.4 Aging aware techno-economic studies of Li-ion BESSs

Recent studies have proposed the utilization of BESS for frequency control service provision since they are capable of responding to frequency changes very fast due to their controllability and flexibility features (Trahey et al., 2020; Wali et al., 2022). However, the participation of BESS in providing frequency services should be profitable for its owner. Thus, a thorough techno-economic study needs to be conducted that includes battery aging costs for Li-ion BESS.

Most available literature does not consider the battery aging effects as part of the techno-economic analysis (Feng et al., 2022; Meschede, Schlachter, Diekmann, Hanke, & von Maydell, 2022; Rancilio et al., 2020; Shafique, Tjernberg, Archer, & Wingstedt, 2021). Few studies consider battery aging as an affecting parameter in cost-based optimization studies. For example, Padmanabhan, Ahmed, & Bhattacharya (2020) developed a novel model for a Li-ion BESS operational cost that estimates the BESS degradation cost according to its discharge rate as well as the depth of discharge. They then proposed a bidding strategy for the BESS to participate simultaneously in energy and spinning reserve capacity markets. However, the paper disregards the responses of BESS to real-time frequency changes and its effects on the operational costs of BESS. Techno-economic analyses on the role of BESS SOC in the EMS of a microgrid has been studied (Sedighzadeh, Esmaili, Jamshidi, & Ghaderi, 2019). The microgrid takes part in energy and reserve markets. The work neglected the effects of BESS cycling aging

on its operations. Iurilli et al. (2019) simulated the behaviour of Li-ion BESS and studied how the battery provides primary control reserve. The controller proposed in Iurilli et al. (2019) received frequency fluctuations and battery SOC as inputs and then returned the power setpoint for the battery along with a simplified inverter and battery model. The authors of Iurilli et al. (2019) also conducted some economic analyses of the BESS. The controller did not work in solving optimization problems and therefore it did not guarantee the most economical set-points.

Therefore, research and development work that can overcome the challenges mentioned above is important to understand the effects of battery aging on the actual profitability of the battery.

## 2.3 BESS Standards and Grid Codes

BESS are becoming an indispensable part of modern power systems, where they find place in keeping the grid stable by providing various ancillary services, increasing grid resilience during grid outages and improving the footprint of RES penetration in the power grids. However, it is important to guarantee its safe use for both, the power grid and the BESSs, which makes it necessary to standardize its utilization with grid codes. Therefore, grid codes similar to that of inverter-based RES technologies are required for BESS installation, including battery safety aspects in their operation (Briceno- & Macdonald, 2022; Gokhale-Welch & Stout, 2019).

As for any other DER related grid codes (“CEI - 0-21 - Reference technical rules for the connection of active and passive users to the LV electrical Utilities | Engineering360,” n.d.; “Home,” n.d.; “IEEE SA - IEEE 1547-2018,” n.d.), BESS grid codes define the following features of operation:

- Ability of the BESS to regulate voltage at the bus which it is connected to the power system;
- Provision of reactive power in support of grid voltage;
- Possibility of active-power curtailment in case of a nonreceptive grid;
- Low- or high-voltage ride-through requirements;
- Low or high frequency ride-through requirements;
- Power system stabilization functions such as damping power oscillations etc.

Grid codes for the operation of BESS in the Finnish context have been explained in further sections, along with introducing other grid codes world over.

### 2.3.1 Finnish BESS Grid Code - SJV2019

Fingrid, the Finnish TSO, has proposed grid code, SJV2019 (Fingrid, 2020), taking into account the shared goals of the European grid connection network. The SJV2019 grid-code specifications are particularly for converter-connected ESSs integrated to the power grid and provide system-wide services. This grid code provides outlines on the utilization of grid-connected ESSs for

1. Withstanding the voltage and frequency fluctuations occurring the power system;
2. Supporting power system operation during disturbances and improving system reliability;
3. Ensuring no adverse events while the energy storage system has been connected to the grid.

According to SJV2019 guidelines, the grid ESS are classified into four categories (Types A–D) based on their capacity of power allocation as shown in Table 2. Some of the key points of the grid codes are as follows:

1. The inverter-based grid ESSs should be connected as a new separate connection or in an existing connection in the power system.
2. The grid-code specifications for these ESS are determined according to Table 1, and as a rule, they are not dependent on the rated capacities or specifications of other production or demand systems connected to the same connection point.
3. If the ESS owner wants to integrate the resources of the ESS into the control system of a power plant or a demand system, the specifications can be reviewed as a whole. The specifications are based on the rated capacity of the integrated system and the connection point's voltage level. Fingrid shall provide detailed specifications in each case upon the connecting party's request.

SJV 2019 provides clear indications regarding the use of different categories of grid ESS for active-power frequency control by means of defining the relevant droop settings. The existing droop settings dictated by SJV2019 have been explained in

detail in Chapter 5, which typically details the frequency of the grid stable defined limits of operation.

Grid codes are region specific and defined particularly by the utility companies for adoption. Other grid codes pertaining to the use of energy storage systems are listed in Table 3 that define specifics of operation of ESS for grid applications (“CEI - 0-21 - Reference technical rules for the connection of active and passive users to the LV electrical Utilities | Engineering360,” n.d.; “Home,” n.d.; “IEEE SA - IEEE 1547-2018,” n.d.).

**Table 2.** Classification of grid energy storage based on capacity

Type category	Connection point's voltage level	Term/condition	Grid energy storage system's rated capacity in production mode $P_{max,p}$
Type A	The connection point's voltage level is less than 110 kV <sup>1</sup>	and *	The grid energy storage system's rated capacity in production mode is at least 0.8 kW but less than 1 MW. ( $0.8 \text{ kW} \leq P_{max,p} < 1 \text{ MW}$ )
Type B	The connection point's voltage level is less than 110 kV <sup>1</sup>	and *	The grid energy storage system's rated capacity in production mode is at least 1 MW but less than 10 MW. ( $1 \text{ MW} \leq P_{max,p} < 10 \text{ MW}$ )
Type C	The connection point's voltage level is less than 110 kV <sup>1</sup>	and *	The grid energy storage system's rated capacity in production mode is at least 10 MW but less than 30 MW. ( $10 \text{ MW} \leq P_{max,p} < 30 \text{ MW}$ )
Type D	The connection point's voltage level is at least than 110 kV <sup>1</sup>	or +	The grid energy storage system's rated capacity in production mode is at least 30 MW. ( $P_{max,p} \geq 30 \text{ MW}$ )

**Table 3.** Other grid codes related to energy storage system

IEEE Standard 2030 series	USA Energy Storage System safety, standards and codes	IEC61850 standard and related developments
1. IEEE Standard 2030™ - Guide for smart grid functional performance, smart grid interoperability reference model	1. Guide for safety in utility integration of ESSs	1. IEC61859 - Communications for power system automation and collection of international standards describing devices in electrical substations and information exchange between them
2. IEEE Standard 2030.3™ - IEEE standard test procedures for electric	2. Associated DER Standards - IEEE Standard 1547™	2. IEC61850.7-420 provides object models for

<b>IEEE Standard 2030 series</b>	<b>USA Energy Storage System safety, standards and codes</b>	<b>IEC61850 standard and related developments</b>
energy storage equipment and systems for electric power system applications		ESS as a DER through IEC TC57 WG17
2. IEEE Standard 2030.2™ - IEEE guide for interoperability of energy storage systems integrated with electric power infrastructure		

### 3 LI-ION BESS MODELING AND CONTROL FOR SHORT-TERM ANM SIMULATIONS

EMTs are short-term changes in the power systems caused by disturbances, for instance, harmonics induced by PEs switching, load variations, power generation variation (high levels in RESs), or transients introduced in the power system during faults (Aggarwal, 2003). By utilization of EMT simulation methods, it is possible to study network dynamics (both harmonics and DC offset in currents and voltages), fast controls of inverters and interactions among them, network components and other adjacent control/management systems (“Knowledge Base | PSCAD,” n.d.; Sano, Yonezawa, & Noda, 2019). Therefore, the controllers designed for ANM including the operations of FERs such as Li-ion BESS and RES-based WTGs and solar power generation must be validated in suitable EMT simulation environments.

Li-ion BESS play a major role as FER in ANM schemes by bridging gaps between non-simultaneous RES-based power generation and demand in the MV and LV distribution networks. The ability of the Li-ion BESS to provide both active power and reactive power flexibility services makes it a potential multipurpose FER for ANM needs (Akagi et al., 2020; Das, Bass, Kothapalli, Mahmoud, & Habibi, 2018b; Saboori, Hemmati, Ghiasi, & Dehghan, 2017). However, to implement ANM schemes effectively, integration and control design of highly flexible Li-ion BESS plays an important role. Consideration of highly nonlinear performance characteristics of Li-ion BESS, affected by multiple factors such as temperature, SOC, C-rate and aging, make control design even more challenging. Therefore, control design, development, and validation of Li-ion BESS controllers and their coordinated control with other FER controllers in a power system by means of EMT simulations are very important.

In studies concerning Li-ion BESS utilization for distribution network flexibility service provision through ANM, it is important to model the nonlinear performance characteristics of the battery accurately. The overall requirements for these studies in EMT simulation environments are

1. Development of an accurate Li-ion BESS SOEC performance model
2. Development of an Li-ion BESS integration methodology (i.e., design and development of controllers for the PE interfaces used for the grid integration purposes)
3. Development of ANM architecture for managing available flexibilities in the power system



4. EMS design (i.e., development of coordinated control of grid-side controllers with DER controllers)

Chapter 3 presents an overview from Publications P2–P5 of the thesis and highlights the following issues:

1. How to model Li-ion BESS for grid integration in EMT simulation studies?
2. How to safely integrate Li-ion BESS in power grids to provide for various grid support application and voltage/frequency control?
3. How are Li-ion BESS managed in the SOC-limited control scheme?
4. How should Li-ion BESS and their controllers be designed in real-time power system dynamic simulations with variable power generation and loads?

### 3.1 Li-ion BESS modeling

Typically, Li-ion BESSs, when connected in power systems, are modeled as an ideal DC source (Chauhan, Reddy, Bhandari, & Panda, 2019) or by using empirical/math-based models (Castaneda et al., 2019)-(Tariq, Maswood, Gajanayake, & Gupta, 2018). Another common technique used is the kinetic battery model (KBM) (Manwell & McGowan, 1993), which was first used to represent lead-acid batteries. Most of the recent literature uses modified KBMs (Bako, Tankari, Lefebvre, & Maiga, 2019; Rodrigues et al., 2018; T. Wang & Cassandras, 2013) for stationary grid applications of Li-ion BESS. KBMs perform well at certain defined conditions but cannot address the nonlinear performance characteristics of Li-ion batteries, that are influenced by various SOCs, temperatures, current rates, and age. Most accurate battery models are provided by physics-based models solved by finite element model-based simulation methods (El Sayed, Ahmed, Habibi, Jimi Tjong, & Arasaratnam, 2014). However, they require enormous computing power in simulations, making it practically impossible to use them for grid integration studies. In general, different Li-ion BESS modeling approaches have varying ranges of computational complexity and accuracy with mathematical models providing least of both. ECM represents the operation of a battery cell in terms of variable resistors and capacitors, whose circuit parameters are determined by means of characterization tests (Nejad, Gladwin, & Stone, 2016). ECMs are considered a trade-off between mathematical and electrochemical models due to their performance metrics.

ECMs provide good accuracy and low computational effort, making them suitable for studies related to stationary grid applications of Li-ion BESS. The SOEC technique, based on Thevenin's circuit model, represents the Li-ion battery in form of resistances and capacitances [6], thereby portraying battery operation comprising of processes such as diffusion, solid electrolyte interface, and charge transfer (Parthasarathy, Hafezi, & Laaksonen, 2020). However, ECM models have to be developed in detail by testing and characterizing the battery cells at different operating conditions.

Fig. 10 shows the proposed dynamic ECM model, i.e., the SOEC model, for Li-ion battery cell (NMC type of cell). The open circuit voltage (OCV) is modeled as an ideal voltage source. The internal resistance is modeled as  $R_i$ . Two RC combinations are suggested for the Li-ion battery cell, so the dynamic behaviour is modeled as  $R_1$ ,  $C_1$ ,  $R_2$  and  $C_2$ . The hysteresis effect and polarization effect in the Li-ion cells can be simulated accurately enough with two RC combinations. Furthermore, the model structure is simpler than that with more RC combinations. As the actual behaviour of the NMC cells is significantly nonlinear, the parameters vary with SOC, temperature, age, and history (number and depth of cycle) of the cell. The next step is to calculate the values of SOEC parameters ( $OCV$ ,  $R_i$ ,  $R_1$ ,  $C_1$ ,  $R_2$ , and  $C_2$ ,) that are variable in nature and are affected by various parameters as shown in Fig. 10. The parametrization process has been developed with the help of the HPPC method, explained in the following section.

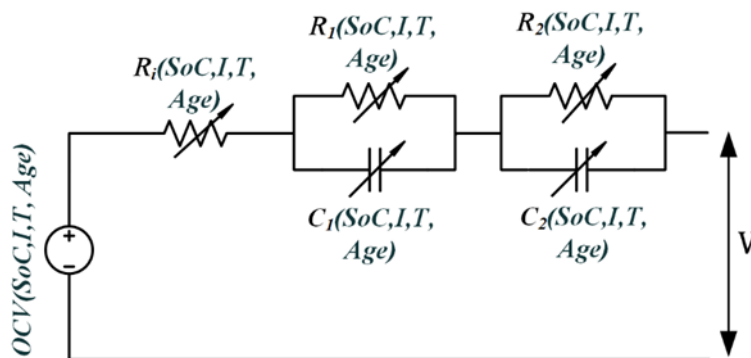
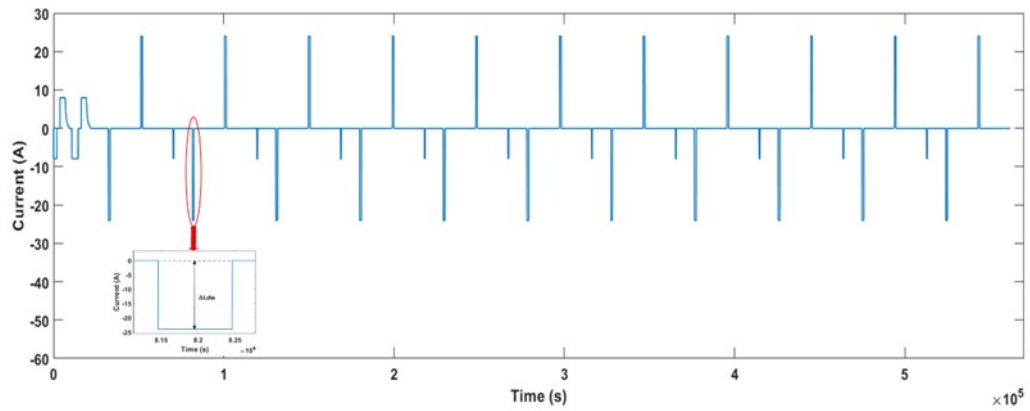


**Figure 10.** SOEC battery cell model (NMC type of cell)

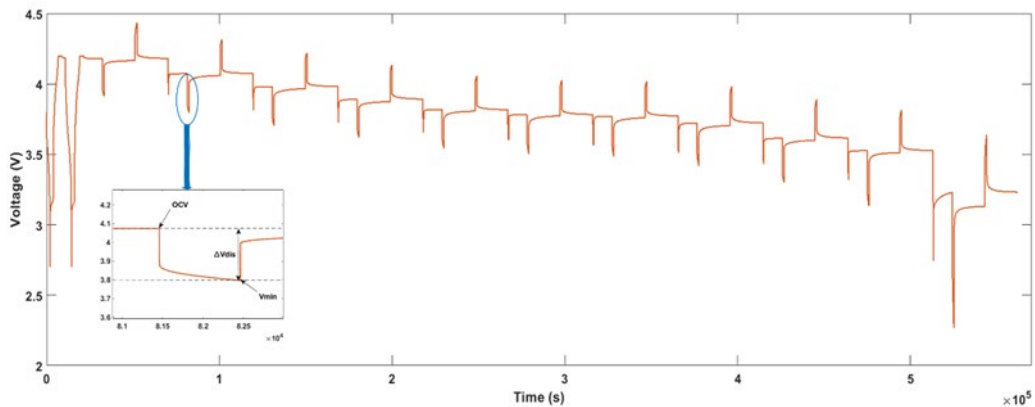
### 3.1.1 SOEC-based battery model parameterization process

Fig. 11 shows the HPPC current profile used to characterize the NMC battery cells. Its corresponding voltage response is shown in Fig. 12. Equivalent-circuit parameters are calculated from the voltage response of the high current discharge pulse at every defined SOC and temperature. Details of the HPPC pulse

characteristics are explained in Arunachala, Parthasarathy, Jossen, & Garche (2016).



**Figure 11.** HPPC current pulse profile



**Figure 12.** HPPC pulse voltage response

OCV is the voltage observed between the battery cell terminals at no-load conditions in the equilibrium/balanced state. The OCV has been modeled as an ideal voltage source, where its values are variable at different SOCs and temperatures. The OCV is captured from the HPPC test profile at the end of each rest phase after the high current charge/discharge pulse, i.e., when the voltage has attained a steady-state value. Other parameters of the SOEC model are evaluated by analyzing the voltage response of the HPPC pulse discharge and charge. A closer view of the voltage response from the HPPC profile at discharge pulse is applied.  $R_i$  is calculated as a function of  $\Delta VO$  using Eq. (1), which is contributed by resistance of at 80% SOC and 25 °C (for that instant) can be seen in the same Fig. 11. It can be also observed that there are time varying voltages ( $\Delta V1$  and  $\Delta V2$ ). Therefore, the equivalent circuit parallel branch resistances,  $R_1$  and  $R_2$ , are

calculated as a function of  $\Delta V_1$  and  $\Delta V_2$ , respectively, by Eqs. (2) and (3). The two RC branches are divided based on short ( $t_1$ ) and long ( $t_2$ ) time transients, which is helpful in calculating  $C_1$  and  $C_2$  using Eqs. (4) and (5) respectively. Equation (6) represents the terminal voltage of the battery cell ( $V_T$ ), which is a function of all the equivalent-circuit parameters.

The HPPC parameterization process must be repeated at every step of temperature, current, and aging intervals to obtain the variable values of SOEC parameters. Hence, a Matlab script was developed to extract the measurements of HPPC tests, particularly the voltage response of high current charge/discharge pulses at every step of SOC and repeated for all the HPPC curves (i.e., 15°C – 45°C experiments, 100%–0% SOC intervals and 0–1600 cycles of charge and discharge). To obtain parameters for the two parallel RC branches in the SOEC model (Fig. 10), the voltage response to the high current pulse was divided into two more time points, where  $t_1$  represents the short-transient response and  $t_2$  represents the long-transient response. Therefore, knowing the values of  $t_1$  and  $t_2$ , the SOEC parameters can be calculated using Eqs. (1)–(5) to get the initial estimates. Initially calculated values at different SOCs and temperatures were then normalized using *lsqfit* in Matlab, which provides the least squares fitting methodology for nonlinear data.

The overall performance of the SOEC battery model is presented in Fig. 13 by comparing experimental and simulated voltage curves using the HPPC load current profile to an HPPC pulse at 25 °C at 0 cycles of charge and discharge. The key observation from this result is that the SOEC model captures the dynamic nonlinear voltage response of the cell very well with an error of almost 0% during the steady-state charge/discharge operations and approximately less than 2% error for the high current pulse profiles from 10% SOC to 100% SOC.

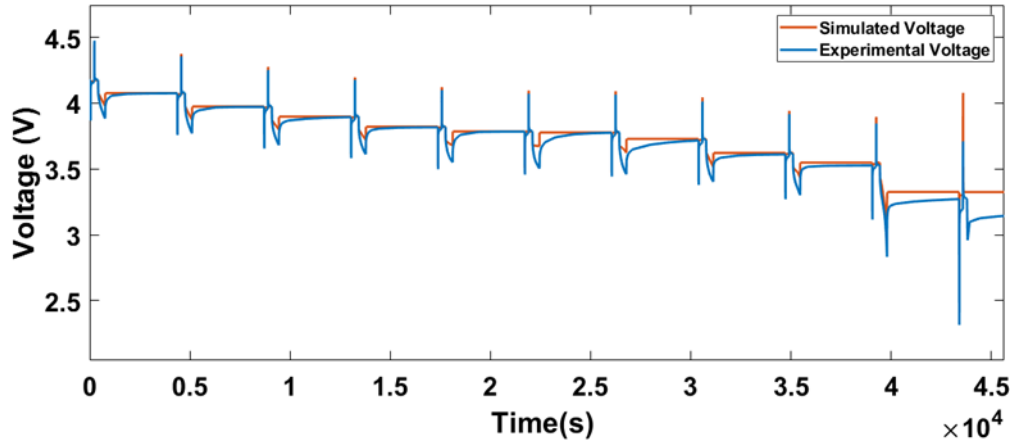


**Figure 13.** Simulation model performance with respect to experimental characteristics

$$R_i = \frac{V_0 - V_1}{I} \quad (1)$$

$$R_1 = \frac{V_1 - V_2}{I} \quad (2)$$

$$R_2 = \frac{V_2 - V_3}{I} \quad (3)$$

$$t_1 = R_1 C_1 \quad (4)$$

$$t_2 = R_2 C_2 \quad (5)$$

$$V_T(t) = V_{OCV} + I(t)R_i + I(t)R_1 \left(1 - e^{-\frac{t}{t_1}}\right) + I(t)R_2 \left(1 - e^{-\frac{t}{t_2}}\right) \quad (6)$$

A battery cell model was developed in the Simscape platform of Matlab/Simulink software. The cell model was scaled up to form a battery pack model to study it for various purposes in smart grid applications. In a battery pack, multiple cells are connected in series to achieve the required voltage levels and multiple strings of serially connected cells have to be added in parallel to Boost the current level. Fig. 14 provides a description of the battery pack model.  $N_S$  represents the series cell elements and  $N_P$  defines the number of parallel strings for a required battery pack. The interconnecting cable resistances are ignored, making it a model with a comparatively fast simulation response. Values of  $N_S$  and  $N_P$  define the voltage and current characteristics of the desired battery packs, respectively. The developed battery pack model was then integrated into the DC/DC Buck–Boost converter

system, which was developed in the SimPowerSystems software platform of Matlab.

### 3.2 Control design of grid-connected Li-ion BESS

PE-based inverters and converters and their control structures are key enabling technologies underlying BESS' growth, utilization, and grid integration. Simultaneously, the PE inverter/converter controls BESS, operation mode, active ( $P$ ), and reactive ( $Q$ ) power flow as well as the current and voltage variations across the battery pack, which affect the performance, health, and lifetime of BESS (Wang et al., 2016). Two-level inverters with DC/DC- and AC/DC-converters are widely used for different applications, including Li-ion BESS integration (with centralized Li-ion BESS at DC bus), due to the maturity of the technology and availability of the commercial solutions. The Li-ion BESS's PE interface also in this thesis includes a DC/DC-converter and an AC/DC-inverter/converter.

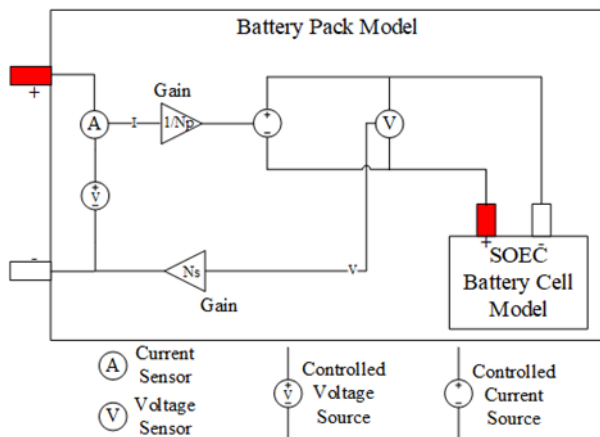


**Figure 14.** Battery pack modeling

A DC/DC Buck–Boost converter can stabilize fluctuating/changing battery voltages. It can also control the charging and discharging of the battery within its safe operating window. The DC–DC conversion stage eliminates low-order current harmonics flowing in the battery since the DC–DC converter isolates the BESS from the inverter DC bus. With the DC–DC converter, BESS can be designed to lower voltage levels (less cells in series). Moreover, it can be used as a protective and current limiting device, which will increase the safety and controllability of the system. Therefore, bidirectional DC/DC Buck–Boost converters have been used in the integration design.

Bidirectional AC/DC-inverters are a necessary part of the PE system in the Li-ion BESS grid integration applications. The main task is to convert the DC voltage to

AC voltage (and vice-versa) and guarantee also, for example, the fulfilment of standard and grid-code requirements (“IEEE 1547-2018 - IEEE Standard for Interconnection and Interoperability of Distributed Energy Resources with Associated Electric Power Systems Interfaces,” n.d.). The AC/DC-converter will be connected to the high-voltage side of the DC/DC-converter, which converts it into 3-phase,  $400 V_{RMS}$  while discharging Li-ion BESS power. Furthermore, a 3-phase LV/LV or MV/LV coupling transformer is usually used to connect the BESS in the power system (Fig. 15). The transformer based solution is favored so far (G. Wang et al., 2016), and for large-scale BESS systems, it could be the preferred solution providing galvanic isolation between the grid and energy storage system.

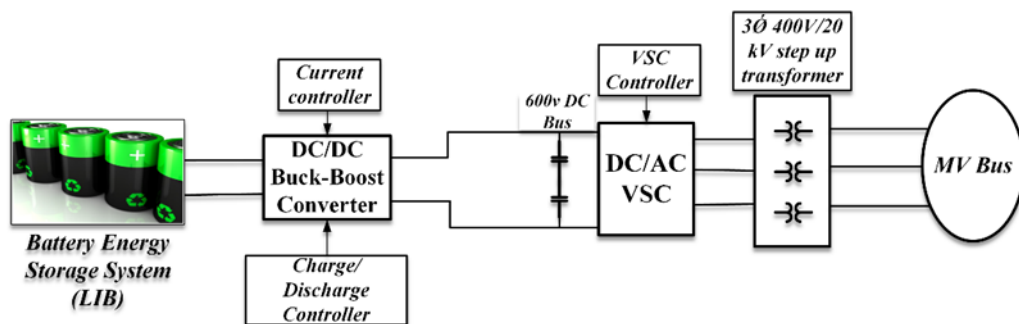


**Figure 15.** Li-ion BESS grid integration modeling

Deriving the accurate design of the power converter controllers, i.e., AC/DC voltage source converter (VSC) and DC/DC BESS Buck–Boost controllers for effective operation, is explained in Sections 3.2.1 and 3.2.2. The overall BESS integration diagram is presented in Fig. 15. Li-ion BESS dynamic characteristics were modeled accurately by considering the influence of parameters such as temperature, DOD, and C-rate (charge/discharge) by means of the SOEC cell model, as explained previously in Section 3.1. This allows the provision of accurate battery parameters such as voltage, power, energy, and SOC, which will be utilized in control design and development of Li-ion BESS for ANM applications.

### 3.2.1 DC/DC bidirectional converter control

A single IGBT with antiparallel diode leg with a switching inductance has been implemented as bidirectional DC/DC Buck–Boost converter for BESS system (D’Antona, Faranda, Hafezi, & Bugliesi, 2016). The average model converter is designed to charge and discharge the batteries through/to the VSC DC bus. A simple PI-controller is designed to control the Buck–Boost converter. Fig. 16 shows the DC/DC Buck–Boost converter current control loop. The converter can work in either the Buck- or Boost-mode. When it works as a Buck converter, the

Boost IGBT is blocked and vice-versa. The sign ( $\pm$ ) of the  $I_{dc,ref}$  defines in which mode it should work. The DC bus is controlled by the VSC d-component control loop so the sign of the PI-controller output defines the active-power flow direction; therefore, there is no need to add an additional voltage control loop in Boost mode (discharging the BESS) to control the voltage level. In both control modes, the PI-controller output provides the duty cycle to the DC/DC Buck or Boost converter.

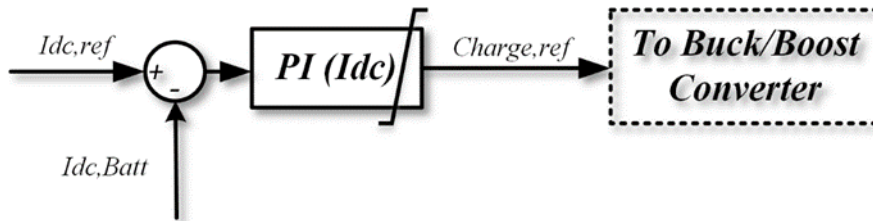


**Figure 16.** Current Controller

In this case, discharge mode works in the range between 20% and 90% of battery SOC, as per the current requirements commanded based on the current required by the converter. For the charging mode, the maximum State of Charge ( $SOC_{Max}$ ) is maintained at 90%, which is typically achieved by constant current charging alone, eliminating the constant voltage (CV) requirements. However, during Li-ion BESS use for grid applications, the CV mode of charging will be barely achieved due system requirements. The battery charge and discharge model are based on the SOC of the system and load requirements. The charge controller triggers the Buck mode of the converter to be switched ON when the SOC goes below 20% and turns it OFF when it reaches a maximum of 90% to maintain battery operation in safe limits.  $I_{dc,ref}$  is communicated to the BESS Buck–Boost converter controller by the upper-level control system. Based on the sign of this reference current, the direction of current flow of the Buck–Boost converter and its controller behaviour is managed.

### 3.2.2 AC/DC voltage source converter control

Fig. 17 describes the AC/DC VSC control scheme i.e. voltage oriented control (VOC) technique (Blaabjerg, Teodorescu, Liserre, & Timbus, 2006). The VOC strategy guarantees fast transient response and high static performance through the current control loop.  $V_{abc}$  and  $I_{abc}$  are transformed to  $V_{dq}$  and  $I_{dq}$  frames, respectively.  $I_{d,ref}$  is obtained by the PI-controller for  $V_{dc}$  and the  $I_{q,ref}$  reference is provided by the outer control loop, input from some other management systems, e.g., ANM that provides the demand of battery power requirements. The active-power output of the converter is controlled by  $I_{d,ref}$ , and  $I_{q,ref}$  controls the



reactive power output. A cross-coupling exists between d- and q-axis components, which affect the dynamic performance of the controller. The  $V_d$  feedforward signal is added to the d-component loop. This feedforward signal is crucial for the d-component control loop. The feedforward signal can be added to the q-component control loop as well but it is not essential for this application. Both  $I_{d,ref}$  and  $I_{q,ref}$  is limited to  $\pm 1.5$  p.u., so the VSC should be designed to provide 150% nominal power for a certain time period during transients. The overall Li-ion BESS integration design for studies related to EMT simulations is explained in detail in Publications P2 and P3 of this dissertation.

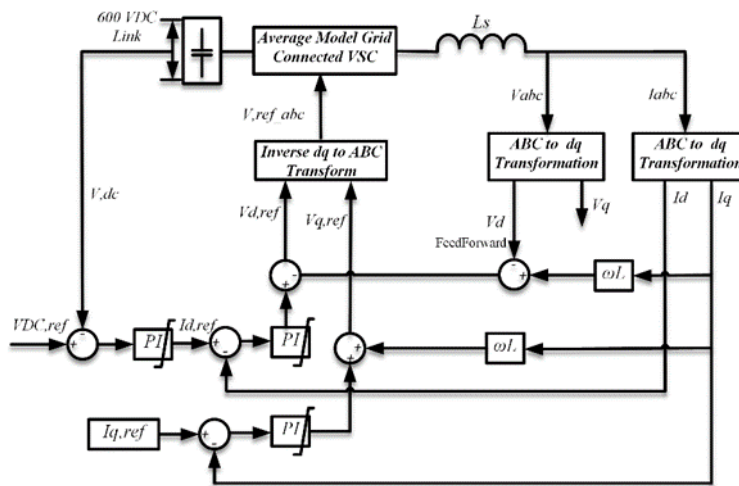


**Figure 17.** VSC controller design

### 3.3 Case Studies – Coordinated control of Li-ion BESS in ANM applications

The robustness of the designed controllers was tested by means of EMT simulations. For this purpose, SSG, a real-life smart grid existing in Finland (see Chapter 1.1.1), was utilized. The SSG has been modified for study purposes to include a Li-ion BESS, which is currently not existing in the grid. The network has been modeled as accurately as possible with the Li-ion BESS integration methodology derived from previous sections.

The cases studied were

1. SSG backup feeding (Publication P4)
2. SSG – Li-ion BESS fast charging (Publication P5)

### 3.3.1 Case 1 – SSG backup feeding

SSG has been reliable in operation in terms of MV voltage regulation and its power quality during the normal mode of operation, i.e., when the grid power is being fed from the Sundom HV/MV substation. However, during Sundom HV/MV substation maintenance operation, the grid power will be fed from the Kuutamolahti HV/MV substation (as in Fig. 18) which is about 5.2 km away, adding on to the overall  $Z_{Grid}$  values (Laaksonen, Parthasarathy, Khajeh, & Shafie-Khah, 2021a). Therefore, for example, rapid WT active-power output variations can be also seen as fluctuating voltage due to a weaker connection point of WT during backup feeding from Kuutamolahti substation.

In this use case, the effect of load variation during lower WT generation during the backup feeding case was modeled. The focus was the management of voltage fluctuations and reactive power flow (within RPW) by the ANM scheme, as explained in the following section. The effectiveness of the developed ANM scheme and the interaction between EMS and DER controllers during this condition has been studied in detail, considering the Li-ion BESS integration aspects. The initial battery SOC was maintained at about 50%, where it could accommodate simultaneous charge/discharge operations. The characteristics of new cells, i.e., unaged cells, are considered for the case study. Simulations were performed for a time period (TS) of 120 seconds.

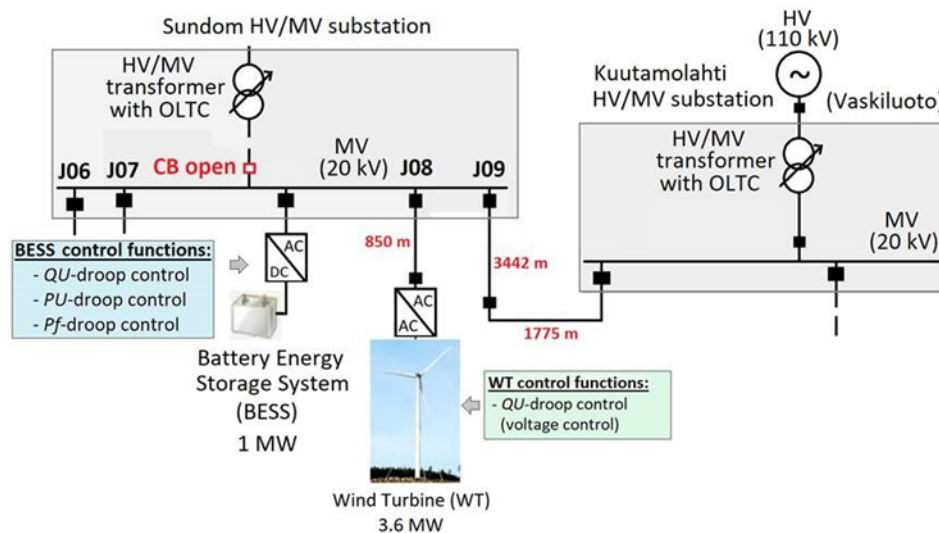


**Figure 18.** SSG one-line diagram during backup feeding case

### 3.3.1.1 ANM architecture with EMS (Case 1)

ANM provides a way to manage the available flexibilities from the inverter-based energy sources in the distribution system in a coordinated manner. The FERs available in SSG are WTG and Li-ion BESS. In addition, the OLTC of HV/MV transformer can be controlled to manage the distribution network voltage level. Table 5 presents details on the characteristics of Li-ion BESS which is integrated to the SSG in the simulated backup feeding scenario. The overall Li-ion BESS modeling and integration methods are as explained in previous sections.

**Table 4.** Li-ion BESS characteristics

Technical Specifications	Values
Nominal DC Voltage	311 V
Peak Voltage	353 V
Cut-off Voltage	235 V
Discharge Power (1C)	1 MW
Nominal Discharge current (1C)	2832 A
Peak Discharge current (3C)	8496 A
Inverter Size	2.5 MVA

The Li-ion BESS that is placed in the MV bus at the HV/MV substation (Fig. 18) will be able to complement the WTG in providing various flexibility services. Li-ion BESS can, for example, be used for power smoothing and it can complement the stochastic nature of wind power generation, i.e., store excess wind power generation and discharge during reduced wind power generation through active-power control and secondarily provide other flexibility/technical ancillary services (e.g., through reactive power control). Li-ion BESS have a multiuse capability based on their characteristics, and the ANM scheme developed in Publication P4 utilizes this capability. The technical ancillary/flexibility services in the ANM scheme are designed based on the available FERs in the MV distribution system. In this case, flexibility services include

1. Managing voltage levels in the MV distribution system (at all the MV feeders) by FERs by controlling both the active and reactive power flows in the power system
2. Maintaining the RPW defined by the Finnish TSO, Fingrid, (*SUPPLY OF REACTIVE POWER AND MAINTENANCE OF REACTIVE POWER RESERVES Guideline*, n.d.) at the HV side of the SSG defined in Section 4.1. Reactive power flow will be controlled from the available FERs to avoid violation of the grid code target limits, thereby supporting DSO to avoid paying the penalty fees to the TSO.

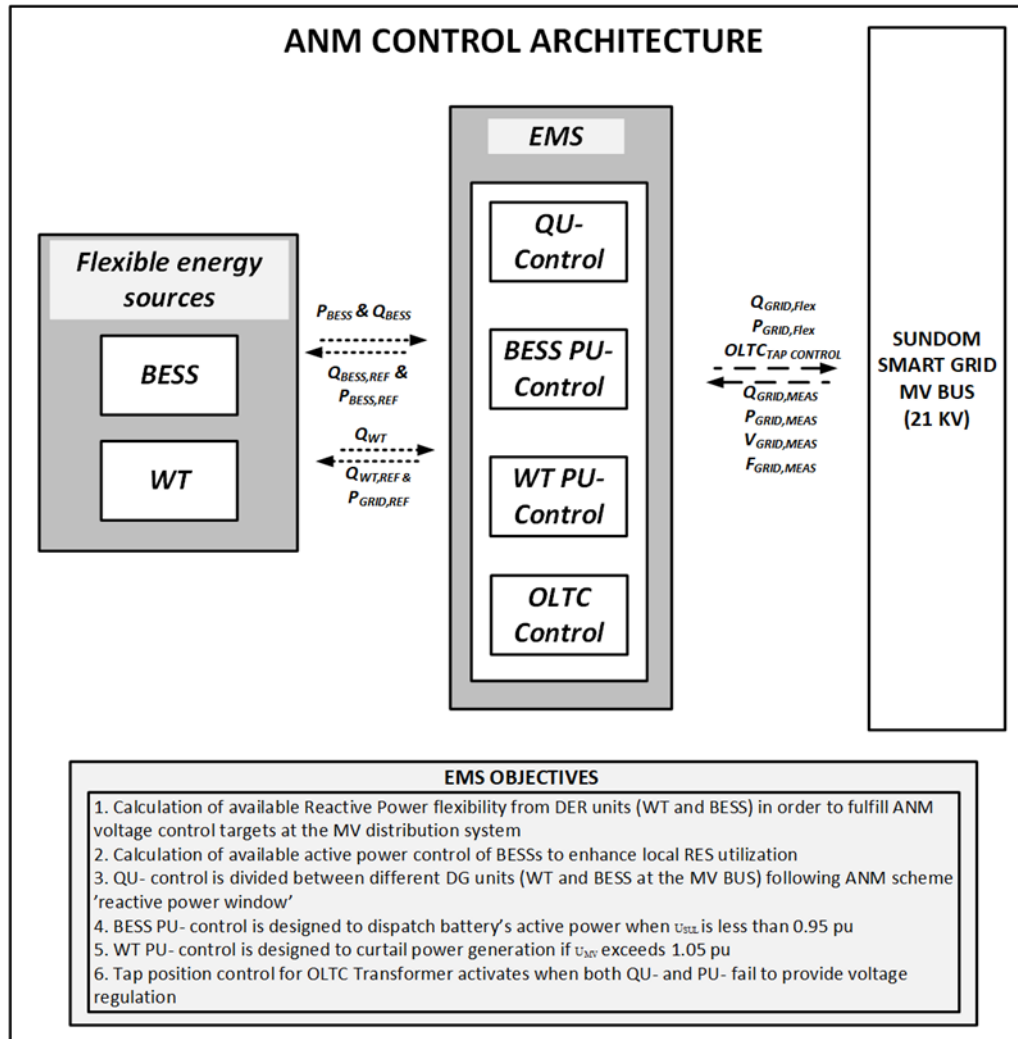


**Figure 19.** Proposed ANM architecture for SSG

The ANM control architecture for SSG is presented in Fig. 19. It describes the management of FERs, i.e., BESS and WTG with the help of EMS. The most important layer of operation in the ANM scheme is the EMS, which is associated with the operation of active and reactive power flows between the MV grid and FERs, in this case Li-ion BESS and WT generator. The objective of the EMS is to maintain  $\underline{U}_{grid,ref}$  within the limits specified by standards and grid codes by controlling the active and reactive power flows at the DSO/TSO interface, especially focusing on the reactive power flow which has been maintained within the limits defined by reactive power window (RPW), specified by the Finnish TSO, Fingrid.

Measured MV grid data such as active power ( $P_{grid,meas}$ ), reactive power ( $Q_{grid,meas}$ ), voltages ( $U_{grid,meas}$ ), and frequency ( $f_{grid,meas}$ ) are given as input (Fig. 19) to the EMS layer. The primary role of the EMS is to constantly monitor the reference

parameters in the MV distribution system. If any of the parameters, i.e.,  $Q_{\text{grid,ref}}$  and  $U_{\text{grid,ref}}$ , are not within the defined threshold values, EMS's secondary functionality of managing the available flexibilities in the MV power system is utilized by generating reference control signals for the various inverter-side controllers. The grid-side controllers that participate in ANM are  $QU$ -, BESS  $PU$ -, WT  $PU$ - control and OLTC-controller as shown in Fig 20. If the voltages, frequency, and reactive power flows are well within the limits defined by target setpoint values based on the applicable standard or grid code, the controllers in the EMS layer remain inactive. However, they constantly monitor the reference parameters in the MV system. In case the defined MV parameters are out of the threshold value, the ANM scheme starts actively mitigating the abnormalities by controlling the grid-side controllers.

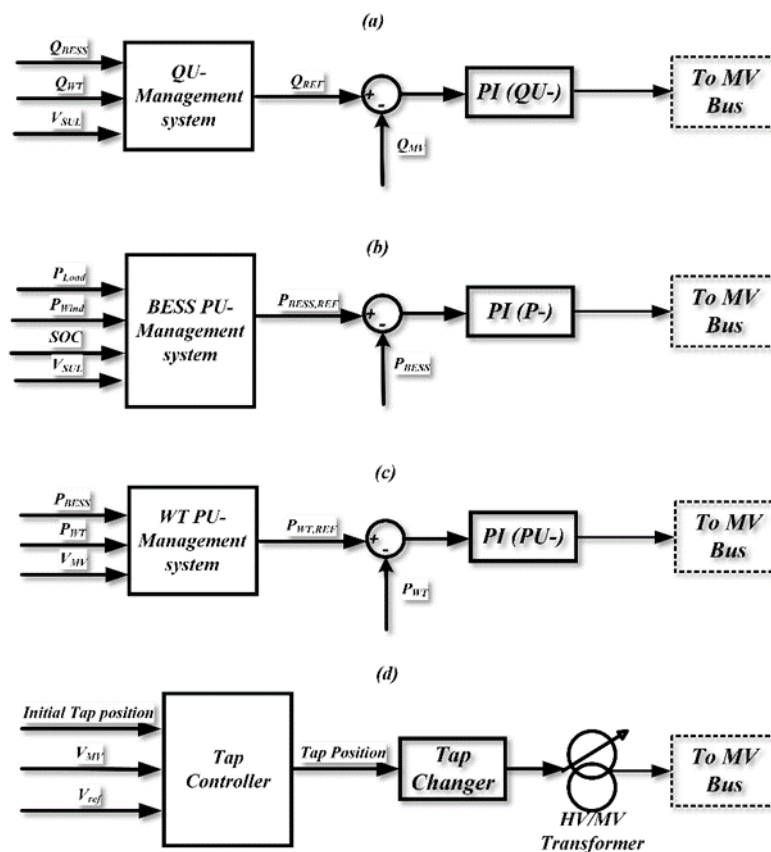


**Figure 20.** a)  $QU$ - control (b) BESS  $PU$ - control (c) WT  $PU$ - control (d) Tap change controller

The total required reactive power control is set according to the requirements of Fingrid's RPW-limits thereby defining the requirements for  $QU$ -control. The reactive power flexibility in the  $QU$ - control are provided by Li-ion BESS and WT generator, i.e.,  $Q_{\text{WIND}}$  and  $Q_{\text{BESS}}$ . If reactive power flow in this situation exceeds

RPW-limits at the TSO/DSO interface,  $Q_{\text{WIND}}$  is regulated to adjust the values as the priority. If  $Q_{\text{WIND}}$  is not sufficient to regulate RPW limits,  $Q_{\text{BESS}}$  will be used.

BESS *PU*-control is utilized to control active-power flow from the Li-ion BESS. Despite the Li-ion BESS' capability of providing both active and reactive power control, they also provide active-power flexibility in terms of both charging and discharging related services. In case the BESS is being charged, their active-power discharge control is disabled, whereas the reactive power discharge control component remains active. *PU*-control was based on the *PU*-droop whose characteristics are defined in Publication P4.

Thus, EMS provides  $Q_{\text{BESS,ref}}$  and  $P_{\text{BESS,ref}}$  to the BESS and  $Q_{\text{Wind,ref}}$  and  $P_{\text{grid,ref}}$  to the WTG. In return, based on the internal control algorithms for BESS and WT defined in the following section, BESS returns relevant  $P_{\text{BESS}}$  and  $Q_{\text{BESS}}$  back to the EMS, whereas WTG returns  $Q_{\text{WT}}$  back to the EMS. These control signals are then forwarded to the grid-side controllers which in turn inject  $Q_{\text{flex}}$  ( $Q_{\text{BESS}}$  and  $Q_{\text{Wind}}$ ) to the MV bus. Similarly, BESS *PU*- controller provides active power from the Li-ion BESS, i.e.,  $P_{\text{BESS}}$ , to regulate voltages at the MV system. The WT *PU*-controller is primarily used to curtail excess active-power generation from WT, and it was activated in this case when MV voltages go beyond the grid code specifications. The design and architecture of the individual control techniques, i.e., *QU*-, *P*-, *PU*- and OLTC- control techniques employed in the ANM management principle are explained as below. The design and development of the EMS controllers shown in Fig. 20 has been explained in detail in Publication P4.

### 3.3.1.2 Results and discussion (Case 1)

Simulation studies involved two subcases where the first subcase being ANM was not active, to record various system parameters, to understand if any ANM schemes are required in the power system, making it the base case scenario. In the second subcase proposed, the ANM scheme has been made active and its efficiency has been validated. The results are presented below.

The results presented in Publication P4 provide a summary of the simulation results and an indication on how the flexibility indices have been utilized based on the ANM objectives and the EMS set-points. The reactive power control requirement,  $Q_{\text{flex}}$ , has been provided only by  $Q_{\text{WIND}}$ , without any interference from  $Q_{\text{BESS}}$ . The results indicate that the  $Q_{\text{flex}}$ , was instrumental in keeping the reactive power flow,  $Q_{\text{MV}}$ , between the HV/MV grids within the limits specified by the RPW. With respect to the results of voltage limits at various MV feeders in the SSG, it has been established that the designed BESS *PU*- droop controller has been

phenomenal in maintaining the MV bus voltages within the values specified by grid codes. The purpose of this PU-droop control loop is to dispatch the exact amount of active power required from the Li-ion BESS, which is derived in Section 3, thereby providing optimum power without over/under-usage of the battery system.

The synergy between the Li-ion BESS converter controls and the EMS controllers (i.e., BESS *PU*- and *QU*- controllers) has been established as a part of ANM design and validated by the simulation results presented in detail in Publication 4, where the EMS controllers provided the required set-points to the individual component (Li-ion BESS and WTG) controllers. Therefore, the designed ANM scheme and its adjoining EMS controllers acted as required to provide RPW and voltage regulation.

### 3.3.2 Case 2: SSG – Li-ion BESS fast charging

Li-ion BESS act as loads when they are being charged. The charging load induces a stress on the distribution network (typical at the BESS connection point), especially when they are being charged at a higher current rate (i.e., fast charging). The effects of Li-ion BESS' charging loads on the distribution network might be severe if there is a request to fast charge batteries at an instance of lower renewable power generation at the distribution levels. The negative impact on the distribution grid in such a case can increase the overall peak load of the network, thereby leading to adverse voltage fluctuations causing harmful effects also on the distribution transformers (Khan, Ahmad, Ahmad, & Saad Alam, 2018; X. Li & Wang, 2019). Therefore, innovative grid solutions such as ANM can be utilized to mitigate such potential network issues.

The SSG was considered as the system under study, where 1 MW Li-ion BESS (Table 2) has been integrated to the MV distribution system. The Li-ion BESS integration design utilized has been explained in detail in Section 3.2. The charge/discharge power of 1C is considered to be at 1 MW.

#### 3.3.2.1 ANM architecture (Case 2)

The ANM scheme designed in this case is quite similar to that in the previous case 1, i.e., to effectively manage the available flexibilities at MV distribution grid of SSG, i.e., from the WTG reactive power ( $Q_{wind}$ ), active and reactive power of Li-ion BESS, ( $P_{BESS}$  and  $Q_{BESS}$ ), and tap positions in OLTC transformers, thereby

providing ancillary services to the system. The objectives to design the ANM architecture include

1. Managing the voltage level in the MV distribution system (at all the MV feeders) by FERs by controlling both the active and reactive power flows in the power system;
2. Maintaining the reactive power flow within the RPW limits defined by TSO Fingrid.

Therefore, the EMS for this case includes  $QU$ -control, Li-ion BESS active-power controller, and OLTC controllers. Inverter-based FERs, i.e., WTG and Li-ion BESS ( $Q_{\text{wind}}$  and  $Q_{\text{BESS}}$ ) participate in  $QU$ -control, providing the required reactive power flexibility  $Q_{\text{Flex}}$ . In this study, the ANM schemes were modeled to utilize the entire range of reactive power control possibility, due to the extremeness of the use case. Li-ion BESS active-power  $P_{\text{BESS}}$  in this case concerns only the charge power defined, i.e., 2 MW. OLTC transformer will be further activated, if  $QU$ -control alone cannot stabilize the MV distribution system voltages. The detailed design and development of all these EMS controllers are explained in Publication P5.

### 3.3.2.2 Results and discussion (Case 2)

In this use case, the Li-ion BESS is charged at a rate of 2C (two times the rated nominal current), equivalent to a 2 MW charge power, which is considered a fast charging method for a 1 MW nominal power Li-ion BESS, during low renewable energy generation. The effects of charging at 2C during low wind power generation have been observed and addressed by the ANM schemes to mitigate their detrimental effects. Two subcases are defined, where the first one shows the strain of charging power on the MV distribution network without any ANM schemes, and the second subcase shows the effect of ANM principles on the MV network stability.

The results presented in Publication P5 provides a summary of the simulation results and an indication on how the flexibility indices have been utilized in the ANM scheme. From the results, it is indicative that the  $Q_{\text{flex}}$  provided by the reactive power control  $QU$ -, was instrumental in keeping the reactive power flow,  $Q_{\text{MV}}$ , between the HV/MV grids, within the limits specified by the RPW. Since this case was investigating the effects of fast charging, the discharging power references were unutilized. With respect to the results of voltage limits at various MV feeders, it has been evident that the voltage stability in the MV distribution system has been maintained within the threshold value defined by the grid codes by allocation of



$Q_{flex}$  and activation of the OLTC transformer, considering the extremity of the study case. Therefore, the designed ANM scheme acted as required to provide RPW and voltage control.

## 4 LI-ION BESS MODELING AND CONTROL FOR LONG-TERM ANM SIMULATIONS

With higher integration of inverter-based energy sources such as RESs (WTGs and PVs) and increasing utilization of devices such as FACTS or HVDC, new types of fluctuations are introduced in the power system, which then needs a more detailed range of time-domain simulation studies. As described in a previous chapter, EMT simulation methods can be used to study fast transients in power systems lasting for a short duration (in order of microseconds to few minutes). Such simulations are computationally intensive and require a longer duration. To study the steady-state fluctuations in the power system for a longer duration, EMT simulations are not feasible. Instead, phasor-domain simulations can be utilized for these long-term simulations. This chapter presents an overview of Publication P6 of the thesis and focuses on Li-ion BESS modeling and control for long-term ANM simulations.

Phasor domain simulations aim to capture the slow dynamics of the power system by assuming that the power-system frequency remains close to its nominal values, i.e., 50 or 60 Hz, unlike transient-stability EMT simulations. Phasor simulations can be performed by replacing the grid differential equations, which are a result of  $R$ ,  $L$ , and  $C$  interactions, with simple algebraic equations. The distributed models of transmission lines are also replaced by lumped models in the phasor simulation mode. The time constants of the fluctuations, captured by the phasor simulations, are typically above 100 ms (Vinicius A. Lacerda, Araujo, Cheah-Mane, & Gomis-Bellmunt, 2022). Therefore, system voltages and currents are represented by equation (7).

$$U = Z * I, \quad (7)$$

where  $U$  and  $I$  are the complex vectors of node voltages and current injections, respectively, and  $Z$  is an impedance matrix. The phasors are assumed to rotate at constant nominal frequency. Thus, the simulation time steps can be increased and the total simulation time can be reduced. The simulation speed in this case can be increased by more than one to three orders of magnitude to EMT simulations.

In Chapter 3, the Li-ion BESS controllers were designed for ANM, and their robustness was validated in the EMT simulation mode. EMT simulation studies provided knowledge on how the battery controllers (whose set-points were provided from accurate Li-ion SOEC battery model) performed when fast transients were introduced in the power system. The coordinated control of the Li-ion BESS with the other grid-side (i.e., from the EMS of the ANM scheme) and PE component controllers (i.e., active and reactive control loops from converters) that

form an inherent part of the ANM architecture were validated with case studies in SSG.

As explained in Chapter 2 (Fig. 6), the time horizon of voltage control in a power system can extend from cycles to days. Therefore, it is important to model the effect of steady-state fluctuations in the power system together with ANM, and their control interactions need to be studied. For this purpose, the phasor simulation mode explained above forms an ideal method to perform long-term power system simulations, particularly to capture steady-state voltage fluctuations (K. H. Sirviö et al., 2020; K. Sirviö et al., 2019). In addition, phasor simulation provides a method to study the effect and interaction of these long-term fluctuations on the power system dynamics and control dynamics of DER and ANM applications.

Another advantage of utilizing the phasor simulation method for longer time periods is that it allows us to study different types of loading characteristics of grid-connected Li-ion BESS more accurately. These load characteristics include, for example, the DOD, C-rate of charge and discharge, and cycling and idle periods of BESS. Such information is vital for the design and development of advanced adaptive control algorithms for grid-connected Li-ion BESS. However, without accurate Li-ion BESS performance models, long-term studies related to their integration in the power grid will not provide accurate results, such as the control set-points, actual thresholds of operation, and their cycling analysis.

SSG (defined in Chapter 1.1.1) has been used as the power system under study in Publication P6 of this thesis, where a 1 MW Li-ion BESS was integrated with the MV distribution system to be utilized as FER. The power system model was developed in the ePhasorSim platform of RT-LAB, which is a real-time simulation platform.

In summary, the following issues had to be overcome to perform simulation studies in phasor simulation mode:

1. Development of the SSG power system model in the ePhasorSim real-time platform including the ANM scheme with Li-ion BESS;
2. Development of an accurate, enhanced Li-ion BESS equivalent-circuit battery model including and describing both the electrical and thermal effects of the battery;
3. EMS design for an ANM scheme (i.e., development of coordinated control of grid-side controllers with DER controllers);

4. Define case studies to validate the overall ANM architecture and its controller's performances in phasor mode simulations.

The focus of the long-term ANM simulation studies in Publication P6 with the enhanced accurate Li-ion BESS mode was on the following issues:

1. Development of the ANM architecture with *QU*-, *PU*-, and *P*- controllers for managing the available flexibilities of various DERs, especially to generate control signals for the BESS and WTG inverters in the MV distribution system of SSG;
2. The utilization of an accurate and enhanced ECM for Li-ion BESS controller development in grid integration studies;
3. Studying the effects of BESS inverter operation on the Li-ion BESS performance, including the thermal effects of Li-ion batteries;
4. Understanding the interaction of the BESS inverter controller with the grid-side controllers in the distribution system.

#### 4.1 Enhanced Li-ion BESS model

The Thevenin-based SOEC battery cell model explained in Chapter 3 (Section 3.1) has been used to represent the dynamic battery model in the long-term ANM simulations of Publication P6 as well. It successfully emulates the model parameters such as multivariable SOC, C-rate, temperature, hysteresis effects, self-discharge, and battery aging. The SOEC is considered as the benchmark model for Li-ion batteries as it describes the charge transfer, diffusion, and solid electrolyte interface reactions in the form of resistors and capacitors (Ates & Chebil, 2022; Mousavi G. & Nikdel, 2014).

In addition, a thermal model of the battery cell has been added to the existing electrical model to understand the temperature changes in the battery cell during its charge and discharge operation due to ANM operations. The SOEC modeling technique can be utilized to estimate the heat generated by the battery cell, which leads to an increase in temperature due to the Joule heating effect. This temperature change affects the performance of the Li-ion battery considerably (Hesse et al., 2017). The major highlight between the model developed in (Arunachala et al., 2016) and the model presented in this paper is the development of the thermal model, which considers both SOC and inner cell temperature as affecting parameters. The inner cell temperature is considered uniform within the

cell and is taken as the average temperature inside the cell. Equation (8) represents the irreversible heat generated by the battery cell due to the Joule effect (Kalogiannis, Jaguemont, Omar, Van Mierlo, & Van den Bossche, 2019). Therefore, temperature changes during the cell operations are determined to provide set-points for the thermal cooling system and the battery management system (BMS).

$$P_{th}(t) = R_i(SOC, T_b)I^2(t) = m_b C_p \frac{dT_b}{dt} + P_a(t) \quad (8)$$

Where,

$m_b$ : mass of the battery [Kg]

$C_p$ : specific heat capacity of the battery [J/Kg.K]

$T_b$ : uniform Temperature inside the battery [K]

$P_a$ : heat transfer rate to the cooling system [W]

$P_{th}$ : heat generated in the battery due to the Joule effect [W]

#### 4.1.1 Enhanced Li-ion BESS model utilization in long-term simulations

The enhanced Li-ion BESS model integration for the long-term phasor mode is presented in Fig. 21. The first block corresponds to the Li-ion battery cell model which has been explained in Chapter 3 (section 3.1). The next block converts the battery cell model to the pack model whose details were also explained in Section 3.1. The detailed inverter models from Chapter 3 designed for EMT simulations are replaced by a simple parameter, i.e.,  $\eta_{\text{Converter}}$ , that provides the particulars of power conversion efficiency of the PE interfaces used in Li-ion BESS integration. The value of  $\eta_{\text{Converter}}$  has been determined from the EMT simulation in a previous chapter. Following the output of the conversion block, the active power supplied by the Li-ion BESS will be obtained. The reactive power block in Fig. 21 dictates the amount of reactive power fed into or from the power grid based on calculations by the ANM scheme.

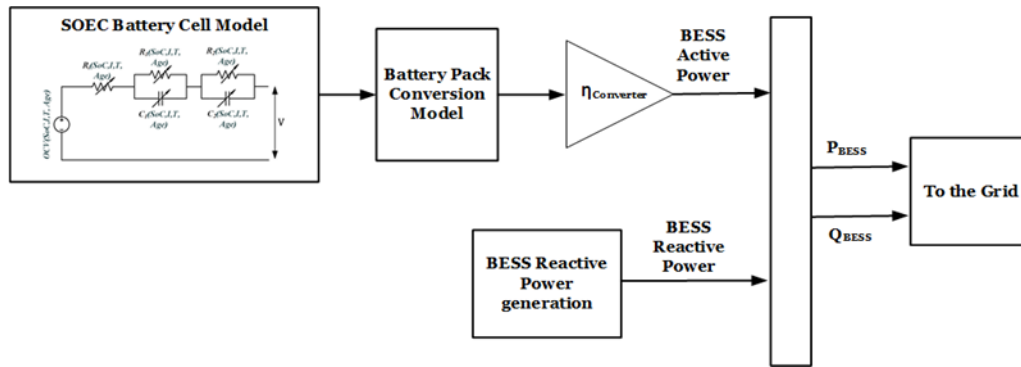


**Figure 21.** Enhanced Li-ion BESS model utilization in long-term simulations

## 4.2 ANM scheme in long-term simulations

Previously, extensive research on various ANM schemes to control the network voltage level and to control reactive power flow between the transmission and distribution network to be maintained within the so-called RPW provided have been studied and validated in the local smart grid pilot SSG (Laaksonen, Sirviö, Aflecht, & Kauhaniemi, 2019; K. Sirviö, Laaksonen, & Kauhaniemi, 2020; K. Sirviö et al., 2019; Sirvio, Valkkila, Laaksonen, Kauhaniemi, & Rajala, 2018). The ANM control architecture for the long-term simulations of Publication P6 in the phasor simulation mode with SSG and enhanced Li-ion BESS model is shown in Fig. 22. Improvement of the local utilization of wind power generation with the aid of BESS is the primary objective of this ANM architecture. Voltage control is the secondary ANM objective. Power system modeling and control studies were performed on the ePhasorSim platform, a real-time simulation from OPAL-RT systems. Details of the ePhasorSim simulation platform has been explained further in Section 4.3.

Measured MV grid data, i.e., active-power ( $P_{GRID,MEAS}$ ), reactive power ( $Q_{GRID,MEAS}$ ), and voltages ( $U_{GRID,MEAS}$ ), are provided as the input to the ANM control architecture. The first layer in the control architecture comprising different control techniques capable of providing technical services to enforce and activate the power management related  $QU$ -,  $P$ - and  $PU$ - control methodologies, which enable these different flexibility services. In this layer, the total required reactive power control to maintain targets for RPW control and  $QU$ - control, the Fingrid codes' requirements, define the overall requirements for  $QU$ -control of flexible energy sources. Along with that, the  $P$ - control for BESS is estimated and dispatched to the next layer. The  $PU$ -control requirements are calculated when  $QU$ -control does not satisfy the standard or grid code voltage limit requirements.

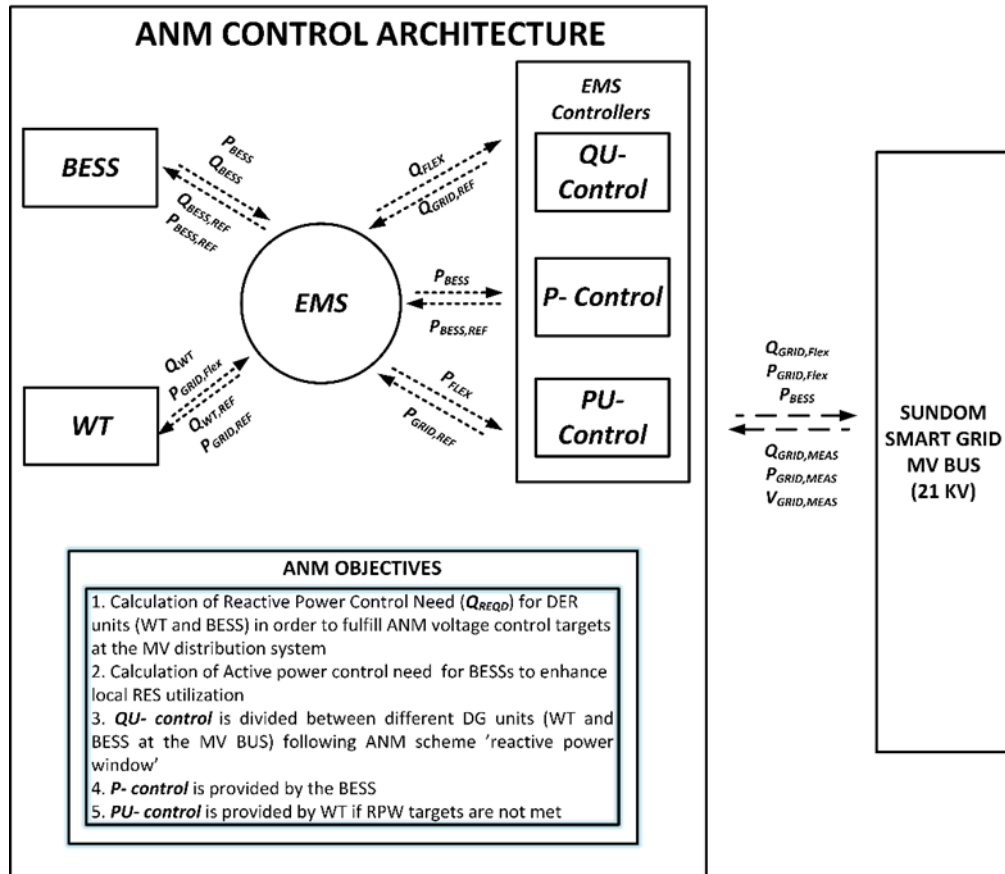


**Figure 22.** Proposed ANM scheme

The next layer of operation in the ANM scheme is the EMS which is associated with the operation of active and reactive power flows from the FERs, in this case BESS and WTG. The grid requirements related reference such as  $Q_{GRID,REF}$ ,  $P_{BESS,REF}$ , and  $P_{GRID,REF}$  are given as input to the EMS layer, where it distributes the related operations to the BESS and WTG based on the availability of their individual flexibilities. Therefore, based on Eqs. (5)–(9), EMS generates reference values  $Q_{BESS,REF}$  and  $P_{BESS,REF}$  to the BESS and  $Q_{Wind,REF}$  and  $P_{GRID,REF}$  to the WTG. Based on the internal control algorithms for BESS and WTG defined in the following section, BESS returns the relevant  $P_{BESS}$  and  $Q_{BESS}$  to the EMS, whereas WTG returns  $Q_{WT}$  to the EMS.

These control signals are then forwarded to the EMS controllers as  $Q_{FLEX}$  ( $Q_{BESS}$  and  $Q_{Wind}$ ) to the *QU-* controller,  $P_{BESS}$  is forwarded to the *P-*controller and  $P_{FLEX}$  is provided to the *PU-* controller layers. All three control layers act in tandem to provide  $Q_{GRID,Flex}$  and  $P_{GRID,Flex}$  to the MV grid, thereby controlling the active and reactive power flows in the HV/MV connection point, regulating the values based on the RPW control requirements. Fig. 23(a), (b) and (c) show the design and architecture of the individual control techniques, i.e., *QU-*, *P-*, and *PU-*controls,

respectively, employed in the ANM management principle. Equations governing the grid-side controllers are explained in detail in Publication P6.

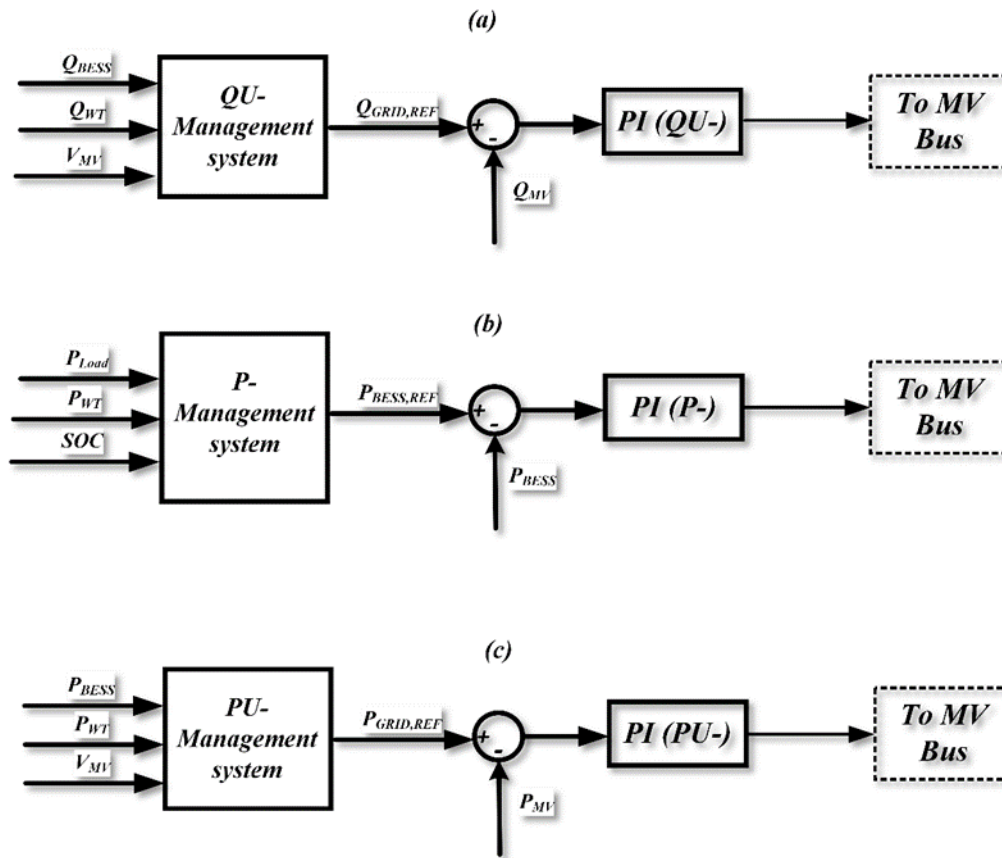


**Figure 23.** EMS Controllers: (a) QU- control (b) P- control (c) PU- control

### 4.3 Utilization of real-time simulation platform for long-term ANM studies

Power system simulations, especially the large-scale ones with detailed DG and DER unit models, are computationally intensive and take a long period to complete few seconds of simulation. To understand various transient and steady-state phenomena in the power system, faster simulation platforms are required. Real-time simulations offer potential platform for faster and more efficient simulations of large-scale power systems. In Publication P6, the ANM scheme defining the role of BESS in enhancing wind power generation and the MV distribution system voltage control are explored through simulation studies in the ePhasorSim platform by OPAL-RT (Panigrahy, Gopalakrishnan, Ilamparithi, & Kashinath, 2017). ePhasorSim is a real-time transient-stability solver used for simulating the slow dynamics of large-scale power systems in real-time. This tool is interfaced



with Matlab/Simulink and compatible with load flow and dynamic data files from PowerFactory simulation software.

Fig. 24 presents the overall architecture for real-time simulation studies in the OPAL-RT interface. Hence, for this study, an SSG model was developed in PowerFactory with accurate data provided by local DSO, Vaasan Sähköverkko and later imported to OPAL-RT to integrate BESSs and design their controllers. The WTG power generation and load utilization data used for power system modeling were extracted from the field as a part of the smart grid pilot. The SSG WTG is of the permanent magnet synchronous generator (PMSG) type with a full-power converter interface, which allows it to absorb or inject reactive power to 100% of its rated power. In this case, the reactive power control ( $QU$ - control) of the WTG is disabled, to record the original characteristics in the SSG without the operation of any FER adhering to IEEE 1547-2018 (IEEE Standard Association, 2018) guidelines. Li-ion BESS integration has been performed as explained in Section 4.1.1.

Simulation studies have been designed for a period of 24 h with a time-step of 1 second. The reasons for selecting the 24-hour time period for simulation studies are as follows:

- The intermittency of WTG power generation on a 24-hour period will be captured;
- Amount of expected charge/discharge Li-ion BESS power can be identified, which tends to provide details on battery utilization prediction for day-ahead markets;
- Simulation studies at the 1 second time-step enable constant monitoring of various controller interactions and aid in improved tuning of controller parameters in a long-term setup.

#### 4.4 Case Studies – Coordinated control of Li-ion BESS in long-term ANM simulations

Three use cases were simulated in Publication P6 to study the utilization of the available flexibility for ANM of the SSG, predominantly voltage control, and for better utilization of wind power generation. None of the flexibilities are utilized in the first case, thereby providing the base case scenario used to compare the second (Case 2: WTG only) and third cases (Case 3: WTG and BESS). All simulations were run for a period of 24 h, mainly to evaluate the different controls of flexible energy

sources and their planning over a period of one full day. In all these cases from Publication P6, SSG is modeled as a grid-connected microgrid, without OLTC in the HV/MV transformer.

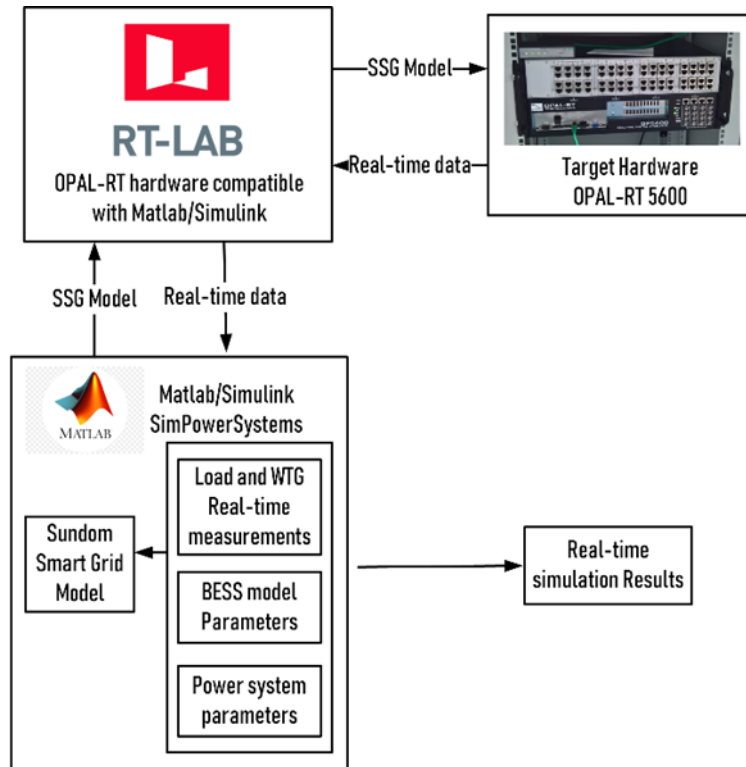


**Figure 24.** SSG real-time simulation setup

#### 4.4.1 Case 1: Without ANM

The first case was designed as a base case scenario for comparison purposes, where SSG is simulated in the ePhasorSim platform without any flexibilities i.e., reactive powers of the WTG and Li-ion BESS and active power of Li-ion BESS. This approach enables us to record the base case parameters such as the active and reactive power flows in the power grid and voltages at the HV and MV feeders. Based on the simulation results, the observations are as follows:

- In the early part of the day, the grid supplies power due to the reduced wind power generation and later starts consuming the power generated from SSG as the WTG power generation increases, causing higher levels of intermittence (active and reactive power flows between HV and MV grids and voltage fluctuations levels at MV grid) in the power system.

- System voltages are measured during the simulation at the HV and MV side of the transformers. The HV side voltage is close to 1 p.u., and the MV side voltage is close to 0.94 pu, mainly due to lack of OLTC.

Detailed graphical results are presented in Publication P6.

#### 4.4.2 Case 2: With ANM (WTG only)

In this case, the WTG's reactive power flexibility in the SSG is utilized to control voltage at the MV distribution system. The reactive power provisioning capability is related to the active-power generation of the WTG, whose details are explained in detail in Ding, Liu, Wang, Zhang, & Wang, 2016; Turitsyn, Šulc, Backhaus, & Chertkov (2010). The *QU*-control algorithm is responsible for the reactive power flexibility service whose details are explained in Chapter 3.

The flexibilities of *QU*-control from the WTG have been utilized to stabilize the MV distribution system's voltages. Because the MV distribution system voltage was less than the target values, *QU*-control of the ANM scheme was activated to provide reactive power to support the local voltage levels. WTG absorbs reactive power in the system to its maximum possible value as defined by the ANM scheme. Despite the maximum flexibility available from *QU*-control of WTG, it has been observed that the voltages in the MV side of the transformer do not remain within the limits defined by the ANM targets for about 14 h, although this flexibility service helped in keeping the voltage stable for about 10 h in a day. Hence, further flexibilities are required in the network to manage the voltage level in the MV distribution system. Detailed graphical results are presented in Publication P6.

#### 4.4.3 With ANM (WTG and BESS)

Li-ion BESS has been integrated to the MV bus of the SSG, where an accurate SOEC model has been used, as explained in Chapters 3.1 and 4.1. Due to its capability in catering to both the active and reactive power requirements of the SSG, the BESS controller includes both *P*-control by regulating the active power of the Li-ion BESS and *QU*-control for reactive power provisioning for ANM requirements commanded by the MV distribution system in SSG.

The Li-ion BESS active-power operations are meant to complement the WTG in the SSG, i.e., discharge battery power when the system load is higher than WTG power generation and charge when its vice-versa. The active-power discharge of Li-ion BESS is controlled by the battery's SOC within their threshold  $SOC_{min}$  and  $SOC_{max}$ , which is set between 20% and 80% in this case. By choosing these

threshold levels, the battery can be charged with a constant current step alone, and the need for CV charging of Li-ion batteries can be eliminated. Furthermore, it helps in keeping some reserve battery capacity for emergencies/contingencies, where the battery needs to be charged. Similarly, the reactive power utilization from the Li-ion BESSs inverter is dependent upon its active power use. Both WTG and Li-ion BESS have been used for reactive power provisioning in the study. The equations commanding charge and discharge power characteristics of the Li-ion BESS and the reactive power provisioning are explained in detail in Publication P6.

Based on the simulation results, when Li-ion BESS participates in  $QU$ -control along with the WTG, the voltages in the MV distribution system are stabilized and maintained above 0.95 p.u. throughout the simulation period of 24 h, thereby satisfying one of the major objectives of the ANM scheme.

The Li-ion BESS characteristics were similar to the ones mentioned in Table 2 in Chapter 3.3. Based on the simulation results, the Li-ion BESS undergoes cycling when the WTG power generation fluctuates. During the beginning of the simulation period, it discharges active power as the load demand is higher than WTG power generation. Somewhere during the 6<sup>th</sup> hour of simulation, the WTG generation exceeds the load demand and the Li-ion BESS charges with a pre-determined value of 500 kW. Toward the end of the simulation, somewhere at hour 20, the battery discharges till its  $SoC_{min}$ . Therefore, the designed  $P$ -controller acted as required in the ANM scheme. The PI-controllers representing control of the flexibilities from BESS ( $P$ -control and  $QU$ -Control) and WTG ( $QU$ -control) are represented in Table 3. This satisfies another major objective of the ANM scheme, i.e., complementing power generation of the WTG and increasing the overall RES penetration in the power system.

The primary advantage of adding the SOEC battery model to the SSG to design their controller principles is to understand the way the battery, as a DC component, responds to the requirements presented by the grid. The results from the SOEC battery model are represented in Fig. 25, which explains various battery characteristics on the DC side due to the demands exerted by the AC side of the power grid. BESS operates with a range of  $SoC_{min}$  and  $SoC_{max}$ , which is as shown in Fig. 25(a), where it operates between 20% and 80% SOC accurately. Fig. 25(b) shows the DC current characteristics on the battery, where the  $P_{dis}$  does not exceed 1 MW and  $P_{chg}$  occurs at 500 kW. The BESS voltage characteristics are shown in Fig. 25(c), which provides an important setpoint for control of power converters employed to integrate battery systems to the grid and Fig. 25(d) presents the DC power characteristics.

**Table 5.** PI-controller parameters of grid-side controllers

Grid-Side Controllers	Kp	Ki
P- Control (Li-ion BESS)	0.005	1
QU- Control (Li-ion BESS)	0.005	1
QU- Control (WTG)	0.3974	0.9196

The charge and discharge operation in the Li-ion BESS are exothermal reactions, which generate heat in the process. This temperature change in the battery cell due to the heat generated during its operation in SSG has been generated with the thermal model of the Li-ion battery cell, as depicted in Fig. 26. This result from the thermal model of the battery provides direct information on the effect of current requirements of the grid on the BESSs thermal characteristics. Hence, the SOEC battery model provides set-points to design battery management systems, i.e., by considering both thermal and electrical characteristics of battery operation. More details about the simulation results can be found in Publication 6.

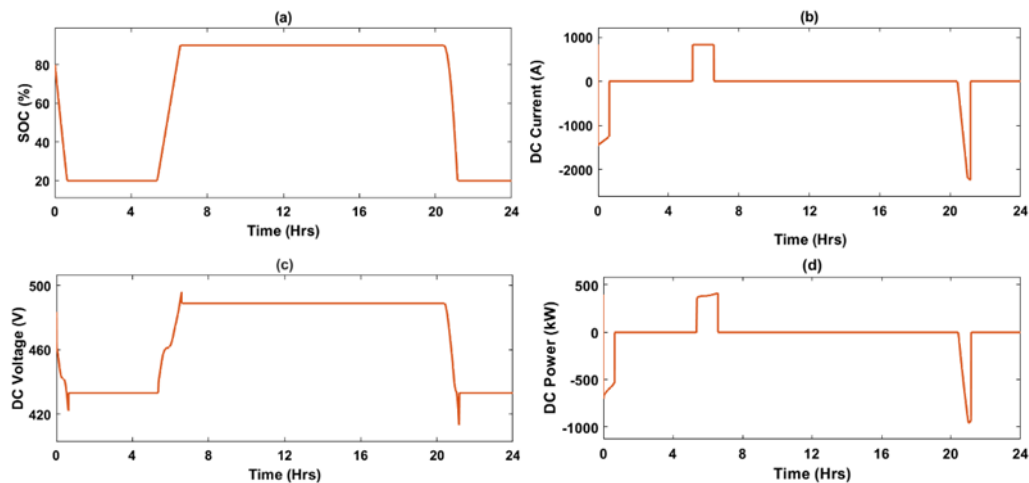


**Figure 25.** Results from the SOEC Model; (a) Battery SoC; (b) Battery DC charge/discharge currents; (c) Battery SOC voltage; (d) Battery DC Power characteristics

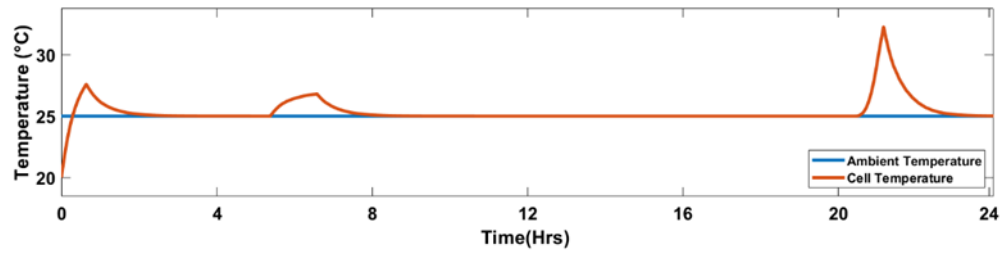


**Figure 26.** Battery cell operational temperature profile

## 5 EFFECT OF BATTERY-AGING MODELING ON CONTROL AND ECONOMIC PROFITABILITY OF LI-ION BESS

The modeling and control development of Li-ion BESSs for short- and long-term ANM studies for flexibility-related services with respect to both active and reactive power has been described in Chapters 3 and 4 as well as in the related publications of this thesis. However, the Li-ion BESS modeling and control design can be improved and enhanced by incorporating technical performance parameters related to its aging characteristics into the model. In Chapter 5, we focus on improving the overall Li-ion BESS control by considering its aging characteristics during modeling. This chapter presents an overview from Publications P7, P8, and P9 of the thesis and discusses the effect of battery-aging modeling on the economic profitability of Li-ion batteries.

Aging of Li-ion batteries is a complex phenomenon, which reduces their capacity and increases their cell resistance with usage (Iurilli, Brivio, & Wood, 2021; Xiong, Pan, Shen, Li, & Sun, 2020). The reduction in the capacity of the Li-ion battery is directly correlated to the reduced energy dispatch, while the increase in cell resistance has been correlated to the reduced power output of the battery, particularly its peak power changes. Tracking such properties of the Li-ion batteries and utilizing them for the development of controllers for their active-power discharge provide the possibility to manage batteries efficiently and safely throughout their lifetime.

The aging of Li-ion batteries also influences the economic aspects of their utilization, which are directly related to the question of how much money a Li-ion BESS operator can make without damaging the BESS? To understand the impact of battery aging on the economic profitability of the Li-ion BESS, a thorough techno-economic analysis must be carried out, including battery-aging curves, as part of the cost-based optimization problem (Abogaleela & Kopsidas, 2019; Kirli & Kiprakis, 2020; Shi, Xu, Tan, Kirschen, & Zhang, 2019).

For the development of accurate battery system control considering the aging characteristics and performing techno-economic analysis when considering battery aging, the major requirement is the development of high-accuracy battery-aging models. First, in Chapter 5, a brief review on various aging characteristics of the Li-ion batteries will be presented. Next, the development of battery-aging models for grid applications is integrated with enhanced Li-ion BESS control and techno-economic studies. Finally, the impact of battery aging will be presented through three case studies, based on Publications P7, P8, and P9 of this thesis.

## 5.1 Li-ion BESS aging modeling in simulation studies

Li-ion BESS aging increases the battery cell resistance and battery loss in capacity over a period of time. The reason for aging is mainly the degradation occurring in the battery components, namely the anode, cathode, and electrolyte. Origins of such degradation mechanisms are related to chemical or mechanical changes in the battery cell, which are again highly dependent on its electrode composition, i.e., type of materials in the anode and cathode (Agubra & Fergus, 2013; C. Lin, Tang, Mu, Wang, & Wang, 2015; Vermeer, Chandra Mouli, & Bauer, 2022; Vetter et al., 2005). Aging of the battery is a continuous process that occurs both during charge or discharge operations and during its idle state. Aging is classified as follows:

- *Cycle aging*: It is defined as the aging that happens while the Li-ion battery is cycling, i.e., undertaking charge and discharge operations.
- *Calendar aging*: The aging of batteries while it is non-operational, i.e., under no load conditions, is defined as calendar aging of the batteries (Krupp et al., 2022)

Cycle and calendar aging in the Li-ion battery cells are complex processes, which are influenced by a multitude of factors, particularly mechanical stresses and chemical side reactions. The rate of the cycle or calendar aging are also influenced by multiple external factors such as SOC, DOD, C-rate of charge and discharge, and ambient temperatures (Barré et al., 2013; Gao, Jiang, Zhang, Zhang, & Jiang, 2018; X. Lin, Khosravinia, Hu, Li, & Lu, 2021a; J. Liu et al., 2020, 2022). Fig. 27 provides an overview on aging of Li-ion battery. The major causes for aging are listed in the first vertical. The second vertical describes the aging mechanisms that occur when the battery cells are linked to the causes from first column on the left. The third column explains the degradation model in Li-ion batteries, which is caused by one or more aging mechanisms from the second column. The last column on the right shows the effects of Li-ion battery aging, i.e., capacity fade or power fade (increase in resistance). The working of Li-ion batteries, their aging mechanisms and degradation modes are explained in detail in Appendix I.

It can be observed from Fig. 27 that Li-ion battery aging is a highly complex process that occurs due to various causes, leading to different aging mechanisms and finally to their particular aging modes. The causes and mechanism for aging vary with types of chemistries in Li-ion batteries, as they are composed of different materials in their anodes and cathodes. However, the common observation in all chemistries due to aging in batteries is the loss of their capacity and power fade, which from the electrical engineering point of view are very important as they have



a direct impact on the control of Li-ion battery systems and the economic profitability due to reduced battery performance characteristics.

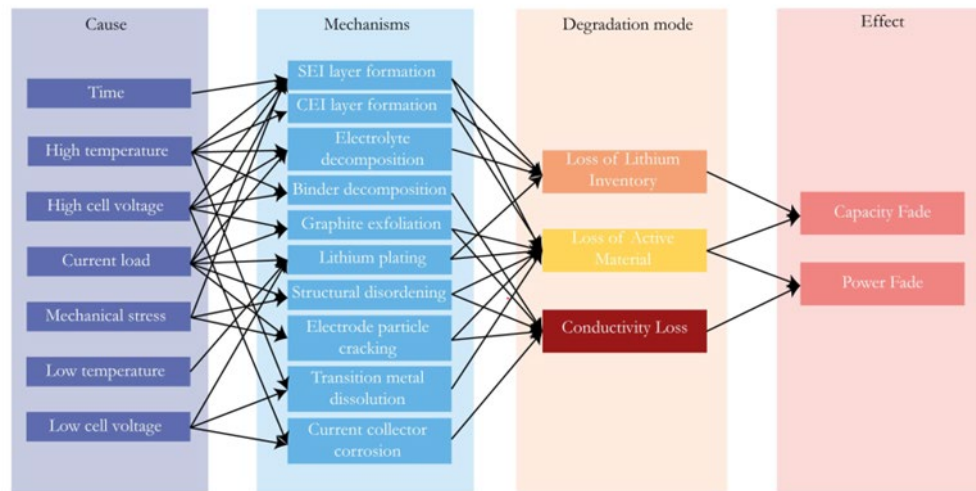


**Figure 27.** Different Li-ion battery-aging processes

### 5.1.1 Need for aging aware control of Li-ion BESS control

Li-ion BESS has become the leading choice in stationary grid applications to provide different flexibility services at all levels of the power systems (Parthasarathy, Sirviö, Hafezi, & Laaksonen, n.d.). Reasons for the wide acceptance are its higher power and energy density, lower self-discharge, slow aging rate, improved safety and high modularity (Choi et al., 2021b). However, the performances of Li-ion BESSs are affected by various parameters such as DOD, SOC, temperature, and aging (Hesse et al., 2017) and performance degradation due to aging mainly leads to changes in battery capacity and increases in resistance, leading to changes in the peak power capability. This peak power change in Li-ion BESS is a function of its SOC and aging. This means that the Li-ion BESS peak power output will differ for a new battery compared to a wear and tear induced cycled BESS.

In existing literature, most studies related to battery modeling and control concentrate on long-term cost-based optimization techniques (Abogaleela & Kopsidas, 2019; Jin, 2022; Kirli & Kiprakis, 2020; Lee et al., 2021; K. Liu et al., 2022; Zhang et al., 2022a). Some of the recent studies (Yang Li et al., 2019, 2020; Reniers, Mulder, Ober-Blöbaum, & Howey, 2018) have also utilized battery-aging models, i.e., their capacity degradation and resistance increase as aging parameters in the power system planning and control studies (predominantly considered as the tertiary control of microgrids). However, the literature focused

on real-time design of BESSs' (e.g. Li-ion BESS) secondary control have not paid attention on their aging characteristics (Allahham et al., 2022; Ryan et al., 2021; Tian et al., 2021; Zhao et al., 2018). Further, according to the authors' best knowledge, the peak power evolution of the Li-ion battery with aging has not been considered as an aging parameter in any of the studies presented in the previous literature. According to the authors' experience in analyzing field data from battery utilization, most battery load in the secondary control has a higher power requirement and DOD when compared to primary control. Therefore, it is important to include the state of age (SOA), i.e., number of operational charge/discharge cycles completed is considered as SOA in this study) and its corresponding peak power capability of the Li-ion BESS in the secondary control design.

Hence, the design for controllers of Li-ion BESS, especially for their secondary and tertiary control must include the aging parameter as an input, i.e., in this case, its evolving peak power capability. Failure to do so might accelerate the overall aging process and may lead to fatality due to internal short circuits, especially when the Li-ion BESSs, which will occur in particular when the battery is nearing its end of life, can no longer offer the expected peak power.

### 5.1.2 Need for aging aware techno-economic analysis of Li-ion BESS

The integration of a higher share of intermittent RESs affects, for example, the frequency control and stability of the power system. Li-ion BESS, as a FER, is capable of addressing the frequency control issues due to their fast controllability and flexible nature (Alsharif, Jalili, & Hasan, 2021; Pusceddu, Zakeri, & Castagneto Gissey, 2021). However, the participation of BESS in providing frequency control services should be profitable for its owner. Thus, a thorough techno-economic study must be conducted for its viability.

As explained earlier, aging of batteries causes degradation in performance characteristics, i.e., changes in capacity and resistance (Liu et al., 2022; Zhang et al., 2021). This directly has an impact on the economic profitability for the BESS owner, due to its reduced power and energy outputs as the battery ages, in addition to battery safety issues (Hasanpor Divshali & Evens, 2020; Khajeh, Firoozi, & Laaksonen, 2022a; Ramos, Tuovinen, & Ala-Juusela, 2021; Wu et al., 2021). Although Lee, Kim, & Kim, 2022; Zhang et al. (2022b) analyzed and scheduled a BESS based on its cycle aging effects, they did not consider these effects if the BESS provides frequency control services through the corresponding marketplace. However, in this chapter, techno-economic analysis will be presented based on

Publication 9, including battery aging consideration as a part of studies related to the economic profitability of BESS.

To develop aging aware Li-ion BESS controllers and for techno-economic analysis (including aging effects), the primary requirement is to develop relevant battery-aging models. Therefore, development of such aging models, the impact of aging on BESS controllers, and its effects on techno-economic studies were analyzed through case studies, as explained in the following sections.

## 5.2 Case studies considering Li-ion BESS aging

The impacts of including battery-aging effects in their control loops and the effects on the economic profitability of the Li-ion BESS for grid application will be explored in this section by means of three case studies based on publications P7, P8, and P9 of this thesis.

The first case study (case 1 from Publication P8) explores the development of adaptive *Pf*-droop controllers instead of conventional droop controllers and their impact on the overall operation of Li-ion BESS in the power system. The battery-aging model for this study has been developed from information available in the datasheet of the battery system that has been installed in Finland, which has been used to provide frequency control by participating in FCR-N markets.

The second case (case 2 from Publication P7) considers modeling of Li-ion BESS adaptive controllers (based on battery-aging characteristics) included in the SSG for ANM applications. The battery-aging model for this study has been developed based on accelerated aging experiments along with characterization tests at different levels of aging, which were conducted under laboratory conditions by battery cell testing and a characterization system at the University of Vaasa (Fig. 38).

The third case study (case 3 from Publication P9) is performed to understand the impact of Li-ion BESS on its economic profitability by means of techno-economic studies. For these studies, a simplified battery model has been developed based on accelerated aging tests in the laboratory that indicates the change in capacity (kWh) of a battery pack with respect to cycle aging.

### 5.2.1 Case 1: Aging aware *Pf*-droop control of Li-ion BESSs

Conventional droop control techniques help in managing the output power of an inverter-based DERs by the local measurement of power system parameters such

as current ( $I$ ), voltage ( $U$ ), and frequency ( $f$ ) (Alaperä & Hakala, 2019). Based on these measurements, the output power (active and reactive power,  $P$  and  $Q$ ) of DERs is dispatched by means of droop curves, as presented in Fig. 28 for a  $Pf$ -droop when BESS is participating on FCR-N frequency control markets. It is very similar to the operation of conventional generators. Conventional droop curves are designed based on Eq. (9), where the required frequency,  $f$ , is a function of  $f_0$ , rated frequency of the DER, droop constant  $K_p$ , DER rated power  $P_0$  and DER power dispatch  $P$ . The value of  $K_p$  which decides the slope of the droop controller is as shown in Eq. (10), which is a function of the difference between the desired and measured frequencies,  $\Delta f$  and maximum active-power  $P_{max}$  of the DER.

However, when Li-ion BESS is considered as a DER, the value of  $P_{max}$  will not be a constant as it is known that their peak power ( $P_{PEAK}$ ) dispatch is influenced by aging. It must be observed that the  $P_{PEAK}$  during both the charging and discharging powers are affected due the capacity fade of battery systems with aging, i.e., their SOH. Hence, this property needs to be integrated in the droop control, making them adaptive in nature. The slope of the adaptive droop control can be facilitated by Eq. (11), which is a function of  $\Delta f$  and  $P_{PEAK}$  (affected by SOH).

Therefore, this case study from Publication P8 proposes an adaptive droop controller that considers the variable  $P_{PEAK}$  as an affecting parameter for Li-ion BESS operation. To do so, an accurate battery-aging model is required, which calculates the Li-ion BESS  $P_{PEAK}$  at different instances of aging. To understand the impact of such adaptive droop controllers in a power system, there is a need for determining how many cycles of charge/discharge a particular BESS has undergone in an application. For this reason, an accurate cycle counter method is needed. The details of the battery-aging model and the cycle counter methodology are explained in the following sections, followed by the proposed droop controller and its development methodology.

$$f = f_0 + K_p(P_0 - P) \quad (9)$$

$$K_p = \frac{\Delta f}{P_{max}} \quad (10)$$

$$K_p = \frac{\Delta f}{P_{PEAK}} \quad (11)$$

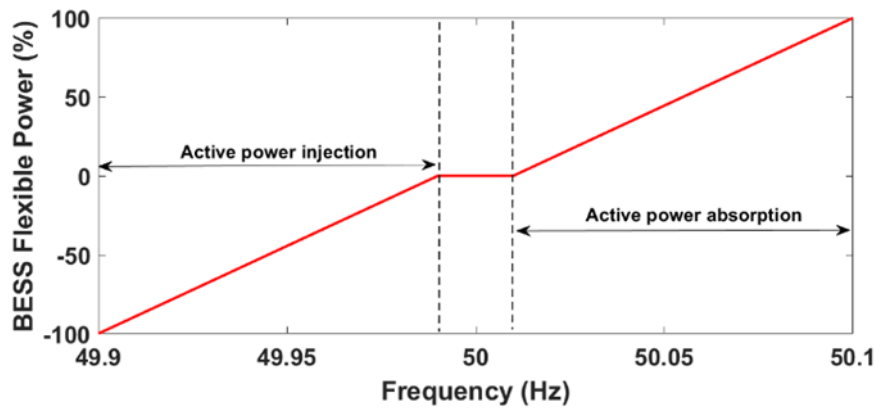


**Figure 28.** Typical active-power-frequency (Pf) -droop curve for BESS participation in FCR-N market

#### 5.2.1.1 Battery-aging modeling

To design an adaptive droop controller, it is necessary to calculate the  $P_{PEAK}$  value of the Li-ion battery with aging. In this study, the aging model includes cycle aging characteristics only. The peak power calculation is based on the aging curve that defines the number of cycles the battery can give at different DODs, as in Fig 29. Data from Fig. 29 provide the number of cycles that the battery can support at different DOD's (0%–100%). The usable capacity ( $CAP_{BESS}$ ) is calculated from Eq. (12), which is just the difference between the battery capacity at the beginning of its life ( $CAP_{BOL}$ ) and its end of life capacity ( $CAP_{EOL}$ ). From both of these values, the capacity lost per cycle at different DODs ( $CAP_{LOSS,DOD}$ ) can be calculated from Eq. (13). The cumulative loss of battery capacity ( $CAP_{LOSS,CUMULATIVE}$ ) when cycled in the field is caused due to different cycle depths. The information on total number of cycles at different DODs is obtained from the result of using the rain-flow-counting algorithm, explained in the next section. Therefore,  $CAP_{LOSS,CUMULATIVE}$  is calculated from (14) where  $N_{DOD_n}$  represents number of battery charge/discharge cycles at DOD,  $n$ . The remaining battery capacity ( $CAP_{REM}$ ) is then calculated by Eq. (15).

However, the parameter of interest for designing adaptive droop controllers is the peak power capability ( $P_{PEAK}$ ) of the battery. SOH, which gives an indication regarding the evolving  $P_{PEAK}$  of the Li-ion BESS, is calculated by Eq. (16).  $P_{PEAK}$  is calculated by Eq. (17), where it is a function of  $P_{PEAK,BOL}$  that corresponds to the Li-ion BESS active-power peak during their beginning of life (BOL) and state of health (SOH).  $P_{PEAK,BOL}$  is obtained from manufacturer's datasheet. Both the calculated  $P_{PEAK}$  and  $P_{PEAK,BOL}$  considered in this study correspond to the peak power of the battery at 100% SOC. By this means, SOH forms an input for the Li-

ion BESS control loop design for their adaptive control considering aging characteristics. The most important input to calculate cycle aging with respect to their DODs (from equations (12) to (17)) is the cycle counter, i.e., the number of cycles that has been completed and their DODs while working for FCR-N operation, which is explained in the following section:

$$CAP_{BESS} = CAP_{BOL} - CAP_{EOL} \quad (12)$$

$$CAP_{LOSS,DOD} = \frac{CAP_{BESS}}{N_{CYC,DOD}} \quad (13)$$

$$\begin{aligned} CAP_{LOSS,CUMULATIVE} & \quad (14) \\ &= \sum_{i=1}^n N_{DOD_1} * CAP_{LOSS,DOD_1} + N_{DOD_2} * CAP_{LOSS,DOD_2} \\ &+ \dots + N_{DOD_n} * CAP_{LOSS,DOD_n} \end{aligned}$$

$$CAP_{REM} = CAP_{BOL} - CAP_{LOSS,CUMULATIVE} \quad (15)$$

$$SOH = \frac{CAP_{REM}}{CAP_{BOL}} \quad (16)$$

$$P_{PEAK} = SOH * P_{PEAK,BOL} \quad (17)$$

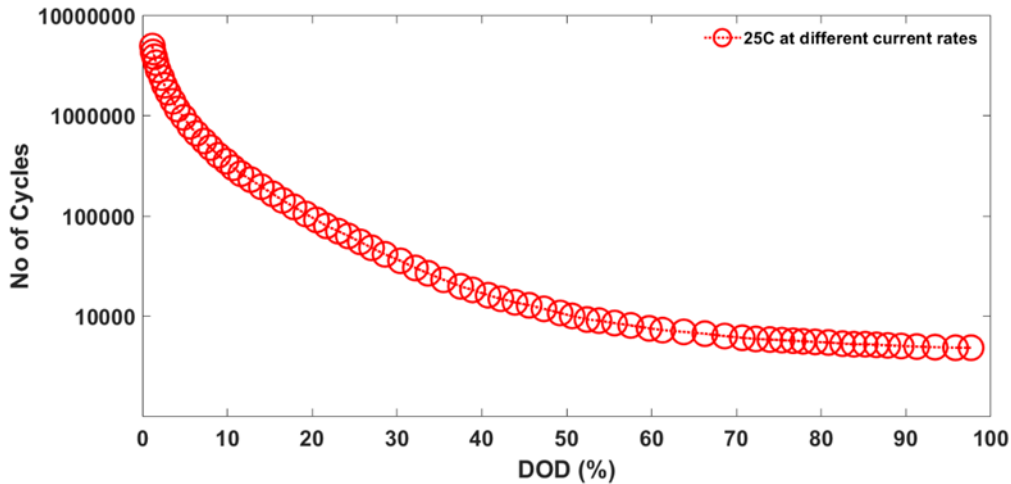


**Figure 29.** Battery cycle aging curve from the manufacturer's datasheet based on DoD

### 5.2.1.2 Rain-flow cycle counting method

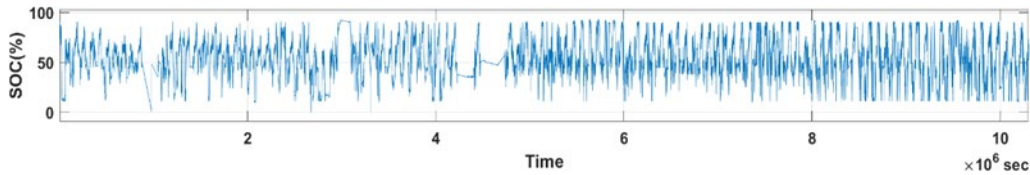
Battery cell-accelerated aging tests in the laboratory are generally performed at higher temperatures and full equivalent cycles of charging and discharging at different current rates to observe aging parameters such as internal resistance and capacity loss (Ghorbanzadeh, Astaneh, & Golzar, 2019; Mureddu, Facchini, & Damiano, 2018). However, when utilized in the field, Li-ion BESSs have different depths of discharges at different cycling depths, typically most of the cycle being micro-cycles (very low DODs). In that case, it becomes difficult to predict the Li-ion BESS aging characteristics in the field. Fig. 30 represents the SOC variations of Li-ion BESSs installed in Finland when utilized for FCR-N services. It can be observed that the cycling characteristics are highly uneven, mainly comprising micro-cycles with very low depths of discharges. Based on the literature, the rain-flow counting technique (Musallam & Johnson, 2012), which is mainly used in reliability analysis, provides an accurate estimate of the overall number of cycles at different DODs. Thus, it provides an avenue to understand the amount of degradation a particular type of battery has undergone in the field usage, based on its accurate calculation of all types of cycles, including micro-cycles as a function of its DOD.

Fig. 31 shows the results from the rain-flow counting algorithms unpacking the information on the cycling characteristics shown in Fig 30. Therefore, from the results, information on the total number of micro-cycles, their DODs, and their occurrences at particular SOCs can be gathered. Based on the results, it is evident that when Li-ion BESS are utilized for FCR-N applications, they perform very high number of micro-cycles at low DODs. Hence, tracking them is of utmost importance due to their contribution to battery aging.

### 5.2.1.3 Developed adaptive Pf- droop for Li-ion BESS

The calculated value of  $P_{PEAK}$ , being a function of SOH, thereby provides the way to introduce Li-ion BESS aging characteristics to be included in the adaptive droop control curve design for BESS. The specification of the BESS used in the study is shown in Table 6; the functionality includes  $Pf$ -control for FCR-N operation, although it supports other applications. The  $P_{PEAK}$  of the Li-ion BESS at different SOH is represented in Table 5, and the values are calculated based on Eq. (14). These values are then utilized to develop adaptive droop control mentioned in Fig. 31, providing inputs of the changing peak power capability of the battery system. The proposed adaptive droop controller, whose droop curve slopes depend on Eq. (11), provides a range of power dispatch considering battery aging. Fig. 32 represents the droop curves at different SOH levels for both charging and

discharging operations of the Li-ion BESS, whose peak power charge/discharge decreases with aging characteristics. Evolution of  $P_{PEAK}$  with aging has been represented in Fig. 32, where adaptive droop characteristics are embedded for Li-ion BESS control to maintain the power dispatch within the allowable limits dictated by the battery's SOH at all times. The following section explains the design of the controller for Li-ion BESS including the proposed droop curve.



**Figure 30.** Measured real-life BESS SOC behaviour when utilized for FCR-N frequency control markets

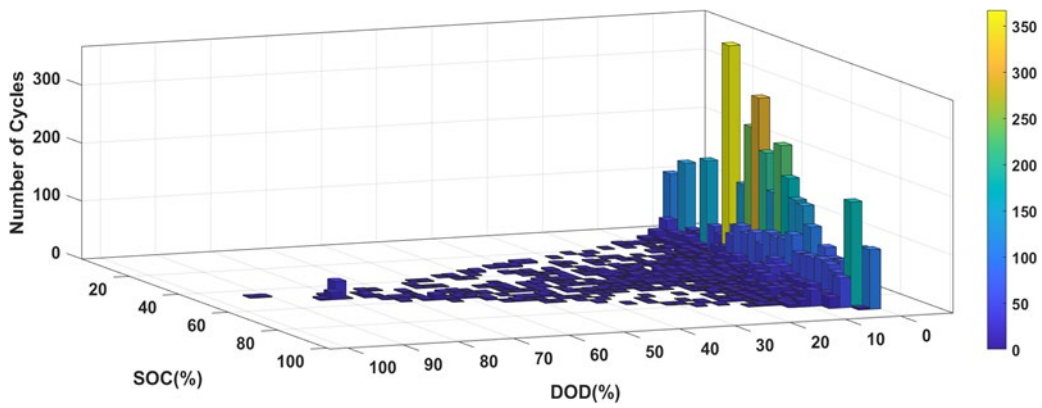


**Figure 31.** Rain-flow counting results on field SOC characteristics

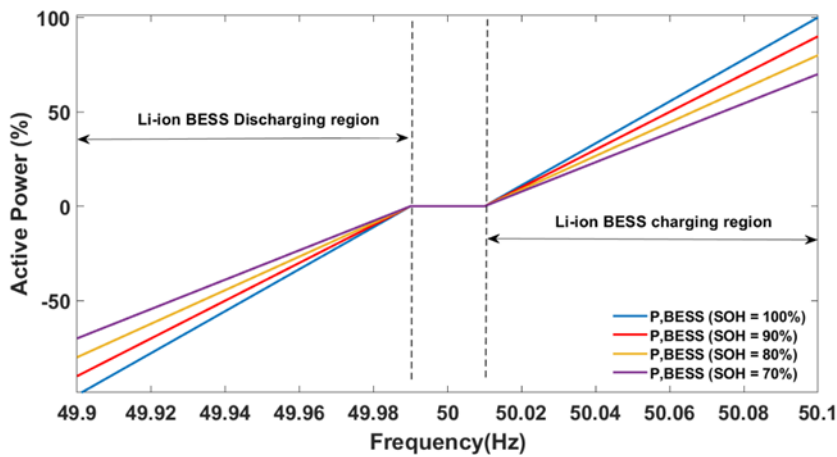


**Figure 32.** Proposed adaptive droop controller



**Table 6.** Li-ion BESS peak power calculations

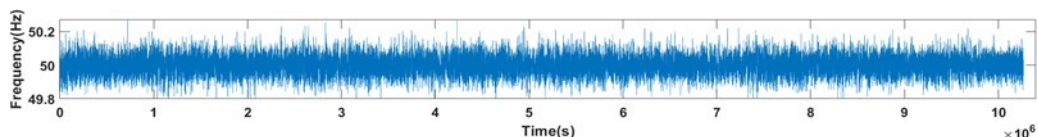
SOH (%)	Peak Power (kW)
100	300
90	270
80	240
70	210

#### 5.2.1.4 Study results discussion and conclusions

To understand the effectiveness and impact of the adaptive droop curves proposed in the previous section, a case study was employed in Publication P8 on an installed Li-ion BESS in Finland. Based on the data set of the installed Li-ion BESS, the peak power supported by this battery system is about 300 kW in the BOL conditions. It is also assumed in this study that the end of life (EOL) conditions is attained when its capacity is reduced by 30%, which provides the peak power calculation to be ~210 kW (see Table 5). However, no commonly agreed EOL definition exists for a BESS from reduced peak power capability (due to aging) viewpoint. In this study, two subcases are considered, where the subcase 1 considers the Li-ion BESS which is at its BOL and the second subcase 2 depicts the operation of Li-ion BESS toward its EOL.

##### a) Subcase 1: Li-ion BESS at BOL

The characteristics of the installed Li-ion BESS are shown in Table 5, which is designed for a continuous nominal power of 100 kW with peak support up to 300 kW (pulsed in nature). In this subcase, the battery is considered at its BOL. The field measurements of the grid frequency for three months, i.e., Dec-2019 to Feb-2020, within the ranges mentioned in Table 5 are shown in Fig. 33. The active power dispatched by the Li-ion BESS to mitigate the frequency fluctuation by means of providing FCR-N service are shown in Fig. 34. They are based on the droop control curve depicted in blue in Fig. 32, which corresponds to the BOL characteristics. It is evident that the range of frequency fluctuations has been predominantly between 49.9 Hz and 50.1 Hz, and the active-power dispatch in the Li-ion BESS has been up to the maximum of 300 kW, by means of the  $Pf$ -droop curve shown in Fig. 28, whose 100% power corresponds to 300 kW.

**Figure 33.** Power System Frequency

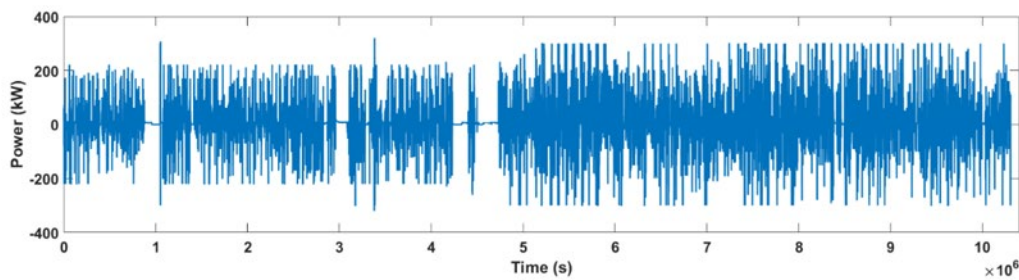


**Figure 34.** Li-ion BESS power dispatch for FCR-N during BOL

Degradation of Li-ion BESS is a serious concern, particularly when it is utilized, for instance, for FCR-N service provision, due to their operation profiles, which seek high power charge/discharge in a shorter span of time based on the field data characteristics. The SOH calculation of the Li-ion BESS due to its cycling, its relative capacity loss, and subsequently, the changes in their peak power capability has been explained above in Section 5.2.1.1. Therefore, to avoid over charging/discharging and to always maintain the Li-ion BESS peak power discharge within the peak power capability, an adaptive droop curve has been designed (see Section 5.2.1.3). This case study has been performed to understand the impacts of the changing Li-ion BESS characteristics (predominantly its peak power characteristics) with respect to aging.

In the previous subcase where a new Li-ion BESS was utilized FCR-N applications, it has been observed that the battery dispatch power reaches its peak limit of 300 kW (Fig. 34). During the Li-ion BESS BOL, all FCR-N loads were supported. In this subcase, we consider the same Li-ion BESS tending toward its EOF, i.e., capacity of the battery has reduced by 30% of its initial value and it has reached its lowest peak power characteristics.

However, based on the proposed SOH sensitive adaptive droop curves, it is evident that the peak power discharge is limited to about 210 kW for the installed Li-ion BESS system toward its EOF. The droop curve dictating Li-ion BESS power flow under these circumstances corresponds to the violet colored line in Fig. 32. The charge/discharge power ranges more than 210 kW were not supported, thereby safeguarding the battery operations within their threshold operational limits. Further, it can be observed that the FCR-N operations seeking more than 210 kW power has not been entertained by the droop curve.

Integrating battery-aging characteristics in the control and planning of Li-ion BESS for grid applications improves the overall utilization of batteries and helps maintain their operations within the safe operating regions. Control of these Li-ion BESSs for FCR-N operation is generally defined by typical  $Pf$ -droop curves as

in Fig. 28. However, the degradation characteristics of the Li-ion battery tend to reduce the peak power charge/discharge capability of the BESS. To address this issue, an adaptive droop curve has been proposed which modifies the Li-ion BESS peak active-power capability based on its SOH. The impact of such adaptive droop curves was analyzed by means of case studies, and it has been established that, as the battery ages, it is advised to omit certain ranges of FCR-N services (preferably high power charge/discharge operation) keeping battery safety in check. Thus, the problem of managing the battery charge/discharge operations can be managed within the threshold of their peak active-power performance. To reduce the computational requirements of counting the cycles of battery usage by the rain-flow counting technique (Section 5.2.1.2), this task should be performed periodically (say for e.g., 30 days interval) rather than in real time, as battery degradation is a slow process and its corresponding peak power characteristics can be updated in the battery inverter control settings.

### 5.2.2 Case 2: Aging aware Li-ion BESS control design for ANM simulations

In this study, SSG (see Section 1.1.1) was considered the power system under study, where an ANM scheme operates. The ANM scheme is the same as that utilized in Chapter 4, where it operates to stabilize system voltages in the MV distribution system and improves WTG penetration with the use of Li-ion BESS integrated in the system. The ePhasorSim real-time simulation platform is used (see Section 4.3) in this study as well. The major addition to the studies conducted previously is the development of an accurate battery model including its aging characteristics for aging aware  $P$ -control in the EMS of the proposed ANM scheme. The primary focus of the proposed new aging aware adaptive  $P$ -control, which deals with the active-power dispatch of Li-ion BESS, is to be aware of the cycle aging of the battery, which is designed to supply charge/discharge power within the battery's peak power capability. Hence, in this study, it is proposed that the battery's evolving peak power characteristics due to aging will be considered as the aging parameter and will be utilized in the  $P$ -control loop for adaptive control design.

To develop the aging aware adaptive  $P$ -control for ANM in SSG, two important components are needed:

1. The Li-ion BESS ECM which considers battery aging as a performance affecting parameter along with its SOC as another influencing parameter
2. The peak power characterization model that accurately calculates the peak power dispatch of the Li-ion BESS at different aging intervals

The development of Li-ion battery SOEC models and the peak power characterization model is derived from experimental characterization of Li-ion batteries in laboratory conditions (see Fig. 38). Their details are described in the following section.

#### 5.2.2.1 Battery characterization and modeling

This section explains the development of peak power characterization models and the ECM utilized for the development of BMS, which forms an integral part of *P*-controller development for ANM scheme.

##### *a) Peak power characterization model*

To calculate the peak power changes in the Li-ion battery, a HPPC test-based method will be utilized in this study. Some of the tests performed for HPPC tests were carried out with battery cell testing and using the characterization test bench at the University of Vaasa (Fig. 35).

The HPPC test was performed at 25°C. At the beginning, the cell is fully discharged and fully charged twice to measure the initial SOC and cell capacity. The HPPC test was performed at 25 °C, at every 10% SOC step starting from 100% SOC to 0% SOC. Prior to pulse sequence, the fully charged battery was maintained at 100% SOC and then rested for 1 h. The pulse power sequence consisted of 3C discharge for 10 s, rest at OCV for 3 min, 3C charge for 10 s, and rest at OCV for 3 min. The aging tests were conducted on the cells at 1C (with CCCV charge/CC discharge methods) cycling regime and 40 °C ambient temperature. Fig. 36 shows the current profile of the HPPC test performed, and Fig. 37 depicts its voltage response for a new cell (i.e., at 0 charge/discharge cycles).

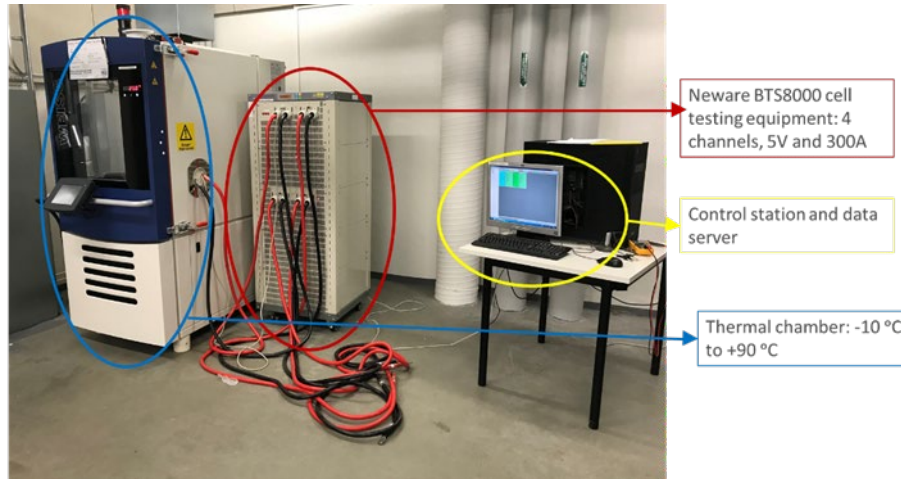


**Figure 35.** Battery cell testing and characterization test bench at University of Vaasa

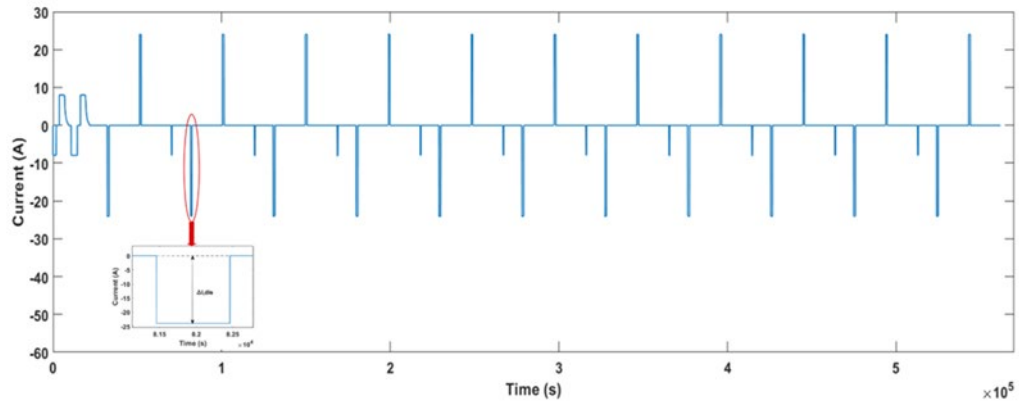


**Figure 36.** HPPC current pulse profile

To calculate the peak power discharge capability of the battery cell at this aging condition, its discharge resistance ( $R_{dis}$ ) at every high current pulse needs to be calculated.  $R_{dis}$  was computed using Eq. (18), where  $\Delta V_{dis}$  and  $\Delta I_{dis}$  are evaluated from the respective voltage and current pulses (see the zoomed images in Fig. 39 and 40). The discharge peak power of the Li-ion battery cell was calculated using Eq. (19), where the OCV and  $V_{min}$  are evaluated from the voltage response of the HPPC test. By repeating this at every 10% step SOC, the overall peak power profile at different DODs at one particular aging condition can be obtained. In the aging test performed in this study, the HPPC test profile was run at intervals specified by number of cycles, i.e., at 0, 500, 800, 1200, and 1600 cycles.

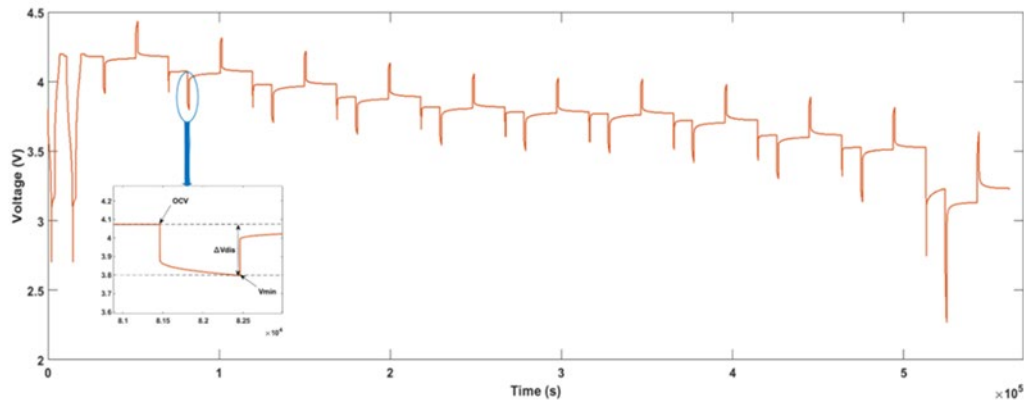


**Figure 37.** HPPC voltage response

The peak power discharge of the Li-ion NMC battery cell was evaluated with the help of HPPC test profiles obtained at different aging conditions. Fig. 38 depicts the peak power output of the Li-ion cell at different aging levels, which were calculated with the help of Eqs. (18) and (19). Similarly, the charge peak powers were calculated using Eqs. (20) and (21) and are presented in Fig. 39. A script was written in the Matlab/Simulink interface for this purpose. The calculated peak power values were then stored in a two-dimensional lookup table whose output was controlled by SOC and aging parameters and then integrated to the BMS control block.

$$R_{dis} = \frac{\Delta V_{dis}}{\Delta I_{dis}} = \frac{V_{t1} - V_{t10}}{I_{t1} - I_{t10}} \quad (18)$$

$$PP_{Dis} = \frac{V_{min} * (OCV - V_{min})}{R_{dis}} \quad (19)$$

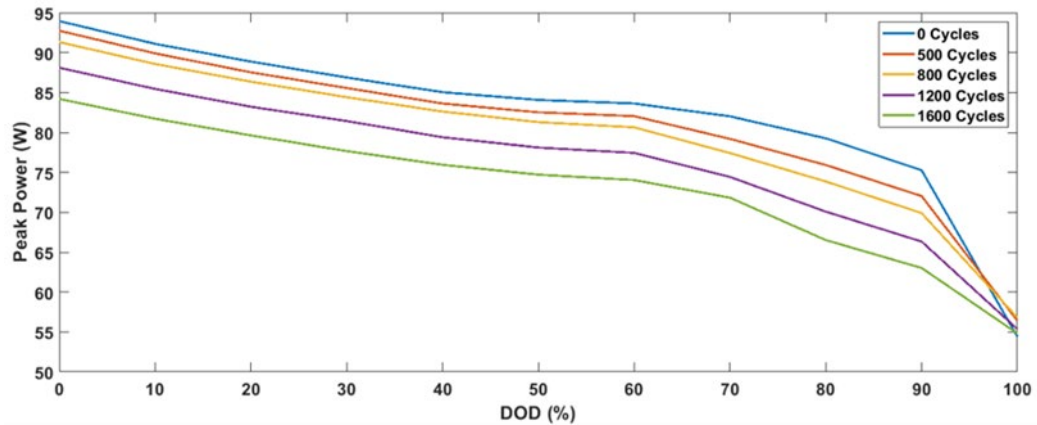
$$R_{cha} = \frac{\Delta V_{cha}}{\Delta I_{cha}} = \frac{V_{t1} - V_{t10}}{I_{t1} - I_{t10}} \quad (20)$$

$$PP_{cha} = \frac{V_{min} * (OCV - V_{min})}{R_{cha}} \quad (21)$$

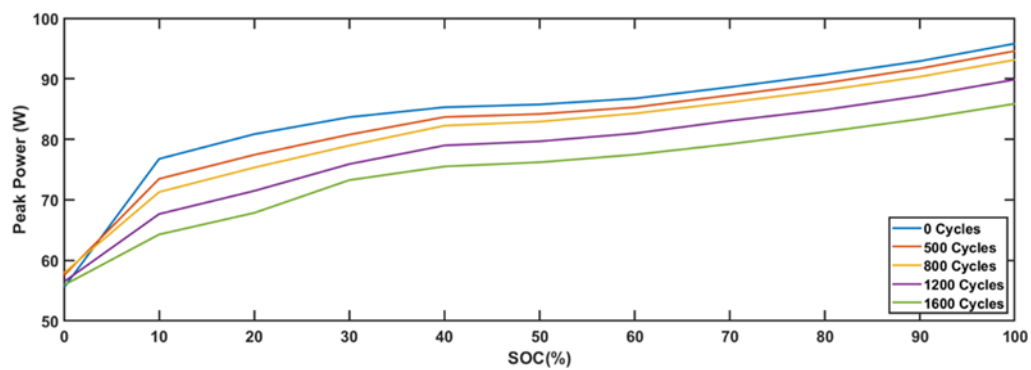
#### a) *ECM of battery*

Fig. 40 shows the proposed dynamic SOEC for the NMC battery cell. OCV is modeled as an ideal voltage source, and the internal resistance is modeled as  $R_i$ . Two RC combinations are suggested for modeling the Li-ion battery cell, so that the dynamic behaviour is modeled with  $R_1$ ,  $C_1$ ,  $R_2$  and  $C_2$ . The model parameters ( $OCV$ ,  $R_i$ ,  $R_1$ ,  $C_1$ ,  $R_2$  and  $C_2$ ) are obtained using HPPC tests (Arunachala et al., 2016), i.e. the HPPC tests were run at different SOC's (from 0% to 100% at 10% intervals) and at different aging intervals (i.e., at 0, 500, 800, 1200 and 1600 cycles of

operation). The battery cell cycle aging test was performed at a 1C charge/discharge rate and 25 °C (Arunachala et al., 2016). A Matlab script was developed to calculate the measurements of SOEC parameters from the HPPC test voltage response (Fig. 37) repeated for all the HPPC curves (i.e., at all the aging intervals).



**Figure 38.** Discharge peak power of Li-ion battery cell at different aging intervals and depending on DOD level



**Figure 39.** Charge peak power of Li-ion battery cell at different aging intervals and depending on SOC level

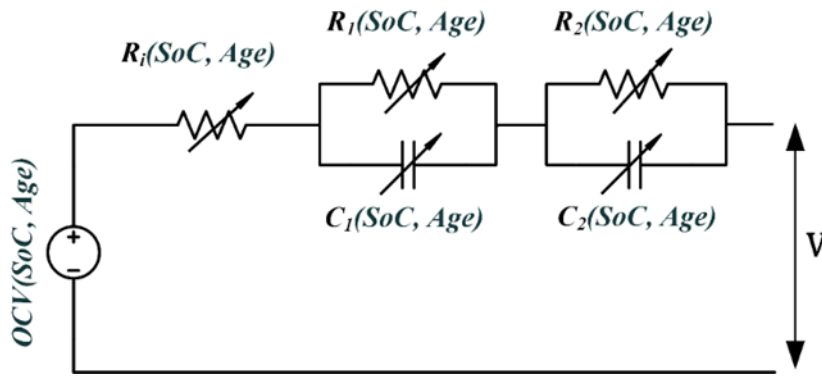


**Figure 40.** Proposed second order equivalent-circuit model

#### 5.2.2.2 ANM scheme with aging aware battery cell model

The ANM scheme is the same as that utilized in Chapter 4, where it operates to stabilize the system voltages in the MV distribution system and improves WTG penetration with the use of the Li-ion BESS integrated in the system (Fig. 21 in Chapter 4). EMS forms the most important block in the overall ANM scheme operations as it provides operational instructions to the FERs, i.e., in this case, Li-ion BESS and WTG. EMS consists of various types of controllers (*QU*-, *P*- and *PU*-controllers) that aid in harnessing the flexibilities offered by WTG and Li-ion BESSs. The objective of EMS is to manage Li-ion BESS charge/discharge operations based on WTG active-power generation and to keep the voltages in the MV bus within the limits specified by standards or grid codes by managing available flexibilities in the power system. The design of *P*- and *QU*-control is as explained below, and that of *PU*-control is presented in Section 4.2.

##### a) *P*-control design

*P*-control of the EMS is designed for the active-power dispatch of Li-ion BESS ( $P_{BESS}$ ) by controlling charge and discharge operations. The Li-ion BESS has been mostly used to complement wind power generation ( $P_{WT}$ ) compared to the power demand ( $P_{Load}$ ). The overall *P*-control layout is shown in Fig. 41. In the first block, the *P*-management system calculates the overall Li-ion BESS active-power utilization possibility ( $P_{BESS,REF}$ ) by taking  $P_{Load}$ ,  $P_{WT}$ , and SOC as inputs and generating  $P_{BESS,REF}$  as the output. The overall maximum active-power discharge expected by the Li-ion BESS is defined by Eq. (22) and that of the overall available power for charge is shown in Eq. (23). Equation (24) generates  $P_{BESS,REF}$ , whose charge and discharge powers are defined by Eqs. (22) and (23), keeping the SOC of the battery within their threshold,  $SOC_{min}$  and  $SOC_{max}$ . The second block in Fig. 44 is obtained by converting  $P_{BESS,REF}$  (which corresponds to battery pack power



containing  $N_s$  cells in series to that of  $N_p$  cells in parallel) to  $P_{CELL,REF}$  (to active-power reference of single cell in the pack) as defined in Eq. (25). This  $P_{CELL,REF}$  is provided as input to the next block called “Aging aware cell model.”

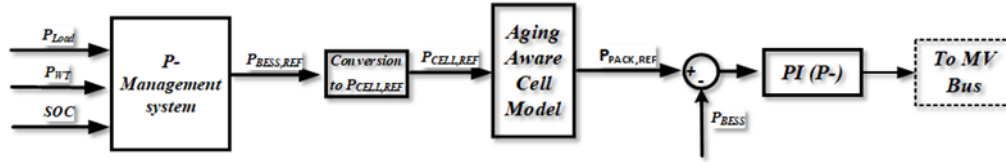


**Figure 41.** Proposed aging aware P-control scheme

$$P_{dis} = P_{Load} - P_{WT} \quad (22)$$

$$P_{chg} = P_{WT} - P_{Load} \quad (23)$$

$$P_{BESS,REF} = \begin{cases} P_{dis}; & (\text{if } SOC_{min} < SOC < SOC_{max} \text{ and } P_{Load} > P_{WT}) \\ P_{chg}; & (\text{if } SOC < SOC_{min} \text{ and } P_{WT} > P_{Load};) \\ 0 & \end{cases} \quad (24)$$

$$P_{CELL,REF} = P_{BESS,REF} / N_s * N_p \quad (25)$$

The design of the aging aware Li-ion battery cell model (third block in Fig. 41) is shown in Fig. 42.  $P_{CELL,REF}$  is the reference power to address the power system needs per cell in the Li-ion battery pack. This block comprises the BMS, which takes  $P_{CELL,REF}$  as input and calculates SOC by the SOC estimation block and the number of completed battery charge/discharge cycles with the help of the age calculator block. Equation (26) provides details on age calculator design, where the cell power is integrated over the period of time and divided by the initial cell energy. The SOC is estimated using the coulomb counting method (Meng et al., 2018), which is shown in Eq. (26).  $SOC_{initial}$  stands for the initial SOC of the cell,  $I_{cell}(t)$  stands for the cell current at time  $(t)$ , and cell capacity refers to its maximum capacity in Ah. The coulomb counting method provides the best accuracy with minimal computational effort in an environment where the measurement noise is minimal, thereby generating the required inputs for the BMS block. The age calculator refers to the calculation of cycle aging or number of completed cycles from the Li-ion battery’s charge/discharge currents, as shown in Eq. (27).

The BMS functionality includes battery cell peak power calculation, an aging aware battery model, and logic-based algorithms to limit the cell charge/discharge power within the peak power (PP) limits defined by the battery cell aging conditions. The details of the PP characterization and battery cell modeling are explained in the following sections. The algorithm explaining the battery cell power dispatch is as shown in Eq. (28), thereby creating a new cell power reference  $P_{CELL,REF,age}$ , which regulates battery cell power to always be within the PP of the battery cell. By modifying Eq. (27),  $P_{BESS,REF,age}$  is obtained, which now provides the battery reference power to the PI- controller, which controls Li-ion BESS. This  $P_{CELL,REF,age}$  is then provided as the reference to the PI-controller, which regulates the Li-ion BESS active-power output,  $P_{BESS}$ .

#### a) *QU-control design*

Reactive power-voltage (*QU*)-control is one of the flexibility services that inverter-based DERs can provide. In this study, the DERs are the WTG and Li-ion BESS. The limitations of active and reactive power contribution for both of these inverter-based sources are explained in detail in Publication P6. The available reactive power support from WTG is defined as  $Q_{wind,av}$ , and that of Li-ion BESS as  $Q_{BESS,av}$ . *QU*-droop is designed for *QU*-control, as shown in Fig 43. The droop controller has been designed to have a maximum reactive power ( $Q_{MAX}$ ) of  $\pm 2$  MVar including both WTG and Li-ion BESS reactive power characteristics. The reason for choosing this particular droop setting has been explained in detail in (Laaksonen, Parthasarathy, Khajeh, & Shafie-Khah, 2021b), which has been mainly attributed to the reason that the reactive power is provided only when the voltage of the system has been violated and there is an absence of the OLTC transformer in the studies conducted. Based on the voltage fluctuation, the droop controller provides the required reactive power reference ( $Q_{ref}$ ). This  $Q_{ref}$  will be satisfied by both the WTG and the Li-ion BESS, but the available reactive power from WT will be prioritized. Equation (29) defines the reactive power dispatch from WTG, and if this reactive power does not satisfy  $Q_{ref}$ , then the reactive power from the Li-ion BESS ( $Q_{BESS}$ ) will be utilized, whose values are defined by Eq. (30).

$$SOC = SOC_{initial} + \frac{\int I_{cell}(t)}{Cell\ Capacity} dt \quad (26)$$

$$Age\ Calculator = \frac{\int P_{cell} dt}{Cell\ Energy} \quad (27)$$

$$P_{CELL,REF,age} = \begin{cases} PP; (if\ P_{CELL,REF} > PP) \\ P_{CELL,REF}; (if\ PP > P_{CELL,REF};) \end{cases} \quad (28)$$

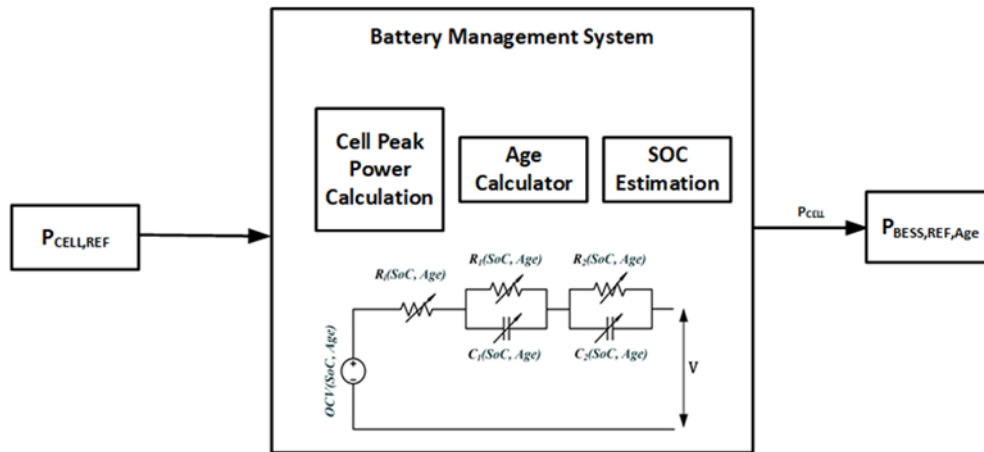


**Figure 42.** Aging aware battery cell model

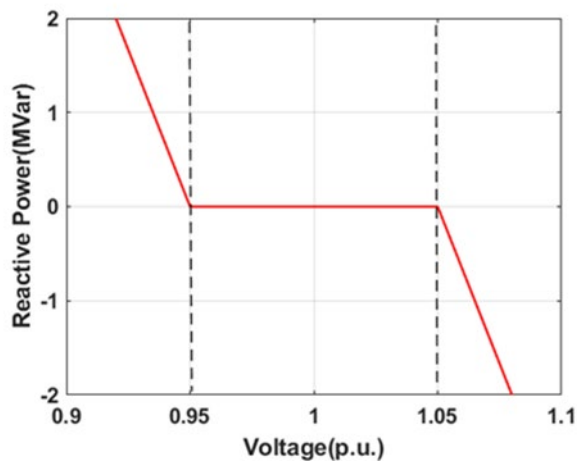


**Figure 43.** Proposed QU-droop control

### 5.2.2.3 Study results discussion and conclusions

The methodology for the development of aging aware adaptive controllers for ANM applications for studying its impact on SSG has been developed and explained in detail in previous sections. In the developed ANM scheme, the role of Li-ion BESS active-power dispatch is to enhance wind power generation and utilization of reactive power flexibilities from WTG and to manage MV distribution system voltage in Li-ion BESS. The impact of such adaptive  $P$ -control on the operation of the ANM scheme in SSG will be explored by means of simulation studies. Simulations are designed to simulate the power system over a long period of time (hours to few days), to validate the effectiveness of the designed ANM secondary controllers ( $P$ -,  $QU$ -, and  $PU$ - controllers) and verify the control set-points provided to them. Such large-scale and longer time horizon power system

simulations are computationally demanding. Therefore, real-time simulations are utilized in these studies from Publication P7.

The real-time simulation models for these studies have been developed on the ePhasorSim platform on the OPAL-RT system, details of which are explained Section 4.3. The power system model of SSG is similar to those in previous studies in Publications P4 and P6, except the change in the battery model which includes their aging characteristics and the Li-ion BESS controllers whose power outputs are governed by their aging aware PP capability. It also has to be noted that in this simulation model, the OLTC of HV/MV transformer is not considered to study threshold limits in the management of flexibilities from available RESs. The major objective of this study is to analyse how battery aging affects its charge/discharge power output and their impact on ANM operations in SSG. Three subcases (1–3) are defined and studied in the following text.

*a) Subcase 1: Base Case (Nonactive ANM scheme)*

In subcase 1, SSG is simulated without flexibilities from BESS and WTG operating in the MV distribution system, which is considered as the base case for comparison purposes. The simulations are performed for a period of three days with a time-step of one second. This approach allows us to record the active and reactive power flows and the voltage measurements at various MV buses in the power system without any ANM being active. The SSG WTG is of PMSG type and is connected to a grid by a full-power converter, thereby allowing it to absorb or inject reactive power to 100% of its rated power. In this case, the *QU*-control of the WTG is disabled to record the original characteristics in the SSG without the operation of any FERs adhering to the IEEE 1547-2018 (IEEE Standard Association, 2018) guidelines. Notably, the presence of the OLTC transformer has been omitted in this case study to understand the capability of flexibility services on voltage stability issues. Based on the simulation results, the voltages at various MV buses are seen to be between 0.94 and 0.95 p.u. (mainly due to omission of OLTC transformer), which is outside the preferred limits determined in standards and/or grid codes. The graphical representation of the results can be found from Publication P7.

*a) Subcase 2: Active ANM scheme and new Li-ion BESS (At 0 cycles of operation)*

From the previous case, it has been understood that the voltages in the MV distribution system are not within the limits specified by standards and grid codes. Hence, in subcase 2, the ANM scheme has been activated, where reactive power flexibilities from Li-ion BESS and the WTG are activated. The characteristics of Li-ion BESS are chosen to be that of a new battery system with 0 charge/discharge

cycles. This is to allow us to understand the power and energy characteristics a new Li-ion BESS can support for ANM scheme needs.

From the simulation results, it has been confirmed that the *QU*-control loop has been activated and helped in boosting the MV distribution system voltages within the threshold specified by the standards and grid codes, i.e., greater than 0.95 p.u. Notably, the reactive power services from WTG alone were enough for *QU*-control. During the simulation period of 3 days, the Li-ion BESS was cycled, i.e., charged or discharged for 14 times. The amount of active-power dispatch (based on *P*-control system of ANM scheme) during each of the cycles when the battery is new can be seen from column 2 of Table 7. The negative sign refers to the discharge power and the positive sign refers to the charge power in Table 6. The graphical results on voltage characteristics and active-power charge and discharge from the Li-ion BESS can be found from Publication P7.

*b) Subcase 3: Active ANM scheme and used Li-ion BESS (After 1200 cycles of operation)*

The objective of this case is to understand the impact of Li-ion BESS aging on its performance, particularly the peak load it can support. In this simulation case, the Li-ion BESS has been considered to have undergone considerable aging, i.e., about 1200 cycles of charge/discharge operations. The power dispatch of aged battery that comes from *P*-control of the ANM scheme is as shown in column 3 of Table 7.

**Table 7.** Li-ion BESS peak power dispatch comparison in Case 2 subcases 2 and 3 (– means discharging of BESS and + charging of BESS)

Cycle number	Subcase 2 Li-ion BESS Active-Power dispatch (kW)	Subcase 3 Li-ion BESS Active-Power dispatch (kW)
1	-631,4	-559,2
2	+603,7	+561,8
3	-556,4	-519,7
4	+438,5	+438,5
5	+174,6	+174,6
6	-282,7	-282,7
7	+264,1	+264,1
8	-310,4	-310,4
9	+478,7	+478,7
10	-345,9	-345,9
11	+44,4	+44,4
12	-52,1	-52,1
13	+183,7	+183,7
14	-537,1	-515,9

It can be observed from Table 7 that the PP outputs are observed to be lesser in magnitude, compared to subcase 2, where the cycles are deep with higher DOD and  $P_{\text{BESS,REF}}$ . From Table 6 it shall be observed that the cycles 1, 2, 3 and 14 which has higher power levels compared to other pulses and  $P_{\text{BESS,REF}}$  are seen to have a dip in the PP dispatch. This is due to the  $P$ -control characteristics, which tends to lower PP of Li-ion BESS with aging. The graphical results can be seen from Publication P7.

An age influenced adaptive  $P$ -control layer (for Li-ion BESS) in the ANM scheme has been proposed in this study from Publication P7, which considers the operational battery SOH (number of completed charge/discharge cycles) as input to the control system. The BMS (within  $P$ -control layer), comprises an accurate SOEC Li-ion battery model that generates accurate voltage, power, and energy characteristics of the Li-ion battery cell, considering battery SOC and SOH as its affecting parameters. The BMS also hosted the PP calculation algorithm, which provides the PP reference of the battery cell at all instances of the SOH. The overall objective of the  $P$ -control layer was to generate the Li-ion BESS active-power reference, which is within the threshold of battery charge/discharge PP capability, which is defined by its SOH and provided by the PP calculation algorithm. Thus, the problem of managing the battery charge/discharge operations always within the threshold of their peak active-power performance is solved.

Based on the simulation results, it can be noted that the designed EMS controllers acted as required in providing flexibilities to manage system voltages within the threshold defined by grid codes. Despite aging aware control of Li-ion BESS using the  $P$ -controller of the EMS, it can be observed that the voltages were maintained within the threshold defined by standards and/or grid codes by the  $QU$ -control scheme. It can also be observed that the cycles with higher power discharge and DOD showed the influence of battery aging by reduced power dispatch with aging and the cycles with lower power discharge and DODs had no impacts on their power dispatch.

### 5.2.3 Case 3: Aging aware techno-economic analysis of Li-ion BESS providing flexibility services

Frequency control and stability of the power system is affected due to large scale addition of inertia-less and intermittent RESs. To mitigate these dynamic disturbances in the system, addition of more FERs is required. Li-ion BESS has been a preferred FER for frequency related services, particularly for frequency containment reserve for normal operation (FCR-N) (Groza, Kiene, Linkevics, & Gicevskis, 2022; Xia Wang, Ying, Wen, & Lu, 2022). Typically, for FCR-N services

in Finland, the battery system operates to frequency deviations from 0 to 0.1 Hz and  $-0.1$  to 0 Hz. However, the power and energy capability of Li-ion batteries decreases with aging. This means the capacity of the battery and its charge and discharge power levels decrease with aging. These changing characteristics must be considered while developing scheduling algorithms based on cost-based optimization studies for Li-ion BESS for stationary grid applications, as it bears a direct outcome on economic profitability for the battery owners.

Therefore, this study presents a method to schedule the charging and discharging power of Li-ion BESS while considering the effects of BESS cycle aging and its economic imposition based on Publication P9 of this thesis. In this simulation study, a 50 kWh BESS is supposed to react to the three-minute frequency changes and the corresponding outcome of battery utilization has been estimated for three months. The major objective of this study is to analyze how the consideration of cycle aging of batteries affects the Li-ion BESS economic outcome when providing services for FCR-N markets.

#### 5.2.3.1 FCR-N frequency control service provision by Li-ion BESS

FCR are deployed to regulate frequency in the power system continuously. FCR-N services react to the frequency changes from 0 to 0.1 Hz and  $-0.1$  to 0 Hz, which can occur due to various reasons such as intermittence from RESs and faults in the power system (Xia Wang et al., 2022). FCR-N is considered as a symmetrical service and market. This means that an FCR-N provider should be able to reserve both upward and downward services at the same time. Thus, a BESS that has the capability to be charged and discharged has good potential to be an FCR-N provider. The full reserve capacity of the FCR-N provider needs to be activated when the frequency goes below 49.9 Hz. Correspondingly, in cases where the frequency goes above 50.1 Hz, the resource should be fully activated with its 100% capacity. When the frequency level is within the range of 49.9–50.1 Hz, the activated capacity needs to be proportional to the magnitude of the frequency changes. In addition, when the frequency deviation occurs, the reserve should be activated in less than 3 minutes and it should not be delayed on purpose (Xia Wang et al., 2022).

When a BESS is an FCR-N provider and it reaches the maximum or minimum level of SOC, the service activation needs to be interrupted until the direction of the frequency changes. A balancing service provider is responsible for scheduling the charging and discharging level of the BESS. The recharging power, SOC management, and forecasting as well as scheduling timetable of BESS can be a challenge when it provides FCR-N services.

A BESS can be deployed as an FCR-N provider. In this way, the BESS is charged whenever the frequency increases from 50 to 50.1 Hz, which means that the system needs downward flexibility. The BESS is discharged in cases where the frequency falls between 50 and 49.9 Hz. In these cases, the system requires upward flexibility. The charging/discharging power needs to be proportional to the frequency deviation. In addition, there should be a local measurement device to direct the BESS toward the right amount and direction of power. Thus, the BESS is managed according to the local frequency measurement.

The monetization of reserves for FCR-N application provider occurs in two steps:

1. It receives a capacity payment for the amount of capacity that is reserved to respond to the frequency deviations.
2. It is paid if its upward flexible capacity is activated.

On the other hand, when downward capacity is activated, the FER, in this case a BESS, which needs to be charged from the power grid, should pay for its own consumption. However, it is worth mentioning that the prices of downward flexibility are always equal to or lower than those of the spot market (Khajeh, Firoozi, & Laaksonen, 2022b). This means that it is always more beneficial for a consumer to consume power based on downward regulation prices rather than spot market prices. Correspondingly, the prices of upward regulation are always equal to or higher than those of the spot market. Hence, it is more beneficial for a producer to provide upward flexibility and sell it into the reserve markets rather than the spot market (Khajeh et al., 2022b).

When Li-ion BESSs are utilized for FCR-N applications, it is understandable that their economics are affected by their changing capacity and power dispatch with cycle aging. Therefore, the techno-economic studies considering the aging characteristics are important, typically while considering their impacts on direct pricing of services. Hence, this study from Publication 9

1. Proposed a method and strategy to schedule the charging and discharging power of a Li-ion BESS that can count the cycle simultaneously and estimate the remaining capacity based on the exhausted cycles.
2. Obtained the economic outcome of a 50 kWh Li-ion BESS that responds to 3 min real measured frequencies and provides FCR-N. This outcome has been calculated with and without cycling effects for comparison purposes.

To carry out the studies mentioned above, the requirements were to develop an aging model, which provides details on the changing capacity of the Li-ion BESS



with respect to the cycles, followed by development of a BESS scheduling algorithm that was based on optimization studies. The final requirement was a cycle counting methodology. Their details are further explained in the following sections.

### 5.2.3.2 Li-ion BESS aging model

In this analysis, the requirement for the battery-aging model is simplified, i.e., the change in energy of a 50 kWh battery pack with respect to different intervals of cycling. To develop this model, experimental data from accelerated aging tests of Li-ion battery cell in laboratory conditions were utilized. The aging tests are explained in Arunachala et al. (2016) in detail. Capacity characterization tests were performed, i.e., the cell capacity in Ah was measured at regular intervals of cycling, in this case at 0, 500, 800, 1200, and 1600 cycles. The cell capacities at different cycling intervals are as shown in Table 8.

The next step was to size a 50 kWh battery pack, whose nominal power is 100 kW and PP is 150 kW. To do so, the first step was to convert the cell capacity in Ah to its energy capability at different cycle intervals in Wh, which is described by Eq. (31). Now, based on these cell energy parameters, a 50 kWh battery pack was designed. This was achieved using Eq. (32), where the energy of the designed pack is based on the energy of the cell times the number of cells in series ( $N_s$ ) and in parallel ( $N_p$ ). Based on this, the energy of the battery pack at different cycling intervals can be calculated. Then, a polynomial regression is deployed to obtain the relationship between the Li-ion BESS capacity and the cycle. Finally, the mean squared error (MSE) criteria are utilized to choose the best fitted function. Regarding our data, the best fitted function that models the Li-ion BESS capacity based on its charging/discharging cycle was a polynomial of degree 4. Fig. 47 depicts the curve fitted on the data, which is an extrapolation from 1600 cycles of testing from the laboratory data.

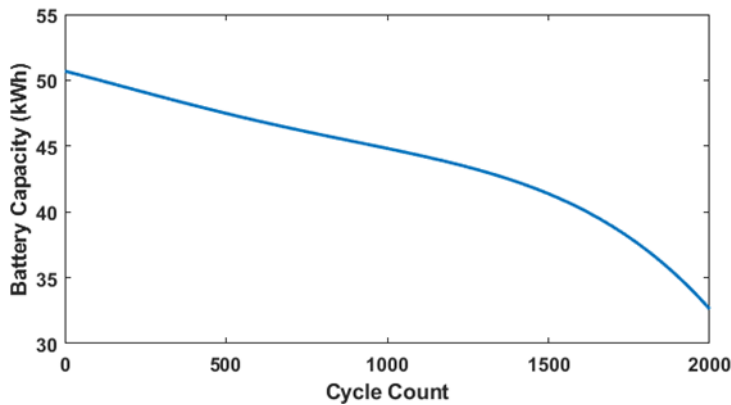
From Fig. 44, it is evident that the cycling of Li-ion BESS can affect its maximum capacity of utilization. For the case of 50 kWh of a Li-ion BESS, its maximum capacity falls to less than 35 kWh after 2000 cycles. Accordingly, it is necessary to consider the BESS cycling effects when the study aims to assess the long-term economic outcome of the Li-ion BESS.

**Table 8.** Cell capacity at different cycles

Cycles	Capacity (Ah)
0	8.06
500	7.55
800	7.30
1200	6.97
1600	6.52

$$E_{Cell}(Cycles) = Cell\ Capacity(Cycles) * V_{cell} \quad (31)$$

$$E_{Pack} = E_{Cell} * N_S * N_P \quad (32)$$

**Figure 44.** Li-ion BESS capacity change with cycle aging

### 5.2.3.3 Li-ion BESS scheduling algorithm

BESS scheduling should be performed according to the volume and direction of the frequency deviation. Moreover, the power of charging/discharging should not result in the Li-ion BESS SOC exceeding its predefined limits. Therefore, a scheduling problem can be developed with the linear programming method. The problem is written separately for scheduling the charging and discharging power, as presented by Eqs. (33)–(41). Here,  $SOC^{min}$  is the lowest allowable SOC, while  $SOC^{max}$  indicates the higher limit defined for the SOC. Furthermore,  $\eta_{ch}$  and  $\eta_{dis}$  denote the Li-ion BESS charging and discharging efficiencies, respectively.  $Cap(Cycle_t)$  is the function that calculates the value of the BESS maximum capacity based on the real-time cycle at  $t$  ( $Cap(Cycle_t)$ ). The derivation of this function has been explained in this section. The cycle is also counted using the method proposed in Section 5.2.3.4.

$P_t$  is the scheduled power determined by solving Eqs. (33)–(40). If the frequency deviation at  $t$ , that is  $FD_t \geq 0$ , the BESS needs to provide downward flexibility by charging the BESS. Thus,  $P_t$  is also positive and the optimization problem (33)–(36) should be solved. Otherwise, if the frequency deviation is negative, the BESS should be discharged. The discharging power can be obtained by solving (37)–(40).

In the optimization problems,  $P^{max}$  is the absolute value of charging/discharging power. As previously stated, an FCR-N provider should be activated with the power that is proportional to the frequency deviation. Regarding FCR-N services, the ratio of the frequency deviation equals  $\frac{FD_t}{0.1}$ . This means that the charging power should be equal to or lower than  $\frac{FD_t}{0.1} \times P^{max}$ , and the discharging power should be equal to or higher than  $\frac{FD_t}{0.1} \times P^{max}$ . If the BESS SOC does not limit the charging/discharging power, optimization problems in Eqs. (33)–(36) and (37)–(40) yield  $P_t = \frac{FD_t}{0.1} \times P^{max}$ . Otherwise, it gives us the highest absolute value of discharging/charging power that maintains the SOC within the permissible range.

*If  $FD_t \geq 0$  then the BESS is charging with  $P_t \geq 0$ :*

$$\max_{P_t} P_t \quad (33)$$

*Subject to:*

$$0 \leq P_t \leq \frac{FD_t}{0.1} \times P^{max} \quad (34)$$

$$SOC_t = SOC_{t-1} + \frac{\eta_{ch} P_t}{Cap(Cycle_t)} \Delta t \quad (35)$$

$$SOC^{min} \leq SOC_t \leq SOC^{max} \quad (36)$$

*If  $FD_t < 0$  then the BESS is discharging with  $P_t < 0$ :*

$$\min_{P_t} P_t \quad (37)$$

*Subject to:*

$$\frac{FD_t}{0.1} \times P^{max} \leq P_t \leq 0 \quad (38)$$

$$SOC_t = SOC_{t-1} + \frac{P_t}{\eta_{dis} \times Cap(Cycle_t)} \Delta t \quad (39)$$

$$SOC^{min} \leq SOC_t \leq SOC^{max} \quad (40)$$

Where:

$$FD_t = freq_t - 50 \quad (41)$$

#### 5.2.3.4 Cycle counting methodology

An online cycle counting method is required for this study, which is based on modifying the method proposed by Gundogdu & Gladwin (2018). According to this method, the first step calculates the SOC change within the predefined time slot. If the SOC increases, it means that the Li-ion BESS was charging. Hence, it adds the SOC increase to the value of a variable denoted by  $SOC_t^{ch}$ . It should be noted that this variable is totally different from the BESS SOC at  $t$  denoted by  $SOC_t$ . The variable  $SOC_t^{ch}$  is just used to calculate the Li-ion BESS cycle. If  $SOC_t^{ch}$  reaches its maximum level, which is one, the cycle increases by 0.5 and the  $SOC_t^{ch}$  is reset to one. Otherwise, the algorithm continues with the current cycle.

Correspondingly, if the SOC decreases during one time slot, the battery was discharging. Hence, the change is added to another variable denoted by  $SOC_t^{dis}$ . This variable is just utilized to calculate the cycle. If  $SOC_t^{dis}$  approaches its minimum level, i.e., zero, the cycle increases by 0.5 and the  $SOC_t^{dis}$  is reset to zero. This algorithm ends when the BESS stops being charged and discharged. Fig. 45 summarizes the method adopted to calculate the Li-ion BESS cycle counting.

#### 5.2.3.5 Case 3: Study results discussion and conclusions

A case study has been designed to observe the economic impacts of the aging aware BESS scheduling algorithm in this section. The proposed methodology was tested on a 50 kWh Li-ion BESS. The frequency data required for the case studies were obtained from “Fingrid Open Data on the Electricity Market and the Power System” (Gundogdu & Gladwin, 2018), Fingrid, the Finnish TSO. The data in use were the frequency recordings from January 1 to March 31, 2021, with a 3-minute time interval. A graphical representation of the frequency data is represented in Fig. 46. The objective of this study is to understand how a 50 kWh, Li-ion BESS can cater to the frequency fluctuation by providing FCR-N services, and how those services may get impacted by battery-aging characteristics. Fig. 47 explains the steps designed to schedule the charging and discharging power of the Li-ion BESS as well as obtain the outcomes in terms of their utilization and economics. The

charging/discharging power of the BESS was scheduled according to the proposed methodology in a previous section.

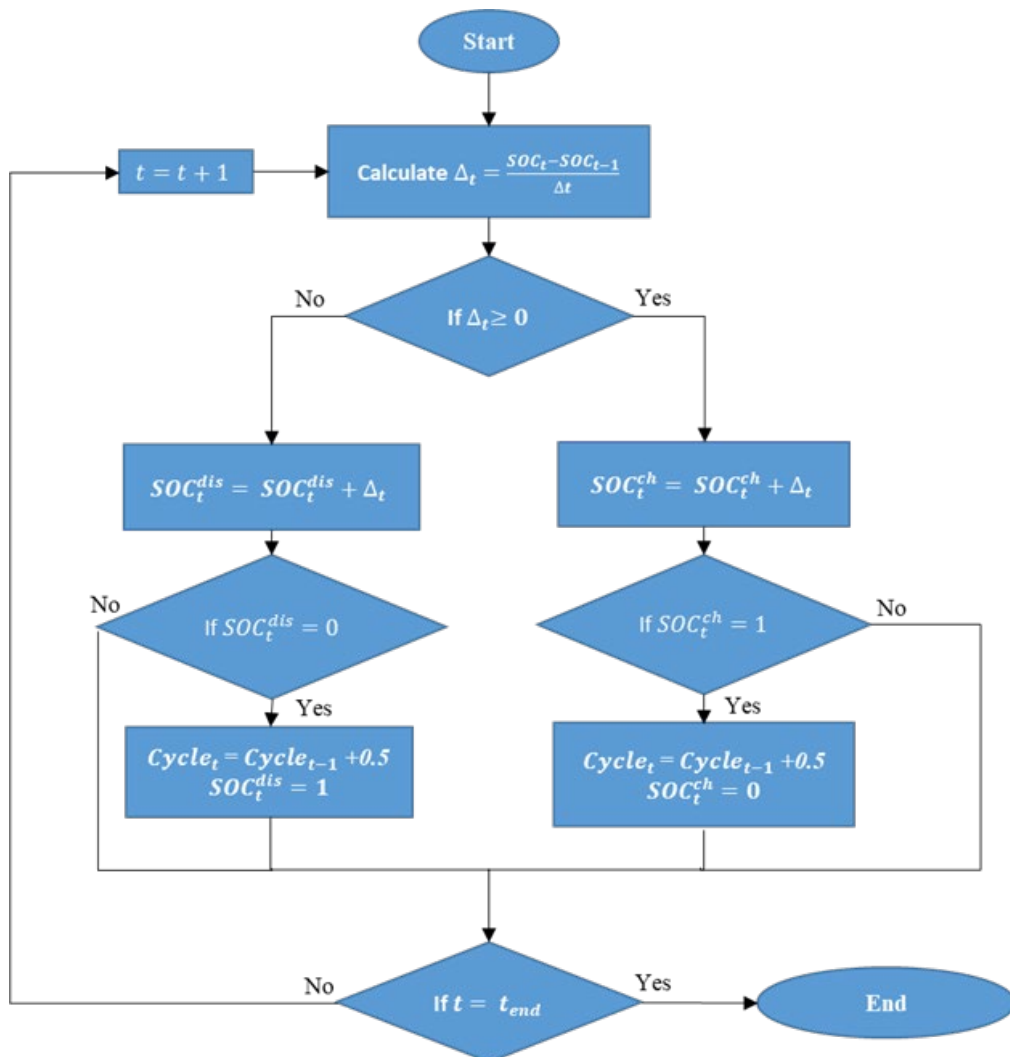


**Figure 45.** Flowchart representing cycle counting methodology

The simulation results are presented in Fig. 48 and 49. They indicate the charging power (negative values for discharging and positive values for charging) as well as the BESS SOC variations. As Fig. 51 and 52 state, BESS continuously reacts to the frequency changes. The initial BESS SOC for the simulation was considered to be 50%.

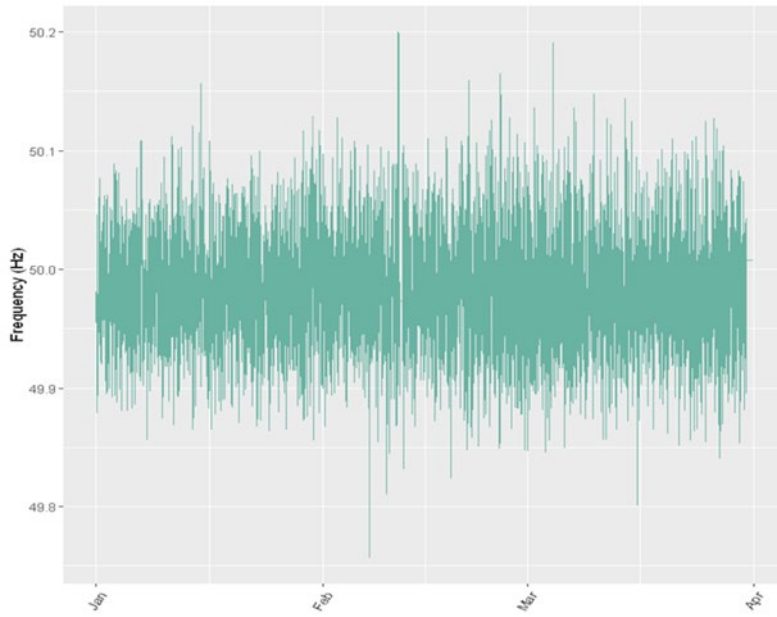


**Figure 46.** Frequencies measured for each three minutes in Jan–March 2021

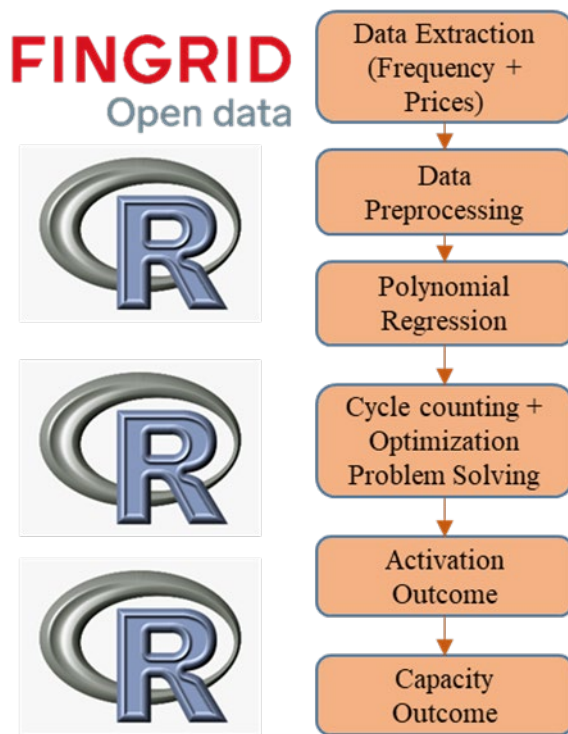


**Figure 47.** The steps to calculate the outcome of the BESS providing FCR-N

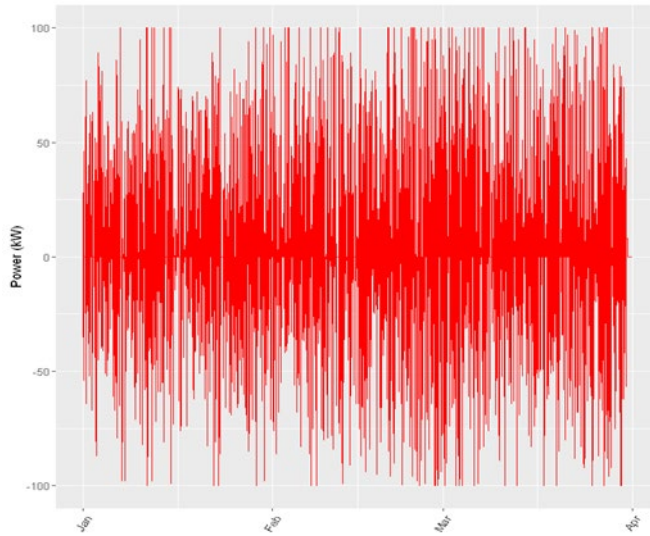


**Figure 48.** Charging/discharging power obtained after scheduling the BESS based on the frequency deviations

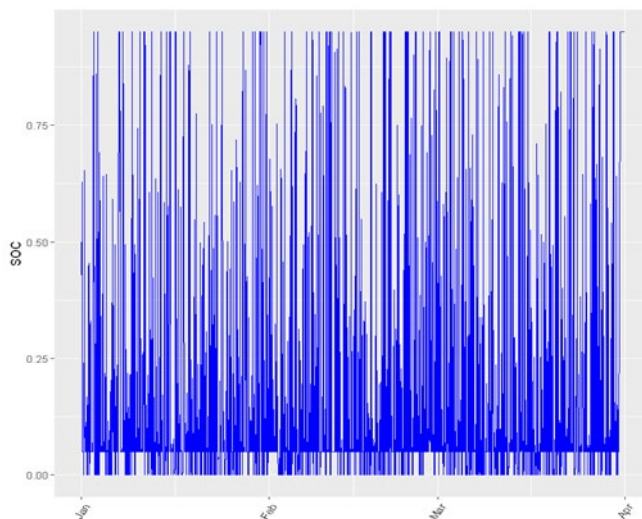


**Figure 49.** BESS SOC variations after responding to the frequency changes

*a) Overall economic analysis*

This subsection analyzes the economic outcomes of the BESS participating in the FCR-N provision. As stated before, the BESS as an FCR-N provider has two resources of the outcome. It receives payment for the capacity it has reserved for providing FCR-N. In 2021, the capacity price for providing 1 kWh FCR-N was equal to 1.25 Cents. The FCR-N is activated by charging and discharging the BESS. Regarding this case study, the BESS was being charged and the prices of downward regulations were paid. It was being discharged and received the prices of

downward regulations. Fig. 53 depicts the upward and downward regulation prices for the defined time period. From Fig. 53, it is evident that the prices of upward regulation are always equal to or higher than those of downward regulation.

The BESS makes profits by receiving the capacity payment and the upward activation payment. However, it should pay according to the downward prices for its charging power. The total activation outcome and capacity outcome were calculated for the BESS regarding the three-month period. The results are shown in Table 9. The table shows a negative activation outcome, which means that in total, the system needed more downward flexibility than the upward one. Hence, the BESS should pay approximately € 169. In contrast, the BESS receives a rather high payment equalling € 1348 for reserving its capacity for the FCR-N service. In total, the BESS paid nearly € 1178 for its three-month participation in providing the FCR-N service.

**Table 9.** Results obtained after scheduling BESS based on the proposed method

Capacity Outcome (cent)	Activation Outcome (cent)	The Number of Cycles	Total Outcome (cent)	Final SOC
134812.5	-16955.199	234	117857.3	0.95

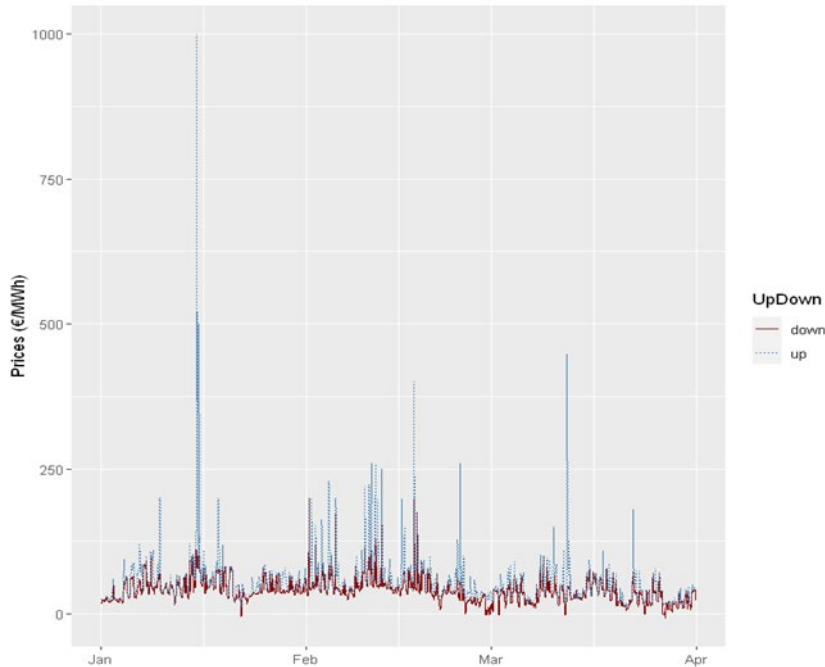


**Figure 50.** Upward and downward regulation prices during January to March 2021



a) *Effect of BESS cycle aging*

From simulation results, the effects of BESS cycling aging in the process of BESS scheduling shall be obtained. For this purpose, two study cases are considered where one considers the aging effect and the other does not for comparison purposes. In this way, BESS capacity has a constant value and is not a function of the cycle. Accordingly, the charging/discharging power is scheduled, and the outcomes are calculated. To analyze the effect of cycling in an economic way, an indicator has been proposed that calculates the total outcome for each cycle. The indicator is denoted by the total outcome per cycle (TOPC), which is calculated for the BESS with and without BESS cycling effects. The results are shown in Table 10. The table states that aging decreases the BESS profits by 6.06 Cent in each cycle. Therefore, it provides information on how Li-ion BESS affects economic profitability when utilized for FCR-N application.

**Table 10.** TOPC indicator with and without cycle aging effects

	<b>With BESS cycling effects</b>	<b>Without BESS cycling effects</b>
TOPC [Cent/kWh]	503.66	509.72

RES rich power systems require more FERs participating in the provision of frequency regulation services. In this regard, BESS is a very potential resource that can provide different types of technical ancillary (i.e., flexibility) services. The FCR-N market needs a symmetrical flexibility service provision. This paper focused on the provision of the FCR-N service by a Li-ion BESS which had the ability to be charged and discharged and was capable of being an FCR-N provider. Further, this paper discussed the participation of a Li-ion BESS in providing FCR-N, considering the effects of BESS cycling aging, particularly their degradation effects, on battery capacity.

This study proposed a methodology that schedules the BESS in a way to be proportional to frequency deviations. The charging/discharging power was based on the direction and volume of the frequency deviation. In addition, the methodology includes the effects of Li-ion BESS cycling on its capacity. Finally, the proposed method was implemented on a 50 kWh Li-ion BESS. The BESS was scheduled according to real frequencies measured for three months, and the economic outcomes were discussed. Furthermore, the results demonstrate that aging can decrease the BESS profits by 6.06 Cent in each cycle.

### 5.3 Conclusions

The application base of Li-ion BESS has increased multi-fold for grid application in recent times, especially their utilization in ANM and frequency control related services. However, their diminishing power and energy characteristics with utilization is a cause of concern for their operation (in terms of safety characteristics) and its economic profitability an issue for the battery system owner. Therefore, in chapter 5, the cycle aging of Li-ion batteries has been considered as an affecting parameter in the design of Li-ion BESS controllers (both ANM scheme and adaptive droop controllers for FCR operations) and in the techno-economic analysis for FCR-N applications in particular. The impact of battery cycle aging on the operations of Li-ion BESS for grid application were analyzed based on three case studies from publications P7, P8, and P9.

For the first case (case 1 from Publication P8), the aging model (PP capability) was developed based on the datasheet characteristics, as this particular type of battery system is already installed in Finland. This case study was designed on the data available from that particular battery system in the field. Including the aging model in the proposed adaptive droop controller in the studies provided information on the impacts of Li-ion BESS power dispatch as the battery ages.

In the second case study (case 2 from Publication P7), an aging model (PP capability) was developed based on the data available from accelerated aging tests conducted in the laboratory. This aging model was directly integrated to the ANM architecture through its *P*-control of the EMS. The battery controller was designed to limit the PP of the battery based on the values commanded by the aging model. The impact of such an ANM scheme was studied by means of simulation studies in SSG, using the real-time simulation platform, OPAL-RT. From the simulation results, it was observed that the deep cycles of charge and discharge (high DOD and C-rate) had changes in its power dispatch commanded by the *P*-control and that of cycles with a lowed C-rate, and the DODs power dispatch remained unaffected.

The third case study (case 3 from Publication P9) required capacity fade of Li-ion batteries in the aging model. Hence, a model was developed based on experimental data available from accelerated aging tests on a Li-ion battery cell. The changing capacity of the cell in Ah's was converted to that of a 50 kWh battery pack under study. The impact of using such aging models in the Li-ion BESS scheduling problem provided a clear understanding of its changing economic profitability, i.e., the profit from new BESS was different from that of an aged BESS.

## 6 CONCLUSIONS

ANM provides an opportunity for efficient management of the FERs for flexibility service provision for DSOs, for various operational requirements, such as, to mitigate voltage and frequency fluctuations. FERs play an essential role by offering different flexibility services for DSOs as well as for TSOs in future RES-based power systems. They provide ways for improved utilization of the existing network capacity without excessive passive network component upgrades and achieving a more reliable and efficient network operation.

Inverter-based BESSs can be seen as ideal FERs due to their potential and versatility in providing multiple active and reactive power related flexibility services for different DSO and TSO needs such as for voltage and frequency control, black start, islanding, load leveling, and peak shaving. Thus, BESSs are useful for bridging the gap between nonconcurrent RES-based power generation and demand at different voltage levels of the power system.

The technical characteristics and modularity of Li-ion batteries have led to their wide utilization in different power system applications. However, their technical characteristics are highly nonlinear and are affected by various factors such as their ambient operational temperature, SOC, DOD, C-rate of charge and discharge, and most particularly, their aging patterns. Such highly variable performance features must be considered while developing Li-ion BESS control schemes and studying their economic profitability in different grid applications. Publication P1 introduces the ANM topics and the role of BESSs. Publications [P2 and P3 contain details on modeling Li-ion BESS integration and modeling for grid applications.

This thesis focused on studying the utilization of Li-ion BESSs for multiple local and system-wide flexibility service provision in case of local (DSO) and system-wide (TSO) needs, especially ANM in electricity distribution networks. The scope included the design and development of a grid-specific ANM control architecture as well as the design and development of the EMS as part of the ANM scheme including control of different FERs [P4], [P5], [P6], and [P7]. A major focus in control design was on the development of accurate control for Li-ion BESSs by including their performance characteristics and features obtained from the developed SOEC [P4]–[P6] and battery-aging models [P7] and [P8]. The thesis also evaluated the effects of variable performance metrics of Li-ion BESSs on economic profitability through techno-economic studies including aging considerations [P9]. The overall battery integration methodology, design, and development of controllers have been enhanced by considering the accurate

performance characteristics of Li-ion BESSs based on the new knowledge obtained compared to the existing literature.

The battery performance models are based on the SOEC technique, which has been developed using HPPC tests in the battery cell test laboratory at the University of Vaasa (Fig. 38, Chapter 5) during the thesis. In addition, Li-ion battery cycle aging models have been developed through accelerated aging tests in the laboratory, which were used in Publications [P8] and [P9].

The general level research targets in this thesis can be briefly summarized as follows:

1. Design and develop ANM scheme functionalities for managing the available flexibilities of various DERs, especially to generate the appropriate control signals for the FERs, particularly Li-ion BESS, inverters in the distribution network.
2. Development of high-accuracy equivalent-circuit battery models capable of emulating battery performance at different SOC, C-rate, temperature, and aging conditions.
3. Integrating the high-accuracy battery models with BESS DC/DC- and AC/DC-inverters in different simulation and operation modes.
4. Development of Li-ion BESS active and reactive power controllers for ANM functionality to support multiuse case scenarios, where the control related to active-power dispatch considers factors such as Li-ion battery aging and their performance at various C-rates and temperatures, along with their SOC being within the safe operating regions.
5. Study the effects of Li-ion BESS inverter operation on the Li-ion BESS performance, including the electrical and thermal effects of Li-ion batteries and understand the Li-ion BESS inverter control interactions and its impacts to the distribution network through multiple case studies.
6. Analyse the effects of Li-ion BESS control on its controller development philosophies and study the aging effects on the economic profitability of Li-ions when it is used for stationary grid applications.

The following sections presents the main contributions of the thesis, possible limitations of the research work, and the potential future research topics.

## 6.1 Main contributions

The main contribution of the thesis are as follows:

### **1. Design of grid specific ANM architecture and its validation**

The thesis proposed the development of an ANM control architecture methodology (grid specific in this case SSG) that manages available flexibility in the distribution system for stable grid operation. The proposed ANM scheme and their adjoining controller operations have been validated by means of various case studies in different simulation environments (i.e., short-term and long-term control validation studies).

### **2. Accurate battery models development for the grid integration studies of Li-ion BESS**

An accurate SOEC model emulating the Li-ion BESS performance characteristics was integrated in the battery integration simulation studies to replace more generic battery models used in existing literature. In short-term control design studies, they provide accurate voltage and SOC reference parameters, and in long-term control design studies, they provide accurate power and energy attributes of the battery in addition to the voltage, SOC, and DOD.

### **3. Improved power system simulation modeling methods**

EMT simulation platform has been utilized to model short-term control validation of ANM schemes, and for long-term control validation, the power system models were developed in the OPAL-RT real-time simulation platform. By integrating accurate battery performance models in both the simulation platforms, the overall power system modeling methodology was improved considerably (for Li-ion battery control design and validation studies) compared to existing methods in the literature.

### **4. Mapping the required battery parameters and performance features for advanced control design and development of Li-ion BESS when they are used for flexibility service provision and ANM schemes**

The complexity of the battery model for various power system related studies depends on the battery parameters that are required for the design and development of its inverter and grid-side controllers. Based on the extensive studies conducted in this thesis, the battery parameter requirement from battery models was understood. Table 11 provides information on mapping relevant battery parameters that are of utmost importance for the design and development of Li-ion BESS controllers (both for short-term and long-term applications) for ANM applications and for techno-economic studies.

**Table 11.** Mapping Battery Parameter Requirement for Controller Development Studies

<b>Battery Parameters</b>	<b>Short-Term Control</b>	<b>Long-Term Control</b>	<b>Long-Term Cost Optimisation Modelling</b>
State of Charge	☒	☑	☑
State of Health	☒	☒	☑
Depth of Discharge	☒	☒	☑
Voltage	☑	☑	☒
Current	☑	☑	☒
Temperature	☒	☒	☑
Battery Aging	☒	☑	☑

### **5. Aging aware adaptive control development of Li-on BESS for ANM simulations and techno-economic studies**

Li-ion battery aging, as explained earlier, causes irreparable damages in the battery system that causes degradation in its performance attributes such as its energy and power dispatch over its lifetime. This thesis developed battery-aging models that consider the evolving PP characteristics of Li-ion BESS in the development of adaptive battery control as part of ANM control architecture for secondary control [P8], developed an adaptive droop controller for a real-life Li-ion BESS which is utilized for frequency control service provision through FCR-N market participation [P7], and developed a simplified Li-ion BESS aging aware model for economic profitability related studies [P9].

## **6.2 Thesis limitations and future research directions**

In this thesis, accurate and enhanced battery integration modeling and control were studied and developed for stationary grid-connected Li-ion BESSs, considering particularly local and system-wide services and applications like ANM and frequency control (FCR-N). It was also proposed to utilize more accurate battery models for techno-economic studies to understand the profitability from

the owners' perspective. In addition to the current contribution, the further possibility of extending the research scope exists. Potential future research topics and areas can be combined under three categories as follows:

### **1. Aging characterization and modeling of Li-ion batteries**

In this thesis, the developed aging model was based on accelerated aging experiments that captured the cycle aging of Li-ion batteries by experimental characterization. When BESSs are utilized for grid applications, they remain in standby mode without cycling for a considerable amount of time. Therefore, an aging model that depicts both cycle and calendar aging of Li-ion batteries is important. Therefore, design, development, and execution of accelerated aging tests for capturing the calendar aging characteristics and integrating with the existing cycle aging model is suggested for further future research.

The PP evolution of Li-ion batteries was considered as the aging parameter for controller development studies in this thesis. For long-term control and techno-economic studies, it is also important to understand the change of resistance and capacity degradation of the batteries, which can provide more accurate and realistic indication regarding the power and energy characteristics of the BESS. Hence, the future scope of work could include development of algorithms that would help in modeling other aging parameters, i.e., resistance change and capacity degradation of the BESS.

To further improve the accuracy of the aging models, it is important to consider real-life field use characteristics of Li-ion batteries while designing aging characterization tests. Therefore, it is suggested that the design and development of accelerated aging tests which are based on the historical or real-time data including the charge/discharge and rest characteristics in an actual application are utilized in future research studies.

### **2. Further development of aging aware adaptive battery controllers for grid applications**

Development of aging aware adaptive battery controllers for grid applications has been a fairly new research topic in the existing literature, and there exists large scope for its further exploration. The repercussion of the proposed development of high-accuracy aging models for BESS requires also further development aging aware Li-ion BESS controllers, i.e., at both the inverter- and grid-side (EMS) controllers for stationary grid-connected BESSs.

With the development of extensive and enhanced aging models for Li-ion BESSs, their threshold points of operation could be further understood, especially in cases where aging models are based on the field measurement data. This will help in utilizing more accurate battery-aging parameters in addition to the PP evolution that has been studied in this thesis. Therefore, further improved novel methodologies for the development of aging aware battery system controllers can be explored in the future. Further, the impact of such aging aware adaptive controllers on the battery system's health and on the power system operation where it provides various services needs to be studied even more in detail.

### **3. Development of techno-economic research methods**

In this thesis, first, an attempt was made to integrate battery-aging models which represents a change in battery capacity (in kWh) with respect to cycle aging conditions for techno-economic analysis to evaluate the economic profitability of the BESS and to develop improved battery scheduling algorithms. The knowledge on this topic has been scarce in the existing research literature. With the proposed development of calendar aging algorithms and other high-accuracy battery-aging models, there exists a scope for improvement in the accuracy of the techno-economic analysis of grid-connected BESSs, providing different system-wide and/or local flexibility services.



## References

\$3.40 Trillion to be Invested Globally in Renewable Energy by 2030, Finds Frost & Sullivan. (n.d.). Retrieved May 24, 2022, from <https://www.frost.com/news/press-releases/3-40-trillion-to-be-invested-globally-in-renewable-energy-by-2030-finds-frost-sullivan/>

Abapour, S., Nojavan, S., & Abapour, M. (2018). Multi-objective short-term scheduling of active distribution networks for benefit maximization of DisCos and DG owners considering demand response programs and energy storage system. *Journal of Modern Power Systems and Clean Energy*, 6(1), 95–106. <https://doi.org/10.1007/s40565-017-0313-0>

Abogaleela, M., & Kopsidas, K. (2019). Battery energy storage degradation impact on network reliability and wind energy curtailments. *2019 IEEE Milan PowerTech, PowerTech 2019*, 1–6. <https://doi.org/10.1109/PTC.2019.8810801>

Active Network Management Enables Addition of 8.5 MW of Renewables to Shetland Islands Grid. (n.d.). Retrieved June 1, 2022, from <https://www.renewableenergyworld.com/storage/active-network-management-enables-addition-of-8-5-mw-of-renewables-to-shetland-islands-grid/>

Scrosati, W.A. Advances in Lithium-Ion Batteries. (2002). *Springer Science & Business Media*. <https://doi.org/10.1007/B113788>

Aggarwal, R. (2003). Electromagnetic transients. *Electrical Engineer's Reference Book: Sixteenth Edition*, 1–16. <https://doi.org/10.1016/B978-075064637-6/50036-8>

Agubra, V., & Fergus, J. (2013). Lithium ion battery anode aging mechanisms. *Materials*, 6(4), 1310–1325. <https://doi.org/10.3390/ma6041310>

Akagi, S., Yoshizawa, S., Ito, M., Fujimoto, Y., Miyazaki, T., Hayashi, Y., ... Yano, T. (2020). Multipurpose control and planning method for battery energy storage systems in distribution network with photovoltaic plant. *International Journal of Electrical Power and Energy Systems*, 116, 105485. <https://doi.org/10.1016/j.ijepes.2019.105485>

Alaperä, I., & Hakala, T. (2019). *25 th International Conference on Electricity Distribution Battery System as a Service for a Distribution System Operator 25 th International Conference on Electricity Distribution Madrid, 3-6 June 2019 Main design characteristics*. (June), 3–6.

Allahham, A., Greenwood, D., Patsios, C., & Taylor, P. (2022). Adaptive receding horizon control for battery energy storage management with age-and-operation-dependent efficiency and degradation. *Electric Power Systems Research*, 209, 107936. <https://doi.org/10.1016/J.EPSR.2022.107936>

Alsharif, H., Jalili, M., & Hasan, K. N. (2021). A comparative analysis of centralised vs. distributed battery energy storage system in providing frequency regulation. *2021 IEEE PES Innovative Smart Grid Technologies - Asia, ISGT Asia 2021*, 1–5. <https://doi.org/10.1109/ISGTASIA49270.2021.9715576>

Anees, A. S. (2012). Grid integration of renewable energy sources: Challenges, issues and possible solutions. *India International Conference on Power Electronics, IICPE*, 1–6. <https://doi.org/10.1109/IICPE.2012.6450514>

Arunachala, R., Parthasarathy, C., Jossen, A., & Garche, J. (2016). Inhomogeneities in large format lithium ion cells: A study by battery modelling approach. *ECS Transactions*, 73(1), 201–212. <https://doi.org/10.1149/07301.0201ecst>

Ates, M., & Chebil, A. (2022). Supercapacitor and battery performances of multi-component nanocomposites: Real circuit and equivalent circuit model analysis. *Journal of Energy Storage*, 53(April), 105093. <https://doi.org/10.1016/j.est.2022.105093>

Bako, Z. N., Tankari, M. A., Lefebvre, G., & Maiga, A. S. (2019). Experiment-based methodology of kinetic battery modeling for energy storage. *IEEE Transactions on Industry Applications*, 55(1), 593–599. <https://doi.org/10.1109/TIA.2018.2866148>

Barré, A., Deguilhem, B., Grolleau, S., Gérard, M., Suard, F., & Riu, D. (2013). A review on lithium-ion battery ageing mechanisms and estimations for automotive applications. *Journal of Power Sources*, 241, 680–689. <https://doi.org/10.1016/j.jpowsour.2013.05.040>

Battery costs rise as lithium demand outstrips supply - Nikkei Asia. (n.d.). Retrieved June 2, 2022, from <https://asia.nikkei.com/Spotlight/Market-Spotlight/Battery-costs-rise-as-lithium-demand-outstrips-supply>

Battery storage system is connected to transmission grid | E&T Magazine. (n.d.). Retrieved June 2, 2022, from <https://eandt.theiet.org/content/articles/2021/06/battery-storage-system-connected-to-transmission-grid/>

Blaabjerg, F., Teodorescu, R., Liserre, M., & Timbus, A. V. (2006). Overview of control and grid synchronization for distributed power generation systems. *IEEE Transactions on Industrial Electronics*, 53(5), 1398–1409. <https://doi.org/10.1109/TIE.2006.881997>

BloombergNEF: Average battery pack prices to drop below US\$100/kWh by 2024 despite near-term spikes - Energy Storage News. (n.d.). Retrieved June 2, 2022, from <https://www.energy-storage.news/bloombergnef-average-battery-pack-prices-to-drop-below-us100-kwh-by-2024-despite-near-term-spikes/>

Boundless. (2015). *Free Energy and Cell Potential*. Retrieved from <https://www.boundless.com/chemistry/textbooks/boundless-chemistry-textbook/electrochemistry-18/cell-potentials-130/free-energy-and-cell-potential-520-1929/>

Braithwaite, J. W., Gonzales, A., Nagasubramanian, G., Lucero, S. J., Peebles, D. E., Ohlhausen, J. A., & Cieslak, W. R. (1999). Corrosion of lithium-ion battery current collectors. *Journal of the Electrochemical Society*, 146(2), 448–456. <https://doi.org/10.1149/1.1391627>

Briceno-Vicente, W. (2022). Grid code requirements in the UK for the connection of BESS in wind systems. *Cigre Science & Engineering*.

Carr, S., Premier, G. C., Guwy, A. J., Dinsdale, R. M., & Maddy, J. (2014). Energy storage for active network management on electricity distribution networks with wind power. *IET Renewable Power Generation*, 8(3), 249–259. <https://doi.org/10.1049/IET-RPG.2012.0210>

Aristizábal, A. J., Herrera, J., Castañeda, M., Zapata, S., Ospina, D., & Banguero, E. (2019). A new methodology to model and simulate microgrids operating in low latitude countries. *Energy Procedia*, 157, 825–836. <https://doi.org/10.1016/j.egypro.2018.11.248>

CEI - 0-21 - Reference technical rules for the connection of active and passive users to the LV electrical Utilities | Engineering360. (n.d.). Retrieved November 1, 2022, from <https://standards.globalspec.com/std/14505609/0-21>

Chauhan, P. J., Reddy, B. D., Bhandari, S., & Panda, S. K. (2019). Battery energy storage for seamless transitions of wind generator in standalone microgrid. *IEEE Transactions on Industry Applications*, 55(1), 69–77. <https://doi.org/10.1109/TIA.2018.2863662>

Choi, D., Shamim, N., Crawford, A., Huang, Q., Vartanian, C. K., Viswanathan, V. V., ... Sprenkle, V. L. (2021a). Li-ion battery technology for grid application. *Journal of Power Sources*, 511, 230419. <https://doi.org/10.1016/J.JPOWSOUR.2021.230419>

Wu, J., Jing, G., & Yi, Z. (2022). Stability analysis and Simulation of power system based on Matlab. *Journal of Physics: Conference Series*, 2260, 12054. <https://doi.org/10.1088/1742-6596/2260/1/012054>

D'Antona, G., Faranda, R., Hafezi, H., & Bugliesi, M. (2016). Experiment on bidirectional single phase converter applying model predictive current controller. *Energies*, 9(4), 233. <https://doi.org/10.3390/en9040233>

Daniel, C., & Besenhard, J. O. (2011). *Handbook of Battery Materials Fundamentals and General Aspects of*.

Das, C. K., Bass, O., Kothapalli, G., Mahmoud, T. S., & Habibi, D. (2018a). Overview of energy storage systems in distribution networks: Placement, sizing, operation, and power quality. *Renewable and Sustainable Energy Reviews*, 91, 1205–1230. <https://doi.org/10.1016/J.RSER.2018.03.068>

Datta, U., Kalam, A., & Shi, J. (2019). The relevance of large-scale battery energy storage (BES) application in providing primary frequency control with increased wind energy penetration. *Journal of Energy Storage*, 23(February), 9–18. <https://doi.org/10.1016/j.est.2019.02.013>

Datta, U., Kalam, A., & Shi, J. (2020). Smart control of BESS in PV integrated EV charging station for reducing transformer overloading and providing battery-to-grid service. *Journal of Energy Storage*, 28, 101224. <https://doi.org/10.1016/j.est.2020.101224>

Davies, D. M., Verde, M. G., Mnyshenko, O., Chen, Y. R., Rajeev, R., Meng, Y. S., & Elliott, G. (2018). Combined economic and technological evaluation of battery energy storage for grid applications. *Nature Energy*, *4:1*, 4(1), 42–50. <https://doi.org/10.1038/s41560-018-0290-1>

de Hoog, J., Timmermans, J. M., Ioan-Stroe, D., Swierczynski, M., Jaguemont, J., Goutam, S., ... Van Den Bossche, P. (2017). Combined cycling and calendar capacity fade modeling of a nickel-manganese-cobalt oxide cell with real-life profile validation. *Applied Energy*, *200*, 47–61. <https://doi.org/10.1016/j.apenergy.2017.05.018>

Ding, K., Liu, J., Wang, X., Zhang, X., & Wang, N. (2016). Research of an active and reactive power coordinated control method for photovoltaic inverters to improve power system transient stability. *China International Conference on Electricity Distribution, CIGRE, 2016*, 1–5. <https://doi.org/10.1109/CIGRE.2016.7576223>

Douglas, J., Creighton, A., Roper, P., & Ault, G. (2007). *Overview of active network management developments and practices in Great Britain*. 21–24.

Edström, K., Gustafsson, T., & Thomas, J. O. (2004). The cathode-electrolyte interface in the Li-ion battery. *Electrochimica Acta*, *50*(2-3 SPEC. ISS.), 397–403. <https://doi.org/10.1016/j.electacta.2004.03.049>

Ahmed, R., El Sayed, M., Arasaratnam, I., Tjong, J., & Habibi, S. (2014). Reduced-order electrochemical model parameters identification and SOC estimation for healthy and aged Li-Ion batteries part I: Parameterization model development for healthy batteries. *IEEE Journal of Emerging and Selected Topics in Power Electronics*, *2*(3), 659–677. <https://doi.org/10.1109/jestpe.2014.2331059>

MEV Team. (2008). *A Guide to Understanding Battery Specifications*. Massachusetts Institute of technology, USA, Tech. Rep.

Feng, L., Zhang, X., Li, C., Li, X., Li, B., Ding, J., ... Chen, H. (2022). Optimization analysis of energy storage application based on electricity price arbitrage and ancillary services. *Journal of Energy Storage*, *55*(PB), 105508. <https://doi.org/10.1016/j.est.2022.105508>

Fingrid. (2020). *Grid Code Specifications for Grid Energy Storage Systems SJV2019. 1*(73), 1–73.

Förster, H., Nissen, C., Siemons, A., Renders, N., Dael, S., Sporer, M., ... European Environment Agency. (2021). *Trends and projections in Europe 2021*.

Gao, Y., Jiang, J., Zhang, C., Zhang, W., & Jiang, Y. (2018). Aging mechanisms under different state-of-charge ranges and the multi-indicators system of state-of-health for lithium-ion battery with Li(NiMnCo)O<sub>2</sub> cathode. *Journal of Power Sources*, *400*(3), 641–651. <https://doi.org/10.1016/j.jpowsour.2018.07.018>

Ghadi, M. J., Rajabi, A., Ghavidel, S., Azizivahed, A., Li, L., & Zhang, J. (2019). From active distribution systems to decentralized microgrids: A review on

regulations and planning approaches based on operational factors. *Applied Energy*, 253, 113543. <https://doi.org/10.1016/J.APENERGY.2019.113543>

Ghorbanzadeh, M., Astaneh, M., & Golzar, F. (2019). Long-term degradation based analysis for lithium-ion batteries in off-grid wind-battery renewable energy systems. *Energy*, 166, 1194–1206. <https://doi.org/10.1016/j.energy.2018.10.120>

Gokhale-Welch, C., & Stout, S. (2019). *Key considerations for adoption of technical codes and standards for battery energy storage systems in Thailand*. Retrieved from [www.nrel.gov/publications](http://www.nrel.gov/publications) (accessed date).

Grey, C. P., & Hall, D. S. (2020). Prospects for lithium-ion batteries and beyond—A 2030 vision. *Nature Communications*, 11(1), 6279. <https://doi.org/10.1038/s41467-020-19991-4>

Growth Opportunities from Decarbonisation in the Global Power Market, 2019–2030. (n.d.). Retrieved May 24, 2022, from <https://store.frost.com/growth-opportunities-from-decarbonisation-in-the-global-power-market-2019-2030.html>

Groza, E., Kiene, S., Linkevics, O., & Gicevskis, K. (2022). Modelling of battery energy storage system providing FCR in Baltic power system after synchronization with the continental synchronous area. *Energies*, 15(11), 3977. <https://doi.org/10.3390/en15113977>

Gundogdu, B., & Gladwin, D. T. (2018). A fast battery cycle counting method for grid-tied battery energy storage system subjected to microcycles. *IEECON 2018 - 6th International Electrical Engineering Congress*. <https://doi.org/10.1109/IEECON.2018.8712263>

Hasanpor Divshali, P., & Evens, C. (2020). Optimum operation of battery storage system in frequency containment reserves markets. *IEEE Transactions on Smart Grid*, 11(6), 4906–4915. <https://doi.org/10.1109/TSG.2020.2997924>

Hawley, W. B., Parejiya, A., Bai, Y., Meyer, H. M., Wood, D. L., & Li, J. (2020). Lithium and transition metal dissolution due to aqueous processing in lithium-ion battery cathode active materials. *Journal of Power Sources*, 466(May), 228315. <https://doi.org/10.1016/j.jpowsour.2020.228315>

Heiskanen, S. K., Kim, J., & Lucht, B. L. (2019). Generation and evolution of the solid electrolyte interphase of lithium-ion batteries. *Joule*, 3(10), 2322–2333. <https://doi.org/10.1016/j.joule.2019.08.018>

Hesse, H. C., Schimpe, M., Kucevic, D., & Jossen, A. (2017). Lithium-ion battery storage for the grid - A review of stationary battery storage system design tailored for applications in modern power grids. *Energies*, 10(12), en10122107. <https://doi.org/10.3390/en10122107>

Holjevac, N., Baškarad, T., Đaković, J., Krpan, M., Zidar, M., & Kuzle, I. (2021). Challenges of high renewable energy sources integration in power systems—the case of croatia. *Energies*, 14(4), EN14041047. <https://doi.org/10.3390/EN14041047>

Home. (n.d.). Retrieved November 1, 2022, from <https://www.entsoe.eu/>

Hu, R., Wang, W., Wu, X., Chen, Z., Jing, L., Ma, W., & Zeng, G. (2022). Coordinated active and reactive power control for distribution networks with high penetrations of photovoltaic systems. *Solar Energy*, *231*, 809–827. <https://doi.org/10.1016/j.solener.2021.12.025>

IEEE 1547-2018 - IEEE standard for interconnection and interoperability of distributed energy resources with associated electric power systems interfaces. (n.d.). Retrieved April 10, 2019, from <https://standards.ieee.org/standard/1547-2018.html>

IEEE SA - IEEE 1547-2018. (n.d.). Retrieved November 1, 2022, from <https://standards.ieee.org/ieee/1547/5915/>

IEEE Standard Association. (2018). IEEE Std. 1547-2018. Standard for Interconnection and Interoperability of Distributed Energy Resources with Associated Electric Power Systems Interfaces. In *IEEE Std 1547-2018 (Revision of IEEE Std 1547-2003)*.

Inal, O. B., Charpentier, J. F., & Deniz, C. (2022). Hybrid power and propulsion systems for ships: Current status and future challenges. *Renewable and Sustainable Energy Reviews*, *156*, 111965. <https://doi.org/10.1016/J.RSER.2021.111965>

Intercalation (chemistry) - Wikipedia, the free encyclopedia. (n.d.). Retrieved June 16, 2015, from [https://en.wikipedia.org/wiki/Intercalation\\_\(chemistry\)](https://en.wikipedia.org/wiki/Intercalation_(chemistry))

Introducing the Phasor Simulation Method - MATLAB & Simulink - MathWorks Nordic. (n.d.). Retrieved June 6, 2022, from <https://se.mathworks.com/help/physmod/sps/powersys/ug/introducing-the-phasor-simulation-method.html>

Iurilli, P., Brivio, C., & Merlo, M. (2019). SoC management strategies in battery energy storage system providing primary control reserve. *Sustainable Energy, Grids and Networks*, *19*, 100230. <https://doi.org/10.1016/j.segan.2019.100230>

Iurilli, P., Brivio, C., & Wood, V. (2021). On the use of electrochemical impedance spectroscopy to characterize and model the aging phenomena of lithium-ion batteries: a critical review. *Journal of Power Sources*, *505*, 229860. <https://doi.org/10.1016/j.jpowsour.2021.229860>

Janakiraman, U., Garrick, T. R., & Fortier, M. E. (2020). Review—Lithium plating detection methods in li-ion batteries. *Journal of The Electrochemical Society*, *167*(16), 160552. <https://doi.org/10.1149/1945-7111/abd3b8>

Jin, X. (2022). Aging-Aware optimal charging strategy for lithium-ion batteries: Considering aging status and electro-thermal-aging dynamics. *Electrochimica Acta*, *407*, 139651. <https://doi.org/10.1016/J.ELECTACTA.2021.139651>

Kalogiannis, T., Jagemont, J., Omar, N., Van Mierlo, J., & Van den Bossche, P. (2019). A comparison of internal and external preheat methods for NMC batteries.

*World Electric Vehicle Journal*, 10(2), 1–16.  
<https://doi.org/10.3390/wevj10020018>

Khajeh, H., Firoozi, H., & Laaksonen, H. (2022a). Flexibility potential of a smart home to provide TSO-DSO-level services. *Electric Power Systems Research*, 205(December 2021), 107767. <https://doi.org/10.1016/j.epsr.2021.107767>

Khajeh, H., Firoozi, H., & Laaksonen, H. (2022b). Flexibility potential of a smart home to provide TSO-DSO-level services. *Electric Power Systems Research*, 205, 107767. <https://doi.org/10.1016/J.EPSR.2021.107767>

Khan, W., Ahmad, A., Ahmad, F., & Saad Alam, M. (2018). A comprehensive review of fast charging infrastructure for electric vehicles. *Smart Science*, 6(3), 256–270. <https://doi.org/10.1080/23080477.2018.1437323>

Kirli, D., & Kiprakis, A. (2020). Techno-economic potential of battery energy storage systems in frequency response and balancing mechanism actions. *The Journal of Engineering*, 2020(9), 774–782. <https://doi.org/10.1049/joe.2019.1053>

Knowledge Base | PSCAD. (n.d.). Retrieved June 8, 2022, from <https://www.pscad.com/knowledge-base/topic-35/v->

Krupp, A., Beckmann, R., Diekmann, T., Ferg, E., Schuldt, F., & Agert, C. (2022). Calendar aging model for lithium-ion batteries considering the influence of cell characterization. *Journal of Energy Storage*, 45, 103506. <https://doi.org/10.1016/J.EST.2021.103506>

Kryonidis, G. C., Kontis, E. O., Papadopoulos, T. A., Pippi, K. D., Nousedilis, A. I., Barzegkar-Ntovom, G. A., ... Papanikolaou, N. P. (2021a). Ancillary services in active distribution networks: A review of technological trends from operational and online analysis perspective. *Renewable and Sustainable Energy Reviews*, 147(March), 111198. <https://doi.org/10.1016/j.rser.2021.111198>

Kryonidis, G. C., Kontis, E. O., Papadopoulos, T. A., Pippi, K. D., Nousedilis, A. I., Barzegkar-Ntovom, G. A., ... Papanikolaou, N. P. (2021b). Ancillary services in active distribution networks: A review of technological trends from operational and online analysis perspective. *Renewable and Sustainable Energy Reviews*, 147, 111198. <https://doi.org/10.1016/J.RSER.2021.111198>

Laaksonen, H., Parthasarathy, C., Hafezi, H., Shafie-Khah, M., & Khajeh, H. (2020). Control and management of distribution networks with flexible energy resources. *International Review of Electrical Engineering (I.R.E.E.)*, 15(3). <https://doi.org/10.15866/iree.v15i3.18592>

Laaksonen, H., Parthasarathy, C., Hafezi, H., Shafie-khah, M., Khajeh, H., & Hatzargyriou, N. (2020). Solutions to increase PV hosting capacity and provision of services from flexible energy resources. *Applied Sciences (Switzerland)*, 10(15). <https://doi.org/10.3390/app10155146>

Laaksonen, H., Parthasarathy, C., Khajeh, H., & Shafie-Khah, M. (2021a). Adaptation of der control schemes and functions during MV network back-up

connection. *SEST 2021 - 4th International Conference on Smart Energy Systems and Technologies*. <https://doi.org/10.1109/SEST50973.2021.9543168>

Laaksonen, H., Parthasarathy, C., Khajeh, H., & Shafie-Khah, M. (2021b). Adaptation of der control schemes and functions during MV network back-up connection. *SEST 2021 - 4th International Conference on Smart Energy Systems and Technologies*, 1–6. <https://doi.org/10.1109/SEST50973.2021.9543168>

Laaksonen, H., Sirviö, K., Aflecht, S., & Hovila, P. (2019). *Multi-objective Active Network Management Scheme Studied in Sandom Smart Grid with MV and LV connected DER Units*. In *Proceedings of 25th International Conference on Electricity Distribution: CIRED 2019: Madrid, 3-6 June 2019*. CIRED.

Lacerda, Vinicius A., Araujo, E. P., Cheah-Mane, M., & Gomis-Bellmunt, O. (2022). Phasor modeling approaches and simulation guidelines of voltage-source converters in grid-integration studies. *IEEE Access*, 10(1), 51826–51838. <https://doi.org/10.1109/access.2022.3174958>

Lawder, M. T., Suthar, B., Northrop, P. W. C., De, S., Hoff, C. M., Leitermann, O., ... Subramanian, V. R. (2014). Battery energy storage system (BESS) and battery management system (BMS) for grid-scale applications. *Proceedings of the IEEE*, 102(6), 1014–1030. <https://doi.org/10.1109/JPROC.2014.2317451>

Lee, Y. R., Kim, H. J., & Kim, M. K. (2021). Optimal operation scheduling considering cycle aging of battery energy storage systems on stochastic unit commitments in microgrids. *Energies*, 14(2), 470. <https://doi.org/10.3390/EN14020470>

Lee, Y. R., Kim, H. J., & Kim, M. K. (2022). Correction to: Lee et al. Optimal operation scheduling considering cycle aging of battery energy storage systems on stochastic unit commitments in microgrids. (*Energies* (2021), 14, 470). *Energies*, 15(6), en15062107. <https://doi.org/10.3390/en15062107>

Li, C., Disfani, V. R., Pecenak, Z. K., Mohajeryami, S., & Kleissl, J. (2018). Optimal OLTC voltage control scheme to enable high solar penetrations. *Electric Power Systems Research*, 160, 318–326. <https://doi.org/10.1016/j.epsr.2018.02.016>

Li, X., & Wang, S. (2019). A review on energy management, operation control and application methods for grid battery energy storage systems. *CSEE Journal of Power and Energy Systems*. <https://doi.org/10.17775/cseejpes.2019.00160>

Li, Yang, Vilathgamuwa, M., Choi, S. S., Farrell, T. W., Tran, N. T., & Teague, J. (2019). Development of a degradation-conscious physics-based lithium-ion battery model for use in power system planning studies. *Applied Energy*, 248(May), 512–525. <https://doi.org/10.1016/j.apenergy.2019.04.143>

Li, Yang, Vilathgamuwa, M., Choi, S. S., Xiong, B., Tang, J., Su, Y., & Wang, Y. (2020). Design of minimum cost degradation-conscious lithium-ion battery energy storage system to achieve renewable power dispatchability. *Applied Energy*, 260(November 2019), 114282. <https://doi.org/10.1016/j.apenergy.2019.114282>



- Li, Yong, Song, J., & Yang, J. (2014). A review on structure model and energy system design of lithium-ion battery in renewable energy vehicle. *Renewable and Sustainable Energy Reviews*, 37, 627–633.  
<https://doi.org/10.1016/J.RSER.2014.05.059>
- Lin, C., Tang, A., Mu, H., Wang, W., & Wang, C. (2015). Aging mechanisms of electrode materials in lithium-ion batteries for electric vehicles. *Journal of Chemistry*, 2015. <https://doi.org/10.1155/2015/104673>
- Lin, X., Khosravinia, K., Hu, X., Li, J., & Lu, W. (2021a). Lithium plating mechanism, detection, and mitigation in lithium-ion batteries. *Progress in Energy and Combustion Science*, 87, 100953.  
<https://doi.org/10.1016/j.pecs.2021.100953>
- Linden, D., & Reddy, T. B. (1995). *Handbook of batteries*. *Fuel and Energy Abstracts*, 4(36), 265.
- Liu, J., Duan, Q., Ma, M., Zhao, C., Sun, J., & Wang, Q. (2020). Aging mechanisms and thermal stability of aged commercial 18650 lithium ion battery induced by slight overcharging cycling. *Journal of Power Sources*, 445, 227263.  
<https://doi.org/10.1016/j.jpowsour.2019.227263>
- Liu, J., Duan, Q., Qi, K., Liu, Y., Sun, J., Wang, Z., & Wang, Q. (2022). Capacity fading mechanisms and state of health prediction of commercial lithium-ion battery in total lifespan. *Journal of Energy Storage*, 46, 103910.  
<https://doi.org/10.1016/j.est.2021.103910>
- Liu, C., Wen, X., Zhong, J., Liu, W., Chen, J., Zhang, J., Wang, Z., & Liao, Q. (2022). Characterization of aging mechanisms and state of health for second-life 21700 ternary lithium-ion battery. *Journal of Energy Storage*, 55, 105511.  
<https://doi.org/10.1016/J.EST.2022.105511>
- Liu, K., Gao, Y., Zhu, C., Li, K., Fei, M., Peng, C., ... Han, Q.-L. (2022). Electrochemical modeling and parameterization towards control-oriented management of lithium-ion batteries. *Control Engineering Practice*, 124, 105176.  
<https://doi.org/10.1016/J.CONENGPRAC.2022.105176>
- Lund, P. D. & Lindgren, J. & Mikkola, J. & Salpakari, J. (2015). Review of energy system flexibility measures to enable high levels of variable renewable electricity. *Renewable and Sustainable Energy Reviews*, 45, 758–807.  
<https://doi.org/10.1016/j.rser.2015.01.057>
- Maeyaert, L., Vandeveldel, L., & Döring, T. (2020). Battery storage for ancillary services in smart distribution grids. *Journal of Energy Storage*, 30, 101524.  
<https://doi.org/10.1016/J.EST.2020.101524>
- Manwell, J. F., & McGowan, J. G. (1993). Lead acid battery storage model for hybrid energy systems. *Solar Energy*, 50(5), 399–405.  
[https://doi.org/10.1016/0038-092X\(93\)90060-2](https://doi.org/10.1016/0038-092X(93)90060-2)

- Masias, A., Marcicki, J., & Paxton, W. A. (2021). Opportunities and challenges of lithium ion batteries in automotive applications. *ACS Energy Letters*, 6(2), 621–630. <https://doi.org/10.1021/acsenergylett.0c02584>
- Meng, J., Luo, G., Ricco, M., Swierczynski, M., Stroe, D.-I., & Teodorescu, R. (2018). Overview of lithium-ion battery modeling methods for state-of-charge estimation in electrical vehicles. *Applied Sciences*, 8(5), 659. <https://doi.org/10.3390/app8050659>
- Meschede, E., Schlachter, U., Diekmann, T., Hanke, B., & von Maydell, K. (2022). Assessment of sector-coupling technologies in combination with battery energy storage systems for frequency containment reserve. *Journal of Energy Storage*, 49(August 2021), 104170. <https://doi.org/10.1016/j.est.2022.104170>
- Mexis, I., & Todeschini, G. (2020). Battery energy storage systems in the United Kingdom: A review of current state-of-the-art and future applications. *Energies*, 13(14), 3616. <https://doi.org/10.3390/EN13143616>
- Miles, M. H. (2001). Recent advances in lithium battery technology. *GaAs IC Symposium. IEEE Gallium Arsenide Integrated Circuit Symposium. 23rd Annual Technical Digest 2001 (Cat. No.01CH37191)*, 219–222. <https://doi.org/10.1109/GAAS.2001.964382>
- Mishra, D. K., Ghadi, M. J., Azizivahed, A., Li, L., & Zhang, J. (2021). A review on resilience studies in active distribution systems. *Renewable and Sustainable Energy Reviews*, 135, 110201. <https://doi.org/10.1016/J.RSER.2020.110201>
- Mousavi G., S. M., & Nikdel, M. (2014). Various battery models for various simulation studies and applications. *Renewable and Sustainable Energy Reviews*, 32, 477–485. <https://doi.org/10.1016/j.rser.2014.01.048>
- Müller, M. (2018). *Stationary Lithium-Ion Battery Energy Storage Systems A Multi-Purpose Technology*. (Doctoral dissertation, Technische Universität München).
- Mureddu, M., Facchini, A., & Damiano, A. (2018). A statistical approach for modeling the aging effects in Li-ion energy storage systems. *IEEE Access*, 6, 42196–42206. <https://doi.org/10.1109/ACCESS.2018.2859817>
- Musallam, M., & Johnson, C. M. (2012). An efficient implementation of the rainflow counting algorithm for life consumption estimation. *IEEE Transactions on Reliability*, 61(4), 978–986. <https://doi.org/10.1109/TR.2012.2221040>
- Nejad, S., Gladwin, D. T., & Stone, D. A. (2016). A systematic review of lumped-parameter equivalent circuit models for real-time estimation of lithium-ion battery states. *Journal of Power Sources*, 316, 183–196. <https://doi.org/10.1016/j.jpowsour.2016.03.042>
- Kurita, A., Okubo, H., Oki, K., Agematsu, S., Klapper, D. B., Miller, N. W.,... & Younkins, T. D. (1993). Multiple time-scale power system dynamic simulation. *IEEE Transactions on Power Systems*, 8(1), 216–223.

Oyj, F. (n.d.). *Appendix 2 to the Yearly Market Agreement and Hourly Market Agreement of Frequency Containment Reserves Unofficial translation The technical requirements and the prequalification process of Frequency Containment Reserves (FCR)*.

Padmanabhan, N., Ahmed, M., & Bhattacharya, K. (2020). Battery energy storage systems in energy and reserve markets. *IEEE Transactions on Power Systems*, 35(1), 215–226. <https://doi.org/10.1109/TPWRS.2019.2936131>

Panigrahy, N., Gopalakrishnan, K. S., Ilamparithi, T., & Kashinath, M. V. (2017). Real-time phasor-EMT hybrid simulation for modern power distribution grids. *IEEE International Conference on Power Electronics, Drives and Energy Systems, PEDES 2016, 2016* (1), 1–6. <https://doi.org/10.1109/PEDES.2016.7914270>

Parthasarathy, C., Hafezi, H., & Laaksonen, H. (2020). Lithium-ion BESS integration for smart grid applications - ECM modelling approach. In *2020 IEEE Power & Energy Society Innovative Smart Grid Technologies Conference (ISGT)* (pp. 1–5).

Parthasarathy, C., Sirviö, K., Hafezi, H., & Laaksonen, H. (n.d.). Modelling battery energy storage systems for active network management – coordinated control design and validation. *IET Renewable Power Generation*, 1–10.

Pinson, M. B., & Bazant, M. Z. (2013). Theory of SEI formation in rechargeable batteries: Capacity fade, accelerated aging and lifetime prediction. *ECS Meeting Abstracts, MA2013-01*(7), 405–405. <https://doi.org/10.1149/ma2013-01/7/405>

Plecas, M., Xu, H., & Kockar, I. (2017). Integration of energy storage to improve utilisation of distribution networks with active network management schemes. *CIGRE Open Access Proceedings Journal, 2017*(1), 1845–1848. <https://doi.org/10.1049/oap-cired.2017.1090>

Pusceddu, E., Zakeri, B., & Castagneto Gisse, G. (2021). Synergies between energy arbitrage and fast frequency response for battery energy storage systems. *Applied Energy*, 283, 116274. <https://doi.org/10.1016/j.apenergy.2020.116274>

Ramos, A., Tuovinen, M., & Ala-Juusela, M. (2021). Battery energy storage system (BESS) as a service in Finland: Business model and regulatory challenges. *Journal of Energy Storage*, 40, 102720. <https://doi.org/10.1016/j.est.2021.102720>

Rancilio, G., Rossi, A., Di Profio, C., Alborghetti, M., Galliani, A., & Merlo, M. (2020). Grid-scale BESS for ancillary services provision: SoC restoration strategies. *Applied Sciences (Switzerland)*, 10(12), 1–18. <https://doi.org/10.3390/APP10124121>

REISHUS CONSULTING. (2017). Electricity ancillary services primer. (August).

Renewable Energy Agency, I. (2018). Power system flexibility for the energy transition, Part 1: Overview for policy makers. Retrieved from [www.irena.org](http://www.irena.org)

Reniers, J. M., Mulder, G., Ober-Blöbaum, S., & Howey, D. A. (2018). Improving optimal control of grid-connected lithium-ion batteries through more accurate battery and degradation modelling. *Journal of Power Sources*, 379, 91–102. <https://doi.org/10.1016/j.jpowsour.2018.01.004>

Rodrigues, L., Leao, E., Montez, C., Moraes, R., Portugal, P., & Vasques, F. (2018). An advanced battery Model for WSN simulation in environments with temperature variations. *IEEE Sensors Journal*, 18(19), 8179–8191. <https://doi.org/10.1109/JSEN.2018.2863549>

Román-Ramírez, L. A., & Marco, J. (2022). Design of experiments applied to lithium-ion batteries: A literature review. *Applied Energy*, 320, 119305. <https://doi.org/10.1016/J.APENERGY.2022.119305>

Ryan, D. J., Razzaghi, R., Torresan, H. D., Karimi, A., & Bahrani, B. (2021). Grid-supporting battery energy storage systems in islanded microgrids: A data-driven control approach. *IEEE Transactions on Sustainable Energy*, 12(2), 834–846. <https://doi.org/10.1109/TSTE.2020.3022362>

Saboori, H., Hemmati, R., Ghiasi, S. M. S., & Dehghan, S. (2017). Energy storage planning in electric power distribution networks – A state-of-the-art review. *Renewable and Sustainable Energy Reviews*, Vol. 79, pp. 1108–1121. <https://doi.org/10.1016/j.rser.2017.05.171>

Sano, K., Yonezawa, R., & Noda, T. (2019). An electromagnetic transient simulation model of grid-connected inverters for dynamic voltage analysis of distribution systems. *Electrical Engineering in Japan*, 206(4), 11–21. <https://doi.org/10.1002/EEJ.23179>

Schuster, S. F., Bach, T., Fleder, E., Müller, J., Brand, M., SEXTL, G., & Jossen, A. (2015). Nonlinear aging characteristics of lithium-ion cells under different operational conditions. *Journal of Energy Storage*, 1(1), 44–53. <https://doi.org/10.1016/j.est.2015.05.003>

Sedighzadeh, M., Esmaili, M., Jamshidi, A., & Ghaderi, M. H. (2019). Stochastic multi-objective economic-environmental energy and reserve scheduling of microgrids considering battery energy storage system. *International Journal of Electrical Power and Energy Systems*, 106, 1–16. <https://doi.org/10.1016/j.ijepes.2018.09.037>

Shafique, H., Tjernberg, L. B., Archer, D. E., & Wingstedt, S. (2021). Energy management system (EMS) of battery energy storage system (BESS) - providing ancillary services. *2021 IEEE Madrid PowerTech, PowerTech 2021 - Conference Proceedings*. <https://doi.org/10.1109/PowerTech46648.2021.9494781>

Shi, Y., Xu, B., Tan, Y., Kirschen, D., & Zhang, B. (2019). Optimal battery control under cycle aging mechanisms in pay for performance settings. *IEEE Transactions on Automatic Control*, 64(6), 2324–2339. <https://doi.org/10.1109/TAC.2018.2867507>

Sirviö, K. H., Mekkanen, M., Kauhaniemi, K., Laaksonen, H., Salo, A., Castro, F., & Babazadeh, D. (2020). Accelerated real-time simulations for testing a reactive

power flow controller in long-term case studies. *Journal of Electrical and Computer Engineering*, 2020. <https://doi.org/10.1155/2020/8265373>

Sirviö, K., Laaksonen, H., & Kauhaniemi, K. (2020). Active network management scheme for reactive power control. (080), 7–8. Retrieved from <https://www.cired-repository.org/handle/20.500.12455/1099>

Sirviö, K., Mekkanen, M., Kauhaniemi, K., Laaksonen, H., Salo, A., Castro, F., ... Babazadeh, D. (2019). Controller development for reactive power flow management between DSO and TSO networks. *Proceedings of 2019 IEEE PES Innovative Smart Grid Technologies Europe, ISGT-Europe 2019*. <https://doi.org/10.1109/ISGTEurope.2019.8905578>

Sirvio, K., Valkkila, L., Laaksonen, H., Kauhaniemi, K., & Rajala, A. (2018). Prospects and costs for reactive power control in sundom smart grid. *Proceedings - 2018 IEEE PES Innovative Smart Grid Technologies Conference Europe, ISGT-Europe 2018*, 1–6. <https://doi.org/10.1109/ISGTEurope.2018.8571695>

Sperstad, I. B., Degefa, M. Z., & Kjølle, G. (2020). The impact of flexible resources in distribution systems on the security of electricity supply: A literature review. *Electric Power Systems Research*, 188(December 2019), 106532. <https://doi.org/10.1016/j.epsr.2020.106532>

Stecca, M., Ramirez Elizondo, L., Batista Soeiro, T., Bauer, P., & Palensky, P. (2020). A comprehensive review of the integration of battery energy storage systems into distribution networks. *IEEE Open Journal of the Industrial Electronics Society*, 1, 1. <https://doi.org/10.1109/ojies.2020.2981832>

*Supply of Reactive Power and Maintenance of Reactive Power Reserves Guideline*. (n.d.).

Tariq, M., Maswood, A. I., Gajanayake, C. J., & Gupta, A. K. (2018). Modeling and integration of a lithium-ion battery energy storage system with the more electric aircraft 270 v DC power distribution architecture. *IEEE Access*, 6, 41785–41802. <https://doi.org/10.1109/ACCESS.2018.2860679>

Tian, N., Fang, H., & Wang, Y. (2021). Real-time optimal lithium-ion battery charging based on explicit model predictive control. *IEEE Transactions on Industrial Informatics*, 17(2), 1318–1330. <https://doi.org/10.1109/TII.2020.2983176>

Trahey, L., Brushett, F. R., Balsara, N. P., Ceder, G., Cheng, L., Chiang, Y. M., ... Crabtree, G. W. (2020). Energy storage emerging: A perspective from the Joint Center for Energy Storage Research. *Proceedings of the National Academy of Sciences of the United States of America*, 117(23), 12550–12557. <https://doi.org/10.1073/PNAS.1821672117/ASSET/E61A4175-7286-4D4A-91DD-18259848BCCD/ASSETS/GRAPHIC/PNAS.1821672117FIG06.JPEG>

Turitsyn, K., Šulc, P., Backhaus, S., & Chertkov, M. (2010). Distributed control of reactive power flow in a radial distribution circuit with high photovoltaic penetration. *IEEE PES General Meeting, PES 2010*, 1–6. <https://doi.org/10.1109/PES.2010.5589663>

Use of Large Scale Energy Storage for Transmission System Support: Energy Storage as Black-Start Resource. (n.d.). Retrieved June 2, 2022, from <https://www.epri.com/research/products/3002001186>

Vazquez, S., Lukic, S. M., Galvan, E., Franquelo, L. G., & Carrasco, J. M. (2010). Energy storage systems for transport and grid applications. *IEEE Transactions on Industrial Electronics*, *57*(12), 3881–3895. <https://doi.org/10.1109/TIE.2010.2076414>

Vennam, G., Sahoo, A., & Ahmed, S. (2022). A survey on lithium-ion battery internal and external degradation modeling and state of health estimation. *Journal of Energy Storage*, *52*, 104720. <https://doi.org/10.1016/J.EST.2022.104720>

Vermeer, W., Chandra Mouli, G. R., & Bauer, P. (2022). A Comprehensive Review on the characteristics and modeling of lithium-ion battery aging. *IEEE Transactions on Transportation Electrification*, *8*(2), 2205–2232. <https://doi.org/10.1109/TTE.2021.3138357>

Vetter, J., Novak, P., Wagner, M. R., Veit, C., Müller, K. C., Besenhard, J. O., ... Hammouche, A. (2005). Ageing mechanisms in lithium-ion batteries. *Journal of Power Sources*, *147*(1–2), 269–281. <https://doi.org/10.1016/j.jpowsour.2005.01.006>

von Lüders, C., Zinth, V., Erhard, S. V., Osswald, P. J., Hofmann, M., Gilles, R., & Jossen, A. (2017). Lithium plating in lithium-ion batteries investigated by voltage relaxation and in situ neutron diffraction. *Journal of Power Sources*, *342*, 17–23. <https://doi.org/10.1016/j.jpowsour.2016.12.032>

Wali, S. B., Hannan, M. A., Ker, P. J., Rahman, M. A., Mansor, M., Muttaqi, K. M., ... Begum, R. A. (2022). Grid-connected lithium-ion battery energy storage system: A bibliometric analysis for emerging future directions. *Journal of Cleaner Production*, *334*, 130272. <https://doi.org/10.1016/J.JCLEPRO.2021.130272>

Wang, A., Kadam, S., Li, H., Shi, S., & Qi, Y. (2018). Review on modeling of the anode solid electrolyte interphase (SEI) for lithium-ion batteries. *Npj Computational Materials*, *4*(1). <https://doi.org/10.1038/s41524-018-0064-0>

Wang, G., Konstantinou, G., Townsend, C. D., Pou, J., Vazquez, S., Demetriades, G. D., & Agelidis, V. G. (2016). A review of power electronics for grid connection of utility-scale battery energy storage systems. *IEEE Transactions on Sustainable Energy*, *7*(4), 1778–1790. <https://doi.org/10.1109/TSTE.2016.2586941>

Wang, H., Li, X., Li, F., Liu, X., Yang, S., & Ma, J. (2021). Formation and modification of cathode electrolyte interphase: A mini review. *Electrochemistry Communications*, *122*, 106870. <https://doi.org/10.1016/j.elecom.2020.106870>

Wang, J., Purewal, J., Liu, P., Hicks-Garner, J., Soukazian, S., Sherman, E., ... Verbrugge, M. W. (2014). Degradation of lithium ion batteries employing graphite negatives and nickel-cobalt-manganese oxide + spinel manganese oxide positives: Part 1, aging mechanisms and life estimation. *Journal of Power Sources*, *269*, 937–948. <https://doi.org/10.1016/j.jpowsour.2014.07.030>

- Wang, T., & Cassandras, C. G. (2013). Optimal control of multibattery energy-aware systems. *IEEE Transactions on Control Systems Technology*, 21(5), 1874–1888. <https://doi.org/10.1109/TCST.2012.2219309>
- Wang, Xia, Ying, L., Wen, K., & Lu, S. (2022). Bi-level non-convex joint optimization model of energy storage in energy and primary frequency regulation markets. *International Journal of Electrical Power & Energy Systems*, 134, 107408. <https://doi.org/10.1016/J.IJEPES.2021.107408>
- Wang, Xueyuan, Wei, X., Zhu, J., Dai, H., Zheng, Y., Xu, X., & Chen, Q. (2021). A review of modeling, acquisition, and application of lithium-ion battery impedance for onboard battery management. *ETransportation*, 7, 100093. <https://doi.org/10.1016/J.ETRAN.2020.100093>
- Welcome - Fingridin avoin data. (n.d.). Retrieved October 27, 2022, from <https://data.fingrid.fi/en/>
- Wu, C., Lin, X., Sui, Q., Wang, Z., Feng, Z., & Li, Z. (2021). Two-stage self-scheduling of battery swapping station in day-ahead energy and frequency regulation markets. *Applied Energy*, 283(December 2020), 116285. <https://doi.org/10.1016/j.apenergy.2020.116285>
- Xiong, R., Pan, Y., Shen, W., Li, H., & Sun, F. (2020). Lithium-ion battery aging mechanisms and diagnosis method for automotive applications: Recent advances and perspectives. *Renewable and Sustainable Energy Reviews*, 131, 110048. <https://doi.org/10.1016/J.RSER.2020.110048>
- Xu, H., & Shen, M. (2021). The control of lithium-ion batteries and supercapacitors in hybrid energy storage systems for electric vehicles: A review. *International Journal of Energy Research*, 45(15), 20524–20544. <https://doi.org/10.1002/ER.7150>
- Zhang, L., Yu, Y., Li, B., Qian, X., Zhang, S., Wang, X., ... Chen, M. (2022a). Improved cycle aging cost model for battery energy storage systems considering more accurate battery life degradation. *IEEE Access*, 10, 297–307. <https://doi.org/10.1109/ACCESS.2021.3139075>
- Zhang, Q., Li, X., Du, Z., & Liao, Q. (2021). Aging performance characterization and state-of-health assessment of retired lithium-ion battery modules. *Journal of Energy Storage*, 40, 102743. <https://doi.org/10.1016/J.EST.2021.102743>
- Zhao, R., Lorenz, R. D., & Jahns, T. M. (2018). Lithium-ion battery rate-of-degradation modeling for real-time battery degradation control during EV drive cycle. *2018 IEEE Energy Conversion Congress and Exposition, ECCE 2018*, 2127–2134. <https://doi.org/10.1109/ECCE.2018.8558368>

## Appendices

### Appendix I: Li-ion battery operation and aging mechanisms

This appendix provides more details and insights regarding the working principles and aging mechanisms of Li-ion batteries as well as other terminologies related to their operations.

The main components of a secondary battery are the positive electrode (Linden & Reddy, n.d.), the negative electrode (Daniel & Besenhard, 2011), and the electrolyte (Miles, 2001). Redox reactions are responsible for the operation of rechargeable batteries, which store and release energy. Oxidation and reduction occur simultaneously in a redox reaction. The oxidation reaction occurs at the anode, which is responsible for the emission of electrons. An oxidation reaction is a reaction in which oxygen is reduced at the end. The cathode receives the electrons emitted from the anode through an external circuit, and a reduction reaction occurs subsequently that ends with the release of oxygen. Electrolytes act as a medium that helps transport ions in the various steps of redox reactions.

The cell voltage of each battery is determined by the choice of anode and cathode material, which can be related to the Gibbs free energy ( $\Delta G$ ) and the equilibrium cell voltage ( $E$ ), as shown in equation (42). The Gibbs free energy with respect to an electrochemical reaction is the chemical potential that is minimized when a system reaches equilibrium at constant pressure and temperature.  $F$  is the Faraday's constant, and  $n$  denotes the number of moles. A negative sign indicates that the chemical reaction is nonspontaneous (Boundless, 2015). The function of the electrolyte is to determine the rate of the reaction.

$$\Delta G = -nFE \quad (42)$$

In Li-ion batteries, the anode is usually composed of a carbon material that can accept and reversibly release significant amounts of lithium. The cathode is usually chosen as a transition metal oxide (e.g., LiCoO<sub>2</sub>), also known as an intercalation compound. Intercalation compounds are those that are capable of reversible insertion of a molecule with layered structures ("Intercalation (chemistry) - Wikipedia, the free encyclopedia," n.d.). Lithium ions are inserted interstitially into the host lattice during discharge and are subsequently extracted during charging without affecting the structural integrity of the cathode. Overall, lithium ions move from the anode to cathode during discharge and vice-versa during charge. At the anode, lithium ions are generated as a result of oxidizing reactions



and are followed by the release of an electron that travels through the external circuit establishing electrical conductivity, as depicted in Fig. 51. The lithium ions generated move toward the cathode region through the electrolyte and recombine with electrons from the external circuit, thereby completing the cathode reaction. This marks the end of the redox reaction. The chemical equations are

### Chemical Reactions

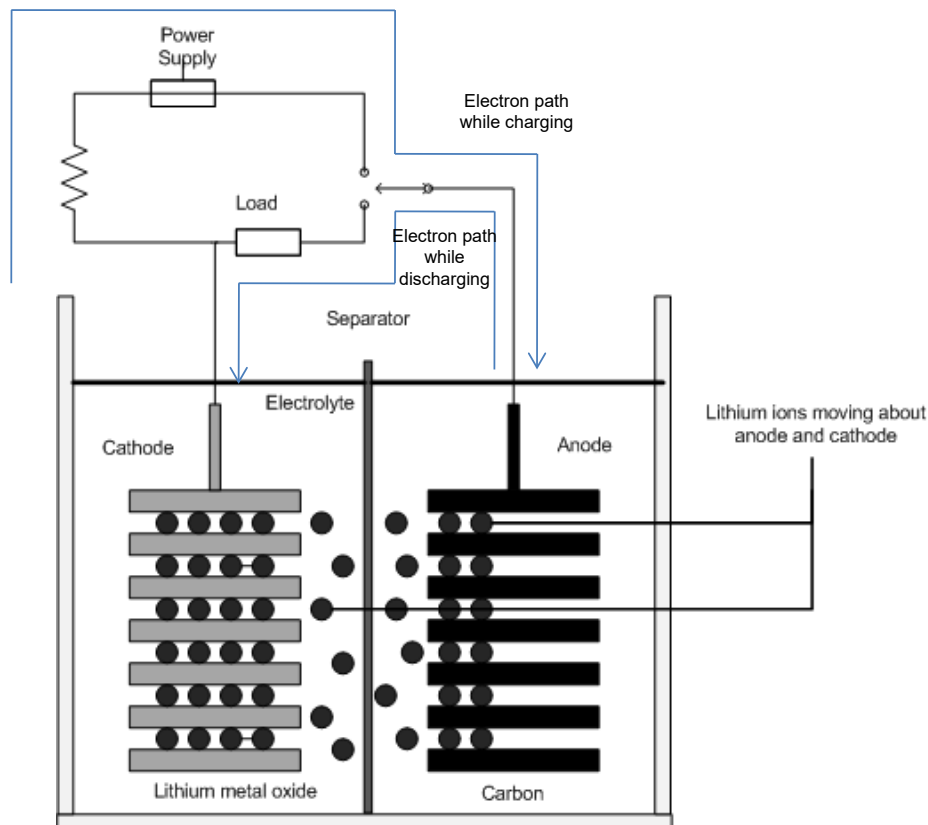
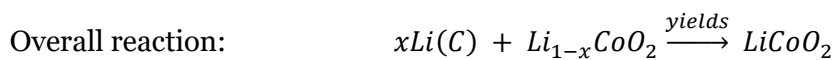
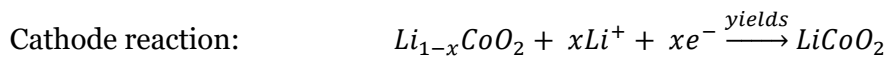


**Figure 51. Working mechanism of Li-ion batteries**

### Electrolyte and Separator

The electrolyte serves as an ionic conductor while guaranteeing electronic insulation. There are several groups of electrolytes: Organic electrolytes, solid-state electrolytes, and ionic liquid electrolytes. Regarding commercial cells, only organic electrolytes using the conducting salt LiPF<sub>6</sub> are currently used on a wider

scale, so the other types will not be considered here. One problem with the alternatives in development is the relatively poor ionic conductivity compared with the latter. Much research has been done to develop a suitable organic electrolyte, as this kind of electrolyte promises higher ionic conductivity and a more practical operation temperature range in comparison with existing electrolytes. However, especially the safety related thermal stability still does not meet the requirements for the application of this type of electrolyte in EVs.

## Appendix I.II: Li-ion BESS aging modes and mechanisms

This part of the appendix describes the terms related to Li-ion battery aging, particularly their aging modes and their aging mechanisms.

### Li-ion BESS aging modes

1. *Loss of lithium inventory (LLI)*: LLI is caused mainly due to loss of cyclable lithium ions, which occurs for various reasons. It directly correlates to loss in capacity of the battery cell in Ah.
2. *Loss of active materials (LAM)*: LAM occurs due to loss or structural degradation in the anode or cathode materials. This causes both capacity loss and power fade in the cells.
3. *Conductivity loss (CL)*: It is also described as contact loss, where the degradation occurs in the electrical parts of the battery cell, such as current collector corrosion and binder decomposition.

### Li-ion BESS aging mechanisms

1. *Anode aging mechanisms*: The anode material in the Li-ion battery contributes majorly to the overall Li-ion battery degradation. The most widely used anode material is graphite, and hence, the discussion on aging will be subjected to graphite as the anode material. The causes for aging in anodes are subjected due to:
  - a. *Solid electrolyte interface (SEI) layer*: The SEI layer is initially formed during the first charge where it forms a layer between electrolyte/electrode interfaces mainly due to the dissolution of electrolyte. The reason for that to occur is that the graphite anode lies outside the electrochemical stability window of the electrolyte. This initial SEI layer provides improved security to the battery by acting as a natural barrier that prevents corrosion of electrodes and

further decomposition of electrolytes. However, when subjected to various operating conditions, such as high SOC (greater than 80%), high temperatures, overcharge and short circuits, this SEI layer grows in magnitudes leading to an overall increase in cell resistance. This growth of the SEI layer is due to loss of cycleable Li-ions and loss to electrode materials, thereby seeing both LLI and LAM processes. Phenomenal growth in the SEI layer in the battery cell leads to breaking off contact with the electrical contacts, such as current collectors in the cell, thereby inducing CL also as an aging mechanism in the SEI growth process (Heiskanen, Kim, & Lucht, 2019; Pinson & Bazant, 2013; A. Wang, Kadam, Li, Shi, & Qi, 2018).

- b. *Lithium plating*: When the battery is subjected to utilization at low SOC, low temperature, and high currents, Li plating is bound to occur, i.e., it leads to loss of lithium ions, which get plated on the anode, which may lead to the formation of dendrite like structures. Lithium plating causes LLI in the cells and causes serious concerns on battery safety due to its nature of causing internal short circuits (Janakiraman, Garrick, & Fortier, 2020; X. Lin, Khosravinia, Hu, Li, & Lu, 2021b; von Lüders et al., 2017). Lithium plating and SEI layer growth are the most common aging mechanisms in Li-ion batteries that majorly contribute to its degradation.
- c. *Transition metal dissolution*: A majority of Li-ion battery cathodes contains transition metals such as nickel, cobalt, manganese, iron, and vanadium and their electrolytes contain the salt  $\text{LiPF}_6$ . At certain conditions of cycling such as high voltages/temperatures, the battery cell produces  $\text{HF}_6$  that increases the overall acidity of the electrolyte, which tends to dissolve transition metals, thereby increasing the impedance and reducing the capacity of the cell (Hawley et al., 2020).
- d. *Mechanical stresses at anode*: When Li ions are intercalated into the anode, it can cause abrupt changes in their volume due to phase transition in those particles. With this condition, when more Li-ions are inserted in the anode, the orientation of the anode molecules changes with respect to their electrical and mechanical properties. Thus, mechanical stresses are caused, which can lead to structural damages in the anode, leading to LAM and LLI (Vetter et al., 2005).

- e. *Current collector corrosion*: Corrosion may lead to contact loss and thus to an increase in contact resistance. Braithwaite et al. (Braithwaite, 1999) showed that the copper anode current collector is especially susceptible to environmentally assisted cracking.
- f. *Changes in the anode morphology*: The reasons for changes in the anode morphology can be attributed to the structural disordering, which regards the inner structure of anode particles and is mainly caused by mechanical stress. The reasons for this may be charging, discharging, variations in temperature, and vibrations. Furthermore, morphological changes at the surface of the graphite particles may occur, which are mainly related to solvent intercalation (Vetter et al., 2005). Secondary reactions of graphite intercalated compounds may also distort the ordered structure at the surface of the graphite particles.

## 2. Cathode aging mechanisms

- a. *CEI layer*: CEI layer stands for cathode electrolyte interface which is a layer that is formed between the cathode and the electrolyte interface. The CEI layer is generally formed during charge/discharge operations of the battery at high voltages. However, the CEI layer's stability and electrochemical properties are not capable of protecting the cathode (Vermeer et al., 2022; H. Wang et al., 2021). Compared to the SEI, the CEI shows low lithium conductivity, and hence, contributes to an increase in resistance. The CEI triggers aging modes LLI and LAM (Edström, Gustafsson, & Thomas, 2004).
- b. *Other Cathode mechanism*: Other aging mechanisms from the cathode are caused by mechanical stresses in them and due to transition metal dissolution in the cathode, but their contribution to aging has been minimal in nature.

## Appendix I.III Li-ion BESS related terminology (Electric & Team, 2008)

- *Full charge*: A cell is considered to be fully charged when it reaches its upper voltage limit and its current is reduced to 5% of the nominal current.

- *Full discharge*: A cell is completely discharged when the voltage reaches its lower limit and the current approaches zero. In this cell, the lower limit of the voltage is 2V.
- *Capacity*: The capacity of the battery is measured in Ampere-hour abbreviated as Ah. This defines the amount of charge stored or supplied by a pouch cell. The capacity of the battery can be obtained from the manufacturer's datasheet.
- *CA*: This is also called the C-rating of the cell. It is a factor of load current which is related to the Ah of a battery. For example, at a load of 5A for a battery rated 5Ah has a C-rating of 1C.
- *Nominal capacity*: The amount of Ah that can be extracted from a battery at room temperature at a particular C-rate from the fully charged condition to the fully discharged condition.
- *State of charge (SOC)*: This expresses the residual capacity that is still left in a cell at a particular moment.
- *Depth of discharge (DOD)*: It is expressed as the percentage of the discharged battery capacity to its maximum capacity. Deep discharge is defined when a battery is discharged to a DOD of 80% or more.
- *Cycle life*: The total number of charge and discharge cycles a cell can provide before its EOL is observed. It depends on the DOD pattern of the cell. It is usually estimated for a particular number of discharge and charge cycles.
- *Terminal voltage (U)*: The voltage observed between battery terminals when a load is connected to it. It varies with SOC and charge or discharge current.
- *Open circuit voltage (OCV)*: The voltage between the battery terminals when there is no load applied across it. It depends on the cells' SOC and increases when the SOC increases.

# Distributed Generation, Storage and Active Network Management

Chethan Parthasarathy<sup>1</sup>, Hosna Khajeh<sup>2</sup>, Hooman Firoozi<sup>3,\*</sup>, Hannu Laaksonen<sup>4</sup> and Hossein Hafezi<sup>5</sup>

Flexible Energy Resource (FER), School of Technology and Innovations, University of Vaasa, 65200 Vaasa, Finland

<sup>1</sup>[chethan.parthasarathy@uwasa.fi](mailto:chethan.parthasarathy@uwasa.fi), <sup>2</sup>[hosna.khajeh@uwasa.fi](mailto:hosna.khajeh@uwasa.fi), <sup>3</sup>[hooman.firoozi@uwasa.fi](mailto:hooman.firoozi@uwasa.fi), <sup>4</sup>[hannu.laaksonen@uwasa.fi](mailto:hannu.laaksonen@uwasa.fi), <sup>5</sup>[hossein.hafezi@uwasa.fi](mailto:hossein.hafezi@uwasa.fi)

\*Corresponding author: Hooman Firoozi ([hooman.firoozi@uwasa.fi](mailto:hooman.firoozi@uwasa.fi))

**Keywords:** *distributed generation, flexible energy resources, energy storage systems, energy management methods, active network management, battery energy storage systems*

## 1. Introduction

Power systems are changing due to global drivers such as climate change and environmental issues as well as increasing dependency on electricity. Therefore, there are needs for (i) large-scale integration of renewable, low-emission (CO<sub>2</sub>) energy sources in high-, medium- and low-voltage (HV, MV and LV) networks, (ii) improving energy efficiency of the whole energy system and (iii) enhance electricity supply reliability. In Fig. 1 the main impacts A)-D) of these changes on power systems are presented.

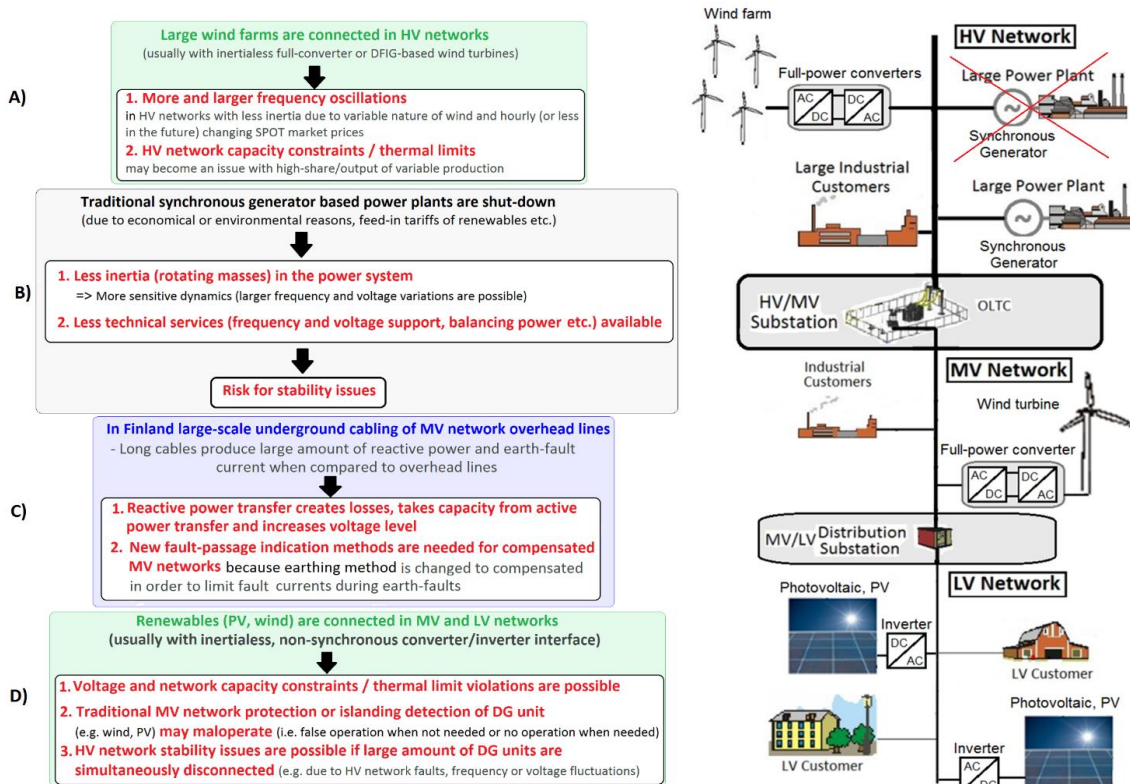


Figure 1. Main impacts of ongoing changes on power systems

Previously distribution grid connected renewable energy sources (RES) and other distributed generation (DG) units were usually required to be disconnected during faults and disturbances. Recent technological advances along with social acceptance have led to an increase in the number of DG units in the electricity distribution networks. Due to constantly increasing number of connected DG units, HV grid stability has become a central issue, and could get worse if, for example, large share of the DG units are disconnected during HV grid faults or frequency disturbances. Therefore, supply reliability and quality with integration of RES is tried to be ensured by setting stricter grid code requirements for the RES and other DG units connected at different voltage levels (HV, MV and LV). These grid codes define, for example, the required HV grid stability supporting functionalities like voltage and frequency fault-ride-through (FRT) requirements of the DG units during HV grid faults and frequency disturbances. These DG unit grid code requirements have been made mainly from HV grid stability point of view and less attention has been paid on distribution network effects (like protection and islanding detection). However, in the future this is not enough. In addition, there is a need for flexibility from distributed energy resources (DER), because DER (controllable generation units, energy storages, controllable loads and electric vehicles) at different voltage levels (HV, MV, and LV) has potential to,

- a) Provide different local (corresponding voltage level) and system-wide (whole power system / HV network) technical flexibility services by active ( $P$ ) and reactive ( $Q$ ) power control which could, in addition to grid codes and regulations, be realized by future technical ancillary service / flexibility markets
- b) Simultaneously improve energy efficiency i.e. reduce the demand for distribution network capacity (coordinated voltage control and congestion management), reduce losses and increase reliability of electricity supply to the customers (intended island / microgrid) operation

But this potential of DG units and full integration of RES cannot be realized without active management of the distribution grids and flexibilities connected in distribution grids. For example, different types of energy storage systems (ESSs) have been deployed extensively as flexible energy resources aiming to increase the flexibility at different levels of the power system including local (distribution network) and system-wide (transmission network) levels. In order to effectively integrate DGs and ESSs and exploit their maximum flexibility potential, appropriate management and control structures are needed. The recent advances in ICT have enabled active participation of these resources, accommodate all DG generation and energy storage options, and also facilitate optimal management of these resources.

Most efficient way to meet energy demand with increasing integration of RESs in the distribution networks is to incorporate innovative solutions, technologies and grid architectures. Developing economically viable yet innovative grid architectures becomes essential with the increased role of non-dispatchable and DGs based on RES. Such solutions are realized by active control of the DGs as part of Active Network Management (ANM) schemes. Smart grids provide the platform to implement ANM schemes, where the DGs are interconnected and inter-communicable in real time to work in tandem to supply energy demands.

In this chapter, an overview of distributed generation, i.e. their classification and role in ANM of smart grid operations and adjoining control methodologies will be addressed in detail. Energy storage systems plays crucial role as flexible energy resources for ANM in smart grids. Their technology types and various applications they tend to be used will be explained. Battery energy storage systems (BESSs), especially Lithium-ion batteries with their current technology and economic maturity are considered as a viable option for stationary grid applications. Design and control of Li-ion battery integration by means of power electronic converters for ANM in medium voltage distribution system, along with managing other flexibility services of DGs are in the scope of this chapter.

## 2. Distributed Generation Sources

DGs have made a significant contribution to producing energy in the last decade. Most energy players and utilities have found that utilizing DGs can decrease their net-costs, as the marginal costs of producing electricity by renewable-based DGs are very low, near to zero [1]. System operators including transmission system operators (TSOs) and distribution system operators (DSOs) can also benefit from the large installation of DGs since they offer benefits for the power systems. The DGs' advantages from the operators' viewpoints can be supporting network voltage and frequency, reducing network losses, reducing transformers loading stress, promoting system reliability, as well as providing the environmental benefits [2]. In addition, end-users who are equipped with DGs are also able to take advantage of the economic benefits of installing DGs. In this way, not only they can be self-sufficient, but they can also sell their production surplus and make profits. DGs mainly assist in satisfying distribution network located demand and they are located in distribution networks (low voltage (LV) and medium voltage (MV) levels). Photovoltaic (PV) panels and wind turbines are currently the most popular renewable-based distributed energy resources that are located in distribution networks. Micro-CHP and fuel cells are the other common DGs which can be adopted in distribution networks. The following sections give more information about these DGs.

### 2.1 PV Panel

There exist various methods estimating the active power produced by a PV module. In one of the first research, the power output of a PV module was proposed to be estimated based on the cell temperature as well as solar irradiance. The cell temperature is in turn dependent on the ambient temperature as stated in (1) [3][4].

$$\theta^{cell} = \theta^{ambient} + G \left( \frac{\theta^{NOCT} - 20}{800} \right) \quad (1)$$

The output power captured by a PV cell is estimated accordingly, utilizing (2).

$$P^{pv} = P^{STC} G (1 + c(\theta^{cell} - 25)) \quad (2)$$

Where, in the above equations,  $c$  indicates the power-temperature coefficient.  $\theta^{cell}$  is the PV cell temperature,  $\theta^{ambient}$  denotes ambient temperature while  $\theta^{NOCT}$  refers to the temperature associated with the nominal



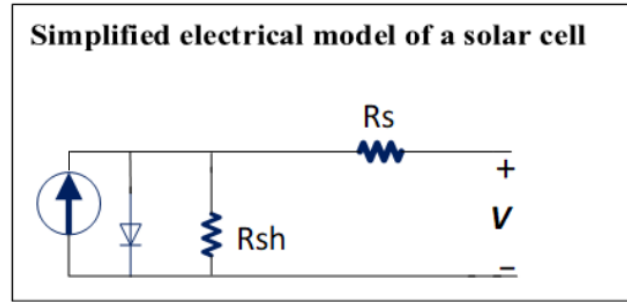


Figure 2. An electrical single diode model for a PV cell

operation of the cell all in [ $^{\circ}\text{C}$ ]. In addition,  $P^{pv}$  and  $P^{STC}$  are the output power of the PV cell and the power produced under the standard test condition, respectively. Finally, the solar irradiance is shown by  $G$  [3].

The output power of PV can be also calculated according to its simplified equivalent circuit illustrated in Fig. 2 [5]. Thus, the following equations are adopted in order to calculate the produced PV power equipped with the boost converter [5]:

$$I^{pv} = I^{ph} - I^{sa} \left( e^{\frac{q(V+IR^s)}{nkT}} - 1 \right) - \frac{V+IR^s}{R^{sh}} \quad (3)$$

$$P^{pv} = \eta^{boost} I^{pv} V^{pv} \quad (4)$$

Where in (3),  $I^{ph}$  denotes the photocurrent and  $I^{sa}$  refers to the saturation current of the diode. Moreover, the series and shunt resistances are represented by  $R^s$  and  $R^{sh}$ , respectively while  $n$  indicates the factor related to the diode ideality,  $k$  is Boltzmann's constant,  $q$  refers to the electron charge, and  $T$  is a parameter expressing the absolute temperature in Kelvin. In (4),  $P^{pv}$  is obtained utilizing  $I^{ph}$ , the open circuit voltage,  $V^{pv}$ , and the efficiency of the boost converter,  $\eta^{boost}$ .

It is worth mentioning that the power produced by a single PV cell is so small. However, PV modules can be connected in parallel and series in various topologies in order to generate more power.

In general, a PV system that is connected to the grid may consist of a boost DC-DC converter, a Maximum Power Point Tracking (MPPT) controller, a voltage source inverter, and some other equipment. The main responsibility of the boost converter is to balance the system while the inverters convert the output DC power of the PV system to the AC power. In order to ensure the efficient operation of the PV panel, the point in which the output power of the PV panels reaches its maximum value should be found. In this regard, an MPPT controller is deployed so as to track the MPP of the panel [6] [7].

## 2.2 Wind Turbine

The active power produced by a wind turbine is dependent on some factors such as the area and location where the wind turbine's rotor blades are spinning (swept area), the wind speed as well as the air mass density. In addition, the output power of the wind turbine is restricted by a coefficient of power denoted by  $c_p$ . If the

coefficient of power equals its optimal value, the maximum wind turbine output is obtained. This value can be calculated by (5) [8].

$$P^{WT} = 0.5c_p^{opt}(\gamma, \beta)A^s \rho^{air}(WS)^3 \quad (5)$$

Where,  $P^{WT}$  is the maximum output of wind power,  $c_p^{opt}(\gamma, \beta)$  is the coefficient of wind power which is a function of speed ration ( $\gamma$ ) and blade pitch angle ( $\beta$ ). the parameter  $A^s$  indicates the swept area in which the rotor spins,  $\rho^{air}$  is the air mass density, and finally  $WS$  is the wind speed.

In the following model, wind power is considered a non-linear function of the wind speed. There also exists another model aiming to explain the linearized relationship between wind power output and the wind power speed. The linear model can be adopted especially for scheduling several energy resources. This model is expressed by (6) [9].

$$P^{WT} = \begin{cases} 0 & WS < WS^{cut-in} \\ \frac{P^r}{WS^r - WS^{cut-in}} WS + P^r \left(1 - \frac{WS^r}{WS^r - WS^{cut-in}}\right) & WS^{cut-in} \leq WS < WS^r \\ P^r & WS^r \leq WS < WS^{cut-off} \\ 0 & WS \geq WS^{cut-off} \end{cases} \quad (6)$$

Where,  $WS$ ,  $WS^r$ ,  $WS^{cut-in}$ ,  $WS^{cut-off}$  are wind speed, rated wind speed, cut-in wind speed, and cut-off wind speed, respectively. Additionally,  $P^r$  denotes the rated power of the wind turbine.

### 2.3 Micro-CHP

A combined heat and power (CHP) is utilized in order to combine the heat with electricity production. A micro-CHP is regarded as a decentralized small-scale CHP located at the customer-level of the electrical network. The micro-CHP is able to simultaneously produce heat and power which increases the efficiency of the system. The maximum capacity of the micro-CHP is usually below 15 kW. The energy efficiency of the CHP unit can be assumed to be constant. However, in practice, the CHP unit's efficiency varies with dynamic operation due to the variation of the output power of the micro-CHP [10]. Moreover, ramping constraints need to be applied in energy scheduling problems since the CHP requires some time to reach the steady-state after its set-point changes [10].

### 2.4 Fuel Cells

A fuel cell can produce electricity by converting the chemical energy originating from hydrogen and oxygen into electricity. Fuel cells can be also located at customer levels and utilized as DGs. In the solid-oxide fuel cell, anode supplies Hydrogen and catalytically split it into a number of protons and electrons. The electrons are then flowing towards the positive side i.e. the cathode by flowing through the external circuit. The oxygen then reacts with the protons and also the electrons flowing in the circuit, forming water formula [11]. The solid-oxide fuel cell can operate in parallel with PV panels, meaning that it can be integrated with solar power. In the night time, when PV panels cannot produce electricity, the fuel cell can be deployed to supply the demand.

### 3. Challenges in DG implementation

The challenges associated with DGs can be different according to the type of DG, the amount of intermittent power injected from renewable-based DGs, the type of distribution network as well as the location of DGs. However, DGs give birth to some new technical challenges in the power system. DGs are mainly installed in the vicinity of residential loads. It results in the bidirectional flow of power in distribution networks.

The connection of DGs to the distribution network exerts significant impacts on voltage profiles and also on the network power flow. These effects can be positive or negative. The positive effects include improving the reliability of supply and reducing losses of power system by bringing the generation closer to consumption. The negative impact is increasing the voltage magnitude at nodes with DGs which may violate the maximum permissible value in the moments with high generation. Accordingly, the voltage control is the most serious challenge and voltage regulation of the distribution network needs more advanced strategy [12]. Moreover, the connection of DGs to the distribution networks exacerbate the challenges related to the traditional Volt-Var control equipment. Traditional and expensive Volt-Var control actions are significantly delayed in order to react to the fast fluctuations resulted from the output power of renewable-based DGs [13]. Besides, the voltage regulation and control devices in the traditional distribution networks are mostly designed to operate without DGs. In this light, the network voltage magnitudes are assumed to decrease along the distribution feeder starting from the substation to the customers. However, with the presence of DGs, the mentioned assumption is no longer valid [14].

In addition to regulation problems, a large standalone DG (like wind turbine) can result in power quality issues, especially in a weak and rural distribution network during the time in which the DG is switched on and off [12]. According to [15], integration of DGs can affect power quality. Voltage dips are a significant event that can occur due to failures of the DG.

In terms of protection, the connection of large number of DGs on the distribution network's feeders has significant influence on the applicable protection practices. DGs can have a major contribution to the short-circuit currents. This issue may, for example, result in unexpected operation of fault indicators which are deployed to locate fault position. Besides, some additional factors should be considered when installing a number of DGs in distribution networks [16]. These factors include the protection of the installed DGs from internal faults, the protection issues associated with the faulted distribution network from the fault currents produced by a DG, and the issues related to islanding detection (anti-islanding / loss-of-mains) as the high DG installation may increase islanding in distribution networks. Also, management of these DGs in the distribution systems needs to be efficiently controlled. Hence, integrating vast amounts of DGs raises multiple challenges related to the distribution system's control, operation and protection. Such challenges are mitigated by innovative distribution grid management architectures reinforcing the need for rapidly controllable flexible energy sources. Following section shall introduce such control architectures in detail.

#### 4. Management-related Solutions

There are several studies implying that active management of distribution networks and also active management of DGs can help to increase the hosting capacity and accommodate higher number of DGs connected to the current networks [17]. Fig. 3 presents an overview of the management-related solutions.

Future active network management methods can enable active control and facilitate the deployment of DGs' available flexibilities during both operation modes including grid-connected and islanded [18]. However, previous studies state that the benefits brought by utilizing DGs are expected to exceed the cost of the active management implementation [16], there exist some uncertainties related to the cost of active management in distribution networks.

From the economic side, the appropriate price control mechanism is needed in order to recover the expenses of applying active network management. Additionally, developing active distribution networks requires new commercial arrangements. In this way, different incentive schemes and market mechanism should be employed to effectively integrate DGs and motivate the owners of these resources to actively participate in different programs. On the other hand, the lack of policies and well-defined regulatory frameworks in the traditional design of distribution networks limits the high utilization of DGs. Hence, supporting DG integration requires appropriate policies applied to the distribution networks.

As previously stated, the growing number of DGs in distribution networks can have both negative and positive impacts on the power system. The active management of DGs, not only is able to decrease the negative impacts but can also enhance the flexibility of the network. In light of this, the following subsections deal with the

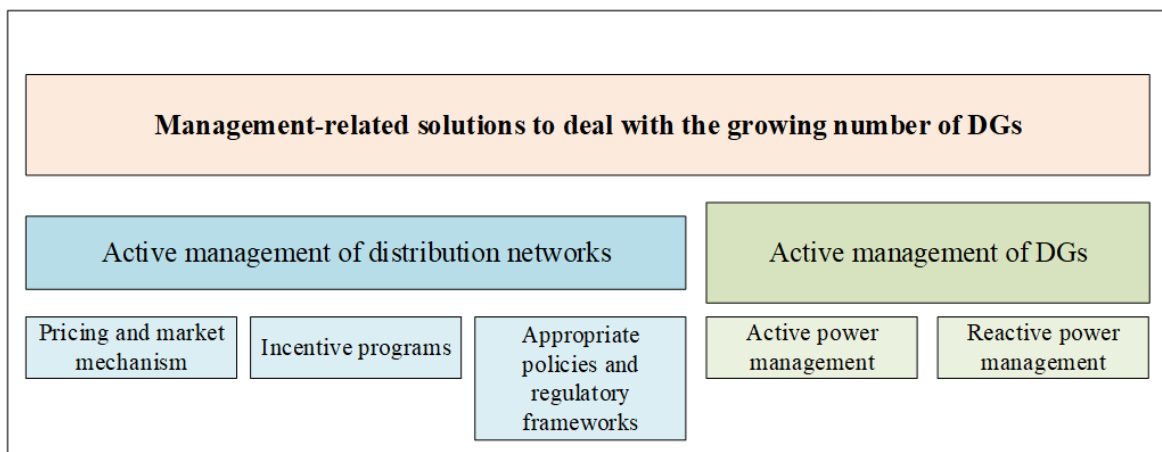


Figure 3. An overview on the management-related solutions of the growing number of DGs in distribution networks

management of active power and reactive power of DGs seeking to help the system operators and enhance the flexibility of the networks.

#### 4.1 DG Inverters' Reactive Power Management

Inverter-based DGs can be regarded as excellent alternatives to resolve the issue related to the rapid response and control of the voltage variation resulted from DGs. Power flowing in feeders is restricted by the line branch's thermal capacity and also by bus voltages along the feeder. When the flow of one of the branches reaches its maximum thermal capacity or one of the bus voltages of the feeder approaches the upper or lower limits, no further power is able to flow the feeder. In this way, DG inverters can assist in increasing the feeder transfer capability by absorbing/injecting the specified amount of reactive power [19].

Inverter-based DGs are equipped with power electronic devices so as to procure the required reactive power in less than 50 milliseconds. This will avoid fast voltage fluctuations stemming from the transient cloud passing [20]. With the help of this feature, inverter-based DGs can be independent on the control actions of traditional distribution system such as deploying capacitor banks, static Var compensators as well as on-load tap changers. Furthermore, DG inverters produce a fast response and also provide more flexible reactive power support. Note that unlike shunt capacitors, the inverters are able to both absorb and inject reactive power to assist in controlling voltage.

In order to highly exploit the flexible capacities of DGs for operating the distribution networks, the reactive power capacity of the DG inverter should be highly utilized. For example, PV inverter can operate to its full capacity during daytime when there exists active power injection. However, both reactive power absorption and injection can be used during evening time when there exists no PV power.

The reactive power of DG's inverters is generally limited by the nominal value of the active power output of the DGs. However, the capacity of inverters may be over-sized to provide surplus reactive power support as well as maintaining the fully active power capability. The maximum reactive power should satisfy the following constraint [21].

$$|Q^{DG}| \leq \sqrt{((1 + OF)S^{DG,r})^2 - (P^{DG,r})^2} \quad (7)$$

In (7),  $OF$  is the over-sizing factor of DG inverter (per unit) in comparison with the normal values of DG units [22].

#### 4.2 DGs Active Power Management

The appropriate management of DGs' active power can be seen as potent DSO-level flexible resources, reducing the need for DSO operational actions which include grid reinforcement and reconfiguration [23]. DGs may be curtailed in a dynamic or static way [24]. The curtailment of DGs is performed in order to increase system flexibility and provide the system with downward flexibility. When the system needs downward flexibility, it has surplus production which violates the balance constraint of the power system. Hence, it should curtail

In the static curtailment, the system operator imposes a predefined threshold related to the injection of active power produced by renewable-based DGs whereas, in dynamic curtailment, the injection of active power is under the full control and may be curtailed due to the network constraints.

Curtailment resulted from network constraints can be performed either voluntary or involuntary [25]. In voluntary cases, an ex-ante agreement was reached between the DG owner and the network operator which specifies the amount of curtailment as well as the possible compensation. It should be noted that the DG owners require to sign the contract voluntarily. The DG owners may also participate in flexibility markets. However, the existing flexibility markets for balancing purposes are designed for large-scale flexibility products. Hence, the DG owners should firstly be aggregated and then participate in selling downward flexibility services. Involuntary curtailment due to network constraints is resulted from an obligation for the network operators including DSOs and TSOs. However, this kind of curtailment may decrease future investment in renewable-based energy resources.

The interactions between DG owners and the DSO have been covered by some research such as IMPROGRES project [25]. This project states that the location of DGs highly depends on regulation and policies designed by the DSO. In order to find the optimal location of DGs, the appropriate cost mechanism should be determined for the DSO. For example, the DG owners may be encountered several curtailments providing that they invest in the locations with high network reinforcement costs. However, curtailment with appropriate compensation can avoid overinvestment in the grid and also motivate renewable DG investors to find the best location in which the reinforcement costs of the grid are the lowest. This may lead to increasing the capability of the grid to host a large amount of renewable-based DG capacities.

### **4.3 Distribution Network Management with DGs**

The increasing number of DGs in distribution networks leads to power systems restructuring the existing management and control architectures. Power systems have been traditionally managed in a centralized way. They consist of generation, transmission, and distribution levels. In a generation level, generators are centrally dispatched through the centralized pool-based markets. The transmission system is then responsible for transmitting the electrical high-voltage (HV) level power to lower-level systems. Transmission networks are also centrally managed by transmission system operators (TSOs). The distribution system delivers electrical power to final customers and end-users. These networks are controlled and operated by DSOs. However, the dramatic growth of DG in distribution networks creates considerable challenges [26]. The traditional centralized architecture fails to exploit potent flexibility capacities of new distribution network located resources such as DGs since in the centralized paradigm, these resources are not able to actively participate in energy and flexibility provision. Accordingly, the power system needs to adopt new control and management methods in order to adapt to the changes associated with the growing number of DGs in distribution networks.

### 4.3.1 Hierarchical Architecture for Distribution Network

The deployment of hierarchical management aims to facilitate the integration of DGs at different levels of the power system. This architecture contains different levels of management. In each level, the related elements are controlled and managed through the external signals receiving from the upstream layers. In other words, the controller in each layer has a certain degree of autonomy which should set its functionalities in accordance with the upstream layers.

Regarding the LV level of distribution networks, at the first hierarchical level, the microgrid is managed and controlled by its control center named a microgrid control center (MGCC). The center is located on the LV side of the MV/LV secondary substation and has some operational functionalities associated with the management and control of the DGs in the MG. The MGCC acts as an interface between the DSO and the MG. At a second hierarchical level, each DG unit is managed and controlled locally through a micro source controller (MC). Loads can be also controlled locally through a load controller (LC) [26]. Fig. 4 describes this kind of control and management structure.

At MV levels of the system, the MGs, the DG units located at MV levels, and MV loads are taken as active cells. The cells are given a certain degree of autonomy. In this regard, the decision making of each cell follows a hierarchical structure. In other words, a central controller is in charge of collecting data from different control units as well as establishing rules for the downstream control units [26]. With regard to the hierarchical structure, consider an aggregator who is responsible for aggregating DGs in the distribution system. In this way, the aggregator negotiates a contract with the owner in order to control their DGs. The aggregator directly controls DGs by sending its control signal to the DGs. The aggregator, itself, receives the control signals from the upper

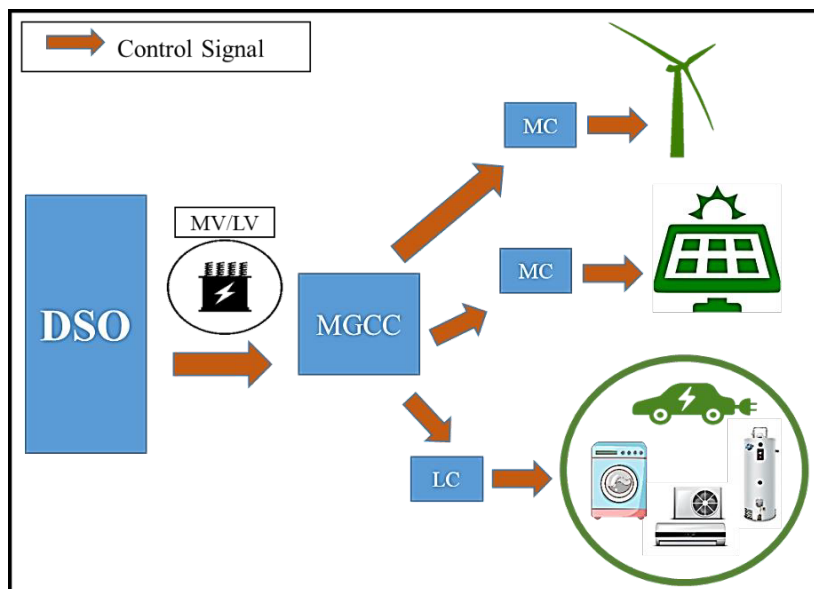


Figure 4. Hierarchical control of DGs located in a microgrid

entity, which can be the DSO. This management method can be regarded as a hierarchical management and control method.

#### 4.3.2 Decentralized Architecture for Distribution Network

Unlike a hierarchical approach, each controller in a decentralized management method has full control over its elements. The recent advances in artificial intelligence enable each controller to act as an independent agent and form the multi-agent system. In this regard, various agents in the distribution grid can communicate with each other aiming to optimize the global objective function. However, each agent has its own objective function. In the decentralized approach, different grid components can be counted as independent agents. For example, flexible loads, electric vehicles, switchers, on-load tap changing, and DGs can have their own objective and autonomous management [26].

For example, consider a DG owner acting as an autonomous agent. It decides for controlling the DG autonomously with the target to maximize its profits by participating in the local market. It controls its resources using an energy management system (EMS). On the other hand, the local market operator (LMO), which can be the DSO or receives signals from the DSO, is responsible for finding the optimal operating points for players based on their offers and bids.

The aim of the local market operator can be maximizing the social welfare of all of the players with respect to the network constraints imposed by the DSO. Therefore, the DG owners have their own autonomous objectives while they follow a community-based objective by participating in the local market. Fig. 5 illustrates the decentralized management method of DGs in the local market environment. The DGs may also participate in flexibility local markets by providing active power and reactive power support for the grid.

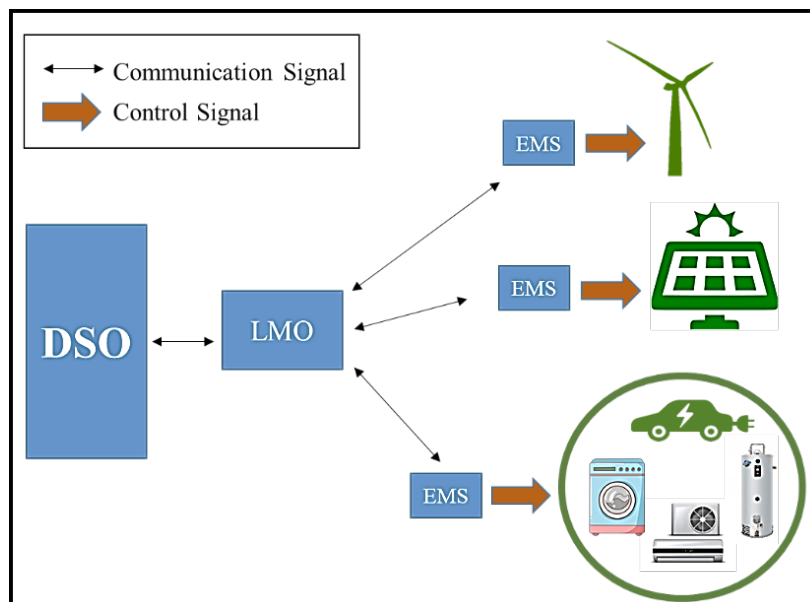


Figure 5. Decentralized control and management of DGs in a local market



An overview of various control architectures provides a clear view on utilization of FESs to mitigate various challenges posed by the integration of DGs in the distribution system. Following section provides a detailed account on utilizing ESSs as FESs in the distribution system, with focus on their classification and range of applications they are capable of tending in smart grid applications.

### 4.3.3 Future Distribution Network Management Architecture - Potential General Approach

In the future distribution grid zones with flexibilities (Fig. 6) i.e. FlexZones could be seen as building-blocks of a smart, flexible and resilient distribution grid as described in Fig. 6. FlexZone could be also called as an active cell, zone with DER or local energy community. Also, for example, one utility grid connected MV or LV microgrid could create one FlexZone (Fig. 6a). FlexZone approach could also create basis to implement new business and market models for flexibilities (flexibility service markets). As illustrated in Fig. 6 there can be different level of FlexZones and higher level FlexZone can consist of multiple lower level FlexZones like grid-connected nested microgrids (i.e. for example one/multiple smaller LV microgrids inside larger MV microgrid).

In the future different local (DSO) active network management (ANM) functionalities could be realized by (de)centralized, hierarchical and coordinated management solutions at HV/MV, MV/LV substations with dedicated management units i.e. FlexZone Units (FZUs), because it is more feasible to distribute also the needed processing and calculation capacity closer to the actual measurement points and controlled flexibilities. With this kind of distributed data processing approach it is possible to avoid too extensive ‘raw data’ transfer and reduce the risk related to loss of one central management unit or communication. However, still fast, secure and

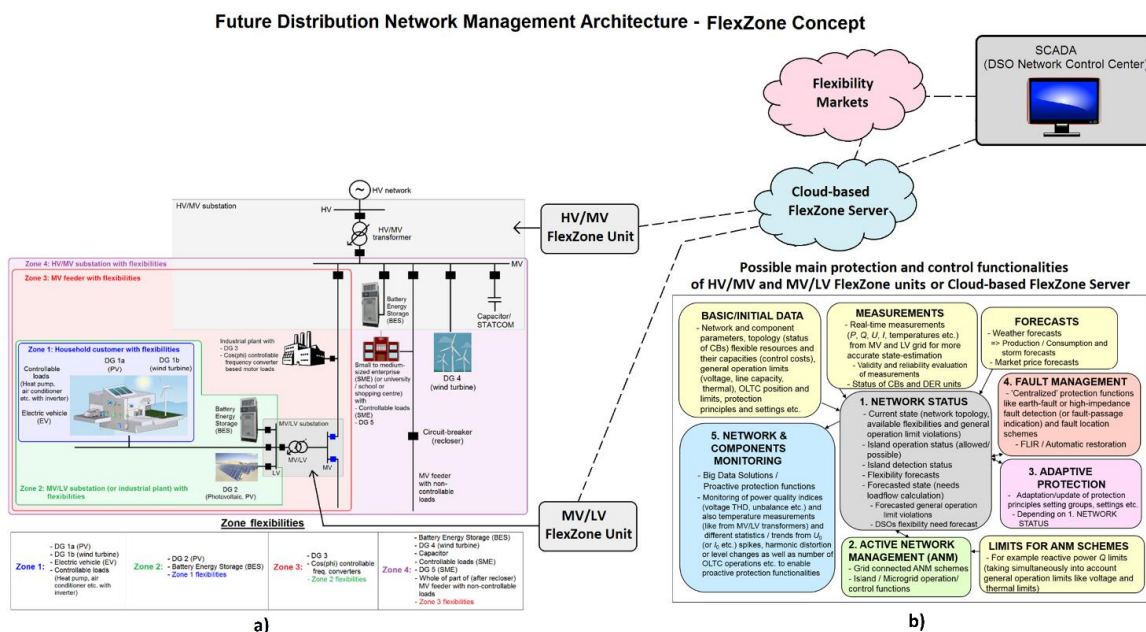


Figure 6. Potential future distribution network management architecture (FlexZone Concept) and a) Different level of FlexZones with possible flexibilities, b) Possible main protection and control functionalities of HV/MV and MV/LV management units

reliable communication between different devices will play essential role in future smart grids with flexibilities to enable the needed management and protection functionalities. HV/MV and MV/LV FZUs could include, in addition to different ANM functionalities, also other functionalities like protection/fault indication & fault location, islanding detection & logic, status monitoring, predictive protection, available flexibilities, flexibility forecasts and historian from flexibilities control/use (Fig. 6b).

Active network management may simultaneously have an effect on protection settings if, for example, the network topology is changed. On the other hand, active management of flexibilities could be used to enable correct and reliable operation of certain islanding detection methods or, for example, due to earth-fault the grid topology may be changed and it may have an effect on active network management functionalities such as voltage control or losses minimization. Therefore, dependencies between active network management and protection functionalities require careful planning and development to enable creation of future-proof solutions for the Smart Grids.

In the future, one alternative could also be that some of the less critical / high-speed communication dependent DSO FZU functionalities (Fig. 6) like, for example, monitoring or predictive protection related big data solutions, flexibility forecasts, some ANM schemes etc. would be alternatively located in cloud servers. This approach could enable more flexible and scalable solutions when only most communication and time-critical protection and islanding detection applications would remain at actual HV/MV or MV/LV FZUs. Communication reliability and cyber security will play more and more important role in the future grid protection and management solutions and, for example, potential short data packet loss should not cause false operation of FZU functionalities (Fig. 6). In possible cloud server based applications role of redundant back-up schemes, like hot-standby or hot-hot schemes, becomes also significant.

## **5. Energy Storage Systems (ESSs)**

Integration of RES has been progressing at a faster pace at all the voltage levels in the power systems, particularly in the low and medium voltage distribution grids. RESs are typically intermittent and low inertia generation sources leading to large voltage and frequency instabilities in the distribution systems compared to traditional centralized power systems. Flexible energy sources are capable of providing stability in the modern power grids with higher RES penetration. ESSs play key roles with their ability to provide multiple flexibility services in smart grids spread over different time ranges. In this section, various ESS technologies capable of acting as flexible energy sources will be explained along with their application ranges for smart grid applications.

### **5.1 ESS Technologies for stationary grid applications**

Energy storage technologies for stationary grid applications are primarily classified based on the nature of energy conversion. From the literature [27]–[29], a brief outline of the classification of energy storage types are defined as below. Also, Fig. 7 provides details on the technologies applicable for grid scale applications.

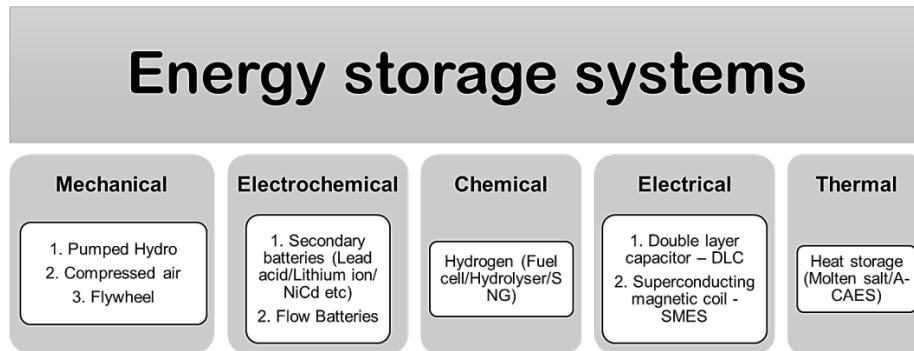


Figure 7. Classification of electrical energy storage systems

1. Mechanical energy storage systems: Stores and convert electrical energy in various forms of kinetic and/or potential energy
2. Electrical energy storage systems: Stores the electrical energy by transforming electrical or magnetic fields with the aid of capacitors and superconducting magnets
3. Electrochemical energy storage systems: Chemical energy of active materials are converted into electrical energy during the discharge phases and vice versa while charging. Simultaneous Redox reactions are responsible for the energy conversion
4. Chemical Energy Storage systems: These systems store energy in the chemical bonds of atoms and molecules and released by electron transfer to generate electrical energy
5. Thermal energy Storage systems: Stores energy in the form of heat or ice, and converted to electrical energy when required

## 5.2 Application of ESSs Smart Grids

Energy storage systems plays a key role in smart grids by bridging gaps in power generation and demand, especially in the modern power grids where higher amount of renewable energy sources are integrated in the MV and LV distribution systems. ESSs are capable of tending multiple applications and services in the distribution systems and are mainly classified based on the duration of their usage. Based on the available literature [30]–[33], three major categories of applications are observed based their local and system wide requirements. Table I provides details on their classification based on their points of usage, i.e. generation, transmission & distribution and end users.

Based on the duration of energy dispatch, they are classified into three major categories [34],

1. Reserve and response ancillary services: Power quality services where dispatch varies between micro-seconds to minutes
  - a. Supply interruptions
  - b. Voltage sags or dips
  - c. Voltage swell
  - d. Harmonic distortion

2. Transmission and distribution grid support: Dispatch time typically varies between few seconds to hours supporting ancillary services in T & D grids to operate as specified by grid codes.
  - a. Grid frequency support
  - b. Voltage control
  - c. Spinning reserve
  - d. Congestion relief
3. Energy management: Application where duration of dispatch varies between several hours to days
  - a. Energy arbitrage
  - b. Load levelling
  - c. Peak shaving
  - d. Black start
  - e. Non-spinning reserve

Fig. 8 provides a pictorial representation of the power ratings and the overall discharge duration required from energy storage technologies for various applications. It defines the requirements or specifications to select various energy storage technologies for particular applications in the smart grid. Based on the requirements defined in Fig. 8, suitable ESS technologies that can be utilized for various grid applications are depicted in Fig. 9. The power/energy requirements for a particular application must match with the characteristics of the ESS technology to be deployed. It is also important to have the detailed load curves while conduction feasibility analysis of ESS technologies considering the fact that the energy & power densities, cost and life-cycle characteristics vary from each ESSs. Based on mix and match of various technologies, it is possible to develop hybrid ESS solutions to cater particular load requirements in the smart grid applications.

From Fig. 9 it is evident that the Lithium ion (Li-ion) based BESSs are capable of tending applications in all the time ranges, i.e. reserve and response applications, T & D grid support and energy management. Also, their superior energy and power densities, shelf and cycle life and low self-discharge makes them an ideal candidate for flexibility applications in smart grids. Hence, Li-ion batteries are modelled to cater various power system applications by the authors of this chapter. Based on [35], integration of lithium ion batteries in the MV distribution system by means of power converters shall be explained. Followed by a case study to verify the operations of the developed converter controls for battery integration.

Table I. Classification of ESS applications.

Generation	Transmission and Distribution	End users
<ul style="list-style-type: none"> <li>▶ Energy Arbitrage</li> <li>▶ Ancillary Services                             <ul style="list-style-type: none"> <li>▶ Frequency Regulation</li> <li>▶ Spinning Reserves</li> <li>▶ Supplemental Reserves</li> <li>▶ Ramping</li> </ul> </li> <li>▶ Capacity                             <ul style="list-style-type: none"> <li>▶ Peak Energy</li> <li>▶ Flexibility</li> </ul> </li> <li>▶ Reliability                             <ul style="list-style-type: none"> <li>▶ Voltage Support/ Reactive Power</li> <li>▶ Black Start</li> <li>▶ Frequency Response</li> </ul> </li> </ul>	<ul style="list-style-type: none"> <li>▶ Update deferral                             <ul style="list-style-type: none"> <li>▶ Reduce circuit and line overload</li> </ul> </li> <li>▶ Grid Resiliency                             <ul style="list-style-type: none"> <li>▶ Outage migration</li> <li>▶ Backup power</li> </ul> </li> <li>▶ Voltage Support/ Power Quality</li> <li>▶ Congestion relief</li> </ul>	<ul style="list-style-type: none"> <li>▶ Reduce demand charges</li> <li>▶ Optimise retail rates</li> <li>▶ Power quality/UPS</li> <li>▶ Onsite renewables</li> </ul>

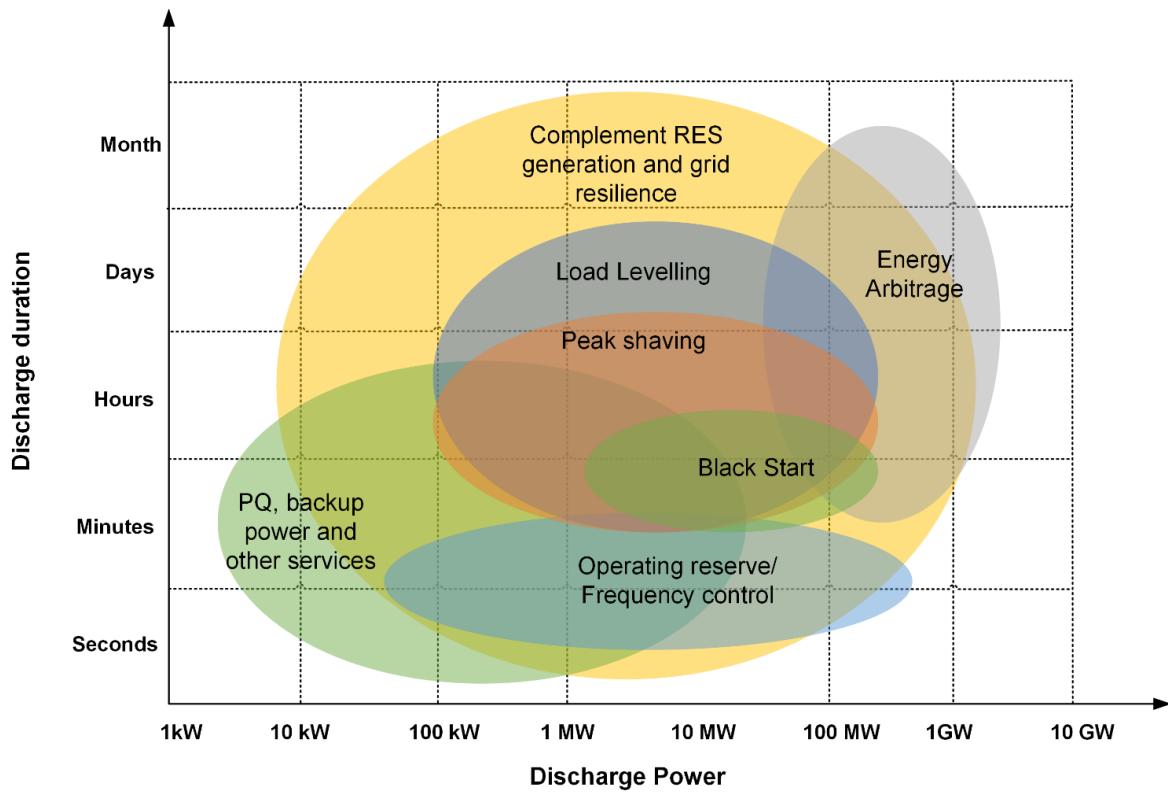


Figure 8. ESS requirements for grid applications

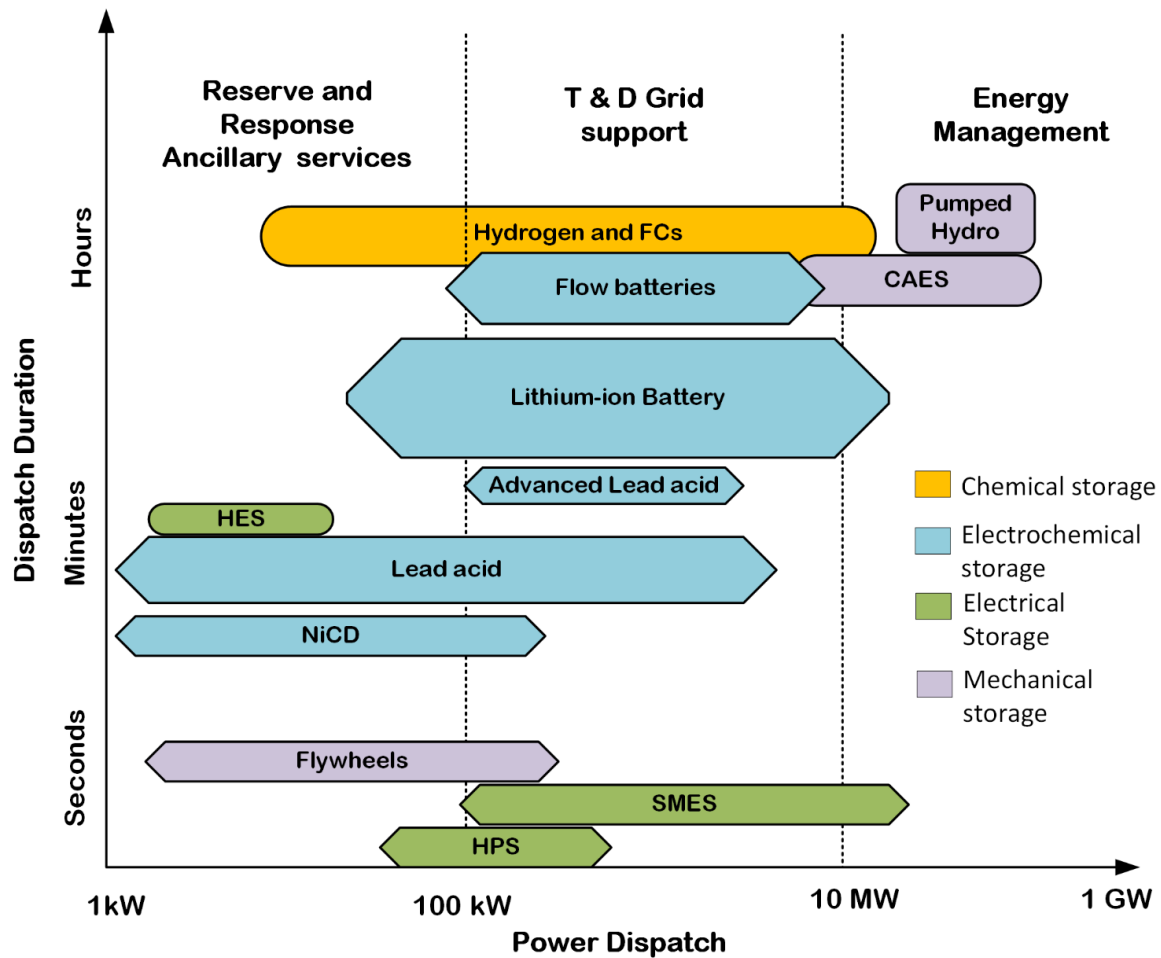


Figure 9. ESS capability for land based applications

## 6. Integration of Battery Energy Storage Systems

Battery energy storage systems (BESSs) are typically inverter based FESs capable of providing both active and reactive power management. Integration of these BESSs follows the same methodology despite being used in centralized or decentralized control architectures. Hence, in this section design and integration methodology of Lithium-ion BESSs to the medium voltage distribution system.

### 6.1 Power Electronic converters

Power electronic (PE) converters provide the vital technology for integration of BESS to the power grids. Maintaining various grid code requirements in the modern distribution systems are satisfied by the PE converters, as most the RESs are connected to the grid through PE. Simultaneously PE interface controls BESS in active (P) and reactive (Q) power flow modes, keeping in view of the current and voltage variations across the battery pack which affects BESS health, performance and lifetime [36]. This section briefly reviews the available and widely used PE topologies for large scale BESSs discussing main parts of the system in detail.

The used configuration and its modelling aspects to integrate BESS to the studied real-life smart grid pilot will be addressed in next section.

Fig. 10 shows the elements of PE units for a typical BESS grid integration which including three main parts;

- DC-DC converter
- DC-AC inverter
- Coupling transformer

In order to design an optimized BESS system, selection and design of each part needs to be investigated in detail. Different parameters affect selection and design of PE units such as power ratio, energy density, response time (speed of system) and grid interconnection requirements.

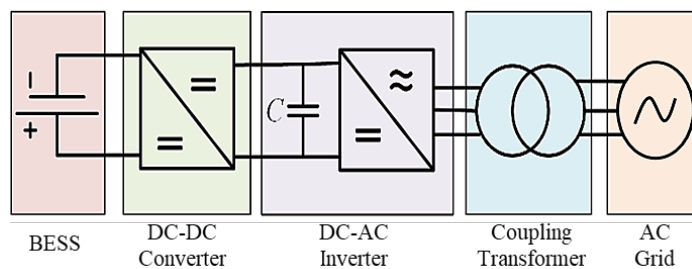


Figure 10. Typical PE units for BESS grid integration

### 6.1.1 DC-DC Converter

Presence of DC-DC converter increases system performance and flexibility, but it also adds losses and costs. Therefore, it is worth considering to connect BESS directly to DC-AC inverter DC bus. BESSs with and without DC-DC converter have been used in recent applications.

#### 6.1.1.1 BESS without DC-DC Converter

PE system design without DC-DC conversion stage could be a cost effective solution in one sense, but it can add complexity to the DC-AC inverter system. Some issues can be linked to this solution. The BESS voltage varies depending on SoC and this introduces DC bus voltage variation which will affect the DC-AC inverter operation performance. Also, safety problems can be associated with this solution since over-voltages or over-currents can happen at BESS side and their management is not easy by only grid side DC-AC inverter. Another possible drawback could be low-order harmonic injection to the battery and this also can affect BESS health and lifetime [37].

#### 6.1.1.2 BESS with DC-DC Converter

Adding a DC-DC conversion stage eliminates above mentioned low-order current harmonics flowing in the battery since the DC-DC converter isolates the BESS from inverter DC bus. With DC-DC converter, BESS can be designed to lower voltage level (less cells in series). Moreover, it can be used as protective and current limiting device which will increase the safety and controllability of the system.

Simple bidirectional Buck-Boost DC-DC converter is widely used due to its simplicity when a lower voltage level is used for BESS side and higher voltage level at the DC bus of the grid side DC-AC inverter. However, Buck-Boost converters have their own intrinsic limits for levelling up/down the voltage [38]. This issue can be dealt with using a full-bridge bidirectional DC-DC converter which also increases the costs and losses (due to increased number of the switching modules).

For high power applications, advanced solutions such as isolated DC-DC converters [39] and isolated dual active bridge (DAB) converters have been proposed [40] which include high frequency isolation transformer (20kHz). This transformer can eliminate need for coupling transformer and since it is working in high frequency, it can decrease the size and weight of the system considerably. These are interesting solutions, but the technology is in research stage and at the moment there are not any commercial solutions available.

### **6.1.2 DC-AC Inverter**

DC-AC inverter is a necessary part of the PE system in the BESS grid integration applications. Main task of it is to convert the DC voltage to the AC voltage and guarantee fulfilment of grid code requirements [41]. Two level inverters are widely used in different applications, including also BESS integration (with centralized BESS at DC bus), due to the maturity of the technology and availability of the commercial solutions. Recently three-level, five-level and more general, multi-level inverters have also been developed and used in wide range of applications.

More specifically, cascaded H-bridge (CHB) converters are used for BESS integration where the BESS can be equally distributed among sub-modules (SMs) in the form of smaller battery packs. However, advanced control algorithms are required in order to ensure balanced SoC for all battery packs.

Modular Multilevel Converter (MMC) is another developing solution in which both centralized BESS at DC bus and distributed BESSs among SMs have been proposed [42]. However, distributed approach can be preferred where the benefits of cascaded structure can be better utilized. With centralized BESS at DC bus, some positive features of MMC structure will be lost [43], [44].

Apart from technology readiness, using CHC and MMC solutions are linked with few issues [36],

- Need for an extra battery management system (BMS) to ensure balanced SoC among the battery modules
- One of the main advantages using CHB or MMC solutions is to eliminate the need for coupling transformer (otherwise these solutions cannot be economically justified), but in BESS application unbalanced SoC can cause DC current injection to the grid (this should be limited to 0.5% according to [41])
- Complexity of the control and system cost.



### 6.1.3 Coupling Transformer

Conventional grid connected PE for BESS system consists of a coupling transformer. Transformer based solution is favoured so far [36] and for large-scale BESS system it could be the preferred solution providing galvanic isolation between grid and energy storage system. However, several transformer-less solutions have been investigated as well. The advantages of using a coupling transformer are,

- DC-AC inverter can work in lower voltage and the transformer can match the voltage level up to kV level
- Inverter AC side passive filter size can be decreased
- It can protect PE devices against grid side faults till certain level
- Losses of the device can be compromised with high efficiency transformers

However, transformers are bulky and heavy units and coupling transformer can increase the weight and size of final installation unit. In medium voltage (MV) level and working with few MWs, the size and weight of coupling transformer itself (in 50 Hz) can be comparatively close or even higher than the rest of system. Isolated DAB converters with high frequency transformers could also be an attractive solution but as mentioned earlier, still DAB commercial solutions does not exist and are in research stage. In addition, it is worth mentioning that correct transformer energization principles should be considered in order to ensure safe and feasible operation conditions.

## 6.2 Grid Code Requirements

IEEE standard considering BESS systems for stationary applications is still in drafting stage, but IEEE standard 1547-2018 [41] and ENTSO-E RfG requirements [45] can be used as a good reference for BESS system PE design from grid code requirements point of view. The standard defines general requirements for power quality (harmonics, reactive power, voltage levels and sag/swells) and DER response to power systems disturbances (such as faults, open phase conditions, voltages and frequency deviation and also islanding situations) i.e. fault-ride-through (FRT) requirements. It can be used as reference to design PE unit but it's focus is mostly on grid side and talks about general requirements and in most cases it leaves the details to the transmission and/or distribution systems operators (TSOs and DSOs) [41].

## 6.3 BESS Integration Design

This section provides an overview on the design and development of power electronics converters for BESS integration to the MV distribution system. Control design and development of voltage source converter (VSC) and DC/DC bidirectional buck-boost converter are explored in detail.

### 6.3.1 BESS Integration Methodology

Li-ion BESSs are best suited for multiple energy storage applications in smart grids, which is evident from their characteristics explained earlier. Hence, they were modelled as flexible energy sources to meet short/medium time energy storage demands in smart grids. Fig. 11 explains to complete BESS integration methodology in the

MV distribution system. Li-ion BESSs are integrated to the MV bus by means of power electronics interfaces, i.e. through DC/DC bidirectional buck-boost converter whose low voltage side is connected to the BESS and the high voltage side is connected to the 600V DC bus. DC/AC VSC converts 600V<sub>DC</sub> to 3-phase, 400 V<sub>RMS</sub>. Coupling transformer converts VSC output to the MV bus voltage which is 21 kV in this case. Equivalent circuit model of Li-ion BESS [35] is utilized in the method. Power electronics converters controller design are explained in the following section.

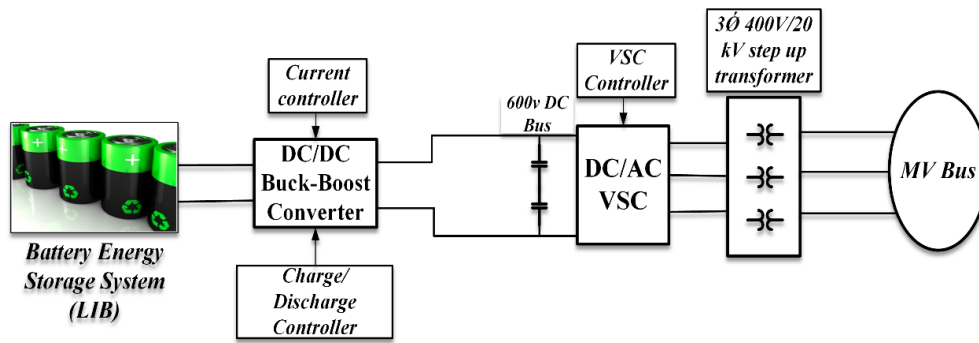


Figure 11. BESS grid integration methodology

### 6.3.2 VSC Controller

VSC controller design is based on voltage oriented control (VOC) technique [46] which is shown in Fig. 12. Primary advantage of the VOC techniques lies in its high static performance and fast transient response through its current control loop. Three phase voltages and currents (i.e.  $I_{abc}$  and  $V_{abc}$ ) are transformed into  $dq0$  frames by means of Park's transformation [47] to  $I_{dq}$  and  $V_{dq}$  frames.  $I_{d,ref}$  is provided by the PI-controller for  $V_{dc}$  management and the  $I_{q,ref}$  is dictated by the reactive power demand for the MV grid application.  $I_{q,ref}$  and  $I_{d,ref}$  controls the active power ( $P$ ) and reactive power ( $Q$ ) outputs respectively. However, the controller's dynamic performance shall be affected by cross coupling between d- and q- axes components. Hence,  $V_d$  feedforward signal is provided to the d-component control loop. Similar Feedforward signal shall be added to the q-component control loop, however, it is not needed in this application. VSC was designed to provide 1.5 times the nominal power to accommodate transient requirements from the grid.

### 6.3.3 Battery Charge and Discharge Controller

Bidirectional Buck-Boost converter acts as the battery charger (buck mode) while charging the batteries and the DC supply converter (boost mode) during discharging scenarios. In this case, it is developed as an average model system with single IGBT and its accompanying anti-parallel diode with a switching inductance [48]. Current control through the converter is provided by a simple PI- controller as shown in Fig. 13. DC bus voltage is regulated and controlled by the VSC's d-component control loop, so the positive or negative sign carried by the PI- controller output defines the  $P$ -flow direction. Hence, an additional DC bus voltage control loop is not necessary in this case in the battery discharging scenarios. During both control modes, i.e. charging or discharging modes, the PI-controller output delivers the duty cycle to the Buck or Boost converter.

To keep the Li-ion BESS in the safe operational threshold, BESS Discharge mode is set in the range between 20 to 90% of the battery State of Charge (SoC). While, charging the batteries the maximum SoC is set at 90% which is provided by the constant current charging technique alone, thereby eliminating constant voltage charging sequence. Adding SoC of the BESS control loops, the battery charging and discharging currents are always maintained within the specifications provided by the manufacturers.

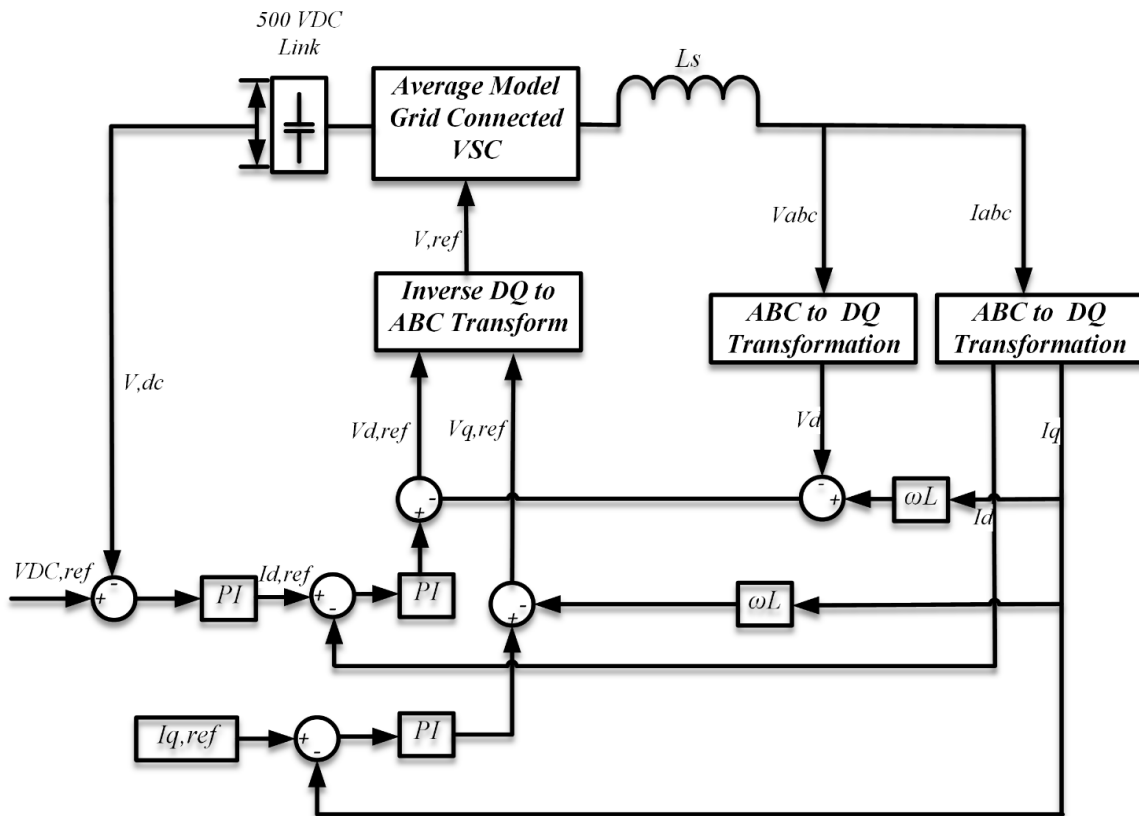


Figure 12. VSC Controller

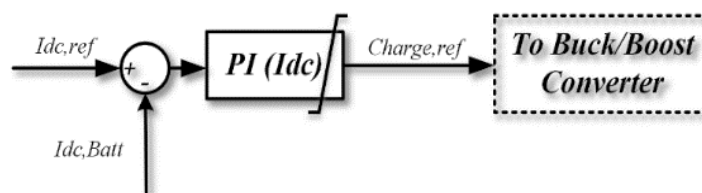


Figure 23. Battery Charge Discharge controller

## 6.4 Case Study and Simulation Results

Integration of Li-ion BESSs to the MV distribution system is validated by means of simulation based on a case study. Grid side controllers provided the  $P_{REF}$  reference to the DC/DC converter stage which is associated with the battery operations. Nature of the designed use case was to validate the stability of VSC and the DC/DC-bidirectional buck boost converter during transient and steady state system behaviour.

Table II presents the characteristics of the Li-ion BESS used in the study. It is sized for a nominal discharge (1C) of 0.335 MW and a peak power discharge (3C) of 1 MW. The DC/DC converter was rated for 3C battery discharge and the VSC is sized at 1.5 MVA. Battery's initial SoC is maintained at 50% which can accommodate both charge and discharge operations as commanded by the grid services.

Table II. Li-ion BESS Specifications

Nominal voltage	312 V
Maximum Voltage	354 V
Minimum Voltage	236 V
Discharge Energy(1C)	335 kWh
Discharge current (1C)	945 A

Table III. Simulation case details

Simulation Time (Secs)	Active Power ref(kW)	Status
T1	670	Discharge
T2	330	Discharge
T3	168	Discharge
T4	-168	Charge

Total simulation time span was considered at 80 seconds. The  $P_{REF}$  given to the BESS is shown in Table III. It corresponds to the various C-rates of battery discharge and changes every 20 seconds during the simulation time period, there by inducing transient instability conditions. In the final time period of simulation, BESS charges at a rate of 0.5C. Such loads are not usually existent upon the BESSs, however, the simulation cases were developed considering extreme events or changes while supporting RESs such as PV/Wind power generation.

Performance of the Li-ion BESS integration through its PE converters are shown in Fig. 14. Battery load current characteristics are as shown in 14(a), where its magnitude changes as set by  $P_{REF}$ . 14(b) shows Li-ion BESS voltage. Voltage fluctuations in the Li-ion BESS are evident. Such accurate voltage characteristics provides set-points for  $V_{dc}$  control in the DC bus. DC power output of the BESS is shown if Fig 14(c), whose characteristics are defined based on the C-rates from Table II. Such large step changes were chosen to observe the DC bus stability and the controller interactions during transient stability conditions. Li-ion BESS SoC changes are as shown in 14(d). The DC bus voltage is presented in 14(e) where it is constantly maintained at 600V, despite changes in Li-ion BESS voltage and current dispatch characteristics. VSC is designed to provide both  $P$  &  $Q$  control capabilities, which is demonstrated after 40 seconds into simulation, where the converter starts to absorb reactive power as shown in 14(f). Therefore, overall design objectives of the Li-ion BESS integration to the MV distribution system is achieved by controlling active and reactive power flows in the power system, maintaining the safe operations of Li-ion batteries.

## Summary and Conclusion

Integration of Distributed generators, i.e. including the renewable energy sources has been ever increasing in the LV and MV distribution systems. Higher penetration of DGs in the power grids comes with its own set of

challenges and multiple innovative ways are needed to mitigate those issues. Active network management of the distribution system, by effective management and control of the available flexibilities plays a crucial role in managing network challenges caused by higher DG penetration. Energy storage systems form a key component in executing ANM schemes by providing both active and reactive power control related flexibilities. Overall, this book chapter provides an overview on DG types, ANM control methodologies, energy storage system (fundamentals, classification and applications) and integration design and methodology for battery energy storage systems in the MV distribution grids.

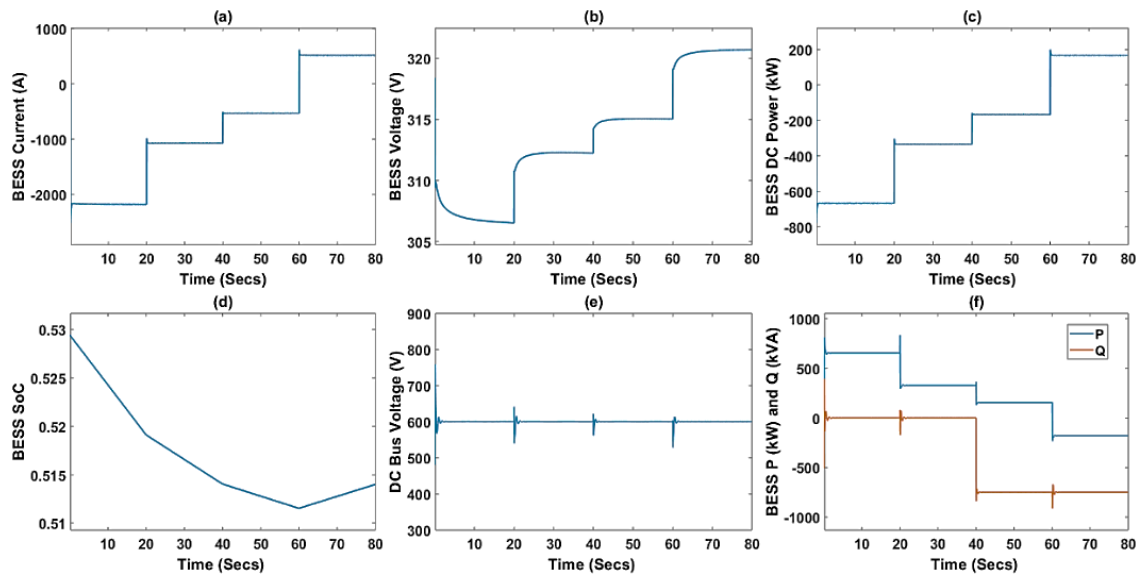


Figure 34. a) Battery Load current (b) Battery Voltage (c) Battery DC Power (d) Battery SoC (e) Battery DC Bus voltage (f) Battery  $P$  and  $Q$  characteristics

## References

- [1] H. Khajeh, A. A. Foroud, and H. Firoozi, "Optimal participation of a wind power producer in a transmission-constrained electricity market," *2017 25th Iran. Conf. Electr. Eng. ICEE 2017*, no. ICEE20 17, pp. 1230–1235, 2017.
- [2] O. S. Nduka and B. C. Pal, "Quantitative Evaluation Of Actual Loss Reduction Benefits of a Renewable Heavy DG Distribution Network," *IEEE Trans. Sustain. Energy*, vol. 9, no. 3, pp. 1384–1396, 2018.
- [3] S. Montoya-Bueno, J. I. Muñoz-Hernández, and J. Contreras, "Uncertainty management of renewable distributed generation," *J. Clean. Prod.*, vol. 138, pp. 103–118, 2016.
- [4] E. Lorenzo, *Solar electricity: engineering of photovoltaic systems*. Earthscan/James & James, 1994.
- [5] D. Çelik and M. E. Meral, "Current control based power management strategy for distributed power generation system," *Control Eng. Pract.*, vol. 82, pp. 72–85, 2019.
- [6] S. Farajdadian and S. M. H. Hosseini, "Optimization of fuzzy-based MPPT controller via metaheuristic techniques for stand-alone PV systems," *Int. J. Hydrogen Energy*, vol. 44, no. 47, pp. 25457–25472, 2019.
- [7] R. AbdelHady, "Modeling and simulation of a micro grid-connected solar PV system," *Water Sci.*, vol. 31, no. 1, pp. 1–10, 2017.
- [8] M. Zaibi, G. Champenois, X. Roboam, J. Belhadj, and B. Sareni, "Smart power management of a hybrid photovoltaic/wind stand-alone system coupling battery storage and hydraulic network," *Math. Comput. Simul.*, vol. 146, pp. 210–228, 2018.
- [9] F. Kalavani, B. Mohammadi-Ivatloo, and K. Zare, "Optimal stochastic scheduling of cryogenic energy storage with wind power in the presence of a demand response program," *Renew. Energy*, vol. 130, pp.

- 268–280, 2019.
- [10] D. Li, X. Xu, D. Yu, M. Dong, and H. Liu, “Rule Based Coordinated Control of Domestic Combined Micro-CHP and Energy Storage System for Optimal Daily Cost,” *Appl. Sci.*, vol. 8, no. 1, p. 8, 2018.
  - [11] W. Bai, M. R. Abedi, and K. Y. Lee, “Distributed generation system control strategies with PV and fuel cell in microgrid operation,” *Control Eng. Pract.*, vol. 53, pp. 184–193, 2016.
  - [12] N. Mahmud and A. Zahedi, “Review of control strategies for voltage regulation of the smart distribution network with high penetration of renewable distributed generation,” *Renew. Sustain. Energy Rev.*, vol. 64, pp. 582–595, 2016.
  - [13] R. A. Walling, R. Saint, R. C. Dugan, J. Burke, and L. A. Kojovic, “Summary of distributed resources impact on power delivery systems,” *IEEE Trans. Power Deliv.*, vol. 23, no. 3, pp. 1636–1644, 2008.
  - [14] S. K. Ibrahim, “Distribution System Optimization With Integrated Distributed Generation,” 2018.
  - [15] S. Ruiz-Romero, A. Colmenar-Santos, F. Mur-Pérez, and A. López-Rey, “Integration of distributed generation in the power distribution network: The need for smart grid control systems, communication and equipment for a smart city - Use cases,” *Renew. Sustain. Energy Rev.*, vol. 38, pp. 223–234, 2014.
  - [16] S. N. Afifi, “Impact of Hybrid Distributed Generation Allocation on Short Circuit Currents in Distribution Systems,” no. March, p. 214, 2017.
  - [17] S. Abapour, S. Nojavan, and M. Abapour, “Multi-objective short-term scheduling of active distribution networks for benefit maximization of DisCos and DG owners considering demand response programs and energy storage system,” *J. Mod. Power Syst. Clean Energy*, vol. 6, no. 1, pp. 95–106, Jan. 2018.
  - [18] H. Laaksonen, K. Sirviö, S. Aflecht, and K. Kauhaniemi, “Multi-objective Active Network Management Scheme Studied in Sandom Smart Grid with MV and LV connected DER Units,” no. June, pp. 3–6, 2019.
  - [19] I. Abdelmotteleb, T. Gomez, and J. P. Chaves-Avila, “Benefits of PV inverter volt-var control on distribution network operation,” *2017 IEEE Manchester PowerTech, Powertech 2017*, pp. 15–20, 2017.
  - [20] M. A. G. De Brito, L. Galotto, L. P. Sampaio, G. De Azevedo Melo, and C. A. Canesin, “Evaluation of the main MPPT techniques for photovoltaic applications,” *IEEE Trans. Ind. Electron.*, vol. 60, no. 3, pp. 1156–1167, 2013.
  - [21] Y. Zhang, Y. Xu, H. Yang, and Z. Y. Dong, “Voltage regulation-oriented co-planning of distributed generation and battery storage in active distribution networks,” *Int. J. Electr. Power Energy Syst.*, vol. 105, no. August 2018, pp. 79–88, 2019.
  - [22] Y. Zhang, Y. Xu, H. Yang, and Z. Y. Dong, “Voltage regulation-oriented co-planning of distributed generation and battery storage in active distribution networks,” *Int. J. Electr. Power Energy Syst.*, vol. 105, pp. 79–88, 2019.
  - [23] H. Khajeh, H. Laaksonen, A. S. Gazafroud, and M. Shafie-Khah, “Towards flexibility trading at TSO-DSO-customer levels: A review,” *Energies*, vol. 13, no. 1, pp. 1–19, 2019.
  - [24] S. Dalhues *et al.*, “Towards research and practice of flexibility in distribution systems: A review,” *CSEE J. Power Energy Syst.*, vol. 5, no. 3, pp. 285–294, 2019.
  - [25] H. Klinge Jacobsen and S. T. Schröder, “Curtailed of renewable generation: Economic optimality and incentives,” *Energy Policy*, vol. 49, pp. 663–675, 2012.
  - [26] M. A. Matos *et al.*, “Control and Management Architectures,” *Smart Grid Handb.*, pp. 1–24, 2016.
  - [27] M. S. Guney and Y. Tepe, “Classification and assessment of energy storage systems,” *Renew. Sustain. Energy Rev.*, vol. 75, no. November 2016, pp. 1187–1197, 2017.
  - [28] M. C. Argyrou, P. Christodoulides, and S. A. Kalogirou, “Energy storage for electricity generation and related processes: Technologies appraisal and grid scale applications,” *Renew. Sustain. Energy Rev.*, vol. 94, no. July, pp. 804–821, 2018.
  - [29] M. Faisal, M. A. Hannan, P. J. Ker, A. Hussain, M. Bin Mansor, and F. Blaabjerg, “Review of energy storage system technologies in microgrid applications: Issues and challenges,” *IEEE Access*, vol. 6, pp. 35143–35164, 2018.
  - [30] M. G. Molina, “Energy Storage and Power Electronics Technologies: A Strong Combination to Empower the Transformation to the Smart Grid,” *Proc. IEEE*, vol. 105, no. 11, pp. 2191–2219, 2017.
  - [31] O. Palizban and K. Kauhaniemi, “Energy storage systems in modern grids—Matrix of technologies and applications,” *J. Energy Storage*, vol. 6, pp. 248–259, 2016.
  - [32] N. Günter and A. Marinopoulos, “Energy storage for grid services and applications: Classification, market review, metrics, and methodology for evaluation of deployment cases,” *J. Energy Storage*, vol. 8, pp. 226–234, 2016.

- [33] European Commission, "COMMISSION STAFF WORKING DOCUMENT Energy storage – the role of electricity," vol. 2020, no. 2013, pp. 1–25, 2017.
- [34] M. Rahman, A. O. Oni, E. Gemechu, and A. Kumar, "Assessment of energy storage technologies : A review," *Energy Convers. Manag.*, vol. 223, no. August, p. 113295, 2020.
- [35] C. Parthasarathy, H. Hafezi, and H. Laaksonen, "Lithium-ion BESS Integration for Smart Grid Applications - ECM Modelling Approach," 2020.
- [36] G. Wang *et al.*, "A review of power electronics for grid connection of utility-scale battery energy storage systems," *IEEE Trans. Sustain. Energy*, vol. 7, no. 4, pp. 1778–1790, 2016.
- [37] A. Bessman, R. Soares, O. Wallmark, P. Svens, and G. Lindbergh, "Aging effects of AC harmonics on lithium-ion cells," *J. Energy Storage*, vol. 21, no. October 2018, pp. 741–749, 2019.
- [38] N. Mohan, T. M. Undeland, and W. P. Robbins, *Power electronics : converters, applications, and design*. John Wiley & Sons, 2003.
- [39] N. M. L. Tan, T. Abe, and H. Akagi, "Design and performance of a bidirectional isolated DC-DC converter for a battery energy storage system," *IEEE Trans. Power Electron.*, vol. 27, no. 3, pp. 1237–1248, 2012.
- [40] J. Everts, F. Krismer, J. Van Den Keybus, J. Driesen, and J. W. Kolar, "Optimal zvs modulation of single-phase single-stage bidirectional dab ac-dc converters," *IEEE Trans. Power Electron.*, vol. 29, no. 8, pp. 3954–3970, 2014.
- [41] "IEEE 1547-2018 - IEEE Standard for Interconnection and Interoperability of Distributed Energy Resources with Associated Electric Power Systems Interfaces." [Online]. Available: <https://standards.ieee.org/standard/1547-2018.html>. [Accessed: 10-Apr-2019].
- [42] M. A. Perez, S. Bernet, J. Rodriguez, S. Kouro, and R. Lizana, "Circuit topologies, modeling, control schemes, and applications of modular multilevel converters," *IEEE Trans. Power Electron.*, vol. 30, no. 1, pp. 4–17, 2015.
- [43] L. Maharjan, S. Member, S. Inoue, and H. Akagi, "A Transformerless Energy Storage System.pdf," vol. 44, no. 5, pp. 1621–1630, 2008.
- [44] H. Akagi, "Classification, terminology, and application of the modular multilevel cascade converter (MMCC)," *IEEE Trans. Power Electron.*, vol. 26, no. 11, pp. 3119–3130, 2011.
- [45] "COMMISSION REGULATION (EU) 2016/ 631 - of 14 April 2016 - establishing a network code on requirements for grid connection of generators."
- [46] F. Blaabjerg, R. Teodorescu, M. Liserre, and A. V. Timbus, "Overview of control and grid synchronization for distributed power generation systems," *IEEE Trans. Ind. Electron.*, vol. 53, no. 5, pp. 1398–1409, 2006.
- [47] "Power Electronics Handbook | ScienceDirect." [Online]. Available: <https://www.sciencedirect.com/book/9780128114070/power-electronics-handbook>. [Accessed: 18-Aug-2020].
- [48] G. D'Antona, R. Faranda, H. Hafezi, and M. Bugliesi, "Experiment on Bidirectional Single Phase Converter Applying Model Predictive Current Controller," *Energies*, vol. 9, no. 4, p. 233, 2016.

# Modelling and Simulation of Hybrid PV & BES Systems as Flexible Resources in Smartgrids – Sundom Smart Grid Case

Chethan Parthasarathy, Hossein Hafezi, Hannu Laaksonen, Kimmo Kauhaniemi  
 School of Technology and Innovation, Electrical Engineering  
 University of Vaasa  
 Vaasa, Finland-65200  
 chethan.parthasarathy@uwasa.fi

**Abstract**— Ever-growing energy needs and larger penetration of renewable energy in the power grids with higher intermittency in power generation cause the need for flexible energy sources. Flexible sources such as distributed generation, demand response, electric vehicles etc. play a dominant role in providing flexibility in services such as frequency, voltage and power balance control in smart grids. Given the present state of technology and economic maturity of battery energy storage systems (BESS), has a lot of potential to fulfill increasing power systems rapid, short-term flexibility needs. In this paper, a case study on hybrid photovoltaic (PV) arrays & lithium ion based BESS as flexible energy sources are integrated in medium voltage (MV) network side in local pilot network, Sundom Smart Grid (SSG). Vaasa, Finland. Sundom Smart grid is modelled based on real time data on energy consumption and generation streamed from network. Role of batteries as a flexible energy source in the PV & BESS hybrid for power balance flexibility application is demonstrated by means of Matlab simulations.

**Keywords**— Microgrid, battery energy storages, lithium ion batteries, Flexible energy sources, DC/DC converter controls, DC/AC VSC controls.

## I. INTRODUCTION

Explosive growth in energy demand and need for its secure supply has posed varied challenges on primary energy availability. Factors such as aging transmission systems, distribution infrastructure, security, reliability and power quality have been motivating development of innovative grid architectures such as microgrids etc. European Union (ETIP-SNET) vision emphasizes on a low-carbon, secure, reliable, resilient, accessible, cost-efficient, and market-based pan-European integrated energy system, capable of supplying the whole economy and paving the way for a fully  $CO_2$ -neutral and circular economy by the year 2050, while maintaining and extending global industrial leadership in energy systems during the energy transition [1]. Smartgrids with decentralized and distributed power generation technologies provide an edge in such innovative solutions by limiting transmission & distribution losses, improved economic dispatch, improved

reliability & power quality and introducing higher degree of flexibility [2].

Strong EU policy framework on cleaner energy has led to rapid increase in the integration of renewable energy systems (RES) such as wind turbine generators (WTG) and PV energy systems in the grids. This enables the need for higher flexibility in distributed power generation considering their intermittency. Intermittent behavior of RES and DGs are due to their dependency on environmental and meteorological conditions, which causes RES energy output to fluctuate for a localized small capacity microgrid (MG) with more than 10% of the RES occupation [3].

BESS play a critical role in providing flexibility in such smartgrids, by acting as small electric power system being able to operate individually in physically islanded or interconnected mode with the utility grids. BESS, along with being a small electric system also has the potential to participate in multitude of services. Apart from facilitating integration of RES, they also play critical roles in energy arbitrage, optimization of sources in MG, power quality improvement and ancillary services such as load following, operational reserve, frequency regulation etc. [4]. Fig. 1 depicts requirement of ESS for a wide range of application in smartgrids.

Lithium ion batteries (LIB) based BESS are gaining prominence for its role in tapping the potential of renewable energy sources due to higher energy and power density [5], with increased safety of battery chemistries in recent times. They are also capable of providing almost all the services mentioned in Fig. 1. LIBs are modular in structure, where scaling up or down the size of the batteries are relatively easier, thereby expanding their importance in smartgrids.

In this paper, a case study about integration of hybrid PV & LIB based BES system in MV network of SSG (in Vaasa, Finland) is studied. Modelling SSG with the battery-PV hybrid system and design of needed DC/DC converters and DC/AC voltage source converter controllers are presented in the following sections.



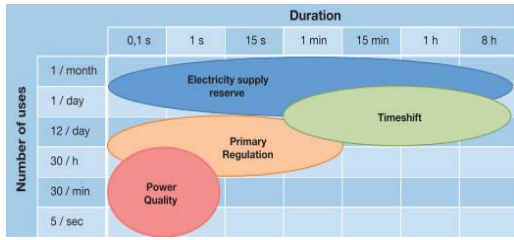


Figure 1. Application of electrical energy storage in microgrids, depending on the frequency and duration of use [6]

II. SUNDOM SMART GRID

SSG is a pilot living lab jointly created by ABB, Vaasan Sähköverkko (DSO), Elisa (communications) and University of Vaasa [7]. The overview of the system is presented in Fig. 2. Real-time measurements are recorded from the MV distribution network on-line, from all four feeders at a HV/MV substation as well as from three MV/LV substations comprising 20 measurement points totally. The measured data is IEC 61850 stream with current and voltage measurements. The sampling rate is 80 samples per cycle. In addition power, frequency, RMS voltages, currents etc. measurements are received by GOOSE messages. The data is collected to servers for providing data also for future research.

III. SSG SYSTEM AND COMPONENT MODELLING

A. Smartgrid system model

SSG is modelled as accurately as possible with available data and grid structure in Matlab/Simulink (Simpowersystems). Distribution system is modelled based on data from the local DSO Vaasan Sähköverkko, including all the LV load distribution points and the distribution lines, which lead to them. At each MV load points, i.e. Vaskiluoto, Sundom and Sulva, multiple LV feeder points exist

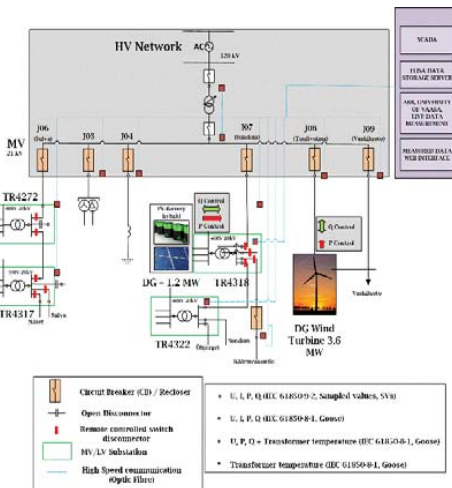


Figure 2. Single line diagram SSG [8]

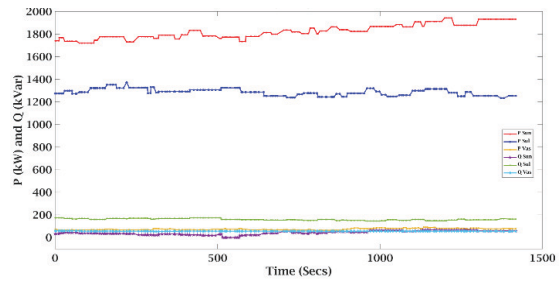


Figure 3. Load Demand at MV buses

Fig. 3 shows the load variations on 30-May-2017 respectively at each MV bus. This period was chosen because the wind power generation was very low (i.e. less than 3.6 MW), which requires implementation of flexible energy resources. Due to the limitation in measurements at distribution side, average load consumption is calculated at each of the MV bus and bus is divided by the number of load centres at each LV distribution points to define load consumption at each LV feeder.

B. Wind Power Modelling

Wind power generation is modelled from the measured active ( $P_{Wind}$ ) and reactive power generation ( $Q_{Wind}$ ) at bus Tuulivoima (J08), which is as shown in Fig 4.  $P_{Wind}$  and  $Q_{Wind}$  are then converted to system currents [9], with MV voltage as reference as explained in (1), (2) and (3). Fig. 5 shows injection of  $I_{abc}$  into the MV grid.

$$[S_{Wind}] = \begin{bmatrix} P_{Wind} \\ Q_{Wind} \end{bmatrix} \quad (1)$$

$$[V_{Grid}] = \begin{bmatrix} Vd & Vq \\ Vq & -Vd \end{bmatrix} \quad (2)$$

$$[Id] = \begin{bmatrix} Vd & Vq \\ Vq & -Vd \end{bmatrix}^{-1} * \begin{bmatrix} P_{Wind} \\ Q_{Wind} \end{bmatrix} \quad (3)$$

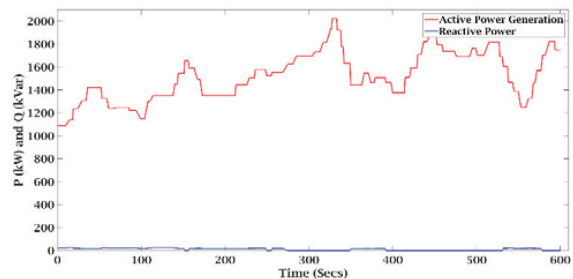


Figure 4. Wind Power Generation

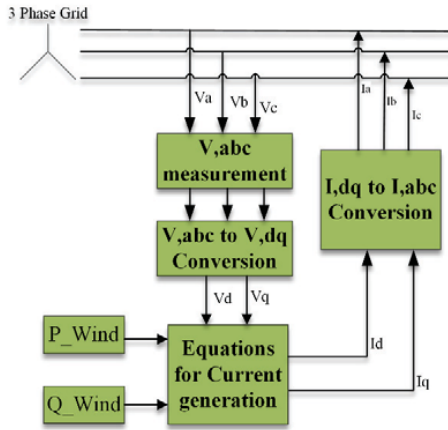


Figure 5. Conversion of PQ\_Wind to Iabc

C. Solar PV & battery hybrid modelling

A 33 kW solar PV distributed generation is currently existent, which is integrated at Sandom (J07) MV bus. A scale up of existing PV production in parallel with lithium ion battery (LIB) based energy storage system forming a hybrid is proposed, as in Fig. 6. The hybrid system is sized to provide a peak output of 1.2 MW reliable power output, where LIB based ESSs shall act as flexible energy sources acting as a short time energy source, complimenting the intermittency in PV power. Details of BESS and PV array are mentioned in Table 1 and 2. BESS is modelled on the basis of Shepherd’s modelling technique [10]. Discharge characteristics of battery (1C, 2C and 3C rates) are as shown in Fig 7. Single diode model with losses [11] are used to model solar PV arrays, whose module current-voltage characteristics are defined by (4) and (5). I-V and P-V characteristics of the PV panel are plotted in Fig 8 at 5 °C and 25 °C, 1000 w/m<sup>2</sup>.

$$I_d = I_o * [e^{-\frac{V_d}{V_T}} - 1] \quad (4)$$

$$V_T = \frac{kT}{q} * nI * N_{cell} \quad (5)$$

- $I_d$  Diode current (A)
- $V_d$  Diode voltage (V)
- $I_o$  Diode saturation current (A)
- $nI$  Diode ideality factor, a number close to 1.0
- $K$  Boltzmann constant (1.3806e-23J. K<sup>-1</sup>)
- $q$  electron charge (1.6022 e<sup>-19</sup>C)
- $T$  cell temperature (K)
- $N_{cell}$  Number of cells connected in series in a module

PV array output is boosted by means of boost converter, whose controller is based on perturb and observe (P & O) MPPT algorithm.

Table I. LIB Size and characteristics

Lithium Ion Battery Characteristics	
Nominal DC voltage	350 V
Peak Voltage	407V
Cut-off Voltage	262V
Capacity (0.5 C)	1110 Ah
Nominal Discharge current (0.5 C)	482A
Peak discharge current (3C)	3330A

Table II. PV size and characteristics

Solar PV Characteristics	
Array type	SunPower SPR-315E-WHT-D
Module Voltage at MPP	54.7 V
Module Open circuit Voltage	64.6 V
Module Current at MPP	5.76 A
Module Max Power	315 W
Total Series Modules	5
Parallel strings	600

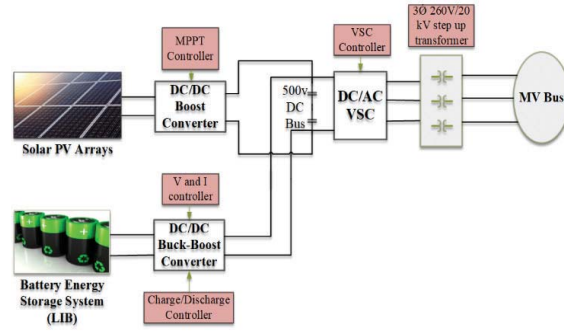


Figure 6. Design of PV and battery hybrid

PV arrays and the lithium ion BESS are integrated in the same DC bus rated at 500V. From Fig. 8, it is evident that PV arrays have a peak power capability of 850 kW with a maximum current generation of up to 4kA. Remaining energy must be provided by the BESS. DC bus is connected to VSC, which is rated at 1.2 MW and is defined as a function of current from PV arrays (I\_PV) and BESS (I\_batt) as in (6). VSC converts 500 Vdc to 3Ø, 260V AC, which is then boosted to MV level by means of a transformer.

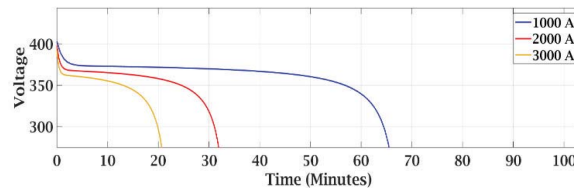


Figure 7. LIB discharge characteristics

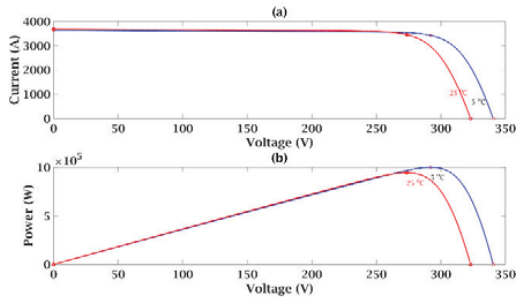


Figure 8. Solar PV array characteristics

$$P_{Inv} = V_{dc,bus} * (I_{PV} + I_{batt}) \quad (6)$$

PV panels have a peak DC output voltage close to 370 V, which is to be boosted to 500 V by means of a boost converter incorporating perturb and observe maximum power point tracking (MPPT) algorithm [12]. In addition, battery stage is connected to the DC bus by means of DC/DC buck-boost converter, where discharging shall be carried out in boost mode and the charging in buck mode. Accurate control for all the power converters are critical considering the nature of application they are serving in this case.

#### IV. CONTROL OF PV AND BATTERY HYBRID

Design and operation of the power converter controllers of the PV and battery hybrid are elaborated in this section. They include DC/AC VSC and DC/DC BESS buck-boost controller designs.

##### A. VSC controller

Fig 9 describes the VSC controller methodology, which is a voltage oriented control (VOC) technique[13][14]. VOC strategy guarantees fast transient response and high static performance through current control loop.  $V_{abc}$  and  $I_{abc}$  are transformed to  $V_{dq}$  and  $I_{dq}$  frames.  $I_{d,ref}$  is obtained by the PI controller for  $V_{dc}$  and the  $I_{q,ref}$  reference is provided by the controller designer based on the application demand. Active power output of the inverter is controlled by  $I_{d,ref}$  and  $I_{q,ref}$  controls the reactive power output.

A cross coupling exists between d- and q- axes components, which shall affect the dynamic performance of the controller. Therefore, it is very imperative to decouple the two axes for better dynamic performance [15]. Controller in Fig. 9 incorporates the decoupling of d- and q- axes.

##### B. Battery Discharge Controller

Average model of boost converter is designed to discharge the batteries through DC bus capacitor. During discharging, the LIB voltage is boosted to 500 Vdc while maintaining DC bus voltage constant for inverter to supply load. Controller design is based on cascade PI controller with outer voltage control and inner current controller as in Fig 10. The second PI controller output provides the duty cycle to boost converter.

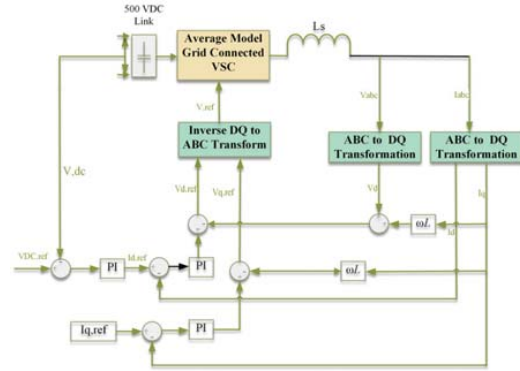


Figure 9. VSC Controller diagram

$$I_{batt} = I_{dc,inv} - I_{PV} \quad (7)$$

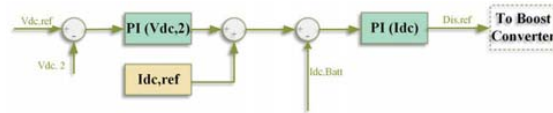


Figure 10. Discharging controller



Figure 11. Charge controller

Discharge mode works in the range between 20% to 90% of battery SoC, as per the current requirements commanded based on the current required by the inverter. During discharge mode, the inverter current requirement limits the battery current to safe operation limits, which is expressed in (7).  $I_{batt}$  is the battery current based on its power rating and  $I_{PV}$  is the Solar PV current.

##### C. Battery Charge Controller

Average model of buck converter is designed to charge the batteries using voltage through DC bus capacitor. Constant current (CC) protocol is employed for charging the battery system, as the maximum State of Charge (SoC, Max), is maintained at 90%, which typically is achieved by constant current charging alone, eliminating constant voltage (CV) requirements. Battery charge and discharge mode is based on state of charge (SoC) of the system. Charge controller triggers buck mode of the converter ON when SoC goes below 20% and turns OFF when it reaches maximum of 90%.

Fig 11 depicts the buck converter controller principle. The difference between nominal voltage value and measured voltage is fed to the PI controller, and the output is considered as the current reference, which is used as reference to the

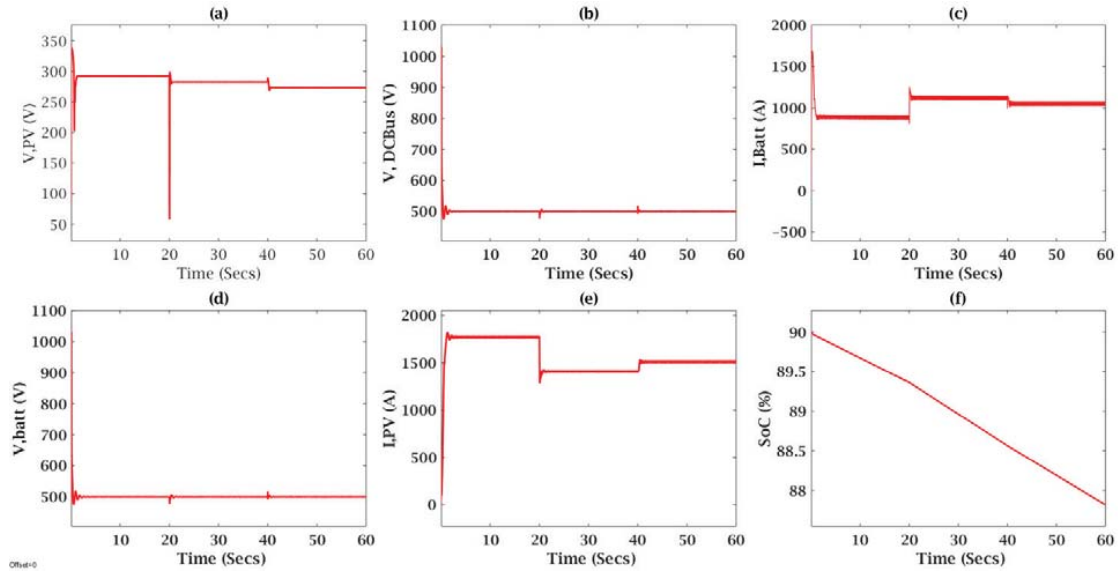


Figure 12. PV array voltage; (b) Controlled voltage at DC bus; (c) Battery current; (d) Controlled battery converter DC voltage ; (e) PV current; (f) Battery SoC;

constant current charge controller. Table 3 presents the regulator gains of PI controllers employed.

V. SIMULATION RESULTS AND DISCUSSION

As explained in section 4, SSG was accurately modelled, both in component and system level by means of the measured characteristics. The case study was performed to validate the role hybrid PV and BESS integration in the MV. The use case study was intended to study the stability of DC/AC converter and battery discharge control by means of DC/DC boost converter, validating it in terms of transient & steady state behavior. It also aids in sizing of BESS for short-term power supply in smart grid applications.

Table III. Controller Coefficients

Controller Coefficients	Kp	Ki
VSC DC voltage regulator	0.5	15
VSC Current regulator	0.3	6
Discharge Controller (V,dc)	0.01	2
Discharge Controller (I,dc)	0.01	1
Charge Controller (Idc)	0.02	0.1

Based on the solar irradiance ( $I_r$ ) and temperature ( $T$ ) characteristics recorded in [16], three different data sets were chosen within total simulation time ( $T_s$ ) is 60 secs, where intermittency is introduced after every 20 seconds.  $I_r$  and  $T$  for  $T_1$  were defined based on the recorded average for the month of July 2017. Similarly,  $T_2$  and  $T_3$  were the average values in June and May 2017 respectively. These PV variable parameters shall aid in studying the robustness of the hybrid system, when wind power generation is not at its peak. Simulations were performed in discrete mode with time steps of 0.0005 seconds.

Table IV. Simulation details

Hybrid PV Simulation Case details		
Time Period (Secs)	Irradiance ( $W/m^2$ )	Temperature ( $^{\circ}C$ )
T1 (0-20)	1000	5
T2 (20-40)	900	15
T3 (40-60)	800	25

Fig 12 explains the performance of PV and BESS for the entire length of simulation period. PV output voltage ( $V_{PV}$ ) reduces at each time steps (i.e. T1 through T3) inducing transients, which is evident from Fig 12(a). Fig 12 (b) displays the DC link voltage ( $V_{DCLink}$ ), which is maintained at 500V despite the transients induced in the system at time periods T2 and T3, thereby verifying the operability of the hybrid system designed. Fig 12 (c) denotes the battery current ( $I_{batt}$ ) discharge characteristics, that are within its safe operating region, which adjusts itself based on the PV intermittency to supply the set requirements. Fig 12 (d) shows DC voltage at the boost converter, which is controlled at 500V. Changes in current generated from PV ( $I_{PV}$ ) in different time periods is evident in Fig 12(e). Fig 12(f) describes the battery SoC, which reduces almost 2% during the simulation period, thereby reinstating its role as short-term power supply source capable of complementing the intermittent generation from renewable energy sources.

Power supply into the SSG system from renewable energy resources is presented in Fig 13. Wind power output is based on data recorded from 0 to 60 seconds (Fig. 4). It is noted that a high level of intermittency appears in this time period starting with a minimal power output, which makes it relevant for the

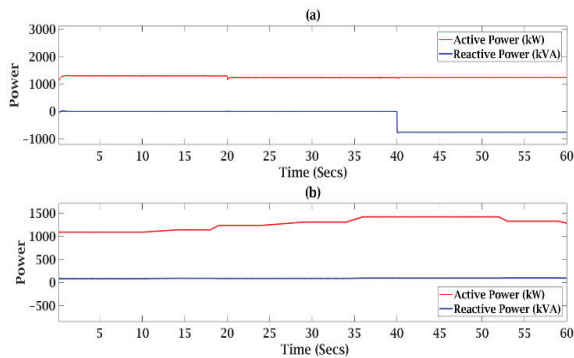


Figure 13. (a) Hybrid PV power characteristics (P & Q); (b) Wind turbine generator power (P & Q) characteristics

study conducted, as flexible energy sources shall complement the wind power output downfall. Fig. 13 (b) replicates the active and reactive power characteristics of the WTG, where P fluctuates. Fig 13. (a) represents the P and Q characteristics of the designed hybrid energy source. Active power output is levelled at 1.2 MW, which serves the purpose it was designed of supplying a constant power, where lithium ion BESS solves PV intermittency issue, by acting as a flexible energy source. Inverter is capable of P & Q control respectively, which is demonstrated in period T3. The inverter absorbs reactive power closer to 400 kVAR, thereby enabling improvement of voltage characteristics as and when the MV grid commands.

## VI. CONCLUSION

Flexible energy resources will play a dominant role in the future of power systems, as there is a phase shift in the integration of renewable energy resources globally. Battery energy storages, especially the lithium ion batteries are in the forefront of such flexible energy services in the coming decades with their promising characteristics, which spreads across multiple applications.

Accurate design and operation DC/AC power conversion system to facilitate integration of PV and battery hybrid energy source is of paramount importance. Also, LIBs are sensitive in terms of their charge and discharge characteristics, which has to be always maintained in their safe operating area, in order to mitigate thermal runaway conditions. In this paper, a design to carefully discharge and charge LIBs within their threshold is designed and validated by simulation in an existing smartgrid (SSG). Also, the inverter design and control (active and reactive power) are validated for the same application. BESS discharge current characteristics derived from the simulation, i.e. Fig. 12 (c), is the primary indicator for capacity sizing of lithium ion batteries. Accurate sizing of ESS resources are critical due to their operating characteristics and economics [17]. In the study, the scenario considered is one of the most critical cases, due to the limited wind power generation, and the battery sized for this application shall aid in tending almost all the other requirements of flexibility.

In future, role of energy storage system for multiple (i.e. short time and longer time) applications will be studied considering SSG as a case, including its role in steady state and transient stabilities by means of OPAL-RT real time simulator.

Such detailed studies shall aid in accurately designing dispatch strategies for BESS tertiary controller in a hierarchically controlled microgrid systems.

## REFERENCES

- [1] T. L. B. N. Hatzigiorgiou, K. Staschus, "A new focus on innovation / implementation and on sector coupling 2016," 2016.
- [2] K. O. Oureilidis and C. S. Demoulias, "An enhanced role for an energy storage system in a microgrid with converter-interfaced sources," *J. Eng.*, vol. 2014, no. 11, pp. 618–625, 2014.
- [3] X. Tan, Q. Li, and H. Wang, "Advances and trends of energy storage technology in Microgrid," *Int. J. Electr. Power Energy Syst.*, vol. 44, no. 1, pp. 179–191, 2013.
- [4] A. Oudalov, T. Degner, F. van Overbeeke, and J. M. Yarza, "Microgrid: Architectures and Control - Chapter 2," *Microgrids Archit. Control*, pp. 1–24, 2003.
- [5] G. Zubi, R. Dufo-López, M. Carvalho, and G. Pasaoglu, "The lithium-ion battery: State of the art and future perspectives," *Renew. Sustain. Energy Rev.*, vol. 89, no. April, pp. 292–308, 2018.
- [6] "www.iec.ch/whitepaper/pdf/iecWP-energystorage-LR-en.pdf." [Online]. Available: <https://www.iec.ch/whitepaper/pdf/iecWP-energystorage-LR-en.pdf>. [Accessed: 07-Dec-2018].
- [7] M. Rita-kasari, "Real-Time Research Lab in the Sundom Smart Grid Pilot," no. 352, pp. 1–4, 2016.
- [8] H. Laaksonen, "Future-proof Islanding Detection Schemes in Sundom Smart Grid," *Cired 2017*, no. June, pp. 12–15, 2017.
- [9] B. N. Singh, V. Khadkikar, and A. Chandra, "Generalised single-phase p-q theory for active power filtering: simulation and DSP-based experimental investigation," *IET Power Electron.*, vol. 2, no. 1, pp. 67–78, Jan. 2009.
- [10] J. Meng, G. Luo, M. Ricco, M. Swierczynski, D.-I. Stroe, and R. Teodorescu, "Overview of Lithium-Ion Battery Modeling Methods for State-of-Charge Estimation in Electrical Vehicles," *Appl. Sci.*, vol. 8, no. 5, p. 659, 2018.
- [11] S. Shongwe and M. Hanif, "Comparative Analysis of Different Single-Diode PV Modeling Methods," *IEEE J. Photovoltaics*, vol. 5, no. 3, pp. 938–946, May 2015.
- [12] M. A. G. de Brito, L. Galotto, L. P. Sampaio, G. de A. e Melo, and C. A. Canesin, "Evaluation of the Main MPPT Techniques for Photovoltaic Applications," *IEEE Trans. Ind. Electron.*, vol. 60, no. 3, pp. 1156–1167, Mar. 2013.
- [13] G. D'Antona, R. Faranda, H. Hafezi, and M. Bugliesi, "Experiment on Bidirectional Single Phase Converter Applying Model Predictive Current Controller," *Energies*, vol. 9, no. 4, p. 233, 2016.
- [14] T. Zhao, Q. Zong, T. Zhang, and Y. Xu, "Study of photovoltaic three-phase grid-connected inverter based on the grid voltage-oriented control," *Proc. 2016 IEEE 11th Conf. Ind. Electron. Appl. ICIEA 2016*, pp. 2055–2060, 2016.
- [15] B. Li, S. Huang, X. Chen, and Y. Xiang, "A simplified DQ-frame current controller for single-phase grid-connected inverters with LCL filters," *2017 20th Int. Conf. Electr. Mach. Syst. ICEMS 2017*, 2017.
- [16] "JRC's Directorate C, Energy, Transport and Climate - PVGIS - European Commission." [Online]. Available: <http://re.jrc.ec.europa.eu/pvgis/>. [Accessed: 25-Nov-2018].
- [17] C. Parthasarathy, S. Dasgupta, and A. Gupta, "Optimal sizing of energy storage system and their impacts in hybrid microgrid environment," in *2017 IEEE Transportation Electrification Conference (ITEC-India)*, 2017, pp. 1–6.

# Lithium-ion BESS Integration for Smart Grid Applications - ECM Modelling Approach

Chethan Parthasarathy, Hossein Hafezi, Hannu Laaksonen  
 School of Technology and Innovation, Electrical Engineering  
 University of Vaasa  
 Vaasa, Finland  
[chethan.parthasarathy@uwasa.fi](mailto:chethan.parthasarathy@uwasa.fi)

**Abstract**— Lithium-ion battery energy storage systems (BESS) with their present state of technology and economic maturity possess huge potential for catering short-term flexibility requirements in smart grid environment. However, it is essential to model in detail the complexity of non-linear battery system characteristics and control of their adjoining power electronic interfaces. More detailed and accurate modelling of components, enables improved overall power system optimization studies by considering both, component and system level aspects simultaneously. Therefore, this paper develops an equivalent circuit model (ECM) for Lithium-ion battery and Lithium-ion nickel-manganese-cobalt (NMC) battery cell is modelled as a second order equivalent circuit (SOEC), including C-rate, temperature, state-of-charge and age effects. Secondly, detailed controller design methodology for DC/DC- and DC/AC-converter interfaces are developed to enable advanced grid integration studies. Overall, BESS integration design was validated by simulation studies in Simulink Simpowersystems platform.

**Index Terms**-- Lithium-ion battery; battery energy storage systems; equivalent circuit battery model; flexible energy sources; Smart grids;

## I. INTRODUCTION

Climate change and environmental issues have reinforced the need for large-scale integration of renewable, low emission energy sources at all voltage level, i.e. high, medium and low voltage, in the power system. Integrating such large amount of variable and usually low-inertia renewable energy sources has significant impacts on traditional centralized power systems. Due to these changes and effects there is increasing need for various type of energy storages for applications with different time-scales. For short-term needs, interest in rapidly controllable stationary BESS applications has increased constantly due to their technological advancements and decreasing costs. Ability to react fast, higher energy and power density, longer cycle and shelf life, low rate of self-discharge, high round trip efficiency and improved safety performance have favored Lithium ion based BESSs also for stationary grid applications. Lithium ion (Li-ion) BESSs are capable to act as flexible energy sources and provide multiple technical ancillary services such as frequency support by controlling active power injection, voltage regulation by reactive etc. [1].

Li-ion batteries are intercalation-based ESSs, which operate as a closed system [2] with very few measurable state variables, which makes it difficult to properly monitor the states of the battery and maintain safe operation. Voltage, current and temperature measurements are typically used to determine or estimate all the other parameters of the battery, such as its State-of-Charge (SoC) and State-of-Health (SoH). Therefore, it is required to understand and model precisely the BESS behaviour under various operating conditions, which affect their performance.

Accurate modelling of battery packs for energy storage applications have been minimal where majority of the literature considers battery systems as an ideal DC voltage source [3] or by utilizing mathematical modelling techniques [4]. Math based kinetic battery models (KBM) were first proposed for lead acid batteries. Modified KBMs [5], [6] are widely used to simulate lithium-ion batteries for smart grid simulations. However, KBMs fail to address the non-linear characteristics of Li-ion batteries, which are also affected by various operating conditions such as SoC, temperature, current rate and age. Physics based electrochemical models [7] are suitable to model the internal behavior of the cell involving huge amount of mathematical computations, which makes them practically impossible to be used for smart grid simulations. Integration of ECM has been presented for electrical vehicle propulsion in [8], considering SoC as the only affecting parameter. Most of the ECM models reported for grid related simulations lack in one or several affecting parameters related to the performance of Li-ion batteries.

Power electronics (PE) is one fundamental enabling technology behind BESS growth, utilization and grid integration determined by different grid code and standard requirements. Simultaneously PE based converter is responsible for safe charge/discharge of BESS, operation mode, active ( $P$ ) and reactive ( $Q$ ) power flow as well as current and voltage variations across the battery pack which will affect BESS performance, health and lifetime [9]. Battery design, sizing and converter control design are more likely to succeed when they are based on more accurate BESS models. Hence, this paper aims to establish an ECM for Li-ion battery inclusive of SoC, temperature, current rate and aging effects. Followed by,

designing DC/DC- and DC/AC- power converter controllers. Overall methodology was validated by integrating Li-Ion BESS to the MV bus of a power system, enabling them as short-term flexible energy sources for smart grids applications. Methodology for ECM for Li-ion BESS is explained in Section II. BESS integration technique, i.e. power electronic controller design for MV grid integration incorporating accurate BESS model is described in Section III.

## II. LI-ION BESS MODELLING

Thevenin-based second order equivalent circuit model (SOEC), technique is versatile, as it successfully emulates the model parameters such as multi-variable SoC, C-rate, temperature, hysteresis effects, self-discharge and battery aging. SOEC is considered as the benchmark model for Li-ion batteries, as it depicts the charge transfer, diffusion and solid electrolyte interface (SEI) reactions in the form of resistors and capacitors. SOEC battery model presented in this paper is based on time domain measurements from hybrid pulse power characterization (HPPC) tests in [10], whose performances are affected by SoC, operating temperature, C-rate and age. Therefore, SOEC model developed strikes a perfect balance between the accuracy and complexity of battery modelling.

Fig. 1 shows the proposed dynamic equivalent circuit model for Li-ion battery cell i.e. NMC type. Open Circuit Voltage (OCV) is modelled as an ideal voltage source. The internal resistance was modelled as  $R_i$ . Two RC combinations are suggested for Li-ion battery cell, so the dynamic behavior is modelled as  $R_1, C_1, R_2$  and  $C_2$ . The hysteresis effect and polarization effect in the Li-ion cells can be simulated accurately enough with the two RC combinations and the model structure is more simple than with more RC combinations. As the actual behavior of the NMC cells is significantly non-linear, all the parameters vary with SoC, temperature, age and history (number and depth of cycle) of the cell.  $OCV, R_i, R_1, C_1, R_2$  and  $C_2$ , are the parameters obtained from experimental characterization of lithium ion battery cell at various SoC's (100% to 0% with a step of 10%), temperature (15°C, 25°C and 45°C), current rates (1C, 2C and 3C) and cycle age (0, 100, 500, 1000, 1500, end of life).  $V$  refers to the battery cell terminal voltage.

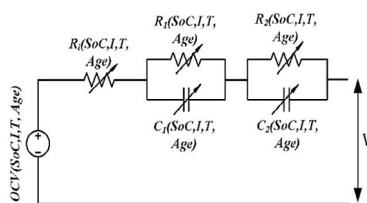


Fig 1. SOEC battery cell model

A closer view of the voltage response from the HPPC profile can be seen in Fig. 2. It shows an immediate voltage drop ( $\Delta V_0$ ) when the current pulse is applied. This is the internal resistance of cell, contributed by resistance of active material, electrolyte, and current collector. It can be also observed that there is a time varying voltage ( $\Delta V_1$  and  $\Delta V_2$ ), which can be

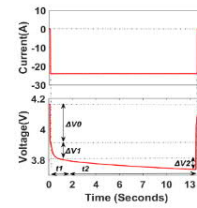


Fig 2. HPPC test response at 100% SoC and 25 °C

interpreted as a presence of additional elements such as capacitor in parallel combination with resistance. The time varying voltage part can be divided into short transient and long transient RC elements due to different time constants ( $t_1$  and  $t_2$ ) in the voltage profile. The output voltage equation for the 2nd order ECM is shown in (1). The mathematical representation of the time constants is shown in (2) and (3). SoC is estimated by coulomb counting method. OCV is evaluated from the voltage response of the HPPC profile at a given SoC interval, at the end of 1 h pause time.

A non-linear least-squares solver optimization algorithm lsqcurvefit (Levenberg-Marquardt) was used to minimize the error for each of the analyzed pulses and the optimized parameters  $R_i, R_1, C_1, R_2$  and  $C_2$  at each SoC and temperature were obtained. The model was further improvised to incorporate the aging effects, by regularly updating the cell parameters at different cycling intervals.

Fig. 3 provides comparison between simulated and experimental discharge voltages at different aging levels of NMC battery cell, at 25 °C and 3C discharge rate that were recorded as a result of accelerated aging tests. The mean relative error was less than to 2% majority of the discharge cycle and in some cases (especially at higher aging) the error was greater than 5%, towards the end of discharge towards 0% SOC. It is evident that overall discharge capacity reduces with aging which in turn reduces overall discharge time. Modelling aging characteristics of battery is critical for smart grid applications, because the BESS state of energy/power is required in order to consider their capability to provide different kind of active power ( $P$ ) related technical ancillary (flexibility) services like frequency support or peak shaving.

Fig. 4 depicts the evolution of ECM parameters with respect to age and SoC in a 3-dimensional plot. Internal resistance ( $R_i$ ) of cell, pertaining to  $\Delta V_0$ , in the HPPC voltage response curve is shown in Fig 4(a), its observed to increase with aging, denoting loss of active materials. Values of  $OCV$  changes are shown in Fig 4(b), whose values decreases over time, predominantly indicating loss of cycleable lithium ions. Figs 4(c)-(d) depict the parameters pertaining to the short transients of the RC branch. It is derived from time varying voltage ( $\Delta V_1$ ) and assumed to highlight the dynamics during of charge transfer process of cell operations. Efficiency of charge transfer process reduces with aging, due to increased  $R_1$  and  $C_1$  values. Figs 4(e)-(f) depict the parameters pertaining to the long transients of the RC branch. It was derived from time varying voltage ( $\Delta V_2$ ) and assumed to show case dynamics during of diffusion process of cell operations.

$$V_T(t) = V_{OCV} + I(t)R_i + I(t)R_1 \left(1 - e^{-\frac{t}{t_1}}\right) + I(t)R_2 \left(1 - e^{-\frac{t}{t_2}}\right) \quad (1)$$

$$t_1 = R_1 C_1 \quad (2)$$

$$t_2 = R_2 C_2 \quad (3)$$

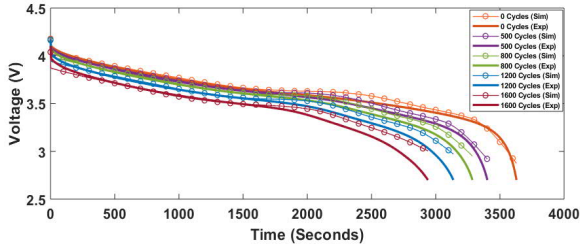


Fig 3. Comparison between simulated and experimental cell discharge voltage with different aging intervals

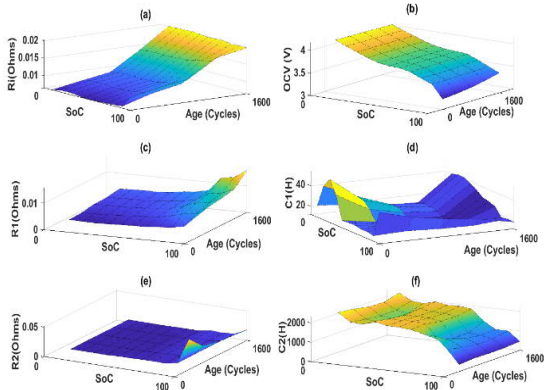


Figure 4. Age dependant ECM Parameters

Cell model was developed in Simscape platform of Matlab/Simulink. Cell model was scaled up to form battery pack model, in order to study it for various purposes in smart grid applications. Multiple cells are connected in series in a battery pack to achieve required voltage levels and multiple strings of serially connected cells have to be added in parallel to boost current level.  $N_S$  represents the series cell elements and  $N_P$  defines the number of parallel strings for a required battery pack. The interconnecting cable resistance are ignored making it a model with fast simulation response comparatively. Values of  $N_S$  and  $N_P$  define voltage and current characteristics of the desired battery packs. Developed battery pack model was then integrated into DC/DC buck-boost converter system, which was developed in SimPowerSystems platform.

### III. BESS INTEGRATION METHOD

Methodology for BESS integration as short-term flexible energy source, to the MV grid of a power system with an improved ECM based battery pack model and their adjoining power electronics control strategies are explained in this section.

#### A. BESS Model for MV Grid Integration

Li-ion (LIB) BESS (NMC type) acts as flexible energy resource which can provide short-time energy supply for multiple different technical ancillary services. Li-Ion BESS dynamic characteristics were modelled. BESS is connected to the power system by means of power electronic interface. In this case, DC/DC buck-boost converter will stabilize fluctuating/changing battery voltage. It will also aid in charging and discharging of batteries within its safe operating window. DC/AC -converter will be connected to the high voltage side of the DC/DC -converter, which converts it into 3-phase, 400  $V_{RMS}$ . Voltage will be boosted to MV level by means of 3-phase transformer thereby completing integration of the battery system. Deriving accurate design of the power converter controllers, i.e. DC/AC voltage-source-converter (VSC) and DC/DC BESS buck-boost controllers for optimal operations are explained further. Overall BESS integration design is presented in Fig 5.

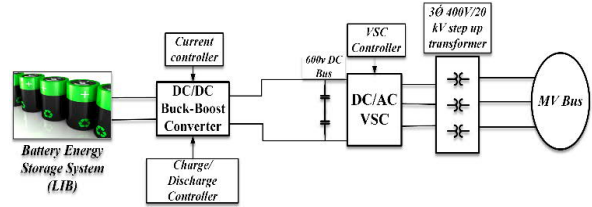


Fig 5. Battery Integration Modelling

#### B. PE Controller Design for BESS Integration

Design and operation of the controllers for BESS converters are developed in this section and they include DC/AC- VSC and DC/DC- BESS Buck-Boost controller.

##### 1) VSC Controller

Fig. 6 describes the VSC controller methodology i.e. voltage oriented control (VOC) technique [11]. VOC strategy guarantees fast transient response and high static performance through current control loop.  $V_{,abc}$  and  $I_{,abc}$  are transformed to  $V_{,dq}$  and  $I_{,dq}$  frames.  $I_{d,ref}$  is obtained by the PI-controller for  $V_{,dc}$  and the  $I_{q,ref}$  reference is provided by the controller designer based on the application demand. Active power output of the converter is controlled by  $I_{d,ref}$  and  $I_{q,ref}$  controls the reactive power output. A cross coupling exists between d- and q- axes components, which shall affect the dynamic performance of the controller.  $V_d$  feedforward signal is added to the d-component loop. This feedforward signal is crucial for d-component control loop. Feedforward signal can be added to the q-component control loop as well but it is not essential for this application. Both  $I_{d,ref}$  and  $I_{q,ref}$  are limited to  $\pm 1.5$  p.u. so the VSC should be designed to provide 150% nominal power for certain time period during transients.

##### 2) Battery Charge and Discharge Controller

A single IGBT with anti-parallel diode leg with a switching inductance has been implemented as bidirectional Buck-Boost converter for BESS system [12]. Average model converter is designed to charge and discharge the batteries through/to the VSC DC- bus capacitor. A simple PI-controller is designed to



control Buck-Boost converter. Fig. 7 shows Buck-Boost converter control loop. The controller is equal, but the converter can work in either Buck mode or in Boost control loop mode. When it works as Buck converter, the Boost IGBT is blocked and vice versa. The sign ( $\pm$ ) of the  $I_{dc,ref}$  defines in which mode it should work. The DC bus is controlled by VSC d-component control loop so the sign of the PI-controller output defines the active power flow direction therefore, there is no need to add additional voltage control loop in Boost mode (discharging the BESS) to control the voltage level. In both control modes, the PI-controller output provides the duty cycle to the Buck or Boost converter.

Discharge mode works in the range between 20% to 90% of battery SoC, as per the current requirements commanded based on the current required by the converter. For the charging mode, the maximum State-of-Charge ( $SoC_{Max}$ ), is maintained at 90 %, which typically is achieved by constant current charging alone, eliminating constant voltage (CV) requirements. Battery charge and discharge model is based on SoC of the system and load requirements. Charge controller triggers Buck mode of the converter ON when SoC goes below 20% and turns OFF when it reaches maximum of 90% to maintain battery operation in safe limits.  $I_{dc,ref}$  is communicated to the BESS Buck-Boost converter controller by upper level control system. Based on sign of this reference current the modality of the Buck-Boost converter and its controller behavior is managed.

#### IV. CASE STUDY AND SIMULATION RESULTS

Simulation based case study is designed to demonstrate integration of more accurate Li-ion BESSs to the MV grid of a power system. Controllers were designed to charge or discharge the battery as and when the grid commands, considering  $P_{ref}$  as the reference for DC/DC- converter stage, which handles battery operations. The use case study was intended to demonstrate the stability of DC/AC- converter and battery charge/discharge controller of the DC/DC- bidirectional buck boost converter, validating their transient and steady state system behavior. It also aids in relevant sizing of BESS for short-term power supply in smart grid applications based on grid current requirements.

Li-ion BESS was sized for a nominal power discharge of 0.334MW at a discharge rate of 1C and peak discharge of 1 MW at 3C. Other battery characteristics are presented in Table 1. DC/DC Buck-Boost converter was rated for 1 MW peak power and DC/AC- inverter was sized for a maximum capacity of 1.5 MVA. Initial battery SoC was maintained at about 50%, where it could accommodate simultaneous charge/discharge operations. Characteristics of new cells, i.e. unaged cells (first-life) are considered for the case study.

Simulations were performed for a time span (TS) of 80 seconds. A set point power reference  $P_{REF}$  based on different C-rates of BESS is shown in Table 2, which is variable every 20 seconds, inducing transient instability conditions. During T1, BESS discharges DC power of 0.668 MW (2C), followed by 0.334 MW(1C) in period T2 and 0.167 MW (0.5C) in T3. Finally, during T4, BESS charges from the grid at rate of 0.5C.

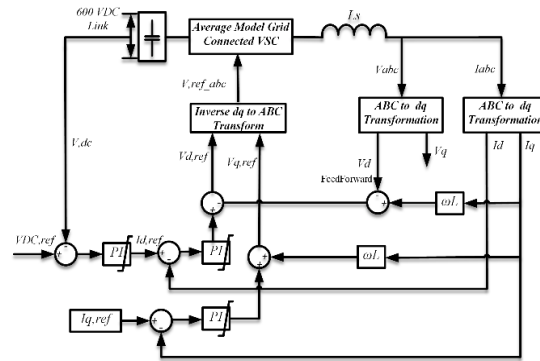


Figure 6. VSC Controller

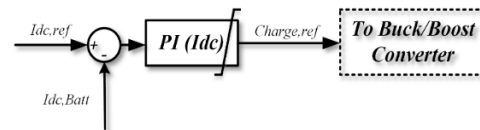


Figure 7. Battery Charge Discharge controller

It was assumed that, BESS shall undergo such cycling characteristics when supporting integration of renewable energy sources such as wind and solar PV, during extreme conditions or changes. In such cases, it is imperative to obtain robust PE converter controller design, as the power output from BESS changes rapidly with alternate charge/discharge pulses, commanded by the grid.

Table I. Li-ion BESS Size and characteristics

Lithium-ion Battery Characteristics	
Nominal DC voltage	311 V
Peak Voltage	353 V
Cut-off Voltage	235 V
Discharge Energy(1C)	334 kWh
Nominal Discharge current (1C)	944 A

Table II- Simulation case details

Time (Secs)	$P_{REF}$ (MW)	BESS Status
T1 (0-20)	0.668	Discharge
T2 (20-40)	0.334	Discharge
T3 (40-60)	0.167	Discharge
T4(60-80)	-0.167	Charge

Fig. 8 explains the performance of ECM based BESS model and its adjoining PE converters for MV grid integration. BESS charge/discharge current characteristics are shown in Fig 8(a), where magnitude of defined BESS current changes are as per the case study requirements. Fig 8(b) depicts the changes in BESS voltage, based on highly accurate ECM battery model, whose performance characteristics are as close to the real hardware. It is evident that the voltage fluctuations are of considerable magnitude during BESS operation. Capturing such changes accurately provides an important set point for tuning DC/DC- and eventually DC/AC- converter controls. Overall, BESS DC power output is shown in 8(c), where the step change depicts the BESS power dispatch characteristics with a magnitude change based on its C-rate capability. Reason to choose such large step change, is to investigate its effect on the DC bus stability during transient operating conditions of the BESS. BESS SoC behavior is presented in Fig 8(d). DC-

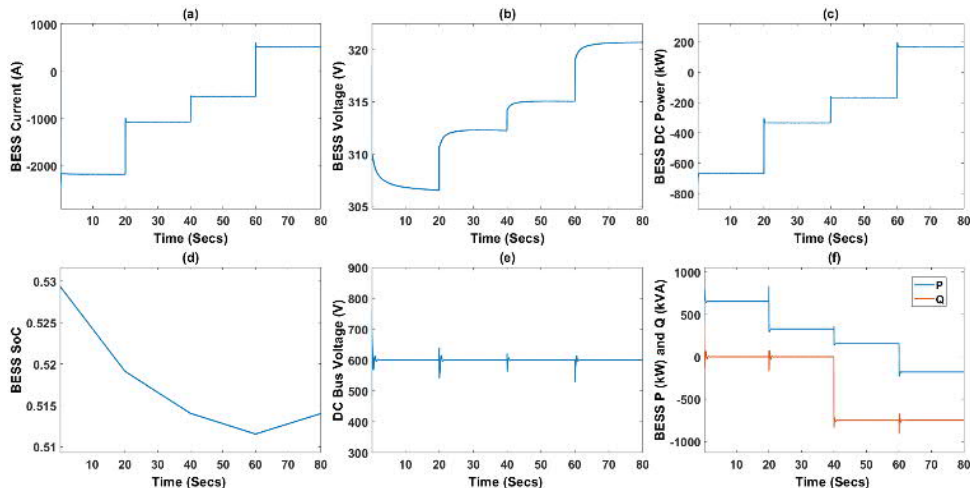


Figure 8. (a) BESS current characteristics (b) BESS Voltage (c) BESS DC power characteristics (d) BESS SoC (e) DC Bus voltage (f) BESS active and reactive power characteristics

bus voltage is constantly maintained at 600V, despite frequent variation of BESS voltage and current rate to the DC/AC-converter stage as shown in Fig. 8(e), thereby, reinforcing robust BESS model and adjoining converter controller design. BESS converter is capable of  $P$  &  $Q$  control respectively, which is demonstrated in a period after 40 seconds of the simulation in Fig. 8(f), where converter absorbs reactive power maintaining constant active power output. Henceforth, enabling improvement and management of voltage level or control of reactive power flow between HV and MV network as and when the MV grid (DSO) requires it.

#### V. CONCLUSION

Li-ion BESSs will play a dominant role as flexible energy sources in the coming decades with their promising characteristics. More detailed modelling of components, like BESS and converter, enables better overall microgrid/smart grid optimization analysis, by considering both component and system level complexities simultaneously. Detailed modelling of BESS and its grid-tied converter in microgrids or larger power systems, also aids to develop better understanding about effect of harmonics in BESS performance, aging etc. Hence, for integration of Li-ion BESS, accurate and detailed design of the DC/DC- and DC/AC- power converters is needed. In this paper, main contribution is the accurate model of Li-ion BESS, which incorporates the dynamic nature of SOEC modelling techniques. And, the design to carefully discharge and charge LIBs within their threshold (DC/DC-converter design) and the converter design and control (active and reactive power), were validated by simulation studies.

In future, role of BESS for multiple applications will be studied considering Sundom Smart Grid (SSG) as a case [13], where short-term and long term planning of BESS are necessary. In such cases, detail battery model with both age and temperature as affecting parameters will play a key role. Also, steady-state and transient stability studies by means of OPAL-RT real-time simulator with the developed new Li-ion battery and converter interface models will be performed.

#### REFERENCES

- [1] S. Vazquez, S. M. Lukic, E. Galvan, L. G. Franquelo, and J. M. Carrasco, "Energy storage systems for transport and grid applications," *IEEE Trans. Ind. Electron.*, vol. 57, no. 12, pp. 3881–3895, 2010.
- [2] M. T. Lawder *et al.*, "Battery energy storage system (BESS) and battery management system (BMS) for grid-scale applications," *Proc. IEEE*, vol. 102, no. 6, pp. 1014–1030, 2014.
- [3] P. J. Chauhan, B. D. Reddy, S. Bhandari, and S. K. Panda, "Battery energy storage for seamless transitions of wind generator in standalone microgrid," *IEEE Trans. Ind. Appl.*, vol. 55, no. 1, pp. 69–77, 2019.
- [4] M. Castaneda, E. Banguero, J. Herrera, S. Zapata, D. Ospina, and A. J. Aristizabal, "A new methodology to model and simulate microgrids operating in low latitude countries," *Energy Procedia*, vol. 157, pp. 825–836, 2019.
- [5] T. Wang and C. G. Cassandras, "Optimal control of multibattery energy-aware systems," *IEEE Trans. Control Syst. Technol.*, vol. 21, no. 5, pp. 1874–1888, 2013.
- [6] Z. N. Bako, M. A. Tankari, G. Lefebvre, and A. S. Maiga, "Experiment-based methodology of kinetic battery modeling for energy storage," *IEEE Trans. Ind. Appl.*, vol. 55, no. 1, pp. 593–599, 2019.
- [7] M. El Sayed, R. Ahmed, S. Habibi, Jimi Tjong, and I. Arasaratnam, "Reduced-Order Electrochemical Model Parameters Identification and SOC Estimation for Healthy and Aged Li-Ion Batteries Part I: Parameterization Model Development for Healthy Batteries," *IEEE J. Emerg. Sel. Top. Power Electron.*, vol. 2, no. 3, pp. 659–677, 2014.
- [8] A. Berrueta, A. Urtaun, A. Ursúa, and P. Sanchis, "A comprehensive model for lithium-ion batteries: From the physical principles to an electrical model," *Energy*, vol. 144, pp. 286–300, 2018.
- [9] G. Wang *et al.*, "A review of power electronics for grid connection of utility-scale battery energy storage systems," *IEEE Trans. Sustain. Energy*, vol. 7, no. 4, pp. 1778–1790, 2016.
- [10] R. Arunachala, C. Parthasarathy, A. Jossen, and J. Garche, "Inhomogeneities in large format lithium ion cells: A study by battery modelling approach," *ECS Trans.*, vol. 73, no. 1, pp. 201–212, 2016.
- [11] F. Blaabjerg, R. Teodorescu, M. Liserre, and A. V. Timbus, "Overview of control and grid synchronization for distributed power generation systems," *IEEE Trans. Ind. Electron.*, vol. 53, no. 5, pp. 1398–1409, 2006.
- [12] G. D'Antona, R. Faranda, H. Hafezi, and M. Bugliesi, "Experiment on Bidirectional Single Phase Converter Applying Model Predictive Current Controller," *Energies*, vol. 9, no. 4, p. 233, 2016.
- [13] H. Laaksonen, K. Sirviö, S. Afleht, and P. Hovila, "Multi-objective Active Network Management Scheme Studied in Sundom Smart Grid with MV and LV Network Connected DER Units," *CIGRE Conference on Electricity Distribution*, Madrid, Spain, 2019. .



# Integration and control of lithium-ion BESSs for active network management in smart grids: Sundom smart grid backup feeding case

Chethan Parthasarathy<sup>1</sup> · Hossein Hafezi<sup>2</sup> · Hannu Laaksonen<sup>1</sup>Received: 28 December 2020 / Accepted: 7 May 2021  
© The Author(s) 2021

## Abstract

Lithium-ion battery energy storage systems (Li-ion BESS), due to their capability in providing both active and reactive power services, act as a bridging technology for efficient implementation of active network management (ANM) schemes for land-based grid applications. Due to higher integration of intermittent renewable energy sources in the distribution system, transient instability may induce power quality issues, mainly in terms of voltage fluctuations. In such situations, ANM schemes in the power network are a possible solution to maintain operation limits defined by grid codes. However, to implement ANM schemes effectively, integration and control of highly flexible Li-ion BESS play an important role, considering their performance characteristics and economics. Hence, in this paper, an energy management system (EMS) has been developed for implementing the ANM scheme, particularly focusing on the integration design of Li-ion BESS and the controllers managing them. Developed ANM scheme has been utilized to mitigate MV network issues (i.e. voltage stability and adherence to reactive power window). The efficiency of Li-ion BESS integration methodology, performance of the EMS controllers to implement ANM scheme and the effect of such ANM schemes on integration of Li-ion BESS, i.e. control of its grid-side converter (considering operation states and characteristics of the Li-ion BESS) and their coordination with the grid side controllers have been validated by means of simulation studies in the Sundom smart grid network, Vaasa, Finland.

**Keywords** Active network management · Battery energy storage systems · Lithium-ion battery · Energy management systems · Equivalent circuit model · Power electronics converter controls

## 1 Introduction

Stochastic and unpredictable nature of the renewable energy sources (RES) and their geographic distribution, often in remote areas with weak electricity distribution network, induce various grid-related challenges. In such situations, managing power balance and grid stability is nonetheless a challenging task, as these factors depend on a number of variables depending on the network topology [1–3]. Challenge of supply reliability and quality with higher integration of RESs has been tried to address by setting stricter grid code requirements and innovative grid control architectures such as active network management (ANM) schemes [4, 5].

Therefore, ANM schemes are utilized to improve the penetration of RESs by managing available flexibilities in the distribution grids and keeping their power quality within the acceptable limits defined by the grid codes [6, 7].

In order to implement ANM schemes, distributed energy resources (DERs) in the distribution network (i.e. MV and LV systems) play an important role in providing flexibility in the power system for local and system wide grid resiliency, along with maximizing network DER hosting capacity [8, 9]. These flexibilities consist of active power ( $P$ -) control and reactive power ( $Q$ -) control of flexible resources like controllable DER units, battery energy storage systems (BESS), controllable loads and electric vehicles (EVs) which are connected in distribution networks, thereby providing different local and system-wide technical services as part of future ANM schemes [4, 10, 11].

BESSs play a major role as flexible energy source (FES) in ANM schemes by bridging gaps between non-concurrent renewable energy sources (RES)-based power generation and demand in the MV and low-voltage (LV) distribution

✉ Chethan Parthasarathy  
chethan.parthasarathy@uwasa.fi

<sup>1</sup> School of Technology and Innovations, Flexible Energy Resources, University of Vaasa, Vaasa, Finland

<sup>2</sup> Faculty of Information Technology and Communication Sciences, Tampere University, Tampere, Finland

networks. Ability of the BESS to provide both active power and reactive power flexibility services makes them a multipurpose FES for ANM needs [12–14]. With current technological maturity, Li-ion BESSs are capable of acting as a cost-efficient FESs and provide multiple technical ancillary/flexibility services like frequency control by controlling active power injection and voltage control by active/reactive power management [15, 16]. From transmission and distribution system operators (TSO/DSOs) point of view, an effective way to utilize BESS for ANM will be to place them in a HV/MV substation or in the MV distribution, e.g. at MV/LV substations. Hence, Li-ion BESSs will be an integral part of the ANM scheme at the MV distribution system for this study.

Efficient operation of ANM schemes highly bank upon the design of energy management system (EMS) [17, 18] which manages the available flexibilities in the distribution system. However, intermittent nature of the RES-based flexible DERs narrows the flexibility provisioning for ANM schemes, thereby challenging their scope of services. Hence, a highly controllable FES will be needed to design the EMS functionalities effectively. Therefore, Li-ion BESSs due to their fast and controllable dynamics will play an important role in the EMS functionalities for multiple flexibility services acting as a buffer to manage flexibilities in the distribution systems.

In [19–23], extensive research on various ANM schemes to maintain system voltage level, as well as to manage the reactive power flow from the DERs within the reactive power window (RPW) provided by the Finnish TSO, Fingrid and ENTSO-E network code [24], have been studied and validated in a local smart grid pilot SSG. From previous results, the reactive power control of wind turbine generator (WTG) was sufficient in order to satisfy RPW requirements on an hourly average data obtained from the SSG MV distribution network. However, it had been recommended to study multi-use capabilities of BESSs in multi-objective ANM schemes by controlling flexibilities in RESs, BESSs and on-load tap changing transformers (OLTCs) [25–27] on a smaller time-step in order to design ANM schemes and services effectively. It was also suggested to study the effect of load curves BESS integration methodology (i.e. the effect of ANM load on the Li-ion BESS converter controllers).

Therefore, the objective of this study is to validate the overall role of Li-ion BESS integration design and its stability for ANM needs, which is often used to mitigate transient instability. Hence, a rule-based [28] EMS has been proposed in Sect. 4 to study the overall power system stability by means of electromagnetic transient (EMT) simulation studies in Matlab/Simulink (SimPowerSystems). Developed EMS design for ANM in the MV distribution system will be based on managing two key network parameters. First objective of the EMS will be to

manage reactive power flow from the DERs between the TSO/DSO interface defined by the reactive power window (RPW) provided by Finnish TSO, Fingrid, and ENTSO-E network codes [24]. The reactive power flow between TSO/DSO interfaces has to comply with the RPW limits to avoid being penalized. Second objective is to manage the MV network voltages which are facing higher fluctuation due to RESs in the network, between the limits set by grid codes. Hence, maintenance of voltage and RPW limits defined by the grid code provides a strong case for implementation of ANM schemes to administer technical ancillary services by effectively managing active and reactive power flows from the available FESs in the distribution network.

To conduct such studies, the requirements are (a) development of accurate Li-ion BESS performance model, (b) Li-ion BESS integration methodology (i.e. design and development of controllers for the power electronic interfaces used for the grid integration purposes) and (c) EMS design (i.e. development of co-ordinated control of grid side controllers with DER controllers).

Design and methodology for integration of Li-ion BESS in the MV distribution system, which are capable to capture and study the fast transient dynamics by means of EMT simulations (i.e. smaller time step system simulation), have been developed and presented in [29, 30]. Hence, in this paper, the developed Li-ion BESS integration design is subjected to the active and reactive power requirements provided by the EMS implementing ANM scheme. EMS focus has been laid on designing coordinated control between the grid side controllers (i.e. the EMS controllers) and Li-ion BESS converter controllers. To validate the developed ANM scheme and the Li-ion BESS integration design, the backup feeding use case in the SSG has been modelled. Under this use case condition, the voltages and the RPW window limits are expected to be under duress, especially at low WTG, which will be addressed by the available flexibility (i.e. Li-ion BESS and WTG) in the MV distribution system with the help of developed EMS thereby providing active network management services.

To summarize, in this paper, the focus has been laid on,

1. Development of EMS architecture for ANM with  $QU$ -, BESS  $PU$ -, WT  $PU$ - and on-load-tap-changer (OLTC) controllers for managing available flexibilities of various DERs, especially to generate control signals for the Li-ion BESS and WTG converters connecting them to the MV distribution system,
2. Utilization of accurate equivalent circuit model (ECM) for Li-ion BESS controller development in grid integration studies
3. Evaluation of Li-ion BESS integration design (i.e. effects of BESS DC/AC voltage source converter and

DC/DC bidirectional buck-boost converter controllers for the ANM load requirements)

- Understanding simultaneous converter interactions between (a) converter + Li-ion BESS, and (b) converter + network management (ANM scheme).

This paper has been organized in the following manner. Sundom smart grid network architecture has been explained in Sect. 2. The reason for underlying voltage fluctuations in the network is presented in Sect. 3. Section 4 explains the ANM architecture and the developed EMS design to manage FESs in the MV distribution system. Developed ANM scheme and their performance with respect to the coordinated control attributes have been validated by means of case studies in Sect. 5.

## 2 Sundom smart grid network

SSG is represented in Fig. 1, which is a pilot living laboratory jointly created by ABB, Vaasan Sähköverkko (DSO), Elisa (communications) and University of Vaasa. Real-time voltage and current measurements (IEC 61,850 standard) are recorded from the MV distribution network, from all four feeders at a HV/MV substation and from three MV/LV substations comprising 20 measurement points in total. Measurement is sampled at 80 samples/cycle. In addition, active and reactive power, frequency, RMS voltages and current

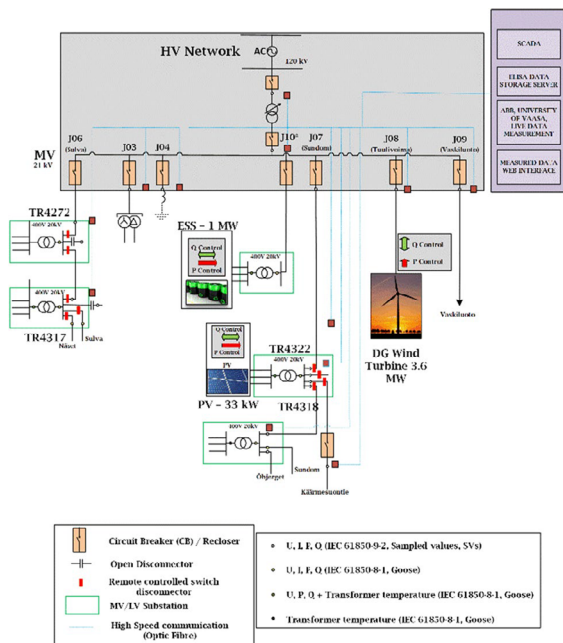


Fig. 1 SSG network diagram

measurements are received by GOOSE messages. SSG is modelled accurately with available data and grid structure, i.e. distribution network structure, loads, generation units, etc., obtained from the local DSO Vaasan Sähköverkko.

Wind power generation is modelled from the measured active power ( $P_{WIND}$ ) and reactive power ( $Q_{WIND}$ ) at bus Tuulivoima (J08), on 30-May-2017.  $P_{WIND}$  and  $Q_{WIND}$  are then converted to system currents, with MV voltage as reference as explained in [31]. Loads at Sulva (J06), Sundom (J07) and Vaskiluoto (J09) feeders are modelled as per the measured data from the MV distribution system.

Li-ion BESS dynamic characteristics were modelled accurately by considering the influence of parameters such as temperature, depth of discharge and C-rate (charge/discharge) by means of second-order equivalent circuit cell model [30]. Li-ion BESS is connected to the power system by means of power electronic interface. In this case, DC/DC bidirectional buck-boost converter will stabilize fluctuating/changing battery voltage. It will also aid in charging and discharging of batteries within its safe operating window. DC/AC -converter will be connected to the high voltage side of the DC/DC -converter, which converts it into 3-phase, 400  $V_{RMS}$ . Voltage will be boosted to MV level by means of 3-phase transformer thereby completing integration of the battery system.

Deriving accurate design of the power converter controllers, i.e. DC/AC voltage-source-converter (VSC) and DC/DC BESS buck-boost controllers for optimal operations is imperative considering the nature of applications they are tending in this study. Overall BESS integration design and their integration methodology along with power electronics controller design are explained in [30]. Developed ANM scheme in Sect. 4 will be utilized to manage flexibilities from WT generator, Li-ion BESS and the HV/MV OLTC transformer in SSG and will be validated in the use case where the loads are varying at low WT generation.

## 3 Problem description—voltage fluctuation

The intermittency of renewable power generation (i.e. wind power in SSG) introduces negative effects on the distribution grid, especially in terms of voltage rise and drop issues [32]. To understand the voltage change issues in the MV network of the SSG, an equivalent circuit of the network is deduced in Fig. 2. The line impedance ( $Z_{Grid}$ ) is represented as  $R_{Grid}$  and  $X_{Grid}$ . The current flow at the point of current coupling (PCC),  $i$ , is represented as  $I_i$ , and the MV bus voltage is measured as  $U_{MV}$ . Wind turbine generator and Li-ion BESS have been represented as current sources with output,  $I_{Wind}$  and  $I_{BESS}$ . The loads in SSG are represented as current sinks, consuming  $I_{Su}$ ,  $I_{Sun}$  and  $I_{Vas}$ .

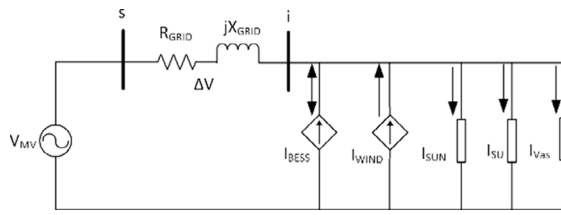


Fig. 2 Equivalent circuit representation of SSG

Eqs. (1)–(6) represent the power flow in the SSG network. The active power flow at the PCC has been represented by (1) and summarized as in (2), where  $P_{Wind}$ ,  $P_{BESS}$  and  $P_{Load}$  represent the active power contribution from the WTG, Li-ion BESSs and load power consumption, respectively.  $P_{Load}$  includes the active power flows of the individual load feeders from Sulva, Sundom and Vaskiluoto ( $P_{Su}$ ,  $P_{Sun}$  and  $P_{Vas}$ ). Similarly, reactive power flow at the PCC is shown in (3), where  $Q_{Wind}$ ,  $Q_{BESS}$  and  $Q_{Load}$  represent the reactive power contribution from the WTG, Li-ion BESSs and load power consumption, respectively.  $Q_{Load}$  includes the reactive power flows of the individual load feeders from Sulva, Sundom and Vaskiluoto ( $Q_{Su}$ ,  $Q_{Sun}$  and  $Q_{Vas}$ ). Equation (4) represents the current distribution at the PCC in the network. Overall power flow at the PCC is shown in (5), where  $S_i$  determines the apparent power flow,  $P_i$  and  $Q_i$  shows their active and reactive power flow components. The injected current at the PCC is represented in (6).

The equivalent circuit for Fig. 1 can be represented as (7), where  $U_{MV}$  represents the MV grid voltage and the  $\Delta V$  determines the voltage deviation in the MV grid. Voltage at the PCC is represented by  $U_i$  in (8) and substituting  $Z_{Grid}$  values (9) is obtained representing voltage at the PCC.

$$P_i = P_{Wind} \pm P_{BESS} - P_{Sun} - P_{Su} - P_{Vas} \tag{1}$$

$$P_i = P_{Wind} \pm P_{BESS} - P_{Load} \tag{2}$$

where,  $P_{Load} = P_{Sun} + P_{Su} + P_{Vas}$

Similarly,

$$Q_i = \pm Q_{Wind} \pm Q_{BESS} - Q_{Load} \tag{3}$$

where,  $Q_{Load} = Q_{Sun} + Q_{Su} + Q_{Vas}$

$$I_i = \pm I_{Wind} \pm I_{BESS} - I_{Load} \tag{4}$$

$$S_i = P_i + jQ_i = U_i \cdot I_i \tag{5}$$

$$I_i = \left( \frac{S_i}{U_i} \right) = \frac{P_i - jQ_i}{U_i} \tag{6}$$

Substituting current  $I_i$  from Eqs. (6) to (9), the overall voltage deviation is represented in (10). The voltage deviation  $\Delta U$  is influenced by both active and reactive power flows in the network. By resolving (10), Eq. (11) is obtained, which shows the voltage deviation due to active power component ( $\Delta U_d$ ) and reactive power component ( $\Delta U_q$ ).

$$U_{MV} = U - I_i Z_{Grid} \tag{7}$$

$$U_i = U_{MV} + I_i Z_{Grid} \tag{8}$$

$$U_i = U_{MV} + I_i (R_{Grid} + jX_{Grid}) = U_{MV} + \Delta U \tag{9}$$

$$\Delta U = \frac{P_i \cdot R_{Grid} + Q_i \cdot X_{Grid}}{|U_i|} + j \frac{P_i \cdot X_{Grid} - Q_i \cdot R_{Grid}}{|U_i|} \tag{10}$$

i.e.  $\Delta U_d = \frac{P_i \cdot R_{Grid} + Q_i \cdot X_{Grid}}{|U_i|}$

$$\Delta U_q = \frac{P_i \cdot X_{Grid} - Q_i \cdot R_{Grid}}{|U_i|} \tag{11}$$

In the SSG’s MV power grid, the magnitude of  $\Delta U_q$  is comparatively smaller than  $\Delta U_d$  but their contribution to voltage deviation is higher than that of the LV distribution system due to the line reactance. However, the purpose of this study is to design and develop effective utilization of Li-ion BESS active power control and to understand and map the effects of MV grid voltage fluctuation on Li-ion BESS and its adjoining power electronic converter controls. Hence, the effect of  $\Delta U_q$  is assumed a constant value. Therefore, by substituting active components of active power flow at the PCC, (12) has been obtained. The magnitude of voltage deviation  $|\Delta U_i|$ , at PCC is represented in (13). It is noted that the only controllable flexible energy source in Eqs. (12) and (13) is the Li-ion BESS, and hence it plays an immense role in regulating voltages in MV distribution network. By substituting Eqs. (12) in (13), we obtain the equation to provision the required change in voltage in (14).

$$\Delta U_d = \frac{(P_{Wind} \pm P_{BESS} - P_{Load}) \cdot R_{Grid} + Q_i \cdot X_{Grid}}{|U_i|} \tag{12}$$

$$|\Delta U_i| = |U_{MV}| + |\Delta U_d| \tag{13}$$

$$|\Delta U| = |U_{MV}| + \frac{(P_{Wind} \pm P_{BESS} - P_{Load}) \cdot R_{Grid} + Q_i \cdot X_{Grid}}{|U_i|} \tag{14}$$

Finally, by rearranging the equation, we obtain magnitude of active power discharge required from BESSs, i.e. in (15) to regulate the required voltages in the MV distribution system. Positive value of  $P_{BESS}$  describes battery charging and

the negative value to that of battery charging. Equation (15) shall form the basis for Li-ion BESS dispatch control operation in the study. The value of  $\Delta U_i$  is as shown in (16), which is the difference between voltage at bus  $i$  and  $U_{ref}$  defines the required voltage correction factor at the MV bus.

$$P_{BESS} = (|\Delta U_i| - |U_{MV}|) \cdot \left[ \frac{|U_{MV}|}{R_{Grid}} \right] - Q_i \cdot \left[ \frac{X_{Grid}}{R_{Grid}} \right] + P_{Load} - P_{Wind} \tag{15}$$

$$|\Delta U_i| = |U_i| - |U_{ref}|, \tag{16}$$

where  $U_{ref}$  is the voltage limits set by grid codes.

### 4 ANM Architecture and EMS Design

In this paper, the ANM management scheme is developed in reference to managing flexibilities from Li-ion BESSs and WT generators in the MV distribution system of SSG. Section 4.1 provides an explanation on the reactive power window requirements in TSO/DSO interface, which forms an inherent condition to be maintained as a part of ANM scheme, along with system voltages and frequency. Developed ANM scheme for Li-ion BESS operation and other available flexibilities in the MV distribution grid is explained in Sect. 4.2 and 4.3 shows the EMS architecture.

#### 4.1 Reactive power window

Based on SSGs existing data, the future reactive power window at the MV side of the HV/MV transformer and its limits are presented in Fig. 3 [20]. The reactive power window and microgrid requirements are combined for the MV distribution system. Limits for the maximum active power are based on the measured data of the year 2016, when  $P_{MAX,IMPORT}$  was 8.3 MW and  $P_{MAX,EXPORT}$  was 1.975 MW. Apart from

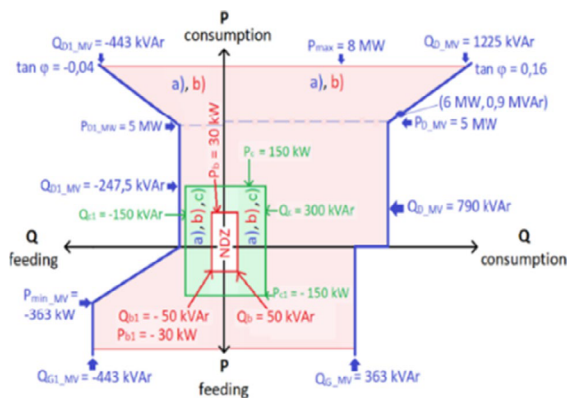


Fig. 3 Reactive power window for SSG at MV (FINGRID)

the Fingrid’s requirements, EU legislations dictate reactive power interactions between TSOs and DSOs. TSO may require DSOs to actively control the exchange of reactive power and subsequently, DSO may require the TSO to consider utilizing the distribution network for reactive power management. The actual reactive power range should not exceed 48% of maximum capacity to import or export of active power ( $P_{max}$ ), when importing (consuming) reactive power  $\cos\phi_{max}$  at 0.9<sub>inductive(ind)</sub> and exporting (producing) reactive power  $\cos\phi_{max}$  at 0.9<sub>capacitive(cap)</sub>. In addition, TSO cannot export reactive power when active power import is below  $0.25 \cdot P_{max}$  as [22]. ANM voltage control threshold is shown in Fig. 4, where the maximum voltage is set at 1.05 pu and the minimum voltage limits are set at 0.95 pu (both HV and MV connection points), which is based on the thermal limit for maximum current flow in the system.

#### 4.2 ANM Architecture design—SSG

Flexibilities provided by the wind turbine (WT) are dependent on its active power generation, which in turn is dependent on the intermittent nature of wind. Thereby, WT alone will not be reliable enough to provide flexibility services in the MV distribution system of SSG. Hence, the Li-ion BESS which is placed strategically in the MV distribution grid will be able to complement WTG in providing various flexibility services in a smart grid.

BESSs when integrated into the MV distribution system of the SSG are primarily designed to complement stochastic nature of wind power generation, i.e. store excess wind power generation and discharge during reduced wind power generation and secondarily used in providing technical ancillary services. Li-ion BESSs have multi-use capability based on their characteristics and hence the ANM scheme developed in this paper is inclusive utilizing such capabilities. The technical ancillary services in the ANM scheme are designed based on the available flexibilities in the MV distribution system. In this case, ancillary services include,

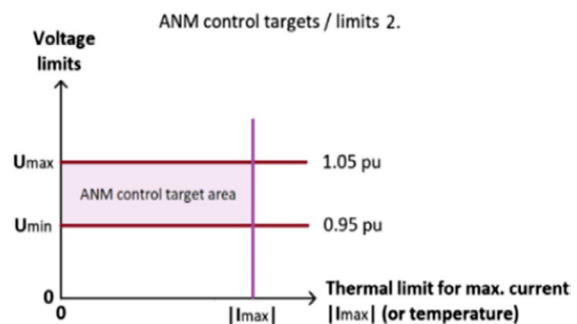


Fig. 4 Voltage control targets at HV and MV connection points

1. Voltage regulation within the threshold (Fig. 4) in the MV distribution system, mainly in all the MV feeders, is the primary objective of this ANM architecture
2. Maintaining the RPW defined by the Finnish TSO, Fin-grid, at the HV side of the SSG is defined in Sect. 4.1. Reactive power flow will be controlled from the available FESs to avoid violation of grid codes, thereby supporting customers to avoid paying the penalty fees to the TSO.

### 4.3 Energy management system

The most important layer of operation in the ANM scheme is the energy management system (EMS)

which concerns with the operation of active and reactive power flows between MV grid and flexible energy sources, in this case, Li-ion BESS and WT generator. Objective of the EMS is to maintain  $U_{grid,ref}$  within the limits specified by grid codes by controlling the active and reactive power flows at the DSO/TSO interface, especially focusing on the reactive power flow which has been maintained within the limits defined by RPW.

The ANM control architecture described in Fig. 5 is designed for implementation in SSG. Measured MV grid data such as active power ( $P_{grid,meas}$ ), reactive power ( $Q_{grid,meas}$ ), voltages ( $U_{grid,meas}$ ), frequency ( $f_{grid,meas}$ ) are given as input to the EMS layer. Primary role of the EMS

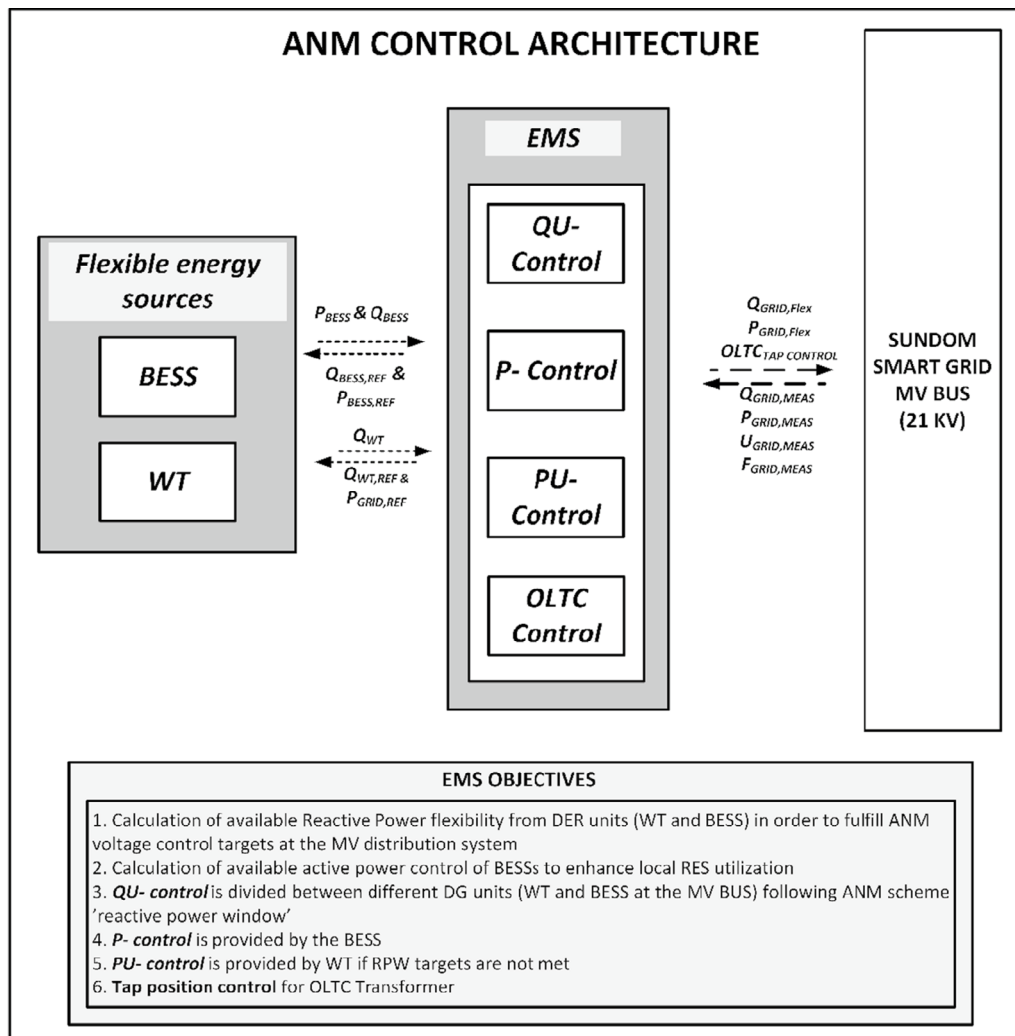


Fig. 5 ANM architecture



is to constantly monitor the reference parameters in the MV distribution system. If any of the parameters, i.e.  $Q_{\text{grid,ref}}$  and  $U_{\text{grid,ref}}$  are not within the defined threshold values, EMS's secondary functionality of managing the available flexibilities in the MV power system is utilized by generating reference control signals for the various grid side controllers. The grid side controllers that participate in ANM are  $QU$ -, BESS- $PU$ -, WT

$$Q_{\text{wind,min}} \leq Q_{\text{wind}} \leq Q_{\text{wind,max}}$$

$$\text{where, } \begin{cases} Q_{\text{wind,min}} = -\sqrt{S_{\text{wind}}^2 - P_{\text{Wind}}^2} \\ Q_{\text{wind,max}} = \sqrt{S_{\text{wind}}^2 - P_{\text{Wind}}^2} \end{cases} \quad (17)$$

$$Q_{\text{BESS,min}} \leq Q_{\text{BESS}} \leq Q_{\text{BESS,max}}$$

$$\text{where, } \begin{cases} Q_{\text{BESS,min}} = -\sqrt{S_{\text{BESS}}^2 - P_{\text{BESS}}^2} \\ Q_{\text{BESS,max}} = \sqrt{S_{\text{BESS}}^2 - P_{\text{BESS}}^2} \end{cases} \quad (18)$$

$$Q_{\text{flex}} = \begin{cases} Q_{\text{MV}} - Q_{\text{rpw,max}}; (\text{if } V_{\text{SUL}} < 0.95\text{PU and } Q_{\text{MV}} > Q_{\text{rpw,max}}) \\ Q_{\text{rpw,max}} - Q_{\text{MV}}; (\text{if } V_{\text{SUL}} > 1.05\text{PU and } Q_{\text{MV}} < Q_{\text{rpw,min}}) \\ 0 \end{cases} \quad (19)$$

$$Q_{\text{wind}} = \begin{cases} Q_{\text{flex}}; (\text{if } Q_{\text{flex}} > 0 \text{ and } Q_{\text{flex}} < Q_{\text{wind,max}}) \\ Q_{\text{wind,max}}; (\text{if } Q_{\text{flex}} > Q_{\text{wind,max}}) \end{cases} \quad (20)$$

$$Q_{\text{BESS}} = \begin{cases} Q_{\text{flex}} - Q_{\text{wind,max}}; (\text{if } Q_{\text{flex}} > Q_{\text{wind,max}}) \\ 0 \end{cases} \quad (21)$$

$$P_{\text{dis}} = \begin{cases} P_{\text{REF}}; (\text{if } P_{\text{REF}} < 1 \text{ MW and } \text{SOC}_{\text{min}} < \text{SOC} < \text{SOC}_{\text{max}}) \\ 1 \text{ MW}; (P_{\text{REF}} \geq 1 \text{ MW and } \text{SOC}_{\text{min}} < \text{SOC} < \text{SOC}_{\text{max}}) \\ 0; (\text{if } \text{SOC} \leq \text{SOC}_{\text{min}}) \end{cases} \quad (22)$$

$$P_{\text{chg}} = \begin{cases} 0; \text{if } \text{SOC} > \text{SOC}_{\text{max}} \\ P_{\text{chg}}; \text{if } \text{SOC}_{\text{min}} < \text{SOC} < \text{SOC}_{\text{max}} \end{cases} \quad (23)$$

$PU$ - control and OLTC- controllers as shown in Fig. 6. If the voltages, frequency and reactive power flows are well within the limits suggested by grid codes, the controllers in the EMS layer stay inactive. However, they constantly monitor the reference parameters in the MV system. In case, the defined MV parameters are out of threshold values ANM scheme starts to activate to mitigate the abnormalities by controlling the grid side controllers. The total required reactive power control is set according to requirements of Fingrid's RPW limits (i.e. Figure 3)

thereby defining the requirements for  $QU$ - control. The reactive power flexibility in the  $QU$ - control is provided by Li-ion BESS and WT generator, i.e.  $Q_{\text{WIND}}$  and  $Q_{\text{BESS}}$ . If reactive power flow in this situation exceeds RPW limits at the TSO/DSO interface,  $Q_{\text{WIND}}$  is regulated to adjust the values as the priority. If  $Q_{\text{WIND}}$  isn't sufficient to regulate RPW limits, the  $Q_{\text{BESS}}$  will be dispatched.

BESS  $PU$ - control is utilized to control active power flow from the Li-ion BESS. Despite Li-ion BESSs capability of providing both active and reactive power control, they also provide active power flexibility in terms of both charging- and discharging-related services. In case the BESSs are being charged, their active power discharge control is disabled, whereas the reactive power discharge control component remains active.

Therefore, EMS provides  $Q_{\text{BESS,ref}}$  &  $P_{\text{BESS,ref}}$  to the BESS and  $Q_{\text{WT,ref}}$  and  $P_{\text{grid,ref}}$  to the WTG. In return, based on the.

internal control algorithms for BESS and WT defined in the following section, BESS returns relevant  $P_{\text{BESS}}$  &  $Q_{\text{BESS}}$  back to the EMS, whereas WTG returns  $Q_{\text{WT}}$  back to the EMS. These control signals are then forwarded to the grid side controllers which in turn injects  $Q_{\text{flex}}$  ( $Q_{\text{BESS}}$  and  $Q_{\text{WT}}$ ) to the MV bus. Similarly, BESS  $PU$ - controller provides active power provisioning from the Li-ion BESS, i.e.  $P_{\text{BESS}}$  in order to regulate voltages at the MV system. WT  $PU$ - controller is primarily used to curtail excess active power generation from WT and activated when voltages at MV bus is greater than 1.0 pu. The design and architecture of the individual control techniques, i.e.  $QU$ -,  $P$ -,  $PU$ - and OLTC- control techniques employed in the ANM management principle are explained as below.

#### 4.3.1 $QU$ - management system

Reactive power ( $Q_{\text{WIND}}$ ) control of WTG system depends on the reactive power output capability. The inverter operating range should be applied accurately before utilizing reactive power control strategy in WTGs. Therefore, the maximum controllable reactive power from the WTG is calculated by (17).  $Q_{\text{WIND,MIN}}$  and  $Q_{\text{WIND,MAX}}$  are the maximum and minimum reactive power output from the WTG. Negative symbol denotes absorbing reactive power and that of positive symbol to generate reactive power.

The reactive power control of BESS is defined by the phasor relationship between the battery inverter operating parameters, for several different levels of BESS active power output ( $P_{\text{BESS}}$ ). When  $S_{\text{BESS}}$  is larger than  $P_{\text{BESS}}$ , the inverter can supply or consume reactive power,  $Q_{\text{BESS}}$ . The BESS inverter can dispatch  $Q_{\text{BESS}}$  quickly (on the cycle-to-cycle time scale) providing a mechanism for rapid voltage regulation. As the output,  $P_{\text{BESS}}$ , approaches  $S_{\text{BESS}}$ , the range of available  $Q_{\text{BESS}}$  decreases to zero, as shown in (18).

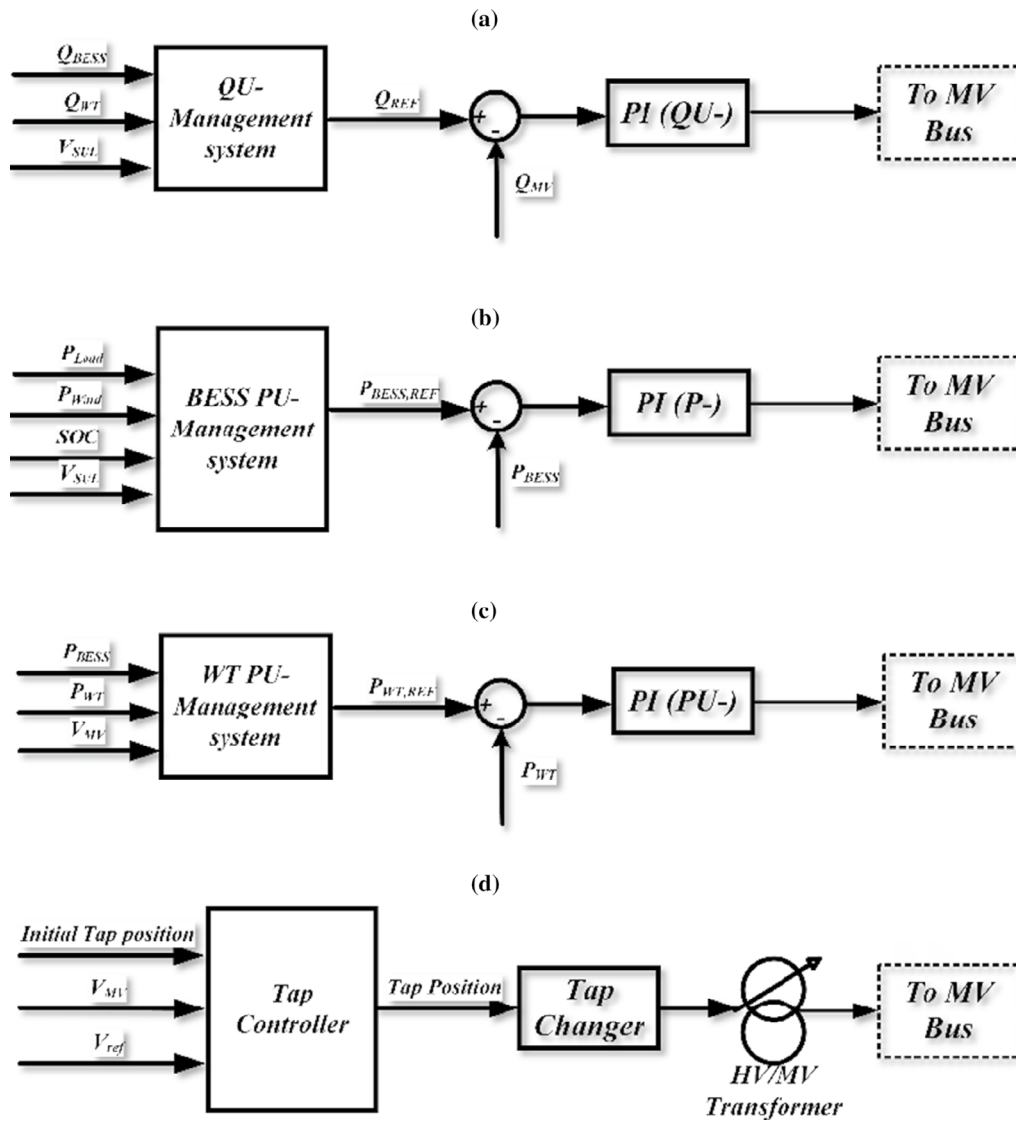


Fig. 6 a QU- control, b BESS PU- control, c WT PU- control, d Tap change controller

$Q_{flex}$ , the flexible reactive power allotted for QU- control is based on (19), whose values are in turn dependant on RPW limits defined in Fig. 3.  $Q_{flex}$  dispatch is provided by  $Q_{WIND}$  and  $Q_{BESS}$  whose magnitudes are defined in Eqs. (20) and (21), respectively. The controller is designed in such a way that the  $Q_{flex}$  allocated shall control the reactive power flow in the TSO/DSO interface within  $Q_{RPW,MIN}$  and  $Q_{RPW,MAX}$  and the Voltage at Sulva feeder,  $U_{SUL}$  which is considered as the reference MV voltage.  $U_{SUL}$  has been under stress during the defined use cases, and the  $Q_{flex}$  flow addressed to regulate this voltage within grid codes.

### 4.3.2 BESS PU- management system

This paper proposes an autonomous PU- droop control scheme for the autonomous operation of the Li-ion BESSs according to voltage measurements at the MV distribution system. The PU- control loop is shown in Fig. 7. It is noted that the reactive power control loop has been decoupled from its active power control loop. The error between measured voltage at connection point and the reference voltage value (here it is considered 0.95 pu) is sent to a PI- controller. The droop value is used as negative feedback gain as shown in

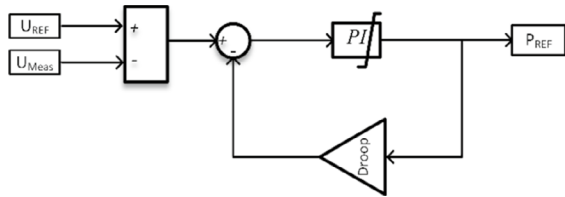


Fig. 7 Droop control loop

Fig. 7. The droop gain of the regulator is set to 0.015 pu (1.5%) per 1 MW. This is a design parameter, which depends on installed network parameters (mention equations) and designed BESS rated power. In this work, the designed system is able to compensate maximum of  $\pm 1.5\%$  voltage drifts.

Figure 8 shows this droop characteristic which has been used in this work. In order to avoid oscillation and instability issues, a  $\pm 0.5\%$  margin has been considered in order to enable/disable the droop control loop as it is illustrated in Fig. 2. The Li-ion BESSs start to discharge power if the reference voltage from the MV bus goes below 0.95 pu and the discharge power is based on the droop coefficient chosen in the study. In case the WT is non-operational, the Li-ion BESS starts to charge when the voltages rise to 1.05 pu or above. In case the WTG is operational, power generation is curtailed based on its own PU- droop control.

BESS internal control algorithms are described by (22) and (23). Battery discharge power ( $P_{DIS}$ ) is provided by the BESS system when  $U_{SUL}$  is lesser than 0.95 pu, and the magnitude of  $P_{DIS}$  is provided by droop characteristics. According to (22), Li-ion BESS will discharge only when its SOC is greater than  $SOC_{MIN}$  adhering to the limitations presented by the battery operational characteristics. Maximum  $P_{DIS}$  has been set at 1C, i.e. 1 MW. Li-ion BESS charging ( $P_{CHG}$ ) is defined by the battery's SOC and must be within their threshold  $SOC_{MIN}$  and  $SOC_{MAX}$  as in (23). Li-ion

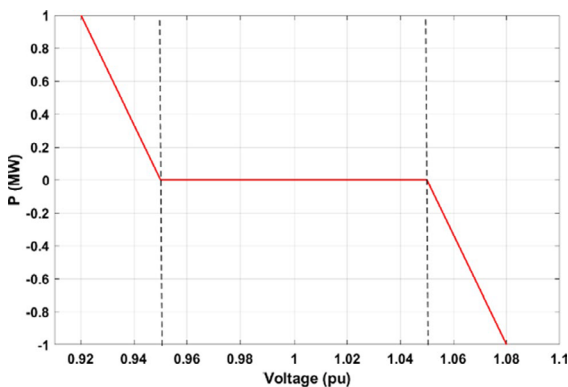


Fig. 8 Li-ion BESS PU- droop characteristics

BESS charging is forbidden when BESS SOC is higher than  $SOC_{MAX}$ . Magnitude of  $P_{CHG}$  is set at a charging rate up to 2C, mainly to observe the MV distribution characteristics when BESS is in different charging modes.

### 4.3.3 WT PU- management system

WT PU- management system is designed keeping in mind the curtailment of renewable energy generation, when the voltage limits exceed 1.05 PU in the MV bus of the system. In order to manage the curtailment, droop control referred in Fig. 9 is utilized for the curtailment of wind power generation.

### 4.3.4 OLTC tap controllers

In the developed ANM scheme, OLTCs are activated to regulate voltages when QU-, QU- and P- controllers fail to provide the required voltage regulation defined by the grid codes in the MV distribution system. OLTC controller receives initial tap position,  $U_{MV}$  and  $U_{REF}$   $V_{ref}$  as inputs. In order to maintain the MV feeder voltages within the grid codes,  $U_{REF}$   $V_{ref}$  of 1 pu is given as input, i.e.  $U_{MV}$   $V_{MV}$   $V_{MV}$  is meant to be controlled at 1 pu. Based on  $V_{ref}$   $U_{REF}$  and  $U_{MV}$   $V_{MV}$   $V_{MV}$  required tap changes are calculated and executed by regulating the voltage at the MV side of the HV/ MV transformer.

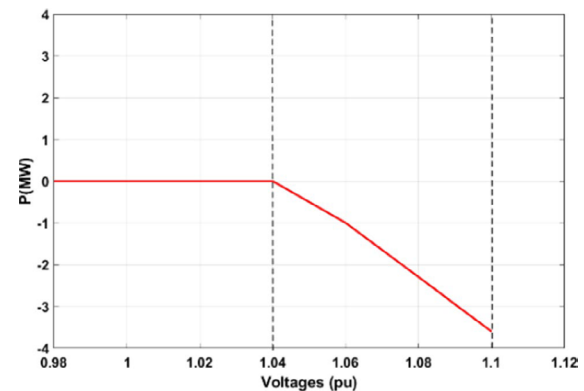


Fig. 9 WT PU- droop settings

### 5 Case study: variable load at low WT generation

SSG has been reliable in operation in terms of MV voltage regulation and its power quality during normal mode of operation, i.e. when the grid power is being fed from Sundom HV/MV sub-stations. However, during Sundom HV/MV substation maintenance operation, the grid power will be fed from Kuutamolahti power station (as in Fig. 10) which is about 5.2 KMs away, adding on to the overall  $Z_{Grid}$  values. Hence, grid disturbances in the form of voltage fluctuations and power quality problems shall

be anticipated, especially when variable load conditions exist at low WTG.

Hence, in this use case, effect of such load variation during lower WT generation during backup feeding case has been modelled. The arising network issues, such as voltage distortion and reactive power flow within RPW, will be addressed by the ANM scheme designed in Sect. 4. The effectiveness of developed ANM scheme and the interaction between EMS and DER controllers during this condition has been studied in detail, considering the Li-ion BESS integration aspects. Initial battery SoC was maintained at about 50%, where it could accommodate simultaneous charge/discharge operations. Characteristics of new cells, i.e. unaged cells are considered for the case study. Simulations were performed for a time period (TS) of 120 s.

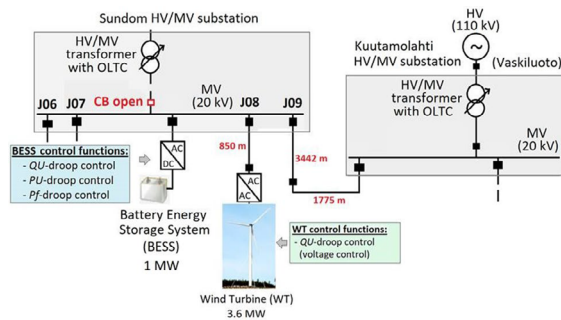


Fig. 10 SSG one-line diagram during backup feeding case

#### 5.1 Without ANM

Figure 11a shows the  $P_{BESS}$  and  $Q_{BESS}$  characteristics of the Li-ion BESS from its MV feeder (J10). Without ANM scheme being active, it is observed that both  $P_{BESS}$  and  $Q_{BESS}$  are at zero values.  $P_{WIND}$  is shown in Fig. 11b and the  $Q_{WIND}$  contribution from wind turbine has been unused in the base case evaluation. Figure 11c depicts the active power characteristics at the MV side of the HV/MV transformer. Negative symbol states that the active power is consumed

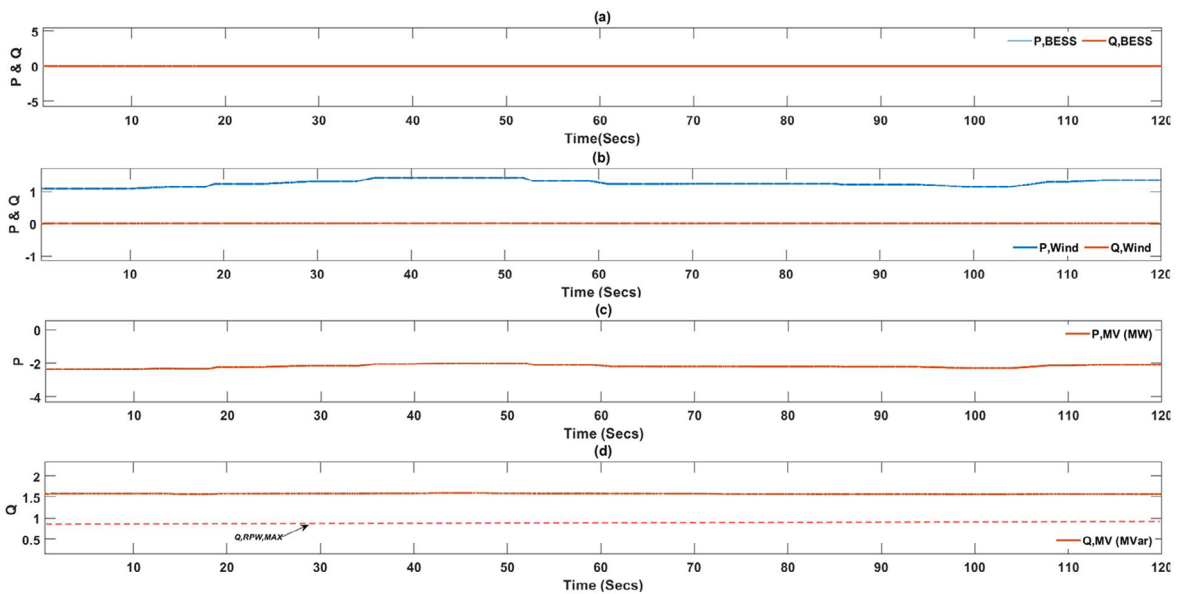


Fig. 11 Case study results (Without ANM): a BESS active and reactive power characteristics, b Wind active and reactive power characteristics, c MV bus active power, d MV bus reactive power

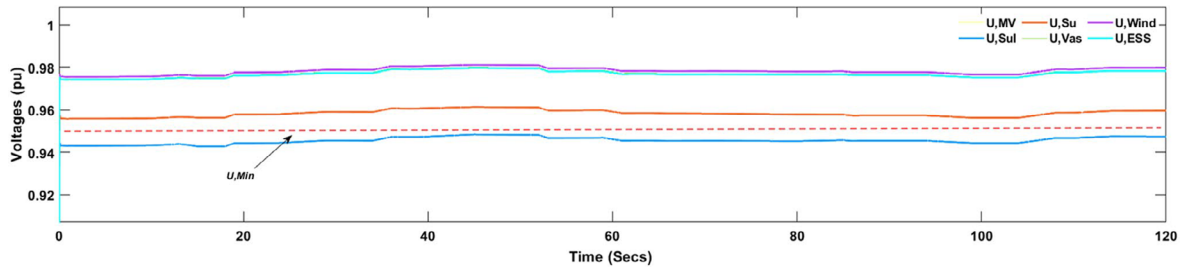


Fig. 12 Case study results (Without ANM): MV bus voltages

by the MV distribution system. Reactive power characteristics are shown in Fig. 11d. It is observed that the  $Q_{MV}$  is higher than the threshold defined by the RPW limits set by FINGRID.

Figure 12 represents the voltages in PU at the various MV feeders in the MV distribution system of SSG. It is observed that the voltages are well within the threshold defined by the grid codes, except the voltage at the Sulva feeder.  $U_{SUL}$  is seen to be lower than 0.95 PU during the simulation time period.

## 5.2 With ANM

Figure 13a shows the  $P_{BESS}$  and  $Q_{BESS}$  characteristics of the Li-ion BESS from its MV feeder (J10) with ANM scheme being active. Magnitude of Li-ion BESS discharge (whose

maximum is set at 1 MW) of  $P_{BESS}$  is defined by the BESS  $PU$ -controller characteristics of the EMS designed to implement ANM scheme, as explained in Sect. 4.3.2.  $P_{WIND}$  and  $Q_{WIND}$  characteristics are as shown in Fig. 13b. The magnitude of  $Q_{flex}$  required to satisfy RPW requirements is shown in (17). The  $Q_{WIND}$  contribution as part of  $Q_{flex}$  is determined by (18). In this case,  $Q_{WIND}$  was alone enough to regulate RPW requirement. Hence,  $Q_{BESS}$  dispatch based on (19) was unused. Figure 13c depicts the active power characteristics at the MV side of the HV/MV transformer. Negative symbol states that the active power is consumed by the MV distribution system. Reactive power characteristics are shown in Fig. 13d. It is observed that the  $Q_{MV}$  has been reduced in magnitude and currently well within the threshold defined by the RPW limits from Fingrid.

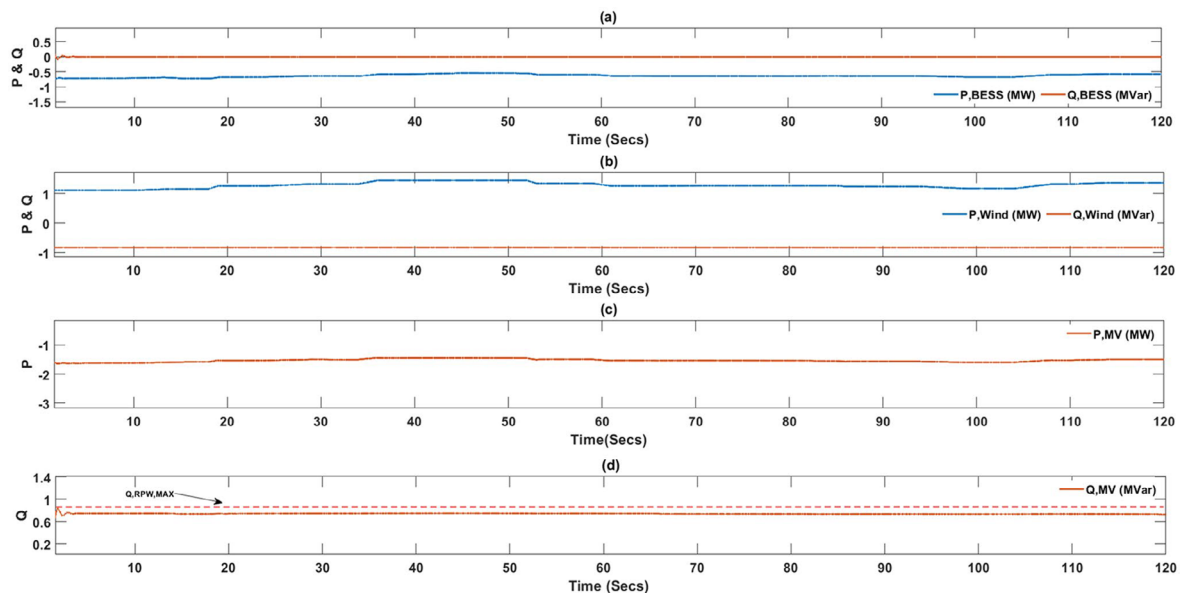


Fig. 13 Case study results (With ANM): **a** BESS active and reactive power characteristics, **b** Wind active and reactive power characteristics, **c** MV bus active power, **d** MV bus reactive power

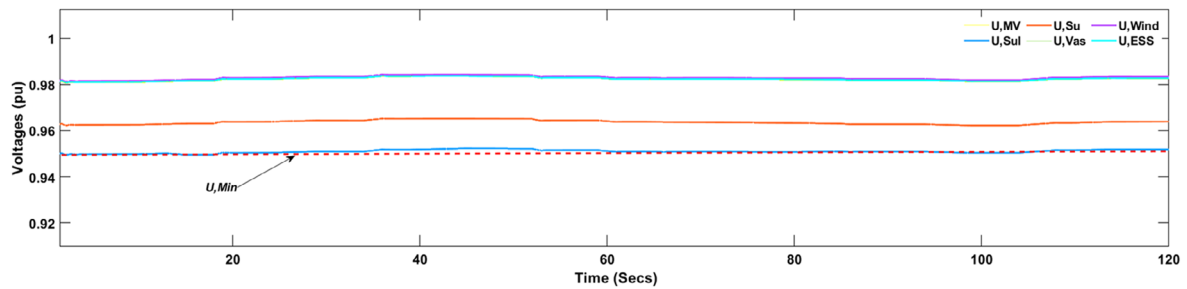


Fig. 14 Case study results (With ANM): MV bus voltages

Fig. 15 BESS DC characteristics: **a** BESS current, **b** BESS voltage, **c** BESS SoC, **d** DC bus voltage

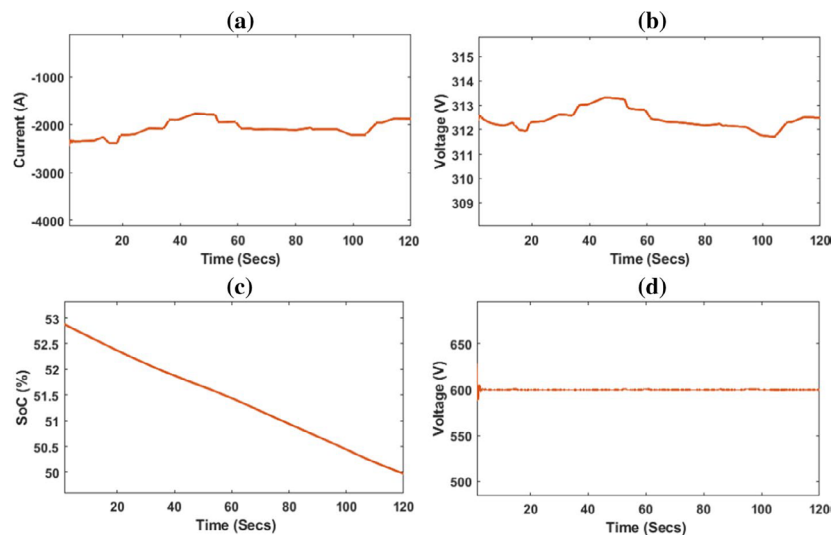


Figure 14 represents the voltages in pu at the various MV feeders in the MV distribution system of SSG. It is observed that the voltages are well within the threshold defined by the grid codes, except the voltage at the Sulva feeder.  $U_{SUL}$  was seen to be lower than 0.95 PU in the beginning of the simulation in the base case evaluation. However, all the MV feeder voltages have improved and well within the voltage limits determined by the grid codes after the EMS dispatched required amounts of flexibility (i.e.  $P_{BESS}$  and  $Q_{WIND}$ ).

Figure 14 explains the DC characteristics of the Li-ion BESS and its adjoining PE converters for MV grid codes, except the voltage at the Sulva feeder.  $U_{SUL}$  was seen to be lower than 0.95 PU in the beginning of the simulation in the base case evaluation. However, all the MV feeder voltages have improved and well within the voltage limits determined by the grid codes after the EMS dispatched required amounts of flexibility (i.e.  $P_{BESS}$  and  $Q_{WIND}$ ).

Figure 15 explains the DC characteristics of the Li-ion BESS and its adjoining PE converters for MV grid integration. BESS charge/discharge current characteristics are shown in Fig. 15a, where magnitude of defined BESS current, in this case, is the BESS discharge current. Figure 15b depicts the changes in BESS operational voltage. BESS SoC behaviour is presented in Fig. 15c. DC-bus voltage is constantly maintained at 600 V, despite frequent variation in BESS voltage and Fig. 15d, thereby, reinforcing robust BESS model and adjoining converter controller integration design for 1 MW charge power.

## 6 Discussion and conclusion

Role of Li-ion BESSs as flexible energy sources in such distribution networks is multi-faceted considering their participation in both active and reactive power related flexibility services. In this study, the developed Li-ion BESS

integration was subjected to the load requirements of ANM schemes in the MV distribution system of SSG, when the WT generation was low and variable load conditions exist. Under such situation, transient instability is seen in the network in terms of voltage regulation. Also, the RPW limits defined by the grid codes are non-adhering to the threshold values. It is imperative that the developed EMS and its adjoining controllers must work in a co-ordinated way with the DER inverter controllers, i.e. Li-ion BESS and the WT generator in order to satisfy the ANM objectives.

Li-ion BESS integration design was validated as a part of the use case. DC/AC voltage source converter and DC/DC bidirectional buck-boost converter and their respective controllers used in the Li-ion BESS performed as per the load requirements provided by the ANM scheme to contain voltage and RPW violation. The stability of the DC bus in Fig. 15d aids in validating the Li-ion BESS integration design being stable even at various transient conditions despite variable WTG and loads.

Table 1 provides a summary of the simulation results and an indication on how the flexibility indices have been utilized based on the ANM objectives and the EMS set-points based on Eqs. (17)–(23). The reactive power control requirement,  $Q_{flex}$ , has been provided only by  $Q_{WIND}$ , without any interference from  $Q_{BESS}$ . From the results, it is indicative that the  $Q_{flex}$ , based on (17), was instrumental in keeping the reactive power flow,  $Q_{MV}$  between HV/MV grids, within the limits specified by the RPW. With respect to the results of voltage limits at various MV feeders, it has been evident that the voltage at the Sulva feeder was below 0.95 pu without any ANM schemes operational. However, with the allocation of  $P_{BESS}$ , whose dispatch value was based on the BESS  $PU$ -droop controller characteristics, voltage at the Sulva feeder was controlled at 0.95 pu. Purpose of this control loop is to dispatch the exact amount of active power required from the Li-ion BESS which is derived in Sect. 3, where the Li-ion BESS dispatch is dictated by (15), thereby providing optimum power without over/under-usage of the battery system.

The synergy between Li-ion BESS converter controls and the EMS controllers (i.e. BESS  $PU$ - and  $QU$ - controllers) has been established as a part ANM design and validated by the simulation results, where the EMS controllers provided required set-points to the individual component (Li-ion BESS and WTG) controllers. Therefore, the designed ANM scheme and its adjoining EMS controllers acted as required to provide RPW and voltage regulation.

In future studies, more use cases such as such as complementing RES intermittency and frequency fluctuations, will be added to the existing ANM control architecture, particularly focusing on the multi-use capability of the Li-ion BESSs. Design and development of adaptive EMS controllers to optimise the control of flexible energy sources in MV distribution systems will be included in the scope of study.

**Table 1** Results summary (mapping flexibility indices)

Simulation step	5 s		20 s		40 s		60 s		80 s		100 s		120 s	
Flexibility indices	No ANM	ANM	No ANM	ANM	No ANM	ANM	No ANM	ANM	No ANM	ANM	No ANM	ANM	No ANM	ANM
$P_{BESS}$ (MW)	0	-0.71	0	-0.67	0	-0.57	0	-0.61	0	-0.64	0	-0.67	0	-0.57
$Q_{BESS}$ (Mvar)	0	0	0	0	0	0	0	0	0	0	0	0	0	0
$Q_{WIND}$ (Mvar)	0	-0.83	0	-0.83	0	-0.83	0	-0.83	0	-0.83	0	-0.83	0	-0.83
$Q_{flex}$ (Mvar)	0	-0.83	0	-0.83	0	-0.83	0	-0.83	0	-0.83	0	-0.83	0	-0.83
$Q_{MV}$ (pu)	1.56	0.73	1.56	0.73	1.56	0.73	1.56	0.73	1.56	0.73	1.56	0.73	1.56	0.73
$U_{SUL}$ (pu)	0.943	0.95	0.944	0.95	0.947	0.951	0.946	0.951	0.945	0.95	0.944	0.95	0.947	0.951

Further, real-time simulation models shall be built for EMS controller test-bed development purposes.

**Funding** Open access funding provided by University of Vaasa (UVA).

**Open Access** This article is licensed under a Creative Commons Attribution 4.0 International License, which permits use, sharing, adaptation, distribution and reproduction in any medium or format, as long as you give appropriate credit to the original author(s) and the source, provide a link to the Creative Commons licence, and indicate if changes were made. The images or other third party material in this article are included in the article's Creative Commons licence, unless indicated otherwise in a credit line to the material. If material is not included in the article's Creative Commons licence and your intended use is not permitted by statutory regulation or exceeds the permitted use, you will need to obtain permission directly from the copyright holder. To view a copy of this licence, visit <http://creativecommons.org/licenses/by/4.0/>.

## References

- Pinson P, Mitridati L, Ordoudis C, Ostergaard J (2017) Towards fully renewable energy systems: Experience and trends in Denmark. *CSEE J Power Energy Syst* 3:26–35. <https://doi.org/10.17775/cseejpes.2017.0005>
- Liang X (2017) Emerging power quality challenges due to integration of renewable energy sources. *IEEE Trans Ind Appl* 53:855–866. <https://doi.org/10.1109/TIA.2016.2626253>
- Ahmed SD, Al-Ismail FSM, Shafiullah M et al (2020) Grid integration challenges of wind energy: a review. *IEEE Access* 8:10857–10878. <https://doi.org/10.1109/ACCESS.2020.2964896>
- Gao X, Sossan F, Christakou K et al (2018) Concurrent voltage control and dispatch of active distribution networks by means of smart transformer and storage. *IEEE Trans Ind Electron* 65:6657–6666. <https://doi.org/10.1109/TIE.2017.2772181>
- Yang Z, Li Y, Xiang J (2018) Coordination control strategy for power management of active distribution networks. *IEEE Trans Smart Grid* 10:5524–5535. <https://doi.org/10.1109/TSG.2018.2883987>
- Palizban O, Kauhaniemi K, Guerrero JM (2014) Microgrids in active network management—part II: system operation, power quality and protection. *Renew Sustain Energy Rev* 36:440–451. <https://doi.org/10.1016/j.rser.2014.04.048>
- Palizban O, Kauhaniemi K, Guerrero JM (2014) Microgrids in active network management—Part I: hierarchical control, energy storage, virtual power plants, and market participation. *Renew Sustain Energy Rev* 36:428–439. <https://doi.org/10.1016/j.rser.2014.01.016>
- Salama HS, Aly MM, Abdel-Akher M, Vokony I (2019) Frequency and voltage control of microgrid with high WECS penetration during wind gusts using superconducting magnetic energy storage. *Electr Eng* 101:771–786. <https://doi.org/10.1007/s00202-019-00821-w>
- Böhm R, Rehtanz C, Franke J (2016) Inverter-based hybrid compensation systems contributing to grid stabilization in medium voltage distribution networks with decentralized, renewable generation. *Electr Eng* 98:355–362. <https://doi.org/10.1007/s00202-016-0425-y>
- Olek B, Wierzbowski M (2015) Local energy balancing and ancillary services in low-voltage networks with distributed generation, energy storage, and active loads. *IEEE Trans Ind Electron* 62:2499–2508. <https://doi.org/10.1109/TIE.2014.2377134>
- Wang L, Bai F, Yan R, Saha TK (2018) Real-time coordinated voltage control of PV inverters and energy storage for weak networks with high PV penetration. *IEEE Trans Power Syst* 33:3383–3395. <https://doi.org/10.1109/TPWRS.2018.2789897>
- Akagi S, Yoshizawa S, Ito M et al (2020) Multipurpose control and planning method for battery energy storage systems in distribution network with photovoltaic plant. *Int J Electr Power Energy Syst* 116:105485. <https://doi.org/10.1016/j.ijepes.2019.105485>
- Das CK, Bass O, Kothapalli G et al (2018) Overview of energy storage systems in distribution networks: placement, sizing, operation, and power quality. *Renew Sustain Energy Rev* 91:1205–1230. <https://doi.org/10.1016/j.rser.2018.03.068>
- Saboori H, Hemmati R, Ghiasi SMS, Dehghan S (2017) Energy storage planning in electric power distribution networks—a state-of-the-art review. *Renew Sustain Energy Rev* 79:1108–1121. <https://doi.org/10.1016/j.rser.2017.05.171>
- Zhang Y, Xu Y, Yang H, Dong ZY (2019) Voltage regulation-oriented co-planning of distributed generation and battery storage in active distribution networks. *Int J Electr Power Energy Syst* 105:79–88. <https://doi.org/10.1016/j.ijepes.2018.07.036>
- Akram U, Nadarajah M, Shah R, Milano F (2020) A review on rapid responsive energy storage technologies for frequency regulation in modern power systems. *Renew Sustain Energy Rev* 120:109626. <https://doi.org/10.1016/j.rser.2019.109626>
- Nour AMM, Hatata AY, Helal AA, El-Saadawi MM (2020) Review on voltage-violation mitigation techniques of distribution networks with distributed rooftop PV systems. *IET Gener Transm Distrib* 14:349–361. <https://doi.org/10.1049/iet-gtd.2019.0851>
- Liu J, Gao H, Ma Z, Li Y (2015) Review and prospect of active distribution system planning. *J Mod Power Syst Clean Energy* 3:457–467. <https://doi.org/10.1007/s40565-015-0170-7>
- Sirvio K, Valkkila L, Laaksonen H et al (2018) Prospects and costs for reactive power control in Sundom smart grid. In: *Proceedings of 2018 IEEE PES Innov Smart Grid Technol Conf Eur ISGT-Europe 2018*, pp 1–6. <https://doi.org/10.1109/ISGTEurope.2018.8571695>
- Sirviö K, Laaksonen H, Kauhaniemi K (2020) Active network management scheme for reactive power control. In: *7–8 Cired Workshop 2018*. <https://www.cired-repository.org/handle/20.500.12455/1099>
- Laaksonen H, Hovila P, Kauhaniemi K (2018) Combined islanding detection scheme utilising active network management for future resilient distribution networks. *J Eng* 2018:1054–1060. <https://doi.org/10.1049/joe.2018.0202>
- Laaksonen H, Sirviö K, Aflecht S, Kauhaniemi K (2019) Multi-objective active network management scheme studied in Sundom smart grid with MV and LV connected DER Units. 3–6, *Cired 2019 conference*. <https://doi.org/10.34890/379>
- Laaksonen H, Parthasarathy C, Hafezi H et al (2020) Control and management of distribution networks with flexible energy resources. *Int Rev Electr Eng* 15:213. <https://doi.org/10.15866/iree.v15i3.18592>
- European Union (2016) DCC: Commission Regulation (EU) 2016/1388 establishing a network code on Demand Connection. *Off J Eur Union* 2016:68. doi:<https://doi.org/10.1017/CBO9781107415324.004>
- Li C, Disfani VR, Pecenek ZK et al (2018) Optimal OLTC voltage control scheme to enable high solar penetrations. *Electr Power Syst Res* 160:318–326. <https://doi.org/10.1016/j.epsr.2018.02.016>
- Muttaqi KM, Le ADT, Negnevitsky M, Ledwich G (2015) A coordinated voltage control approach for coordination of OLTC, voltage regulator, and DG to regulate voltage in a distribution feeder. *IEEE Trans Ind Appl* 51:1239–1248. <https://doi.org/10.1109/TIA.2014.2354738>



27. Long C, Ochoa LF (2016) Voltage control of PV-rich LV networks: OLTC-fitted transformer and capacitor banks. *IEEE Trans Power Syst* 31:4016–4025. <https://doi.org/10.1109/TPWRS.2015.2494627>
28. Zia MF, Elbouchikhi E, Benbouzid M (2018) Microgrids energy management systems: a critical review on methods, solutions, and prospects. *Appl Energy* 222:1033–1055. <https://doi.org/10.1016/j.apenergy.2018.04.103>
29. Parthasarathy C, Hafezi H, Laaksonen H, Kauhaniemi K (2019) Modelling and simulation of hybrid PV & BES systems as flexible resources in smartgrids—Sundom smart grid case. In: *IEEE PES PowerTech Conf 2019*. <https://doi.org/10.1109/PTC.2019.8810579>
30. Parthasarathy C, Hafezi H, Laaksonen H (2020) Lithium-ion BESS Integration for Smart Grid Applications—ECM modelling approach ISGT NA. <https://doi.org/10.1109/ISGT45199.2020.9087741>
31. Li B, Chen M, Cheng T et al (2018) Distributed control of energy-storage systems for voltage regulation in distribution network with high PV penetration. In: *2018 UKACC 12th Int Conf Control Control 2018* 9:169–173. <https://doi.org/10.1109/CONTROL.2018.8516803>
32. COMMISSION REGULATION (EU) 2016/ 631 - of 14 April 2016 - establishing a network code on requirements for grid connection of generators <http://data.europa.eu/eli/reg/2016/631/oj>

**Publisher's Note** Springer Nature remains neutral with regard to jurisdictional claims in published maps and institutional affiliations.

# Control and Co-ordination of Flexibilities for Active Network Management in Smart Grids – Li-ion BESS Fast Charging Case

Chethan Parthasarathy, Hannu Laaksonen

School of Technology and Innovation, Flexible energy sources group, Electrical Engineering  
University of Vaasa  
Vaasa, Finland  
[chethan.parthasarathy@uwasa.fi](mailto:chethan.parthasarathy@uwasa.fi)

Hossein Hafezi

Faculty of Information Technology and Communication Sciences, Electrical Engineering  
Tampere University  
Tampere, Finland  
[hossein.hafezi@tuni.fi](mailto:hossein.hafezi@tuni.fi)

**Abstract**— Fast charging of Lithium-ion battery energy storage systems (Li-ion BESSs) when utilized in the medium voltage (MV) distribution networks may introduce its own stress on the network under certain operating modes, especially when combined with intermittent renewable power generation. In such situations, active network management (ANM) schemes by managing available flexibilities in the MV network is a possible solution to maintain operation limits defined by grid codes. The studies in this paper are related to the utilization ANM schemes for MV distribution network in Sundom Smart Grid, Vaasa, Finland. The aim of this study is to capture the stresses induced by fast charging of Li-ion BESSs during low wind power generation and utilization of ANM schemes to mitigate those arising issues. The effect of such ANM schemes on integration of Li-ion BESS, i.e. control of its grid-side converter (considering operation states and characteristics of the Li-ion BESS) and their coordination with the grid side controllers to enforce network ANM schemes have been analyzed in detail. Particularly, the effect of AC load on the DC characteristics of Li-ion BESSs has been evaluated in this simulation study.

**Index Terms**-- Active Network Management; Battery Energy Storage Systems; Lithium ion battery; Equivalent Circuit Model; Power Electronics Converter Controls;

## I. INTRODUCTION

Battery energy storage systems (BESS) play a major role as flexible energy sources (FES) in active network management (ANM) schemes by bridging gaps between non-concurrent renewable energy sources (RES)-based power generation and demand in the medium-voltage (MV) and low-voltage (LV) distribution networks. Ability of the BESS to provide both active power and reactive power flexibility services, makes them a multipurpose FES for ANM needs [1], [2]. With current technological maturity, Li-ion BESSs are capable of acting as a cost-efficient FESs and provide multiple technical ancillary/flexibility services like frequency control by controlling active power injection and voltage control by reactive power management [3], [4].

However, Li-ion BESSs will act as system load when they are being charged. The charging load shall induce stresses on the distribution system (typical at the BESS integration location), especially when they are being charged at a higher current rate (i.e. fast charging). The effects of Li-ion BESSs charging load on the distribution network might be severe, if there is a request to fast charge batteries at an instance of lower renewable power generation at the distribution levels. The negative impact to the distribution grid in such instance shall lead to increase in the overall peak load of the network, there by leading to adverse voltage fluctuations causing detrimental effects on the distribution transformers [5], [6]. Therefore, innovative grid solutions such as ANM schemes are utilised to mitigate such arising network issues.

Reactive power flow from the distributed energy resources (DERs) between the TSO/DSO interface has been defined by the reactive power window (RPW) provided by Finnish TSO, Fingrid, and ENTSO-E network codes [7]. The reactive power flow between TSO/DSO interfaces have to comply within the RPW limits to avoid being penalised. Hence, maintenance of voltage and RPW limits defined by the grid code provides a strong case for implementation of ANM schemes to administer technical ancillary services by effectively managing active and reactive power flows from the available FESs in the distribution network.

In [8]–[10], extensive research on various ANM schemes to maintain system voltage level as well as manage the reactive power flow from the DERs within the RPW provided by the Finnish TSO, Fingrid and ENTSO-E network code [7] have been studied and validated in a local smart grid pilot, Sundom Smart grid (SSG). From previous results, the reactive power control of wind turbine generator (WTG) was sufficient in order to satisfy RPW requirements on an hourly average data obtained from the SSG MV distribution network. However, it was recommended to study multi-use capabilities of BESSs in multi-objective ANM schemes by controlling flexibilities in

RESSs, BESSs and on-load tap changing transformers (OLTCs) [11] on a smaller time-step in order to design ANM controllers and services effectively.

Primary role of Li-ion BESSs i.e. their slow dynamics (control of voltages and active power characteristics) over an extended time period was previously studied [12], where the authors tend to support and complement active power generation of WTG on a day-to day basis.

Design and methodology for integration of Li-ion BESS in the MV distribution system, which are capable to capture and study the fast transient dynamics by means of electromagnetic transient (EMT) simulations (i.e. smaller time step system simulation) has been presented in [13]. Therefore, in this paper, the developed Li-ion BESS integration design is subjected to an extreme network event, i.e. fast charging of the batteries under low renewable power generation. Under this condition, the voltages and the RPW window limits are expected to be under duress. Hence, an ANM scheme has been designed to provide ancillary services addressing the network issues. The ability of the developed ANM scheme to provide required ancillary services and the stability of Li-ion BESS integration (i.e. adjoining power electronic controller performance) under extreme conditions are validated by EMT simulation studies in Matlab/Simulink (SimPowerSystems).

## II. GRID COMPONENTS AND MODELLING

Sundom Smart Grid (SSG) is shown in Fig. 1, which is a pilot living lab jointly created by ABB, Vaasan Sähköverkko (DSO), Elisa (communications) and University of Vaasa [10]. Measurements of active and reactive power, frequency, RMS voltages and currents are received by GOOSE messages from all the MV feeders. SSG is modelled accurately with available data and grid structure, i.e. distribution network structure, measured loads, generation units etc. obtained from the local DSO Vaasan Sähköverkko. WTG in SSG is rated at 3.6 MW and its modelling details are explained in [13].

Li-ion BESS dynamic characteristics were modelled accurately by considering the influence of parameters such as temperature, depth of discharge and C-rate (charge/discharge) by means of second order equivalent circuit cell model [13]. Li-ion BESS has been connected to the power system by means of power electronic interfaces. Detailed Li-ion BESS integration and its power electronics converter control design has been explained in [13].

## III. ANM CONTROL METHODOLOGY

ANM schemes provide improved ways to manage available flexibilities from the inverter-based energy sources in the distribution grid. Hence, in this study the ANM scheme has been developed to effectively manage the available flexibilities at MV distribution grid of SSG, i.e. WTG reactive power ( $Q_{wind}$ ), active and reactive power of Li-ion BESS, ( $P_{BESS}$  and  $Q_{BESS}$ ) and tap positions in OLTC transformers, thereby providing ancillary services to the system. Active power, reactive power and OLTC controllers explained below will aid in providing the ancillary services, which include,

1. Voltage regulation within the threshold in the MV distribution system, mainly in all the MV feeders,

2. Maintaining reactive power flow within the RPW limits defined by Fingrid

### A. Reactive Power Control

Aim of the reactive power controller is the manage voltage regulation by means of  $QU$ - control and regulate TSO/DSO reactive power flows within the threshold defined by RPW limits defined by Finnish TSO, Fingrid (Fig .2). According to the grid codes, all the MV feeder voltages must stay within 0.95 to 1.05 pu.

The maximum controllable reactive power from the WTG is calculated by (1).  $Q_{wind,min}$  and  $Q_{wind,max}$  are the minimum and maximum reactive power output from the WTG respectively. The reactive power control of BESS is defined by the phasor relationship between the battery inverter operating parameters. As the output,  $P_{BESS}$ , approaches apparent BESS power ( $S_{BESS}$ ), the range of available  $Q_{BESS}$  decreases to zero, as shown in (2).  $Q_{BESS,min}$  and  $Q_{BESS,max}$  are the minimum and maximum reactive power output from the Li-ion BESS. Positive symbol of the reactive powers means it is capacitive and of negative value shows it's inductive in nature.

$Q_{flex}$  is meant to control  $U_{SUL}$  because it has been under maximum stress during the defined use cases.  $Q_{flex}$ , the flexible reactive power allotted for  $QU$ - control is based on (3), whose values are in turn dependant on RPW limits defined in Fig. 2. Based on Fig. 2,  $Q_{rpw,max}$  is defined as the maximum allowed reactive power that can be consumed by the HV/MV transformer (denoted by positive sign) and  $Q_{rpw,min}$  provides set-points minimum allowed limits for reactive power export by the HV/MV transformer (denoted by negative sign). The reactive power control from both  $Q_{BESS}$  and  $Q_{wind}$  constitutes the overall  $Q_{flex}$ . The controller is designed in such a way that the  $Q_{flex}$  allocated shall control the reactive power flow in the TSO/DSO interface within  $Q_{rpw,min}$  and  $Q_{rpw,max}$  and

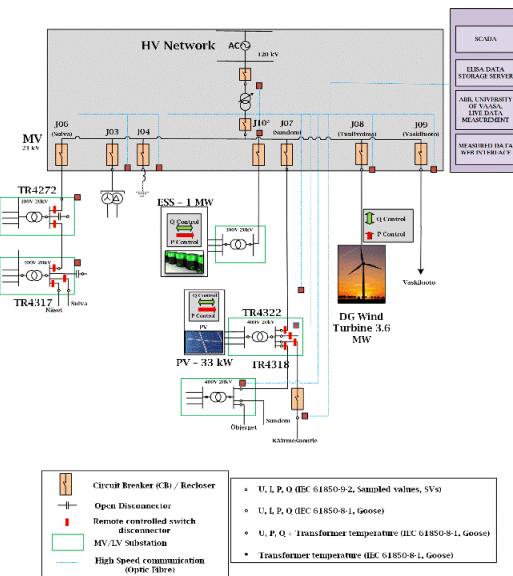


Figure 1. Sundom Smart Grid single line diagram

$$Q_{wind,min} \leq Q_{wind} \leq Q_{wind,max} \tag{1}$$

$$\text{where, } \begin{cases} Q_{wind,min} = -\sqrt{S_{wind}^2 - P_{Wind}^2} \\ Q_{wind,max} = \sqrt{S_{wind}^2 - P_{Wind}^2} \end{cases}$$

$$Q_{BESS,min} \leq Q_{BESS} \leq Q_{BESS,max} \tag{2}$$

$$\text{where, } \begin{cases} Q_{BESS,min} = -\sqrt{S_{BESS}^2 - P_{BESS}^2} \\ Q_{BESS,max} = \sqrt{S_{BESS}^2 - P_{BESS}^2} \end{cases}$$

$$Q_{flex} = \begin{cases} Q_{wind,max} + Q_{BESS,max}; & (\text{if } U_{SUL} < 0.95 \text{ PU and } Q_{rpw,min} < Q_{MV} < Q_{rpw,max}) \\ -(Q_{wind,max} + Q_{BESS,max}); & (\text{if } U_{SUL} > 1 \text{ pu and } Q_{rpw,min} < Q_{MV} < Q_{rpw,max}) \\ 0; & (\text{if } (0.95 \text{ pu} < U_{SUL} < 1 \text{ PU})) \end{cases} \tag{3}$$

$$P_{dis} = \begin{cases} P_{Load} - P_{Wind}; & (\text{if } (P_{Load} - P_{Wind}) < 1 \text{ MW}) \\ 1C; & (\text{if } SOC > SOC_{min}) \\ 0; & (\text{if } (SOC) < SOC_{min}) \text{ and } P_{dis} > 1 \text{ MW} \end{cases} \tag{4}$$

$$P_{chg} = \begin{cases} 0; & \text{if } SOC > SOC_{max} \\ P_{chg}; & \text{if } (SOC_{min} < SOC < SOC_{max}) \end{cases} \tag{5}$$

manage voltage at Sulva feeder,  $U_{SUL}$  which is considered as the reference MV voltage since it has been under maximum stress during the defined use cases.  $U_{SUL}$  is considered as the reference point for voltage control as it tends to have the highest voltage drop in base case simulation (explained in detail in section IV).

**B. Active Power Control**

Li-ion BESS discharge power ( $P_{dis}$ ) is defined by logical conditions stated in (4), where it is designed to discharge power when the load requirement ( $P_{Load}$ ) is higher in magnitude than  $P_{wind}$ . According to the first condition in the equation, the magnitude of  $P_{dis}$  is calculated as the difference between  $P_{Load}$  and  $P_{wind}$ , and this active power output is expected from Li-ion BESS, if  $(P_{Load} - P_{wind})$  is less than 1MW. If  $(P_{Load} - P_{wind})$  is higher than 1 MW, then  $P_{dis}$  magnitude is fixed at 1C rate, i.e. 1 MW, given the Li-ion BESSs state of charge ( $SOC$ ) is higher than its minimum,  $SOC_{min}$ . If none of the two conditions is met,  $P_{dis}$  is set to 0 MW.

Li-ion BESS charging ( $P_{chg}$ ) is defined by (5).  $P_{chg}$  is regulated by Li-ion BESS's  $SOC$ , which has to be regulated within the maximum  $SOC$ ,  $SOC_{max}$ . According to the first condition in (5), Li-ion BESS must stop charging if the  $SOC$  reaches  $SOC_{max}$ . Charging operations are always undertaken if the ANM scheme requires it to do, when the  $SOC$  is between  $SOC_{max}$  and  $SOC_{min}$ .

**C. OLTC Tap Controllers**

In the developed ANM scheme, OLTC's are activated to regulate voltages when both active and reactive power controllers fail to provide the required voltage regulation defined by the grid codes in the MV distribution system. OLTC controller receives initial tap position,  $U_{MV}$  and  $U_{REF}$  as inputs. In order to maintain the MV feeder voltages within the grid codes,  $U_{REF}$  of 1pu is given as input, i.e.  $U_{MV}$  is meant to be controlled at 1pu. Based on  $U_{REF}$  and  $U_{MV}$ , required tap changes are calculated and executed by regulating the voltage at the MV side of the HV/MV transformer.

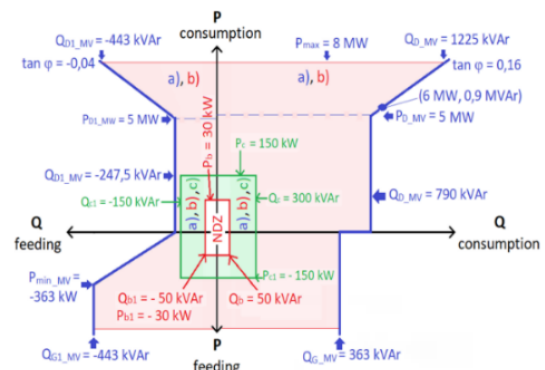


Figure 2. Reactive Power Window at HV/MV substation of SSG

#### IV. CASE STUDIES: FAST CHARGING OF BESS

Li-ion BESS characteristics used in the study is shown in Table I. In this use case, Li-ion BESS is charged at a rate of 2C, equivalent to 2 MW charge power, which is considered as fast charging method for a 1MW nominal power Li-ion BESS, during low renewable energy generation. The effects of charging at 2C during low wind power generation has been observed and then addressed by the ANM schemes to mitigate their detrimental effects. Two sub-cases are defined, where the first one shows the strain of charging power on the MV distribution network without any ANM schemes and the second sub-case shows effect of ANM principles on the MV network stability.

Table I. Li-ion BESS characteristics

Lithium Ion Battery Characteristics	
Nominal DC Voltage	311 V
Peak Voltage	353 V
Cut-off Voltage	235 V
Discharge Power (1C)	1 MW
Nominal Discharge current (1C)	2832 A
Peak Discharge current (3C)	8496 A
Inverter Size	2.5 MVA

##### A. Without ANM

Fig 3(a) shows  $P_{BESS}$  and  $Q_{BESS}$  characteristics of the Li-ion BESS from its MV feeder (J10). BESS is charged with 2 MW power (positive symbol denotes battery charging) and its reactive power control has been deactivated.  $P_{wind}$  is shown in Fig 3(b) and the  $Q_{wind}$  contribution from wind turbine has been unused in the base case evaluation. Fig 4(a) depicts the active power characteristics at the MV side of the HV/MV transformer. Negative symbol states that the active power is consumed by the MV distribution system. Reactive power characteristics are shown in Fig 4(b). It is observed that the  $Q_{MV}$  is higher than the threshold defined by the RPW limits set by FINGRID.

Fig. 5 represents the voltages (pu) at various MV feeders in the MV distribution system of SSG. It is observed that the MV voltages are well within the threshold defined by the grid codes, except the voltages at the Sulva and Sundom feeders.  $U_{SUL}$  and  $U_{SU}$  was seen to be lower than 0.95 pu throughout the simulation period in the base case evaluation. Hence, both MV feeder voltages and RPW limits were distorted in the use case without ANM schemes.

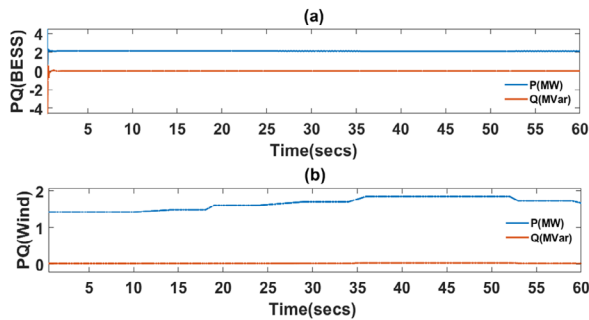


Figure 3. Simulation results (Without ANM): (a) BESS Active and reactive power characteristics (b) Wind Active and reactive power characteristics

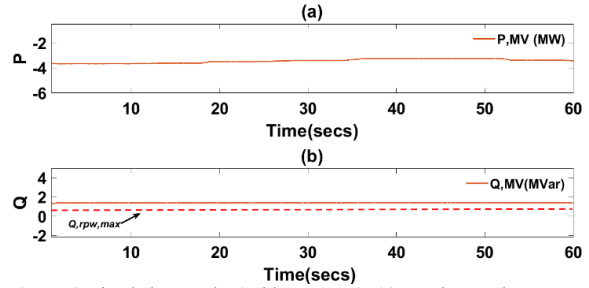


Figure 4. Simulation results (Without ANM): (a) MV bus Active power (b) MV bus reactive power

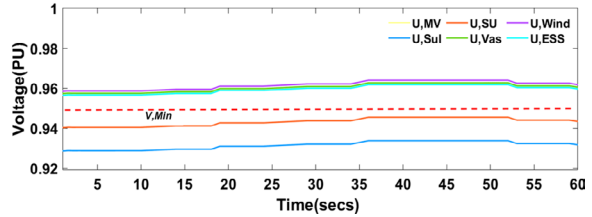


Figure 5. Simulation results (Without ANM): MV bus voltages

##### B. With ANM

Fig 6(a) shows the active  $P_{BESS}$  and  $Q_{BESS}$  characteristics of the Li-ion BESS from its MV feeder (J10). BESS is charged with 2 MW power and its maximum reactive power allocation have been activated according to the ANM schemes. Allocation from the  $Q_{BESS}$  has been designed as per (2).  $P_{WIND}$  is shown in Fig 6(b) and  $Q_{wind}$  contribution from the wind turbine has been utilized to maximum, as designated by (1), to stabilise MV feeder voltages. Fig 7(a) depicts the active power characteristics at the MV side of the HV/MV transformer. Reactive power characteristics are shown in Fig 7(b). It is observed that the  $Q_{MV}$  has been reduced in magnitude and currently well within the threshold defined by the RPW limits from FINGRID.

Fig. 8 represents the voltages in pu at various MV feeders in the MV distribution system of SSG. With the reactive power control alone, it is evident that the voltage at  $U_{SU}$  had been improved within the grid code requirements after  $Q_{flex}$  has been allocated as per first condition in (3). However,  $U_{SUL}$  still has a magnitude less than 0.95 pu, and hence the tap position changes in the OLTC transformer after 5 seconds into simulation, thereby regulating all MV feeder voltages within limits.

Fig. 9 explains DC characteristics of the Li-ion BESS and its adjoining power electronic converters for MV grid integration. BESS charge/discharge current characteristics are shown in Fig 9(a), where magnitude of defined BESS current, in this case the BESS charge current. Fig 9(b) depicts the changes in BESS operational voltage. Overall, BESS DC charge power is shown in 9(c), BESS  $SOC$  behaviour is presented in Fig 9(d). DC- bus voltage is constantly maintained at 600V, despite frequent variation of BESS voltage and current rate to the DC/AC- converter stage as shown in Fig. 9(e), thereby, reinforcing robust BESS model and adjoining converter controller design for 2 MW charge power at low

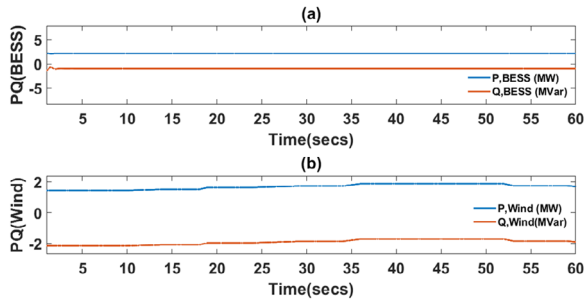


Figure 6. Simulation results (With ANM): (a) BESS Active and reactive power characteristics (b) Wind Active and reactive power characteristics

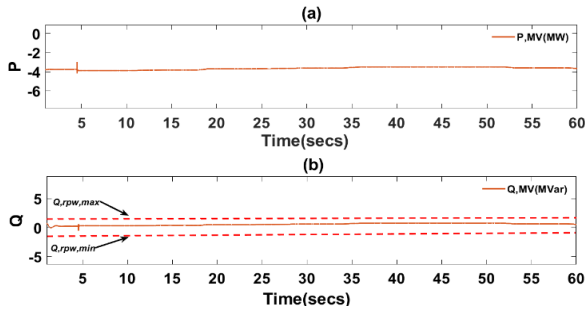


Figure 7. Simulation results (With ANM): (a) MV bus Active power (b) MV bus reactive power

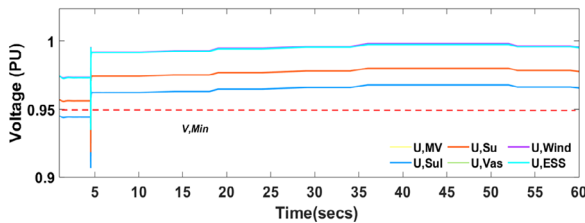


Figure 8. Simulation results (With ANM): MV bus voltages

WTG output. The ambient temperature of battery operations is assumed to be 25 °C which is represented in Fig 9(f). Recorded field temperature measurements will be introduced in the future studies. Accurate Li-ion BESS and its integration modelling was important to understand the effects of AC load requirements on the DC characteristics of the battery, especially to regulate their operation within safe limits while maintaining DC bus voltage stable.

### V. CONCLUSION

Role of Li-ion BESSs as flexible energy sources in such distribution networks are multi-faceted considering their participation in both active and reactive power related flexibility services. The use case of fast charging of Li-ion BESSs, especially during low renewable power generation induces its own strain in the distribution system in the form of voltage distortions and reactive power flows barring the RPW limits of the SSG. In such cases, active network management schemes provide a basis to mitigate arising network stability issues by actively managing available flexibilities in the MV distribution network of the SSG, where penetration of inverter based flexible energy sources are increasing at a faster pace.

In this study, the ANM schemes were modelled to utilise the entire range of reactive power control possibility, due to the extremeness of the use case. Table II provides a summary of the simulation results and an indication on how the flexibility indices have been utilised based on the equations, (1)-(5) which forms the basis of ANM control schemes.  $Q_{wind}$  and  $Q_{BESS}$  were allocated based on their maximum limits defined in (1) and (2) respectively. From the results, it is indicative that the  $Q_{flex}$  based on (3), was instrumental in keeping the reactive power flow,  $Q_{MV}$  between HV/MV grids, within the limits specified by the RPW. Since, this case was investigating the effects of fast charging, (4) which provides set-points for discharging were unutilized. With respect to the results of

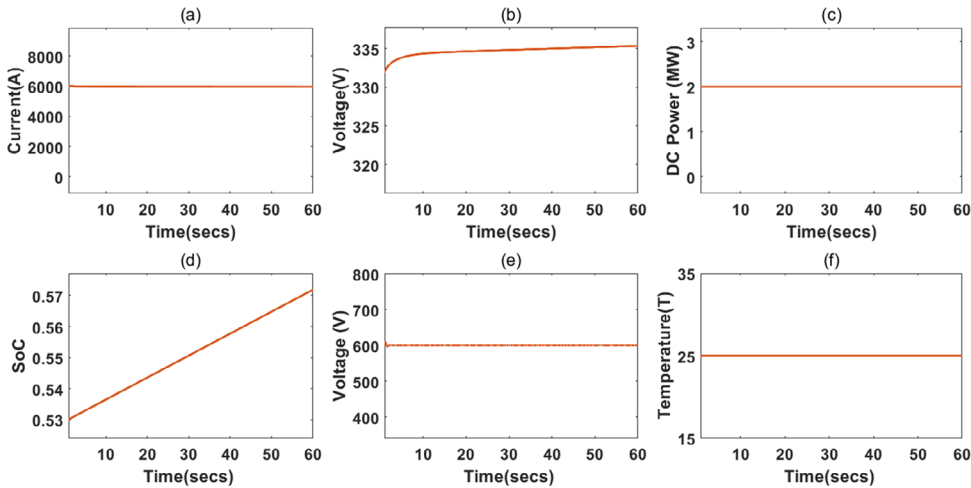


Figure 9. (a) BESS Current (b) BESS Voltage (c) BESS DC Power (d) BESS SOC (e) DC Bus voltage (f) Ambient operational temperature

Table II. Simulation Result Summary

Simulation Step	5 Secs		10 Secs		20 Secs		30 Secs		40 Secs		50 Secs		60 Secs	
	No ANM	ANM	No ANM	ANM	No ANM	ANM	No ANM	ANM	No ANM	ANM	No ANM	ANM	No ANM	ANM
$Q_{BESS}$ (Mvar)	0	0,5	0	0,5	0	0,5	0	0,5	0	0,5	0	0,5	0	0,5
$Q_{wind}$ (Mvar)	0	2,05	0	2,05	0	1,96	0	1,92	0	1,88	0	1,88	0	1,94
$Q_{flex}$ (Mvar)	0	2,55	0	2,55	0	2,46	0	2,42	0	2,38	0	2,38	0	2,44
$Q_{MV}$ (pu)	<b>1,8</b>	<b>0,43</b>	<b>1,8</b>	<b>0,44</b>	<b>1,8</b>	<b>0,45</b>	<b>1,8</b>	<b>0,44</b>	<b>1,8</b>	<b>0,46</b>	<b>1,8</b>	<b>0,46</b>	<b>1,8</b>	<b>0,45</b>
$U_{SUL}$ (pu)	<b>0,924</b>	<b>0,938</b>	<b>0,924</b>	<b>0,96</b>	<b>0,93</b>	<b>0,962</b>	<b>0,932</b>	<b>0,963</b>	<b>0,934</b>	<b>0,965</b>	<b>0,934</b>	<b>0,965</b>	<b>0,933</b>	<b>0,963</b>
$U_{SU}$ (pu)	<b>0,94</b>	<b>0,955</b>	<b>0,94</b>	<b>0,975</b>	<b>0,942</b>	<b>0,976</b>	<b>0,943</b>	<b>0,976</b>	<b>0,945</b>	<b>0,978</b>	<b>0,945</b>	<b>0,978</b>	<b>0,944</b>	<b>0,977</b>

voltage limits at various MV feeders, it has been evident that the voltages at Sulva and Sundom feeders were below 0.95 pu without any ANM schemes operational. However, with the allocation of  $Q_{flex}$ , voltage at the Sundom feeder improved, but Sulva was still barring the MV voltage limits. Hence, at about 5 seconds into simulation, OLTC were activated, thereby improving the voltage at Sulva feeder. Therefore, the designed ANM scheme, acted as required to provide RPW and voltage regulation. In future, more adaptive and accurate ANM schemes will be designed and modelled for real-time simulations to optimise the control of flexible energy sources in the MV distribution systems.

#### VI. REFERENCES

- [1] M. Faisal, M. A. Hannan, P. J. Ker, A. Hussain, M. Bin Mansor, and F. Blaabjerg, "Review of energy storage system technologies in microgrid applications: Issues and challenges," *IEEE Access*, vol. 6, pp. 35143–35164, 2018.
- [2] N. Günter and A. Marinopoulos, "Energy storage for grid services and applications: Classification, market review, metrics, and methodology for evaluation of deployment cases," *J. Energy Storage*, vol. 8, pp. 226–234, 2016.
- [3] Z. Yang, Y. Li, and J. Xiang, "Coordination Control Strategy for Power Management of Active Distribution Networks," *IEEE Trans. Smart Grid*, vol. 10, no. 5, pp. 5524–5535, 2018.
- [4] U. Akram, M. Nadarajah, R. Shah, and F. Milano, "A review on rapid responsive energy storage technologies for frequency regulation in modern power systems," *Renew. Sustain. Energy Rev.*, vol. 120, no. November 2019, p. 109626, 2020.
- [5] W. Khan, A. Ahmad, F. Ahmad, and M. Saad Alam, "A Comprehensive Review of Fast Charging Infrastructure for Electric Vehicles," *Smart Sci.*, vol. 6, no. 3, pp. 256–270, 2018.
- [6] X. Li and S. Wang, "A review on energy management, operation control and application methods for grid battery energy storage systems," *CSEE J. Power Energy Syst.*, 2019.
- [7] European Union, "DCC: Commission Regulation (EU) 2016/1388 establishing a network code on Demand Connection," *Off. J. Eur. Union*, vol. 2016, no. 14 April 2016, p. 68, 2016.
- [8] H. Laaksonen, C. Parthasarathy, H. Hafezi, M. Shafie-khah, and H. Khajeh, "Control and Management of Distribution Networks with Flexible Energy Resources," *Int. Rev. Electr. Eng.*, vol. 15, no. 3, p. 213, Jun. 2020.
- [9] K. Sirviö, H. Laaksonen, and K. Kauhaniemi, "Active Network Management Scheme for Reactive Power Control," no. 080, pp. 7–8, 2020.
- [10] H. Laaksonen, K. Sirviö, S. Aflecht, and K. Kauhaniemi, "Multi-objective Active Network Management Scheme Studied in Sundom Smart Grid with MV and LV connected DER Units," no. June, CIRED 2019.
- [11] K. M. Muttaqi, A. D. T. Le, M. Negnevitsky, and G. Ledwich, "A Coordinated Voltage Control Approach for Coordination of OLTC, Voltage Regulator, and DG to Regulate Voltage in a Distribution Feeder," *IEEE Trans. Ind. Appl.*, vol. 51, no. 2, pp. 1239–1248, 2015.
- [12] C. Parthasarathy, K. Sirviö, H. Hafezi, and H. Laaksonen, "Modelling Battery Energy Storage Systems for Active Network Management – Coordinated Control Design and Validation," *IET Renew. Power Gener.*, pp. 1–10, Accepted: 03/08/2021.
- [13] C. Parthasarathy, H. Hafezi, H. Laaksonen, and K. Kauhaniemi, "Modelling and Simulation of Hybrid PV & BES Systems as Flexible Resources in Smartgrids – Sundom Smart Grid Case," *IEEE PES PowerTech Conf.*, 2019.
- [14] C. Parthasarathy, H. Hafezi, and H. Laaksonen, "Lithium-ion BESS Integration for Smart Grid Applications - ECM Modelling Approach," ISGT NA 2020.

# Modelling battery energy storage systems for active network management—coordinated control design and validation

Chethan Parthasarathy<sup>1</sup>  | Katja Sirviö<sup>1</sup> | Hossein Hafezi<sup>2</sup>  | Hannu Laaksonen<sup>1</sup>

<sup>1</sup> School of Technology and Innovation, Flexible energy resources, University of Vaasa, Yliopistoranta 10, Vaasa, Finland

<sup>2</sup> Faculty of Information Technology and Communication Sciences, Tampere University, Tampere, Finland

## Correspondence

Chethan Parthasarathy, School of Technology and Innovation, Flexible energy resources, University of Vaasa, Yliopistoranta 10, Vaasa, Finland.  
Email: [chethan.parthasarathy@uwasa.fi](mailto:chethan.parthasarathy@uwasa.fi)

## Abstract

Control of battery energy storage systems (BESS) for active network management (ANM) should be done in coordinated way considering management of different BESS components like battery cells and inverter interface concurrently. In this paper, a detailed and accurate lithium-ion battery model has been used to design BESS controls, thereby allowing improved overall power system control design optimisation studies by simultaneously considering both component and system-level aspects. This model is utilised to develop a multi-objective ANM scheme (a) to enhance utilisation of wind power generation locally by means of active power ( $P$ )- control of BESSs; (b) to utilise distributed energy resources (i.e. BESS and wind turbine generators) to maintain system voltage within the limits of grid code requirements by reactive power/voltage ( $QU$ )- and active power/voltage ( $PU$ )- controls. BESS control strategies to implement the ANM scheme, are designed and validated through real-time simulation in an existing smart grid pilot, Sundom Smart Grid (SSG), in Vaasa, Finland.

## 1 | INTRODUCTION

The stochastic and unpredictable nature of the renewable energy sources (RES) and their geographic location, often in remote areas with weak electrical grids, present upcoming network issues, where relatively small-sized RESs are connected to the power grid in the LV/MV distribution systems. Managing power balance and power system stability (especially system voltages) is a challenging task in such situations. Therefore, innovative ANM schemes designed to manage available flexibilities in the LV/MV distribution system play a pivotal role in raising the network RES hosting capacity and managing different network parameters (voltage, reactive power flow and frequency) within the threshold values dictated by grid codes.

RES based distributed energy resources (DERs) in the MV and LV distribution network play an important role in providing flexibility in the power system for local and system-wide grid resiliency, and maximising network DER hosting capacity [1–3]. These flexibilities consist of active power ( $P$ ) and reactive power ( $Q$ )- control of flexible resources, such as, controllable DER units, battery energy storage system (BESS), controllable

loads and electric vehicles (EVs) which are connected in distribution system operator's (DSOs) grids providing different local and system-wide technical services as part of future ANM schemes [4–8].

ANM principles in [4–6] were modelled to dispatch flexibilities in the distribution system for the day-ahead market through mathematical optimisation techniques. Whereas, [7, 8] consider voltage regulation by means of reactive power control considering DER power capability curve limits and grid codes in an existing MV grid. Such studies provide details on the overall  $P$ - and  $Q$ -optimal dispatch for RESs and BESSs in the LV/MV distribution systems. However, network management studies considering the effect of such optimal dispatch on the operation of DERs and their grid-side and/or component level controllers are minimal. Considering the economic and technical aspects of DERs, especially BESSs, it is imperative to model their performance characteristics in detail.

BESSs because of their fast and controllable dynamics have the potential to provide multiple different flexibility services in stationary grid applications, especially in the ANM schemes acting as a buffer, to manage flexibilities in the distribution

This is an open access article under the terms of the [Creative Commons Attribution License](https://creativecommons.org/licenses/by/4.0/), which permits use, distribution and reproduction in any medium, provided the original work is properly cited.

© 2021 The Authors. *IET Renewable Power Generation* published by John Wiley & Sons Ltd on behalf of The Institution of Engineering and Technology



systems. From transmission and distribution system operators (TSO/DSOs) point of view, an effective way to utilise BESSs for ANM, will be to place them in an HV/MV substation or the MV distribution for example at MV/LV substations. Their benefits [9] include,

1. Increase the capacity to transfer active power by storing the energy at times of higher RES generation, avoiding the cost for additional transfer capacity
2. Secure reliable LV-network distribution to all or the most critical customers in cases of MV-network fault by utilising intended island operation
3. The storage capacity of MV/LV substations can be increased in a modular way for example, when customer reliability requirements or RES integration in LV network increase
4. Local compensation of reactive power produced by underground cables by decreasing the reactive power exchange in the MV network, thereby reducing network losses and increasing active power flow
5. Continuously control reactive power flow through the distribution system to minimise frequent tap changes in OLTC when the amount of flexibilities is higher in a system [10]

In addition to local flexibility services, BESSs can also provide a variety of system-level technical ancillary/flexibility services [9]. The utilisation of BESSs for single purpose such as improving electricity supply reliability (intended islanded or microgrid operation) or increasing RES penetration in the distribution network may not be economically viable, considering its robust ability to participate in multi-use case scenarios [11]. Hence, the developed ANM scheme is based on the multi-use capability of BESSs.

Lithium-ion (Li-ion) BESSs are capable of acting as flexible energy sources and providing multiple technical ancillary/flexibility services including frequency support by controlling active power injection and voltage regulation by reactive power control [12–14]. Ability to react fast, higher energy and power density, longer cycle and shelf life, low self-discharge rate, high round trip efficiency and improved safety performance have favoured Li-ion based BESSs for stationary grid applications. However, Li-ion batteries are intercalation-based energy storage systems, which operate as a closed system [15] with very few measurable state variables, which makes it difficult to monitor the states of the battery properly. Therefore, it is required to understand model precisely the Li-ion BESS behaviour under various operating conditions, unlike in recent research [16–18], where generic or most basic Li-ion battery models are considered.

In this paper, the equivalent circuit model (ECM) is developed for nickel-manganese-cobalt-oxide (NMC) cathode based Li-ion battery and used to design BESS control topologies. In terms of performance, ECMs are highly accurate than the kinetic battery models (KBM)/modified KBMs [19, 20] and mathematical models [21]. ECMs [22–26] are computationally less intensive compared to the Physics-based electrochemical models [27]. In this study, second-order equivalent circuit (SOEC) of Li-ion BESSs has been proposed and placed strate-

gically in the MV distribution grid harnessing its utilisation for multi-objective ANM scheme.

In order to maximise the multi-use capabilities of BESSs for distribution systems, controllers such as reactive power/voltage ( $QU$ -), active power/voltage ( $PU$ -) and active power ( $P$ -) controls are designed to act in co-ordination with each other. In previous research [28, 29], BESS integration to the MV bus of SSG was studied in detail considering the fast dynamics of the power systems, where the grid was modelled in EMT mode capturing the power system fast transients in detail. However, the slow dynamics that is control of voltages over an extended time will be modelled in the scope of this paper. Overall, in this paper, the focus was laid on,

1. Development of ANM architecture with  $QU$ -,  $PU$ - and  $P$ -controllers for managing available flexibilities of various DERs, especially to generate control signals for the BESS and wind turbine generator (WTG) inverters in the MV distribution system
2. The utilisation of accurate ECM for Li-ion BESS controller development in grid integration studies
3. Studying the effects of BESS inverter operation on the Li-ion BESS performance, including the thermal effects of Li-ion batteries
4. Understanding the interaction of BESS inverter controller with the grid side controllers in the distribution system

In this paper, the SOEC model for Li-ion BESS grid integration studies includes  $SoC$ , temperature, current rate and ageing effects explained in Section 2. The ANM architecture to manage flexible energy sources and its underlying controller design for a stable MV distribution system is presented in Section 3. Validation of the developed ANM scheme is implemented in Section 4, by managing the available flexibilities in MV distribution system in SSG network.

## 2 | LI-ION BATTERY MODEL

Thevenin-based SOEC model is a versatile technique [25]. It successfully emulates the model parameters such as multi-variable  $SoC$ , charge-rate (C-rate), temperature, hysteresis effects, self-discharge and battery ageing. SOEC is considered the benchmark model for Li-ion batteries, as it depicts the charge transfer, diffusion and solid electrolyte interface reactions in the form of resistors and capacitors.

Figure 1 shows the proposed dynamic equivalent circuit model for the NMC type Li-ion battery cell. Open circuit voltage (OCV) is modelled as an ideal voltage source, and the internal resistance is modelled as  $R_i$ . Two RC combinations are suggested for modelling Li-ion battery cell, so that the dynamic behaviour is modelled as  $R_1$ ,  $C_1$ ,  $R_2$  and  $C_2$ . The hysteresis and polarization effects in the Li-ion cells can be simulated accurately enough with the two RC combinations. The model structure is simpler compared to more RC combinations. The model parameters ( $OCV$ ,  $R_i$ ,  $R_1$ ,  $C_1$ ,  $R_2$  and  $C_2$ ) are obtained by hybrid pulse power characterization (HPPC) tests [30].

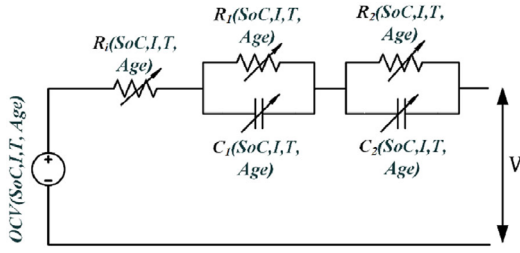


FIGURE 1 SOEC battery cell model

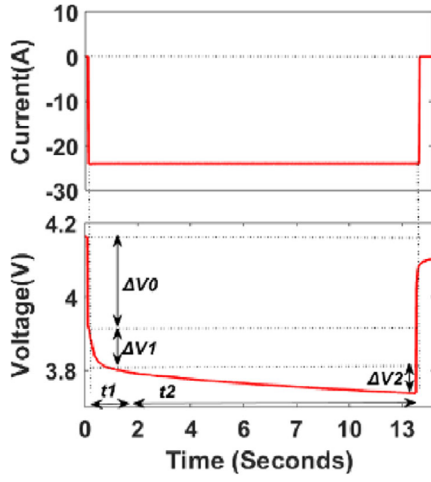


FIGURE 2 HPPC test response at 100% SoC and 25 °C

A closer view of the voltage response from the HPPC profile can be seen in Figure 2. It shows an immediate voltage drop ( $\Delta V_0$ ) when the current pulse ( $I$ ) is applied. This result is the internal resistance of the cell, which is contributed by resistance of active material, electrolyte and current collector. It can be also observed that there is a time-varying voltage ( $\Delta V_1$  and  $\Delta V_2$ ), which can be interpreted as a presence of additional elements such as a capacitor in parallel combination with resistance. The time-varying voltage part can be divided into short transient and long transient RC elements due to different time constants ( $t_1$  and  $t_2$ ) in the voltage profile. The output voltage equation for the second order ECM is shown Equation (1). The mathematical representation of the time constants is shown in Equations (2) and (3). OCV is evaluated from the voltage response of the HPPC profile at a given  $SoC$  interval, at the end of 1 h pause time.

$SoC$  is estimated by using coulomb counting method (CC) [26]. CC method provided the best accuracy with minimal computational effort in an environment where the measurement noise was minimal [31], such as measurements from battery cyclers. Hence, the  $SoC$  calculation from the CC method has been considered as the reference value in this study. The overall performance of the SOEC battery model is depicted in Figure 3 by comparing experimental and simulated voltage curves using the HPPC load current profile.

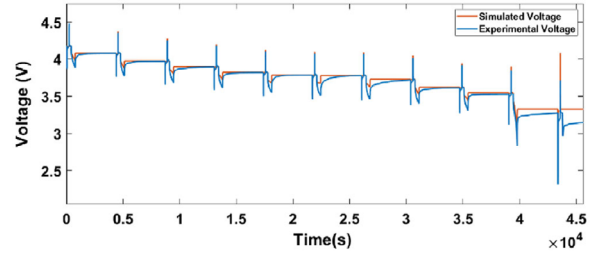


FIGURE 3 Battery model performance (HPPC profile)

The SOEC modelling technique can be utilised to estimate heat generated by battery cell, which leads to the temperature increase due to Joule heating effect. This temperature change affects the performance of the Li-ion battery considerably [13]. The major highlight between the model developed in [30] and the model presented in this paper is the development of the thermal model, which considers both  $SoC$  and inner cell temperature as affecting parameters. The inner cell temperature is considered uniform within the cell and taken as the average temperature inside the cell. Equation (4) represents the irreversible heat generated by the battery cell due to the Joule effect [32]. Therefore, temperature changes during the cell operations are determined providing set points for the thermal cooling system and the battery management system.

$$V_T(t) = V_{OCV} + I(t) R_i + I(t) R_1 \left(1 - e^{-\frac{t}{t_1}}\right)$$

$$+ I(t) R_2 \left(1 - e^{-\frac{t}{t_2}}\right) \quad (1)$$

$$t_1 = R_1 C_1 \quad (2)$$

$$t_2 = R_2 C_2 \quad (3)$$

$$P_{ib}(t) = R_i(SoC, T_b) I^2(t) = m_b C_p \frac{dT_b}{dt} + P_a(t) \quad (4)$$

where,

$m_b$ : mass of the battery [Kg]

$C_p$ : Specific heat capacity of the battery [J/Kg K]

$T_b$ : Uniform Temperature inside the battery [K]

$P_a$ : Heat transfer rate to the cooling system [W]

$P_{ib}$ : Heat generated in battery due to Joule effect

### 3 | ACTIVE NETWORK MANAGEMENT

In [33–36] extensive research on various ANM schemes to maintain system voltage by control of reactive power flow from the DERs within the reactive power window (RPW) provided by the Finnish TSO, Fingrid and ENTISO-E standards have been studied and validated in a local smart grid pilot SSG. RPW

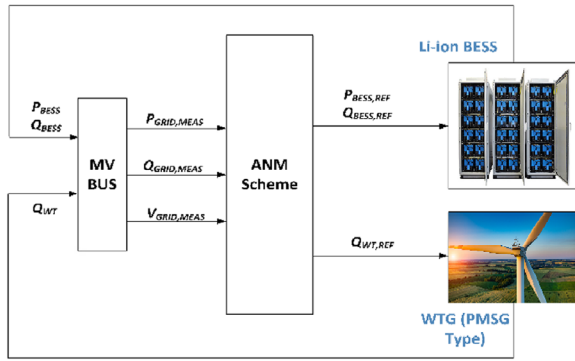


FIGURE 4 Flexibility management schematic in SSG MV grid

specified by Fingrid at the HV side of the TSO/DSO interface is represented in [36] and the requirement at the MV side is presented in [37]. The maximum active power limits are based on the measured data from year 2016, when imported grid power was 8.3 MW and the exported was 1.975 MW. According to the grid codes, the ANM voltage control is set to a maximum voltage of 1.05 pu, and the minimum voltage limits are set at 0.95 pu (both HV and MV connection points), which is based on the thermal limit for maximum current flow in the system. From previous results, the reactive power control of WTG was adequate to satisfy RPW conditions. However, it was recommended to study multi-use capabilities of BESSs such as, active power control flexibility, primarily to improve RES hosting capacity and reactive power control utilisation to complement WTG

Proposed flexibility management schematic for the MV grid of SSG is shown in Figure 4. The ANM architecture developed in Section 3.1, forms the basis to deploy flexibility management in the MV distribution system. The ANM scheme in-turn depends on the functionalities of the energy management system (EMS) and its adjoining controllers to provide technical ancillary services. Details of the ANM architecture, EMS functionalities and the EMS controller design to provide flexibility management is explained further in this section.

### 3.1 | Active network management architecture with BESS

BESSs integrated to the SSG MV bus are primarily designed to complement the stochastic nature of wind power generation, that is, store excess wind power generation and discharge during reduced wind power generation. Secondly, they are used to provide technical ancillary services. The WTG primarily caters maintaining the HV side of the grid within the RPW. However, the reactive power ( $Q_{WT}$ ) control flexibilities provided by the WTG are dependent on the active power generation ( $P_{WT}$ ), which in turn is dependent on the intermittent nature of wind. There by, WTG alone may not be sufficient to provide flexibilities in a power system, especially with respect to the reactive

power compensation by the WTG. Hence, BESS placed strategically in the MV distribution grid will be able to complement WTG in providing various technical services in the MV distribution side of the smart grid.

The ANM control architecture described in Figure 5 was designed to implement in SSG to manage flexibilities offered by WTG and Li-ion BESS. Enhancing local utilisation of wind power generation with the aid of BESSs is the primary objective of this ANM architecture. Voltage regulation within the threshold in the MV side of the grid constitutes the secondary objective. Measured MV grid data, that is active power ( $P_{GRID,MEAS}$ ), reactive power ( $Q_{GRID,MEAS}$ ) and voltages ( $V_{GRID,MEAS}$ ) is provided as the input to the control architecture. The first layer in the control architecture consists of different control techniques, capable of providing technical services to enforce ANM.  $QU$ -,  $P$ - and  $PU$ -control methodologies helps in managing different available flexibilities in the power system. In this layer, the total required reactive power control is required to maintain targets for RPW control and  $QU$ -control, the Fingrid codes' requirements, thereby defining the overall requirements for  $QU$ -control of flexible energy sources. Along with that, the  $P$ -control for BESSs is estimated and dispatched to the next layer.  $PU$ -control requirements are calculated when  $QU$ -control does not satisfy the grid code requirements.

The next layer of operation in the ANM scheme is the EMS which concerns with the operation of active and reactive power flows from the flexible energy sources, in this case BESS and WTG. Grid requirement references such as  $Q_{GRID,REF}$ ,  $P_{BESS,REF}$  and  $P_{GRID,REF}$  are given as input to the EMS layer, where it distributes the related operations to the BESS and WTG based on the availability of their individual flexibilities. Therefore, based on Equations (5)–(9), EMS generates reference values  $Q_{BESS,REF}$  and  $P_{BESS,REF}$  to the BESS and  $Q_{WT,REF}$  and  $P_{GRID,REF}$  to the WTG. Based on the internal control algorithms for BESS and WTG defined in the following section, BESS returns relevant  $P_{BESS}$  and  $Q_{BESS}$  to the EMS, whereas WTG returns  $Q_{WT}$  to the EMS.

These control signals are then forwarded to the EMS controllers as  $Q_{FLEX}$  ( $Q_{BESS}$  and  $Q_{WT}$ ) to the  $QU$ -controller,  $P_{BESS}$  is forwarded to the  $P$ -controller and  $P_{FLEX}$  is provided to the  $PU$ -controller layers. All the three control layers act in tandem to provide  $Q_{GRID,Flex}$  and  $P_{GRID,Flex}$  to the MV grid, there by controlling the active and reactive power flows in the HV/MV connection point regulating the values based on the RPW control requirements.

Figure 6(a–c) shows the design and architecture of the individual control techniques, that is  $QU$ -,  $P$ - and  $PU$ -controls respectively employed in the ANM management principle defined. Their overall operations are explained as below.

#### 3.1.1 | $QU$ -management system

Voltage regulation at the MV side ( $V_{MV}$ ) of the HV/MV connection point is the primary objective of this control loop by

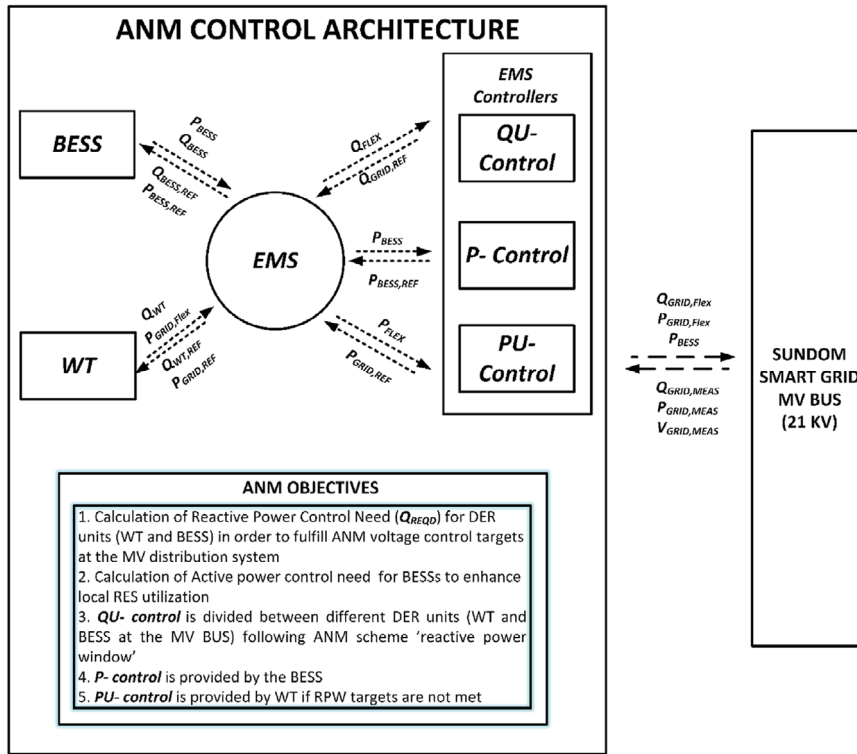


FIGURE 5 ANM scheme and its adjoining EMS controller operations

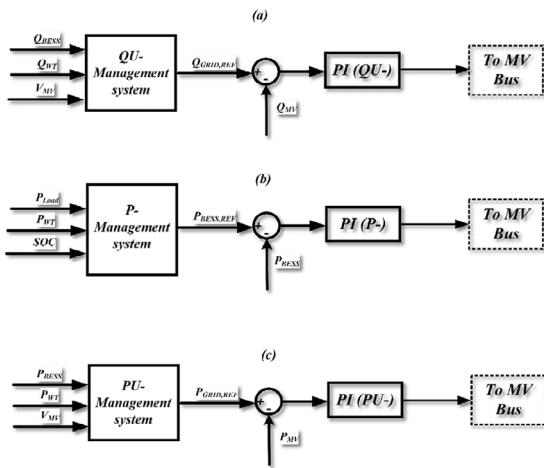


FIGURE 6 (a) QU-control, (b) P-control and (c) PU-control

controlling the available flexibilities (i.e.  $Q_{WT}$  and  $Q_{BESS}$ ) when its voltage falls below 0.95 p.u. The decoupling between reactive power control and the active power control of the distributed energy sources in this case WTG and BESS have to be clearly defined to avoid controller interactions. Hence, for both the DERs when in QU-control mode, their maximum possible reac-

tive power support is taken into account by the control algorithms.

$Q_{WT}$  control of WTG system depends on the reactive power output capability. The inverter operating range should be applied accurately before utilising reactive power control strategy in WTGs so that the maximum active power generation from the wind turbine is not disturbed. Therefore, the maximum controllable reactive power from the WTG is calculated by Equation (5).  $Q_{WT,min}$  and  $Q_{WT,max}$  are the maximum and minimum reactive power output from the WTG.  $S_{WT}$  denotes apparent power of the WTG. The negative symbol denotes absorbing reactive power and that of positive symbol to generate reactive power.

P-control of the BESS was set higher in the hierarchy so that its main goal is to enhance wind power penetration by controlling the charging and discharging  $P_{BESS}$  as per the grid's requirement. However, the reactive power control of BESS is defined by the phasor relationship between the battery inverter operating parameters as in Equation (6), for several different levels of BESS active power output ( $P_{BESS}$ ). When  $S_{BESS}$  is larger than  $P_{BESS}$ , the inverter can supply or consume reactive power,  $Q_{BESS}$ . The BESS inverter can dispatch  $Q_{BESS}$  quickly (on the cycle-to-cycle time scale) providing a mechanism for rapid voltage regulation. As the output,  $P_{BESS}$  approaches  $S_{BESS}$  (apparent power of Li-ion BESS), the range of available  $Q_{BESS}$  decreases to zero.

### 3.1.2 | $P$ -management system

Due to its capability in catering both active and reactive power requirements of the SSG, BESS control includes both  $P$ -control by regulating  $P_{BESS}$  and  $QU$ -control by regulating  $Q_{BESS}$ , there by satisfying the ANM requirements commanded by the MV distribution system in SSG.

Li-ion BESS active power control in the MV distribution system shown in Equation (7), which is primarily designed to charge ( $P_{chg}$ ), when the wind power generation exceeds load demand and discharge power ( $P_{dis}$ ) during higher demand than its wind power production, which is controlled by the battery's  $SOC$  within their threshold  $SOC_{min}$  and  $SOC_{max}$ . Overall active power discharged by the BESS is defined by Equation (8) and the BESS is charged with a power of 500 kW as with a C-rate of 0.5 C as shown in Equation (9).

$$Q_{WT,min} \leq Q_{WT} \leq Q_{WT,max}$$

$$\text{where, } \begin{cases} Q_{WT,min} = -\sqrt{S_{WT}^2 - P_{WT}^2} \\ Q_{WT,max} = \sqrt{S_{WT}^2 - P_{WT}^2} \end{cases} \quad (5)$$

$$Q_{BESS,min} \leq Q_{BESS} \leq Q_{BESS,max}$$

$$\text{where, } \begin{cases} Q_{BESS,min} = -\sqrt{S_{BESS}^2 - P_{BESS}^2} \\ Q_{BESS,max} = \sqrt{S_{BESS}^2 - P_{BESS}^2} \end{cases} \quad (6)$$

$$P_{BESS} = \begin{cases} P_{dis}; & (\text{if } SOC_{min} < SOC < SOC_{max} \text{ and } P_{Load} > P_{WT}) \\ P_{chg}; & (\text{if } SOC < SOC_{min} \text{ and } P_{WT} > P_{Load};) \\ 0 \end{cases} \quad (7)$$

$$P_{dis} = P_{Load} - P_{WT} \quad (8)$$

$$P_{chg} = 0.5C \quad (9)$$

### 3.1.3 | $PU$ -management system

$PU$ -management system is designed to keep in mind the curtailment of renewable energy generation, when the voltage limits exceed 1.05 pu in the system's MV bus. To manage the curtailment droop control referred in Figure 7 is utilised for the curtailment of wind power generation.

## 4 | RESULTS AND DISCUSSION

Dynamic voltage stability simulation is the key component in control and dynamic security assessment tools. The ultimate goal in this field has always been to perform these

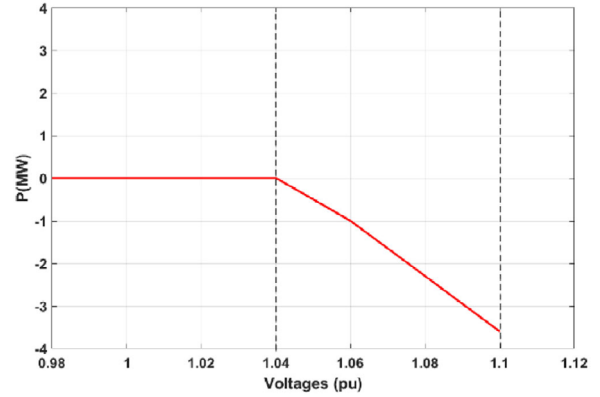


FIGURE 7 PU-droop settings

simulations as fast as real-time for realistic power systems. However, mathematical modelling and numerical solutions are computationally heavy for large-scale systems. On the other hand, continuous growth in electricity demand and the consequent expansion of power grids create new and complex problems. Thus, real-time simulations offer methods for quick and efficient simulations of large-scale systems that are necessary.

To ensure secure functioning of BESSs in smart grids, extensive real-time phasor simulations, where active and reactive power control system design and validation of BESSs over an extended period (i.e. hours to a day) are necessary. They provide accurate setpoints for the battery system controllers. Such simulations are equivalent to developing and verifying secondary and tertiary controllers for BESSs, in a hierarchically controlled power system topology. In this paper, the ANM scheme defining the role of BESS in enhancing wind power generation and MV distribution system voltage control is explored through simulation studies in the ePhasorSim platform by OPAL-RT [38].

ePhasorSim is a real-time transient stability solver used for simulating slow dynamics of large scale power systems in real-time. This tool is interfaced with Matlab/Simulink and compatible with load flow and dynamic data files from PowerFactory simulation software. Hence, for this study SSG model was developed in PowerFactory by the data provided by Local DSO, Vaasan Sähköverkko and later imported to OPAL-RT to integrate BESSs and design their controllers. Three cases are designed to study the utilisation of available flexibility for ANM of the SSG, predominantly voltage control and better utilisation of wind power generation. None of the flexibilities are utilised in the first case, thereby providing the base case scenario used to compare second (WTG as flexibility source) and third case (WTG and BESS as flexibility sources). All the simulations run for a period of 24 h, mainly in order to evaluate the different controls of flexible energy sources and their planning over a period of one full day. In all the cases, SSG is modelled as a grid-connected microgrid, without on-load tap changer (OLTC) in the HV/MV transformer. Therefore,

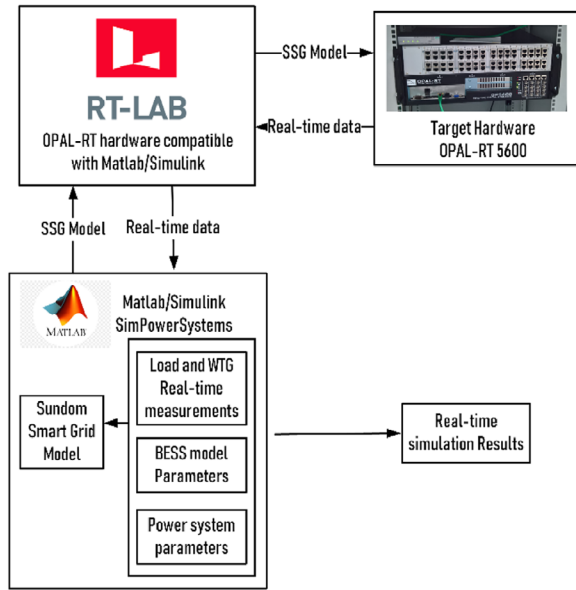


FIGURE 8 SSG real-time simulation set-up

relying on flexibility services available in the grid for voltage regulation.

#### 4.1 | Case 1: Without ANM

The real-time simulation environment is presented in Figure 8. SSG is represented in Figure 9, which is a pilot living lab jointly created by ABB, Vaasan Sähköverkko (DSO), Elisa (communications) and University of Vaasa [39]. Real-time voltage and current measurements (IEC 61850 standard) recorded from the MV distribution network, from all four feeders at an HV/MV substation and three MV/LV substations comprising 20 measurement points in total. Measurements are sampled at 80 samples/cycle. In addition measurements of, active and reactive power, frequency, RMS voltages, currents etc. are received by GOOSE messages. Figure 10 represents SSG with Li-ion BESS integrated to the MV grid.

The base case scenario where SSG is simulated without BESS in the MV distribution system is shown in Figure 9. This approach enables us to record the active and reactive power flows at the HV/MV interface and active power flow of the WTG. The SSG WTG is of permanent magnet synchronous generator type, thereby allowing it to absorb or inject reactive power to 100% of its rated power. In this case, the reactive power control ( $QU$ -control) of the WTG is disabled, to record the original characteristics in the SSG without the operation of any flexible energy resources adhering to IEEE 1547–2018 [40] guidelines.

$P_{WT}$  and  $Q_{WT}$  generation from the wind turbine is shown in Figure 11(a), where negative symbol denotes power generation. Figure 11(b) shows the active ( $P_{HV}$ ) and reactive power ( $Q_{HV}$ ) flow from the HV side of the HV/MV transformer. In the early

part of the day, grid supplies power due to the reduced wind power generation and later it starts to consume power generated from SSG. The flexibilities provided by the reactive power control of the WTG is unused to record the system parameters in the base case scenario.  $V_{HV}$  and  $V_{MV}$ , the system voltages measured during the simulation, from the HV and MV side of the transformers respectively. The SSG as a grid-connected micro-grid, proves to be a very stiff grid on the HV side with  $V_{HV}$  close to 1 pu. Whereas, the voltage in the MV side of the transformer is close to 0.94 pu (Figure 11(c)), which is well under the limitations commanded from the Fingrid's RPW. Hence, there exists a need from flexible energy sources to regulate system voltage at the MV grid, in the absence of OLTC. Hence, the following cases are defined to utilise the available flexibilities to stabilise voltage in the MV distribution system.

#### 4.2 | Case 2: ANM flexibilities (WTG only)

In this case, the WTG's reactive power flexibility in the SSG is utilised to control voltage at the MV bus, adhering to the modified standards explained in Section 3.  $P_{WT}$  of the WTG is the recorded measurement data. However,  $Q_{WT}$  control of WTG system depends on the reactive power output capability based on  $QU$ -control calculations.

The flexibilities of  $QU$ -control from the WTG have been utilized to stabilise MV distribution system's voltages. The WTG absorbs reactive power in the system to its maximum possible value as defined by the ANM scheme determined in Section 3. Active and reactive power flows from the WTG is shown in Figure 12(a), where the instantaneous  $Q_{WT}$  is determined by Equation (5). The voltages at the HV and MV side of the HV/MV transformer in SSG is presented in Figure 12(b). Despite the maximum flexibility available from the  $QU$ -control of WTG, it is observed that the voltages in the MV side of the transformer, does not stay within limits defined by the ANM targets. Hence, further flexibilities are required in the network to regulate voltage at the MV distribution system.

#### 4.3 | Case 3: ANM flexibilities (WTG and BESS)

Li-ion BESS and its integration in MV grid using power converters (bus J10\*) are shown in Figure 10. BESS has been modelled based on the SOEC method as explained in Section 2. Li-ion BESS characteristics are presented in Table 1.

Due to its capability in both catering both active and reactive power requirements of the SSG, BESS controllers should include both  $P$ -control by regulating  $P_{BESS}$  and  $QU$ -control by regulating  $Q_{BESS}$ , there by satisfying the ANM requirements commanded by the MV distribution system in SSG. BESS internal control algorithms are described by Equations (7)–(9). Li-ion BESS active power control in the MV the distribution system is shown in Equation (7), which is primarily designed to  $P_{drg}$ , when the wind power generation exceeds load demand and  $P_{dis}$  during higher demand than its wind power production,

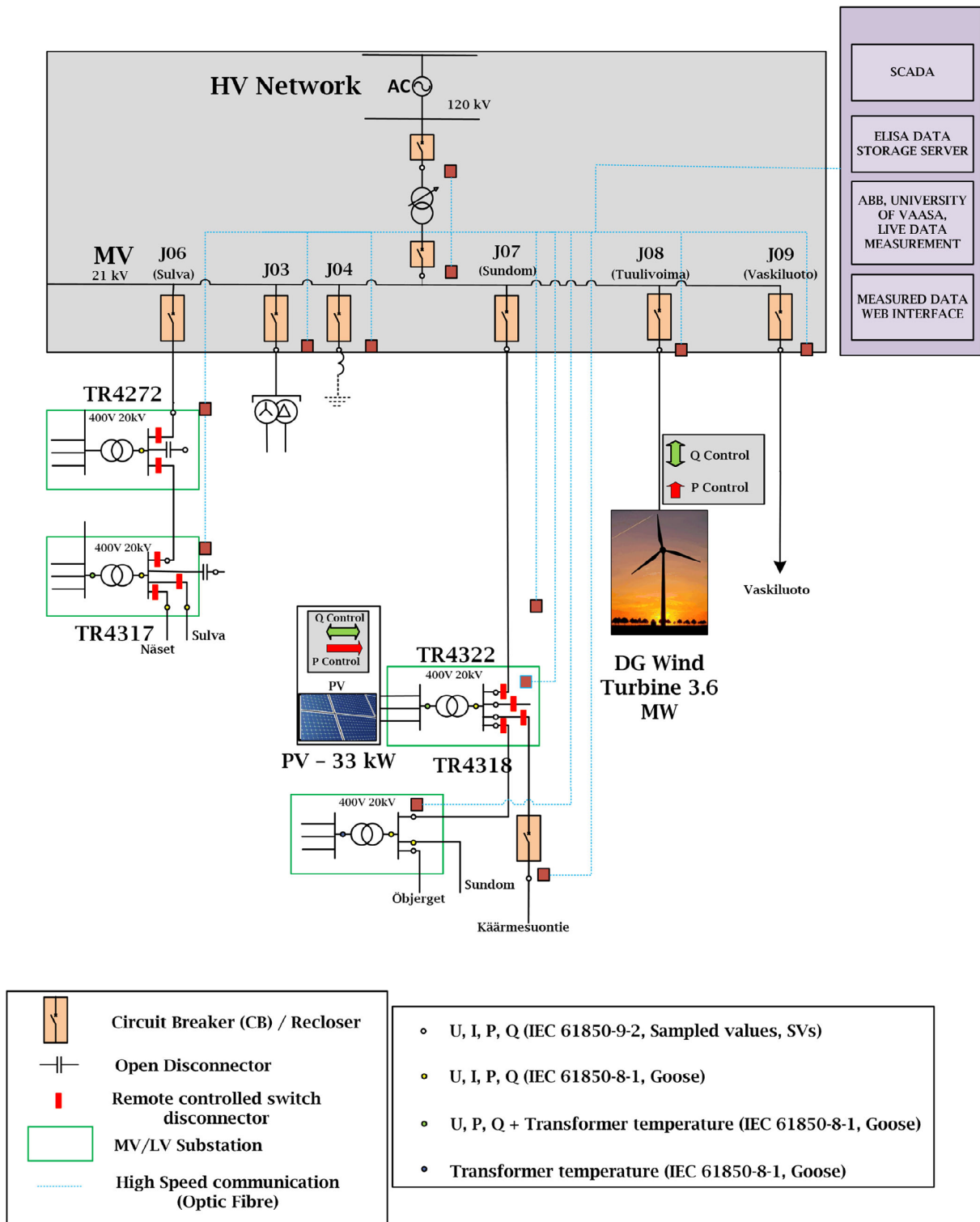


FIGURE 9 Existing SSG network

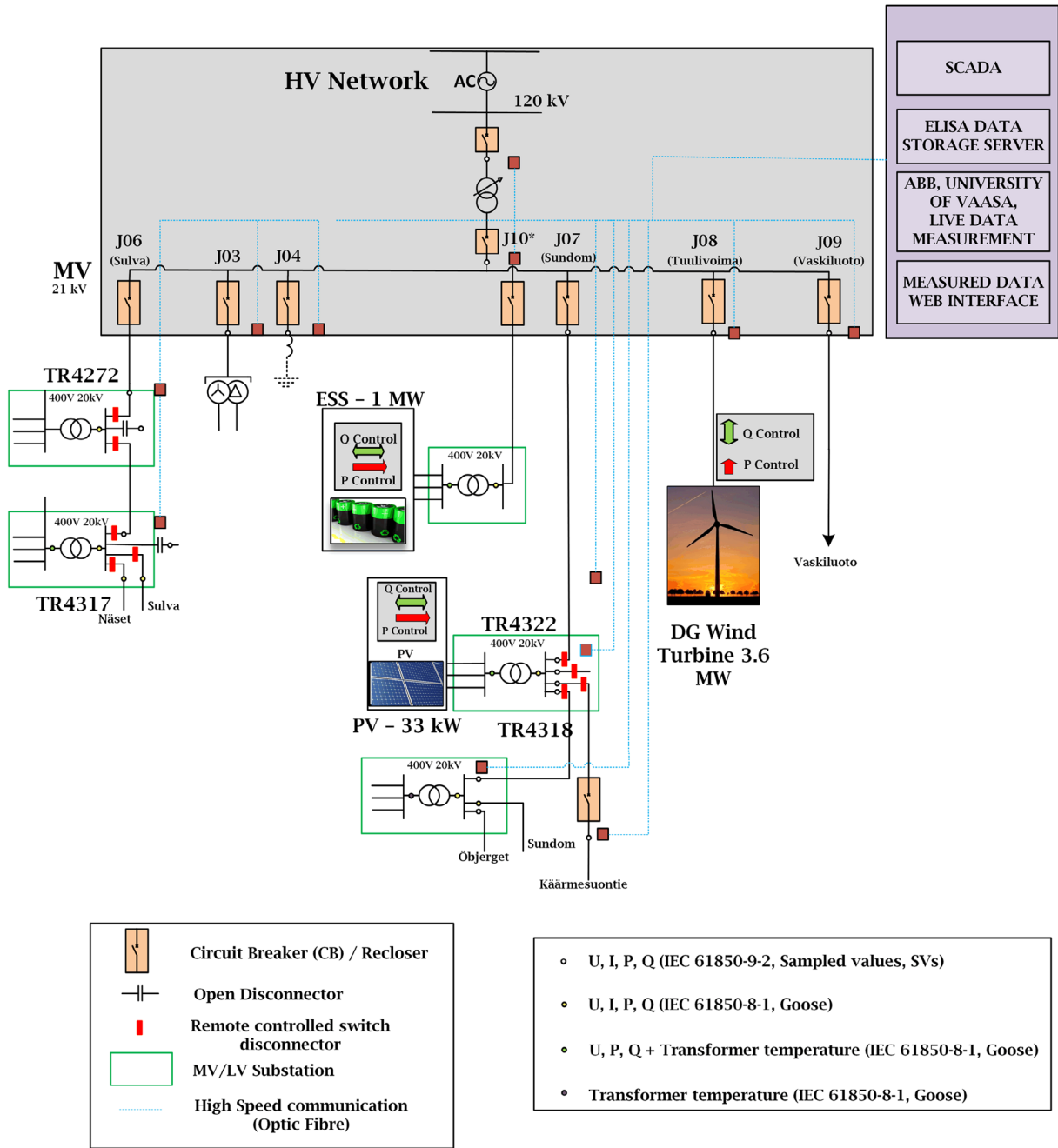


FIGURE 10 SSG with Li-ion BESS

which is controlled by the battery's  $SoC$  within their threshold  $SoC_{min}$  and  $SoC_{max}$ . Overall active power discharged by the BESS is defined by Equation (8) and the BESS is charged with a power of 500 kW as with a C-rate of 0.5 C as shown in Equation (9). Simulations are run by integrating Li-ion BESSs in the MV distribution system and their respective controllers are evaluated. Figure 13(a) presents active and reactive power of the BESS, following the commands set by Equations (7)–(9). During the

beginning of the simulation  $P_{Load}$  is greater than  $P_{WT}$ . Hence, the BESS begins to discharge active power, with any reactive power flow due to the grid's reference set. However, during the course of the day,  $P_{WT}$  increases and is able to cater the load demand requirements and also capable of charging the BESS. Over this period, it is noted that the maximum reactive support from BESS is utilised due to its requirement to regulate MV bus voltage except the time during BESS charge. In that



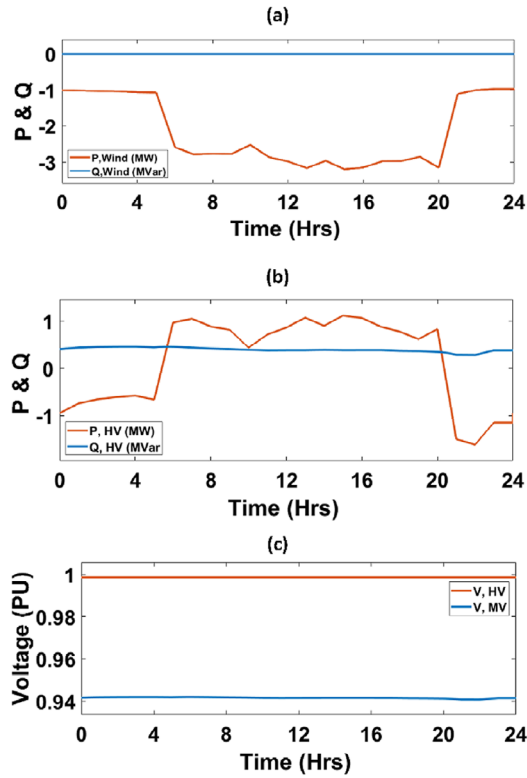


FIGURE 11 Case (1) results: (a) Active and reactive power flow at the HV side. (b) Active and reactive power of WTG. (c) Voltages in HV and MV grids

TABLE 1 Li-ion BESS characteristics

Lithium-ion battery characteristics	
Nominal DC voltage	525 V
Peak voltage	597 V
Cut-off voltage	397 V
Discharge energy(1C)	1 MWh
Nominal discharge current (1C)	2104 A

instance, reactive power flow is controlled by Equation (6). MV and HV bus voltages are presented in Figure 13(b), where both the voltages are within the threshold values determined by the ANM control architecture. The primary advantage of adding the SOEC battery model to the SSG to design their controller principles is to understand the way battery as a component responds to the requirements presented by the grid. Figure 14 explains various battery characteristics on the DC side due to the demands exerted by the AC side of the power grid. BESS operates with a range of  $SoC_{min}$  and  $SoC_{max}$ , which is as shown in Figure 14(a), where it operates between 20% and 90%  $SoC$  accurately. Figure 14(b) shows the DC current characteristics on the battery, where  $P_{dis}$  operation does not exceed 1MW and  $P_{chg}$  happens at 500 kW. BESS voltage characteristics are shown in Figure 14(c), which provides an important set-point

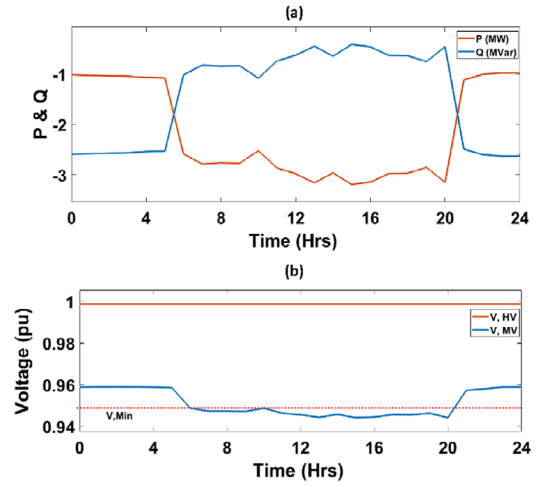


FIGURE 12 Case (2) results: (a) Active and reactive power of WTG. (b) Voltages in HV and MV grid

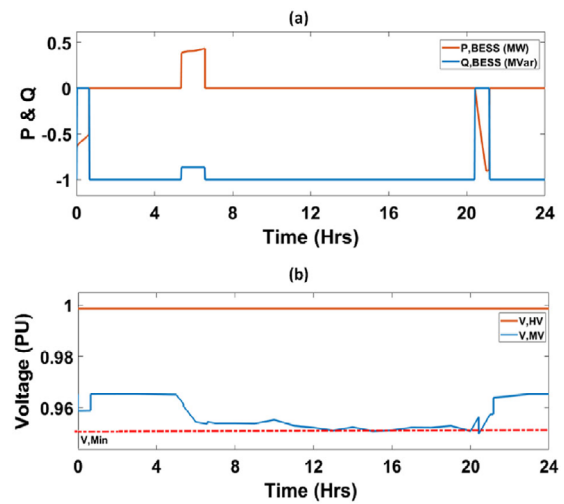


FIGURE 13 Case (3) results: (a) BESS active and reactive power (b) HV and MV voltages

for control of power converters employed to integrate battery systems to the grid and Figure 14(d) presents the DC power characteristics. The PI-controllers representing control of the flexibilities from BESS and WTG are represented in Table 2.

When the BESS is subjected to the current profile in Figure 14(b), the temperature changes in the battery cell due to

TABLE 2 PI controller coefficients

Grid side controllers	Kp	Ki
$P_{BESS}$	0.005	1
$Q_{BESS}$	0.005	1
$Q_{WT}$	0.3974	0.9196

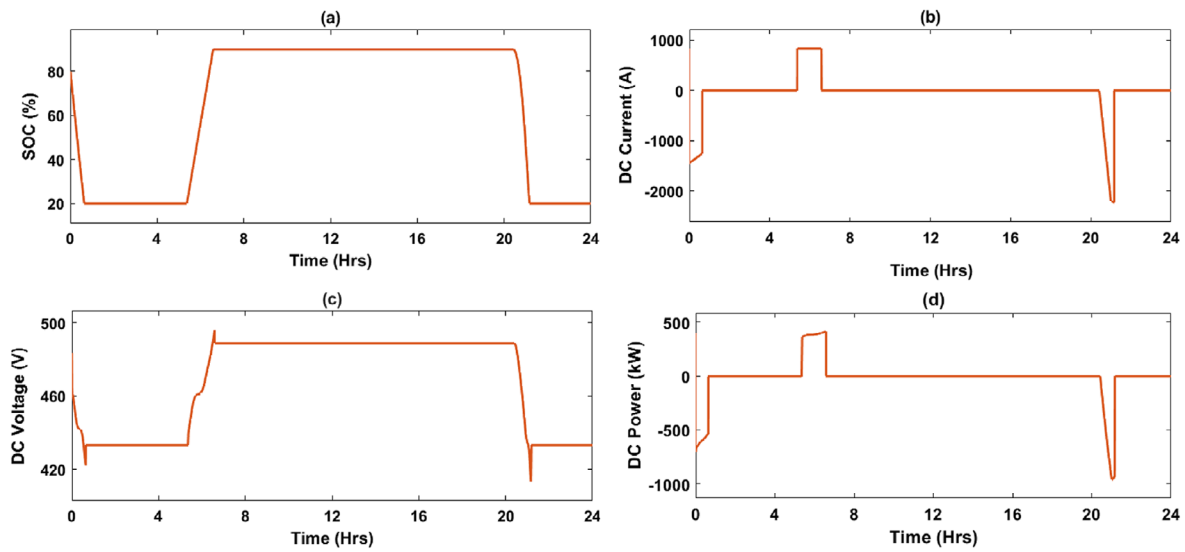


FIGURE 14 (a) Battery SoC; (b) Battery DC charge/discharge currents; (c) Battery SC voltage; (d) Battery DC power characteristics

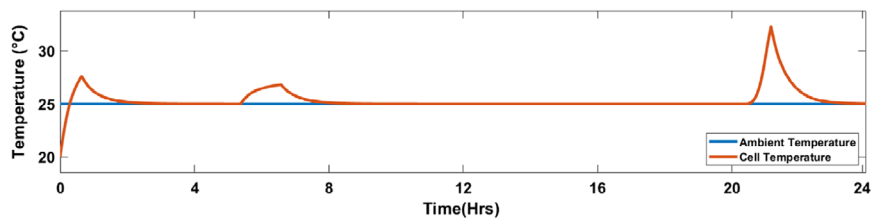


FIGURE 15 Battery cell operational temperature profile

the heat generated during its operation is represented in Figure 15. It is assumed that the ambient temperature is 25 °C. This result from the battery thermal model provides direct information on the effect of grid current requirements on the BESSs thermal characteristics. Hence, the SOEC battery model provides set points to design battery management systems, that is by considering both thermal and electrical characteristics of battery operation.

## 5 | CONCLUSION

Li-ion BESSs will play a dominant role as flexible energy sources for stationary grid applications because of their versatile nature, tending multi-objective applications in ANM schemes and their capability to participate in active and reactive power flexibility markets. However, the Li-ion BESSs are highly non-linear in performance with stringent safety requirements due to their characteristics. It is important to include the parameters affecting battery performance while designing grid-scale controllers for BESS to cater to the power system requirements. Hence, in this paper ANM control schemes were developed by utilising the second-order equivalent circuit battery model, an accurate

representation of battery operations keeping the battery characteristics in safe operational areas. Li-ion BESS controls were designed to cater effective management of available flexibilities in the MV distribution system. Such studies allow validating the BESS-ANM control schemes and provide a detailed analysis on the impact of such load curves on the BESS performance attribute.

In future, more use cases will be added on to the existing multi-use scenarios of the BESS for managing flexibilities in a medium voltage distribution system, especially with respect to catering system frequency related challenges and the effects of Li-ion BESS aging will be included for smart grid applications.

## ORCID

Chethan Parthasarathy  <https://orcid.org/0000-0002-2926-9367>

Hossein Hafezi  <https://orcid.org/0000-0003-1859-6263>

## REFERENCES

1. Usman, M., Coppo, M., Bignucolo, F., Turr, R.: Losses management strategies in active distribution networks: A review. *Electr. Power Syst. Res.* 163(7), 116–132 (2018)

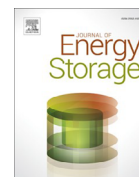
2. Christakou, K.: A unified control strategy for active distribution networks via demand response and distributed energy storage systems. *Sustain. Energy, Grids Networks*. 6, 1–6 (2016)
3. Palizban, O., Kauhaniemi, K., Guerrero, J.M.: Microgrids in active network management—Part II: System operation, power quality and protection. *Renew. Sustain. Energy Rev.* 36, 440–451 (2014)
4. Karagiannopoulos, S., et al.: Active distribution grids offering ancillary services in islanded and grid-connected mode. *IEEE Trans. Smart Grid*. 11(1), 623–633 (2020)
5. Christakou, K., Paolone, M., Abur, A.: Voltage control in active distribution networks under uncertainty in the system model: A robust optimization approach. *IEEE Trans. Smart Grid*. 9(6), 5631–5642 (2018)
6. Luo, E., et al.: Two-stage hierarchical congestion management method for active distribution networks with multi-type distributed energy resources. *IEEE Access*. 8, 120309–120320 (2020)
7. Calderaro, V., et al.: A smart strategy for voltage control ancillary service in distribution networks. *IEEE Trans. Power Syst.* 30(1), 494–502 (2015)
8. Mendonca, T.R.F., Green, T.C.: Distributed active network management based on locally estimated voltage sensitivity. *IEEE Access*. 7, 105173–105185 (2019)
9. Stecca, M., et al.: A comprehensive review of the integration of battery energy storage systems into distribution networks. *IEEE Open J. Ind. Electron. Soc.* 1(1), 1–1 (2020)
10. Li, C., et al.: Optimal OLTC voltage control scheme to enable high solar penetrations. *Electr. Power Syst. Res.* 160, 318–326 (2018)
11. Münderlein, J., et al.: Analysis and evaluation of operations strategies based on a large scale 5 MW and 5 MWh battery storage system. *J. Energy Storage*. 24(5), (2019)
12. Vazquez, S., et al.: Energy storage systems for transport and grid applications. *IEEE Trans. Ind. Electron.* 57(12), 3881–3895 (2010)
13. Hesse, H.C., et al.: Lithium-ion battery storage for the grid - A review of stationary battery storage system design tailored for applications in modern power grids. *Energies*. 2107, 10(12), (2017)
14. Müller, M.: Stationary Lithium-Ion Battery Energy Storage Systems A Multi-Purpose Technology. Ph.D. thesis, TUM (2018)
15. Lawder, M.T., et al.: Battery energy storage system (BESS) and battery management system (BMS) for grid-scale applications. *Proc. IEEE*. 102(6), 1014–1030 (2014)
16. Datta, U., Kalam, A., Shi, J.: Smart control of BESS in PV integrated EV charging station for reducing transformer overloading and providing battery-to-grid service. *J. Energy Storage*. 28, 101224, (2020)
17. Iurilli, P., Brivio, C., Merlo, M.: SoC management strategies in battery energy storage system providing primary control reserve. *Sustain. Energy, Grids Networks*. 19, 100230 (2019)
18. Datta, U., Kalam, A., Shi, J.: The relevance of large-scale battery energy storage (BES) application in providing primary frequency control with increased wind energy penetration. *J. Energy Storage*. 23(2), 9–18 (2019)
19. Wang, T., Cassandras, C.G.: Optimal control of multibattery energy-aware systems. *IEEE Trans. Control Syst. Technol.* 21(5), 1874–1888 (2013)
20. Bako, Z.N., et al.: Experiment-based methodology of kinetic battery modeling for energy storage. *IEEE Trans. Ind. Appl.* 55(1), 593–599 (2019)
21. Castaneda, M., et al.: A new methodology to model and simulate microgrids operating in low latitude countries. *Energy Procedia*. 157, 825–836 (2019)
22. Imran, R.M., Li, Q., Flaih, F.M.F.: An enhanced lithium-ion battery model for estimating the state of charge and degraded capacity using an optimized extended kalman filter. *IEEE Access*. 8, 208322–208336, (2020)
23. Kim, T., et al.: An on-board model-based condition monitoring for lithium-ion batteries. *IEEE Trans. Ind. Appl.* 55(2), 1835–1843 (2019)
24. Yang, J.: A closed-loop voltage prognosis for lithium-ion batteries under dynamic loads using an improved equivalent circuit model. *Microelectron. Reliab.* 100–101(7), 113459 (2019)
25. Nejad, S., Gladwin, D.T., Stone, D.A.: A systematic review of lumped-parameter equivalent circuit models for real-time estimation of lithium-ion battery states. *J. Power Sources*. 316, 183–196 (2016)
26. Meng, J., et al.: Overview of lithium-ion battery modeling methods for state-of-charge estimation in electrical vehicles. *Appl. Sci.* 8(5), 659 (2018)
27. El Sayed, M., et al.: Reduced-order electrochemical model parameters identification and soc estimation for healthy and aged li-ion batteries part i: parameterization model development for healthy batteries. *IEEE J. Emerg. Sel. Top. Power Electron.* 2(3), 659–677 (2014)
28. Parthasarathy, C., et al.: Modelling and simulation of hybrid pv & bes systems as flexible resources in smartgrids – sundom smart grid case. In: *IEEE PES PowerTech Conference*, Milan, Italy, pp. 1–6 (2019)
29. Parthasarathy, C., Hafezi, H., Laaksonen, H.: Lithium-ion bess integration for smart grid applications - ccm modelling approach. *IEEE Power & Energy Society Innovative Smart Grid Technologies Conference (ISGT)*, Washington, DC, USA, (2020)
30. Arunachala, R., et al.: Inhomogeneities in large format lithium ion cells: A study by battery modelling approach. *ECS Trans.* 73(1), 201–212 (2016)
31. Nemounekhkhah, B., et al.: Comparison and evaluation of state of charge estimation methods for a verified battery model. In: *2020 International Conference on Smart Energy Systems and Technologies (SEST)*, Istanbul, Turkey, pp. 1–6 (2020)
32. Kalogiannis, T., et al.: A comparison of internal and external preheat methods for NMC batteries. *World Electr. Veh. J.* 10(2), 1–16 (2019)
33. Laaksonen, H., et al.: Multi-objective active network management scheme studied in sundom smart grid with mv and lv connected der units. *CIREC 2019*, Madrid, Spain, (2019)
34. Sirviö, K., et al.: Controller development for reactive power flow management between dso and tso networks. *IEEE PES Innovative Smart Grid Technologies Europe (ISGT-Europe)*, Bucharest, Romania, pp. 1–5 (2019)
35. Sirviö, K., Laaksonen, H., Kauhaniemi, K.: Active network management scheme for reactive power control. *Cired Workshop 2018 on Microgrids and Local Energy Communities*, Ljubljana, Slovenia, 7–8, (2020)
36. Sirvio, K., et al.: Prospects and costs for reactive power control in sundom smart grid. *IEEE PES Innovative Smart Grid Technologies Conference Europe (ISGT-Europe)*, Sarajevo, Bosnia and Herzegovina, p. 1–6, (2018)
37. Laaksonen, H., Hovila, P., Kauhaniemi, K.: Combined islanding detection scheme utilising active network management for future resilient distribution networks. *J. Eng.* 2018(15), 1054–1060 (2018)
38. Panigrahy, N., et al.: Real-time phasor-emt hybrid simulation for modern power distribution grids. *IEEE International Conference on Power Electronics, Drives and Energy Systems (PEDES)*, Trivandrum, India, p. 1–6 (2017)
39. Laaksonen, H.: Future-proof Islanding Detection Schemes in Sundom Smart Grid. *24th International Conference on Electricity Distribution (CIREC 2017)* Glasgow, Scotland, pp. 12–15 (2017)
40. IEEE Standard Association, *IEEE Std. 1547–2018. Standard for Interconnection and Interoperability of Distributed Energy Resources with Associated Electric Power Systems Interfaces.* (2018)

**How to cite this article:** Parthasarathy, C., Sirviö, K., Hafezi, H., Laaksonen, H.: Modelling battery energy storage systems for active network management—coordinated control design and validation. *IET Renew. Power Gener.* 1–12 (2021).  
<https://doi.org/10.1049/rpg2.12174>



Contents lists available at ScienceDirect

Journal of Energy Storage

journal homepage: [www.elsevier.com/locate/est](http://www.elsevier.com/locate/est)

Research papers

## Aging aware adaptive control of Li-ion battery energy storage system for flexibility services provision

Chethan Parthasarathy<sup>a,\*</sup>, Hannu Laaksonen<sup>a</sup>, Eduardo Redondo-Iglesias<sup>b</sup>, Serge Pelissier<sup>b</sup><sup>a</sup> Flexible Energy Resources, Electrical Engineering, University of Vaasa, Vaasa, Finland<sup>b</sup> LICIT-ECO7 Lab, Univ Eiffel, ENTPE, Univ Lyon, Bron, France

## ARTICLE INFO

## Keywords:

Lithium ion battery  
 Battery aging characterisation  
 Power system control and modelling  
 Active network management

## ABSTRACT

Battery energy storage systems (BESSs) play a major role as flexible energy resource (FER) in active network management (ANM) schemes by bridging gaps between non-concurrent renewable energy sources (RES)-based power generation and demand in the medium-voltage (MV) and low-voltage (LV) electricity distribution networks. However, Lithium-ion battery energy storage systems (Li-ion BESS) are prone to aging resulting in decreasing performance, particularly its reduced peak power output and capacity. BESS controllers when employed for providing technical ancillary i.e. flexibility services to distribution (e.g. through ANM) or transmission networks must be aware of changing battery characteristics due to aging. Particularly of importance is BESSs' peak power changes aiding in protection of the Li-ion BESS by restricting its operation limits of it for safety reasons and improving its lifetime in the long run. In this paper, firstly an architecture for ANM scheme is designed considering Li-ion BESSs as one of the FERs in an existing smart grid pilot (Sundom Smart Grid, SSG) in Vaasa, Finland. Further, Li-ion BESS controllers are designed to be adaptive in nature to include its aging characteristics, i.e. tracking the changing peak power as the aging parameter, when utilised for ANM operation in the power grid. Peak power capability of the Li-ion nickel-manganese-cobalt (NMC) chemistry-based battery cell has been calculated with the experimental data gathered from accelerated aging tests performed in the laboratory. Impact of such aging aware and adaptive Li-ion BESS controllers on the flexibility services provision for power system operators needs will be analysed by means of real-time simulation studies in an existing SSG pilot.

### 1. Introduction

Modern power systems landscape is changing rapidly in order to facilitate reduction on fossil fuel utilization and tackle climate change issues. This has led to large and rapid integration of renewable energy sources (RES) in medium voltage (MV) and low voltage (LV) distribution networks. One of the major issues in RES integration, arises from their intermittency in power generation which causes fluctuation in system parameters such as its frequency and voltage [1,2].

Active network management (ANM) provides an opportunity for efficient management of the flexible energy sources (FERs) for flexibility services provision for distribution system operators (DSOs) increasing needs related, for example, to voltage fluctuations [3,4]. FERs play an essential role by offering multiple different flexibility services for DSOs as well as for transmission system operators (TSOs). They provide ways for improved existing network capacity utilization without excessive passive network component upgrades and simultaneously more reliable

and efficient network operation. In the development of future-proof ANM methods FER controllers play a major role. For example, inverter-based resources such wind turbine generators are capable of participating in flexibility services provision by its reactive power control dependent on local voltage target value or simultaneous active power output. However, flexibility services feasible provision requires design of suitable controllers for different purposes (flexibility service needs).

Inverter-based BESSs can be seen as ideal flexibility services providers due to their potential and versatility in providing multiple active ( $P$ ) and reactive power ( $Q$ ) related flexibility services for different DSO and TSO needs like, for example, for voltage and frequency control, black start, islanding, load leveling and peak shaving [5,6]. Thereby, BESSs are very useful for bridging gap between non-concurrent RES-based power generation and demand at different voltage ( $U$ ) levels of the power system.

Recently, Li-ion battery energy storage systems (Li-ion BESSs) have become the forefront choice for utilization in land-based grid support

\* Corresponding author.

E-mail address: [chethan.parthasarathy@uwasa.fi](mailto:chethan.parthasarathy@uwasa.fi) (C. Parthasarathy).<https://doi.org/10.1016/j.est.2022.106268>

Received 18 May 2022; Received in revised form 24 October 2022; Accepted 26 November 2022

Available online 5 December 2022

2352-152X/© 2022 The Authors. Published by Elsevier Ltd. This is an open access article under the CC BY license (<http://creativecommons.org/licenses/by/4.0/>).

Nomenclature			
BESS	battery energy storage systems	$P_{dis}$	battery active power discharge
FER	flexible energy resources	$P_{chg}$	battery active power charge
ANM	active network management	$P_{Load}$	total load power
RES	renewable energy sources	$P_{WT}$	wind turbine active power generation
LV	low voltage	$P_{BESS, REF}$	Li-ion BESS active power reference without age consideration
MV	medium voltage	$SOC_{min}$	SOC minimum limits
NMC	Nickel-Manganese-cobalt battery chemistry	$SOC_{max}$	SOC maximum limits
TSO	transmission system operator	$P_{CELL, REF}$	Li-ion battery cell reference without age consideration
SOH	state of health	$N_s$	number of battery cells in series
SOC	state of charge	$N_p$	number of battery cells in parallel
SSG	second order smart grid	$P_{cell}$	battery cell power
DER	distributed energy resources	$P_{CELL, REF, age}$	Li-ion battery cell reference without age consideration
DSO	distribution system operator	$SOC_{initial}$	initial battery SOC
EMS	energy management system	$I_{cell}$	current per cell
WTG	wind turbine generator	$Q_{wind}$	reactive power contribution from WTG
BMS	battery management system	$Q_{ref}$	reactive power reference
PP	peak power	$Q_{wind, av}$	available reactive power from WTG
HPPC	hybrid pulse power characterisation test	$Q_{BESS}$	reactive power contribution from Li-ion BESS
SEI	solid electrolyte interface	$R_{dis}$	DC discharge resistance of battery cell
CCCV	constant current constant voltage	$PP_{Dis}$	peak power during battery cell discharge
CC	constant current	$R_{cha}$	DC charge resistance of battery cell
DOD	depth of discharge	$PP_{cha}$	peak power during battery cell charge
SOEC	second order equivalent circuit	$P_{BESS, REF, age}$	Li-ion BESS active power reference with age consideration

applications, by acting as a FER which is capable of providing multiple flexibility services for ANM operations in the distribution system [7]. Nowadays, Li-ion BESSs are commercially available for large-scale for grid applications with power ratings in the range of hundreds of MWs. The power and energy density, lower self-discharge, slow aging rates, improved safety and high modularity in their construction are some of the reasons behind adoption of Li-ion batteries for grid applications [8].

However, performance of Li-ion BESSs are affected by various parameters such as depth of discharge (DOD), state of charge (SOC), temperature and aging [9]. Further, performance degradation due to aging, mainly leads to change in battery capacity and their peak power capability. This peak power changes in Li-ion BESS is a function of its SOC and aging. This means that the Li-ion BESS peak power output will differ for a new battery compared to a wear and tear induced cycled BESS. Hence, the design for controllers of Li-ion BESS, especially for their secondary and tertiary control must include aging parameter as an input, i.e., in this case its evolving peak power capability. Failure to do so might accelerate the overall aging process and may lead to fatality due to internal short circuits, especially when expected peak power can no longer be offered by the Li-ion BESSs, which shall happen particularly when the battery is nearing its end of life.

In existing control related studies in literature, Li-ion BESSs have been used extensively. For example, in [10] Li-ion BESS has been utilised to develop a test model for various grid related control studies and the battery model in this study was developed based on equivalent circuit model with SOC, C-rate and temperature as affecting parameters. A fuzzy logic based coupling of voltage and frequency control was established for BESS in [11]. The control design also considered battery's state of health (SOH) (an empirical model) to define control parameters, but considered capacity loss with SOC and DOD as affecting parameters. Distributed secondary control for a multi-BESS distribution system was proposed in [12] where the objective was to compensate deviations introduced by droop control and improve SOC balancing among multiple BESS units, without considering battery aging effects.

In existing literature, most of the studies related to battery modelling and control concentrate on long-term cost-based optimization techniques [13–18]. Some of the recent studies [19–21] have also utilised

battery aging models, i.e., their capacity degradation and resistance increase as aging parameters in the power system planning and control studies (predominantly considered as the tertiary control of microgrids). However, the literature focused on real-time design of BESSs' (e.g. Li-ion BESS) secondary control have not paid attention on their aging characteristics [22–25]. Further, according to authors' best knowledge, the peak power evolution of the Li-ion battery with aging has not been considered as an aging parameter in any of the studies presented in the previous literature. According to the authors' experience in analyzing field data from battery utilization, majority of the battery load in the secondary control has higher power requirement and DOD when compared to primary control. Therefore, it is important to include state of age (SOA), i.e., number of operational charge/discharge cycles completed is considered as SOA in this study and its corresponding peak power capability of the Li-ion BESS in the secondary control design.

Therefore, the scope of this paper is as follows,

1. Development of ANM architecture with  $QU$ -,  $PU$ - and  $P$ -controllers for managing available flexibilities of various distributed energy resources (DER), especially to generate control signals for the inverters of the Li-ion BESS and wind turbine generator (WTG) connected in the MV distribution network.
2. Primary focus has been on the development of Li-ion BESS  $P$ -control for ANM functionality related to active power dispatch control in which battery utilization in terms of age calculation in number of cycles of charge/discharge completed is also considered. In addition,  $P$ -control is designed to supply charge/discharge power within the battery's peak (active) power capability.
3. In order to develop  $P$ -control for ANM, accurate equivalent circuit battery model and peak power evolution model for Li-ion BESS has been developed in detail. These are needed in the battery management system (BMS) which considers battery SOC and age calculation as affecting parameters.
4. Understanding the Li-ion BESS inverter control interactions and its impacts to the distribution system by means of case studies in an existing smart grid (SSG) in Finland.

2. Study case – Sundom Smart Grid

Sundom Smart Grid (SSG) is represented in Fig. 1, which is a pilot living lab jointly created by ABB, Vaasan Sähköverkko (DSO), Elisa (ICT) and University of Vaasa [26]. Real-time voltage and current measurements (IEC 61850 standard) are sent from the MV distribution network, from all four feeders at HV/MV substation and three MV/LV substations comprising 20 measurement points in total. Measurements are sampled at 80 samples/cycle. In addition, active and reactive power, frequency, RMS voltages, currents etc. measurements are received by Generic Object Oriented Substation Event (GOOSE) messages. SSG doesn't have a Li-ion BESS at the moment, but for study purposes it is added on to the MV distribution network model as shown in Fig. 1.

3. Active network management scheme

Flexible distributed energy resources (DER) in the distribution network (at MV and LV level) plays an important role in providing flexibility services, e.g. as part of distribution network ANM scheme, in

the power system for local (DSO) and system-wide (TSO) needs in order to improve grid resiliency and DER (e.g. solar photovoltaic, PV) and electric vehicles (EVs) hosting capacity. These potential flexibility services consist of active (P) and reactive (Q) power control of flexible DER like controllable DG units, energy storages, controllable loads and EVs which are connected to the DSOs network. In this paper, ANM scheme is developed and studied for management of flexibilities in the MV distribution system, particularly focusing on the BESS control design. The developed scheme is then validated in an existing smart grid environment (Sundom Smart Grid). Fig. 2 represents the proposed ANM control architecture proposed in this paper.

BESSs integrated to the SSG MV bus are primarily designed to complement the stochastic nature of wind power generation, i.e., store excess wind power generation and discharge during reduced wind power generation. Secondly, they are used to provide technical ancillary services. These services include management of the voltages (according to grid codes) and improving RES penetration by complementing WTG power generation. Details on the grid codes specifications are explained in [27,28]. The following sub-section explains the development of

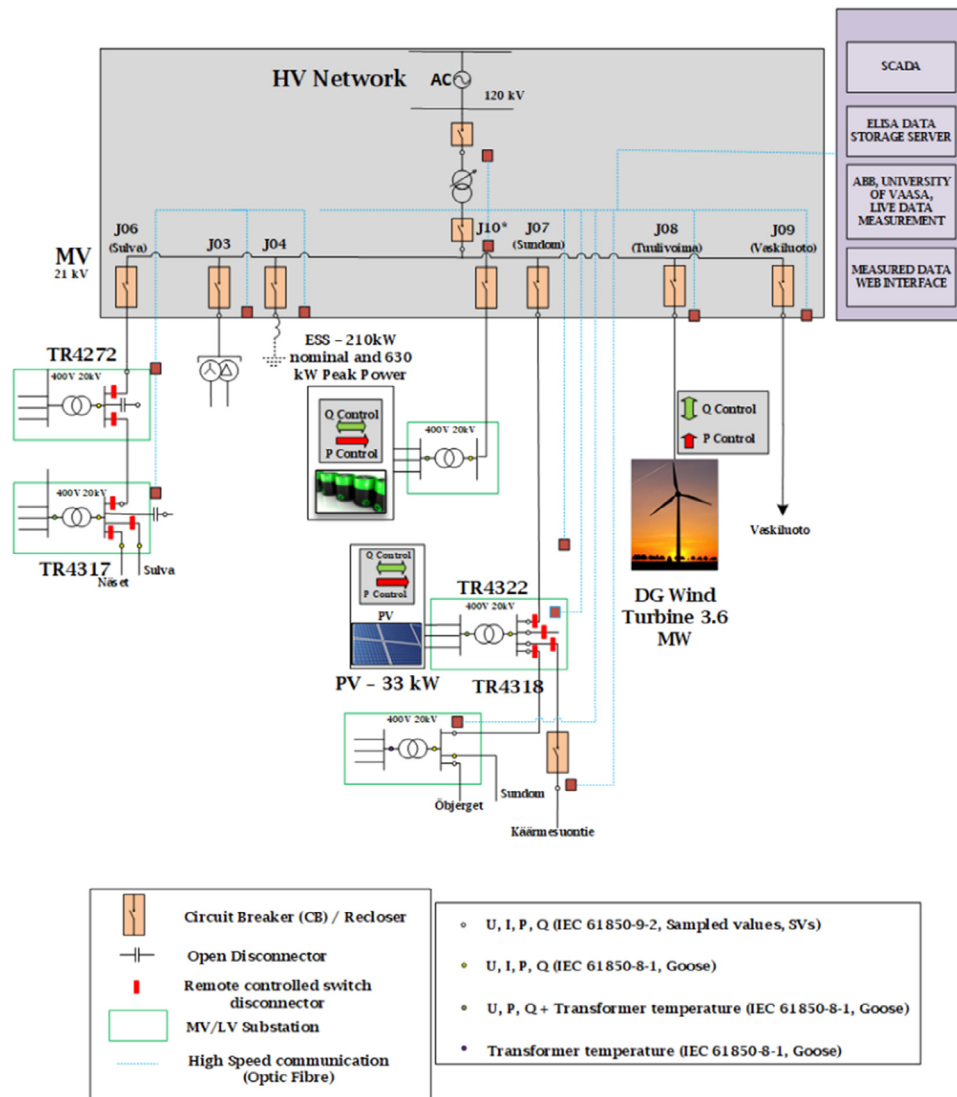


Fig. 1. Sundom Smart Grid network with Li-ion BESS.

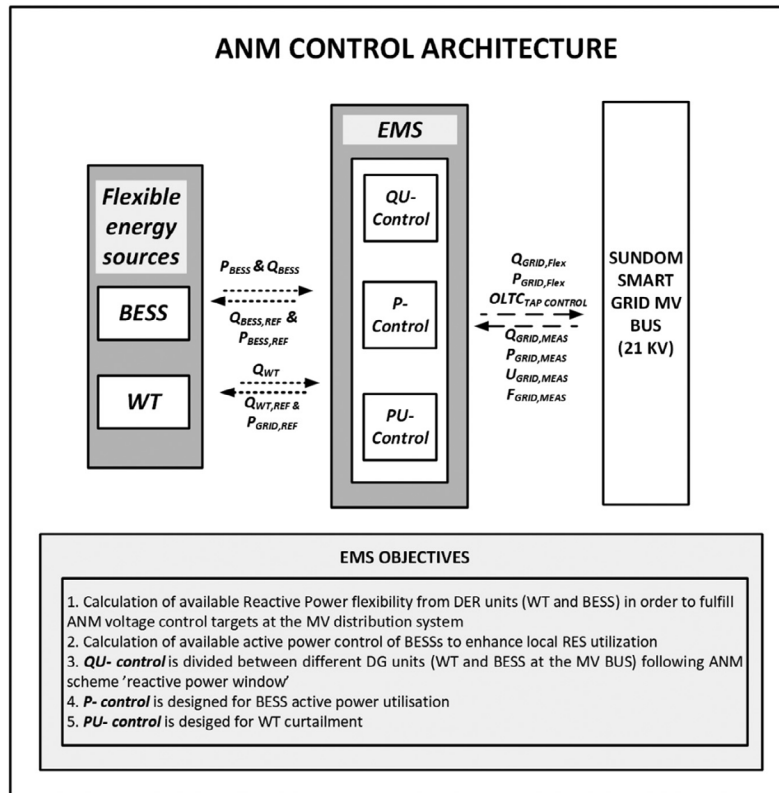


Fig. 2. ANM control architecture.

energy management system (EMS) for providing ANM services, followed battery characterisation and modelling in order to develop elaborate controllers for the Li-ion BESSs.

3.1. Energy management system

Energy management system (EMS) forms the most important block in the overall ANM scheme operations as they provide operational instructions to the flexible energy sources, i.e. in this case Li-ion BESS and WTG. EMS consists of various types of controllers (QU-, P- and PU-controllers) that shall aid in harnessing the flexibilities offered by WTG and Li-ion BESSs. Objective of EMS is to manage Li-ion BESS charge/discharge operations based on WTG active power generation and to keep the voltages in the MV bus within the limits specified by grid codes, by managing available flexibilities in the power system.

3.1.1. P-control

P-control of the EMS is designed for the active power dispatch of Li-ion BESS ( $P_{BESS}$ ), by controlling charge and discharge operations. The Li-ion BESS has been mostly used to complement wind power generation ( $P_{WT}$ ) compared to the power demand ( $P_{Load}$ ). The overall P-control

layout is shown in Fig. 3. First block, P-management system calculates the overall Li-ion BESS active power utilization possibility ( $P_{BESS, REF}$ ), by taking  $P_{Load}$ ,  $P_{WT}$  and SOC as inputs and generate  $P_{BESS, REF}$  as the output. Overall maximum active power discharge expected by the Li-ion BESS is defined by Eq. (1) and that of overall available power for charge is shown in Eq. (2). Eq. (3) generates  $P_{BESS, REF}$ , whose charge and discharge powers are defined by Eqs. (1) and (2) keeping the SOC of the battery within their threshold,  $SOC_{min}$  and  $SOC_{max}$ . In order to avoid minor deviations by the algorithm in Eq. (3), the charge functionality of the Li-ion BESS has been defined at the SOC lesser than or equal to  $SOC_{min}$ . The second block in Fig. 3 corresponds from converting  $P_{BESS, REF}$  (which corresponds to battery pack power containing  $N_s$  cells in series to that of  $N_p$  Cells in parallel) to  $P_{CELL, REF}$  (to active power reference of single cell in the pack) as defined in Eq. (4). This  $P_{CELL, REF}$  is provided as input to the next block called "Aging aware cell model".

$$P_{dis} = P_{Load} - P_{WT} \tag{1}$$

$$P_{chg} = P_{WT} - P_{Load} \tag{2}$$

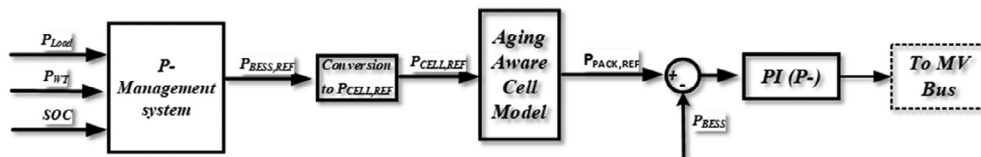


Fig. 3. P-control scheme.

$$P_{BESS,REF} = \begin{cases} P_{dis}; & (\text{if } SOC_{min} < SOC < SOC_{max}) > \text{and } P_{Load} > P_{WT} \\ P_{chg}; & (\text{if } SOC \leq SOC_{min} \text{ and } P_{WT} > P_{Load}); \\ 0 & \end{cases} \quad (3)$$

$$P_{CELL,REF} = P_{BESS,REF} / N_s * N_p \quad (4)$$

The design of aging aware Li-ion battery cell model (third block in Fig. 3) is shown in Fig. 4.  $P_{CELL,REF}$  is the reference power to address the power system needs per cell in the Li-ion battery pack. This block comprises of battery management system (BMS) which takes  $P_{CELL,REF}$  as input and calculates SOC by SOC estimation block and the number of completed battery charge/discharge cycles with the help of age calculator block. SOA refers to the calculation of cycle aging or number of completed cycles from the Li-ion battery's charge/discharge currents. Eq. (5) provides details on age calculator design, where the cell power is integrated over period of time and divided by the cell initial cell energy providing the Battery's SOA. SOC is estimated by using coulomb counting method [29], which is shown in Eq. (7).  $SOC_{initial}$  stands for the initial SOC of the cell,  $I_{cell}(t)$ , stands for cell current at time (t) and cell capacity refers to its maximum capacity in Ah. Coulomb Counting method provided the best accuracy with minimal computational effort in an environment where the measurement noise has been minimal, there by generating required inputs for BMS block.

$$SOA = \frac{\int P_{cell} dt}{Cell\ Energy} \quad (5)$$

$$P_{CELL,REF,age} = \begin{cases} PP; & (\text{if } P_{CELL,REF} > PP) \\ P_{CELL,REF}; & (\text{if } PP > P_{CELL,REF}); \end{cases} \quad (6)$$

$$SOC = SOC_{initial} + \frac{\int I_{cell}(t) dt}{Cell\ Capacity} \quad (7)$$

The BMS functionality houses cell peak power calculation, aging aware battery model and logic based algorithms to limit the cell charge/discharge power within the peak power (PP) limits defined by battery cell aging conditions. The details of the PP characterisation and battery cell modelling are explained in the following sections. The algorithm explaining battery cell power dispatch is as shown Eq. (6), thereby creating a new cell power reference  $P_{CELL,REF,age}$ , which now regulates battery cell power always within the PP of the battery cell. By modifying Eq. (4),  $P_{BESS,REF,age}$  is obtained which now provides the battery reference power to the PI-controller, which controls Li-ion BESSs. This  $P_{CELL,REF,age}$  is then provided as the reference to the PI-controller which regulated the Li-ion BESS active power output,  $P_{BESS}$ .

### 3.1.2. QU-control

Reactive power-voltage (QU)-control is one of the flexibility services which inverter-based DER can provide, in this study wind turbine generator (WTG) and Li-ion BESS. The limitation of active and reactive power contribution for both these inverter-based sources are explained in detail in [30]. The available reactive power support from WTG is

defined as  $Q_{wind,av}$ , and that of Li-ion BESS as  $Q_{BESS,av}$  QU-droop has been designed for QU-control as shown in Fig. 5. The droop controller has been designed to have a maximum reactive power ( $Q_{MAX}$ )  $\pm 2$  MVar. Based on the voltage fluctuation, the droop controller provides the required reactive power reference ( $Q_{ref}$ ). This  $Q_{ref}$  will be satisfied by both WT generator and Li-ion BESS, but prioritising the available reactive power from WT first. Eq. (8) defines the reactive power dispatch from WTG and if this reactive power doesn't satisfy  $Q_{ref}$ , then reactive power from the Li-ion BESS ( $Q_{BESS}$ ) will be utilised whose values are defined by Eq. (9).

$$Q_{wind} = \begin{cases} Q_{ref}; & (\text{if } Q_{ref} < Q_{wind,av}) \\ Q_{wind,av}; & (\text{if } Q_{ref} > Q_{wind,av}) \end{cases} \quad (8)$$

$$Q_{BESS} = \begin{cases} Q_{ref} - Q_{wind}; & (\text{if } Q_{ref} > Q_{wind,av}) \\ 0 & \end{cases} \quad (9)$$

### 3.1.3. PU-control

PU-management system is designed to keep in mind the curtailment of renewable energy generation, when the voltage limits exceed 1.05 pu in the MV bus. To manage the curtailment, PU-droop control presented in Fig. 6 is utilised for the wind power generation.

### 3.2. Battery characterisation and aging modelling

Widely adopted battery aging models are based on Arrhenius equation [31,32] that facilitates capturing degradation of battery cells as well due to ambient temperature as an affecting parameter. However, in this paper, we have assumed that the battery systems that are being utilised on the field for stationary grid applications has its own thermal management system that regulates the ambient temperature within a certain range (a constant value) preferred by the operator. Therefore, the aging model been built upon the assumption that the ambient temperature of the battery system shall remain constant when operated for grid applications, typically in room temperatures. It has to be noted that aging model developed in this paper has been based on accelerated aging tests that has been performed at room temperature. Therefore, Li-ion BESS that has been used for ANM applications in this paper, has been assumed to contain a battery thermal management system that is capable of regulating battery ambient temperature at room temperature. The focus of the aging model is to determine evolving PP characteristics due to cycle aging of Li-ion batteries, which has been embedded in control design of Li-ion BESSs.

This section explains the development of PP characterisation models (aging models) and equivalent circuit models utilised in previous section

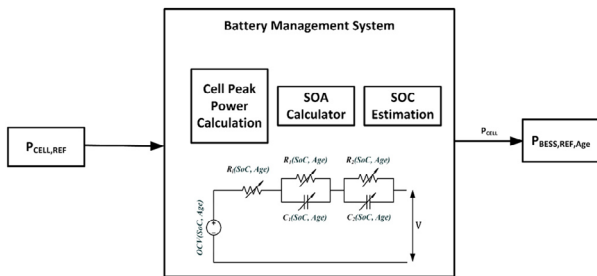


Fig. 4. Aging aware battery cell model.

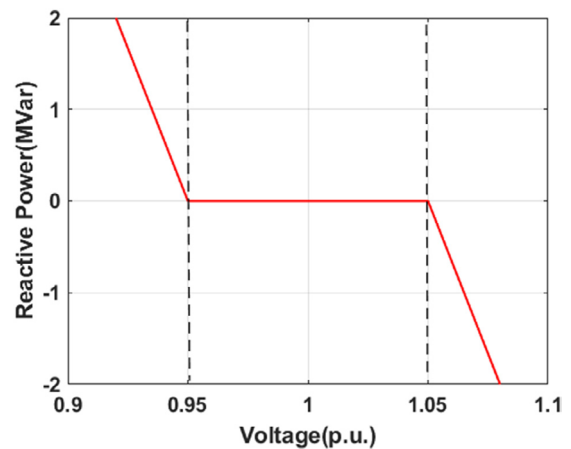


Fig. 5. Proposed QU-droop control.



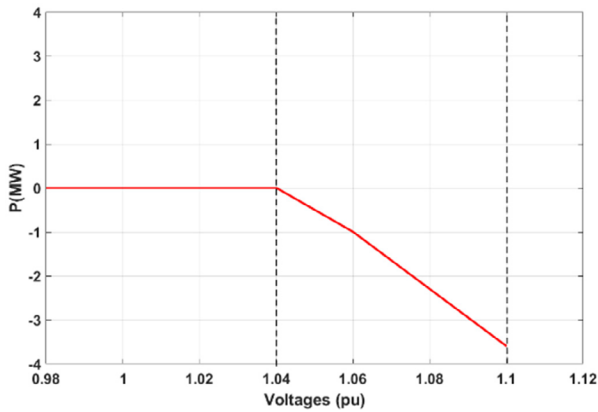


Fig. 6. PU-droop settings.

in the development of BMS which forms integral part of the P-controller development for ANM scheme.

### 3.2.1. Peak power characterisation model

Li-ion BESSs suffer performance degradation due to aging caused by phenomena's such as loss of cycleable lithium ions or active materials, growth of SEI (solid electrolyte interphase) layer, etc. [33], which in turn are a result of calendar and cyclic aging [34,35] of the battery cells. Due to aging, it has been observed that the Li-ion battery capacity reduces and its internal resistance increases, leading to reduction in PP discharge supported by Li-ion BESS. In this study, for development of aging aware Li-ion BESS controllers it is imperative to calculate the PP changes of the battery with aging and SOC. This model will be included in the cell PP calculation block of the BMS. The methodology to extract cell PP changes is explained below.

To calculate the PP changes of Li-ion battery, hybrid pulse power characterisation (HPPC) test based method will be utilised in this study. The HPPC test was performed at 25 °C. At the beginning the cell is fully discharged and fully charged 2 times to measure initial SOC and cell capacity. The HPPC test was performed at 25 °C, at every 10 % SOC step starting from 100 % SOC to 0 % SOC. Prior to pulse sequence, the fully charged were maintained at 100 % SOC and then rested for 1 h. The pulse power sequence consisted of 3C discharge for 10 s, rest at open circuit voltage (OCV) for 3 min, 3C charge for 10 s and rest at OCV for 3 min, followed by partial discharge of 10 % SOC and finally a rest of 1 h. This process was repeated till the battery cell reached 0 % SOC. The aging tests were conducted on the cells at 1C (CCCV charge/ CC discharge) cycling regime and 40 °C ambient temperature. Fig. 7 shows the current profile of the HPPC test performed and Fig. 8 depicts its

voltage response for a new cell (i.e. at 0 charge/discharge cycles).

The rationale behind using high current pulse of 3C for 10s has been majorly due to cell characteristics as mentioned by manufacturers' datasheet. This 8 Ah, NMC cell has a continuous maximum discharge C-rate of 2C and its pulsed maximum C-rate has been mentioned as 3C at 10s. Hence, while designing the high current pulse for HPPC test, we chose 3C rate at 10s. This pulse characteristics of the battery cell defines the highest possible current extraction from a particular cell and hence the PP characterisation model has been developed based on this method.

In order to calculate the PP discharge capability of the battery cell at this aging condition, its discharge resistance ( $R_{dis}$ ) at every high current pulse needs to be calculated.  $R_{dis}$  has been computed by Eq. (10), where  $\Delta V_{dis}$  and  $\Delta I_{dis}$  are evaluated from the respective voltage and current pulses (see the zoomed images in Figs. 7 and 8). The discharge PP of the Li-ion battery cell has been calculated by Eq. (11), where the OCV and  $V_{min}$  are evaluated from the voltage response of the HPPC test. By repeating this at every 10 % step SOC, the overall PP profile at different depths of discharge (DODs) at one particular aging condition. In the aging test performed in this study, the HPPC test profile has been run at the intervals of specified by number of cycles, i.e. at 0, 500, 800, 1200 and 1600 cycles. PP discharge of the Li-ion NMC battery cell has been evaluated with the help of HPPC test profiles obtained at different aging conditions. Fig. 9 depicts the PP output of the Li-ion cell at different aging levels, which were calculated with the help of Eqs. (10) and (11). Similarly, charge PPs were calculated with the help of Eqs. (12) and (13), which is represented by Fig. 10. A script was written in Matlab/Simulink interface for this purpose. The calculated PP values were then stored in a two-dimensional lookup table whose output will be controlled by SOC and aging parameters and then integrated to the BMS control block.

$$R_{dis} = \frac{\Delta V_{dis}}{\Delta I_{dis}} = \frac{V_{t1} - V_{t10}}{I_{t1} - I_{t10}} \quad (10)$$

$$PP_{Dis} = \frac{V_{min} * (OCV - V_{min})}{R_{dis}} \quad (11)$$

$$R_{cha} = \frac{\Delta V_{cha}}{\Delta I_{cha}} = \frac{V_{t1} - V_{t10}}{I_{t1} - I_{t10}} \quad (12)$$

$$PP_{cha} = \frac{V_{min} * (OCV - V_{max})}{R_{cha}} \quad (13)$$

### 3.2.2. Equivalent circuit battery model

Li-ion battery model capable of emulating its performance at different SOC and age intervals forms the second requirement for BMS design and development. For this purpose, second order equivalent circuit model (SOEC) based on Thevenin's circuit model [36] representing the dynamic response of the Lithium-ion battery including its

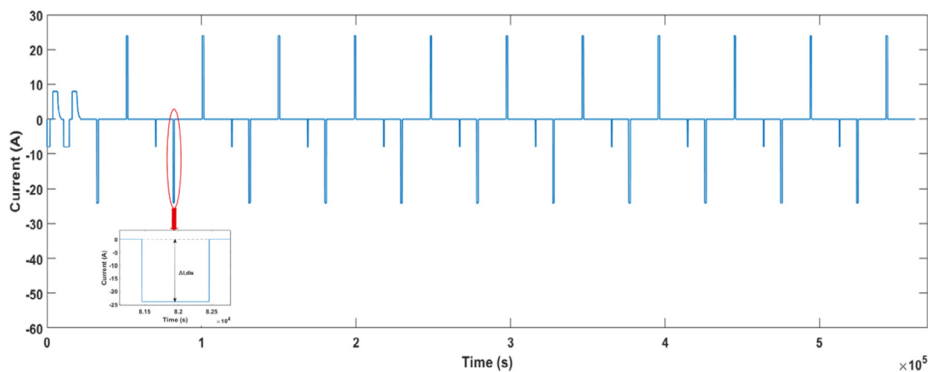


Fig. 7. HPPC current pulse profile.

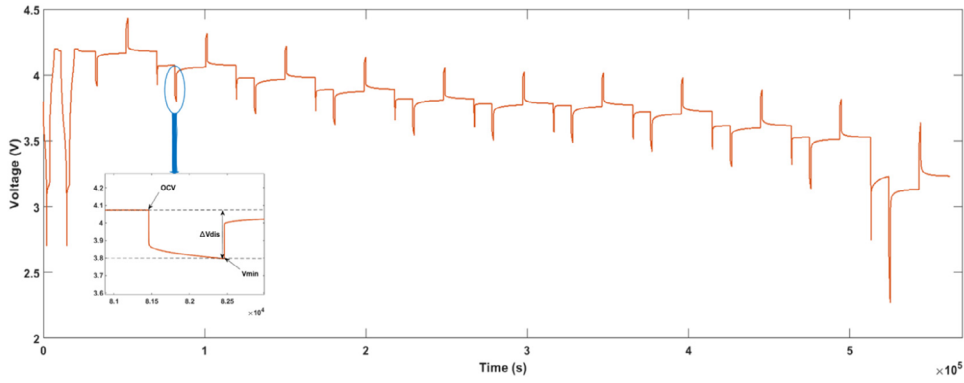


Fig. 8. HPPC voltage response.

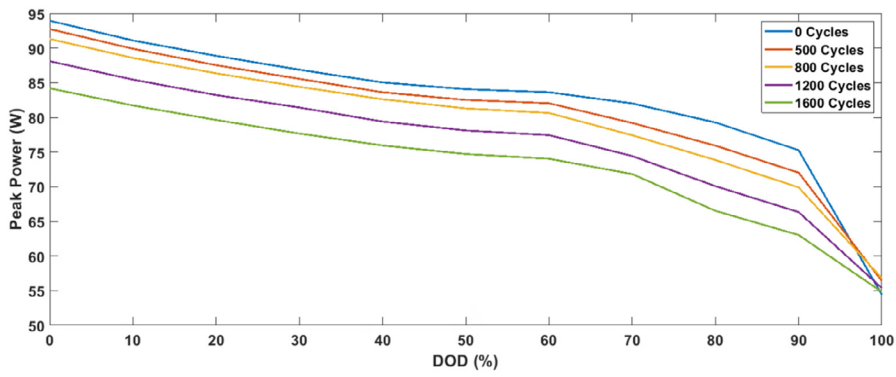


Fig. 9. Discharge peak power of Li-ion battery cell at different aging intervals.

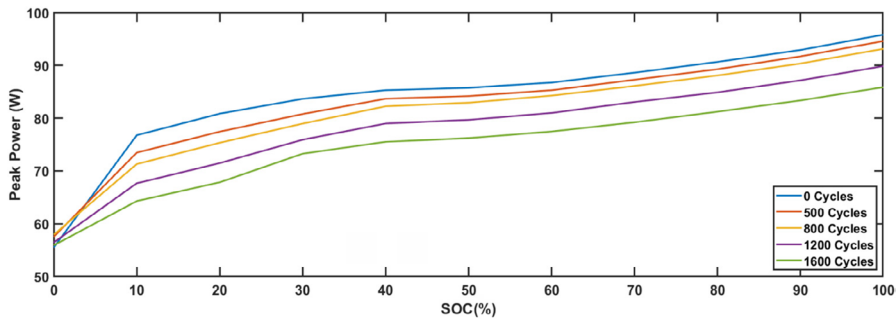


Fig. 10. Charge peak power of Li-ion battery cell at different aging intervals.

performance affecting parameters such as SOC, current-rate (C-rate) and battery age has been chosen. SOEC model denotes the processes occurring inside the battery cell such as charge transfer, diffusion and solid electrolyte interface (SEI) layer in the form of resistors and capacitors.

Fig. 11 shows the proposed dynamic SOEC for the NMC battery cell. OCV is modelled as an ideal voltage source, and the internal resistance is modelled as  $R_i$ . Two RC combinations are suggested for modelling Li-ion battery cell, so that the dynamic behaviour is modelled as  $R_1$ ,  $C_1$ ,  $R_2$  and  $C_2$ . The model parameters ( $OCV$ ,  $R_i$ ,  $R_1$ ,  $C_1$ ,  $R_2$  and  $C_2$ ) are obtained by HPPC tests [37], i.e. the HPPC tests were run at different SOC's (from 0% to 100% at 10% intervals) and at different aging intervals (i.e. at 0, 500, 800, 1200 and 1600 cycles of operation). The battery cell cycle aging test was performed at 1C charge/discharge rate and 25 °C [37]. A

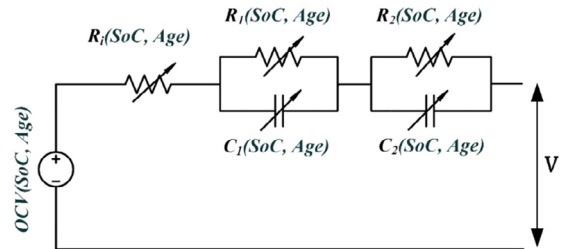


Fig. 11. Proposed second order equivalent circuit model

Matlab script was developed to calculate the measurements of SOEC parameters from HPPC test voltage response (Fig. 8) repeated for all the HPPC curves (i.e at all the aging intervals).

#### 4. Case study evaluation

SSG network (explained in Section 2) has been the power system under study to access the developed ANM scheme and its operations to manage MV voltage stability and boosting renewable power penetration by neat utilization of Li-ion BESSs. It is important to simulate the power system over a long period of time (hours to few days), in order to validate the effectiveness of the designed ANM secondary controllers ( $P$ -,  $QU$ -, and  $PU$ -controllers) and verify the setpoints provided to them. The control setpoints for Li-ion BESS have considered their aging as an affecting parameter in the control loop. Such large scale and longer time horizon power system simulations are computationally demanding and in order to perform accurate analysis, real-time simulations provide an avenue for quick and efficient approach. In the developed ANM scheme, the role of Li-ion BESS active power dispatch is to enhance wind power generation and reactive power flexibilities from WTG and Li-ion BESS is to manage MV distribution system voltage. The simulation models for these studies are developed in ePhasorSim platform by OPAL-RT, details of which are explained in [30].

The real-time simulation environment is presented in Fig. 12. The power system model of the modified SSG with Li-ion BESS in MV distribution system explained in Section 2. The power system model is based on the system parameters of the SSG provided by the local DSO and that of power generation details from WTG are based on the actual site data. The details of the power system model is similar to the

previous studies undertaken by the authors [30,38], except the change in battery model which includes their aging characteristics and the Li-ion BESS controllers whose power outputs are governed by their aging aware PP capability. It has to be noted that in this simulation model services from the on-line tap changer (OLTC) transformer wasn't available, reason being to study management of flexibilities from available sources. The major objective of this study is to analyse how battery aging affects its charge/discharge power output and their impact on ANM operations in SSG. Case studies are defined in the following section to conduct these analyses.

##### 4.1. Case 1: base case (non-active ANM scheme)

In this case, SSG is simulated without flexibilities from BESS and WTG operating in the MV distribution system, which is considered as the base case study. The simulations are performed for a period of 3 days with a time step of 1 s. This approach enables us to record the active and reactive power flows and the voltage measurements at various MV buses in the power system without any ANM being active. The SSG WTG is of permanent magnet synchronous generator (PMSG) type and connected to grid by full-power converter, thereby allowing it to absorb or inject reactive power to 100 % of its rated power. In this case, the reactive power control ( $QU$ -control) of the WTG is disabled, to record the original characteristics in the SSG without the operation of any flexible energy resources adhering to IEEE 1547–2018 [39] guidelines.

Fig. 13 shows the voltages at various MV buses whose values are seen to be between 0.94 and 0.95 p.u. The active power generation from WTG for 3 days is recorded in Fig. 14(a) and (b) provides details on reactive power contribution from WTG and Li-ion BESSs.

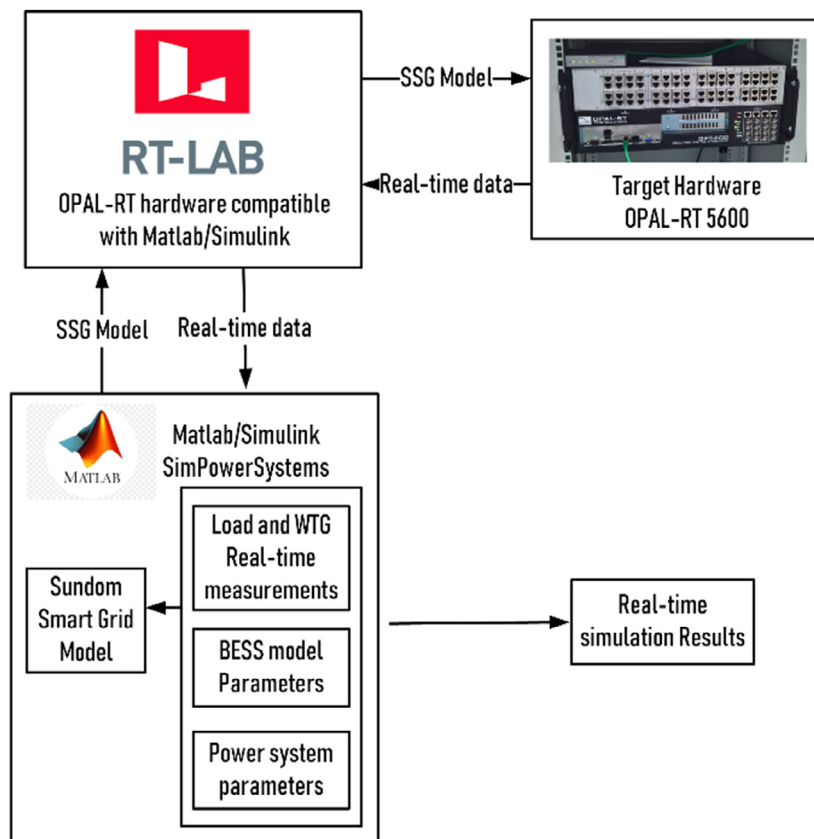


Fig. 12. Real-time simulation setup.

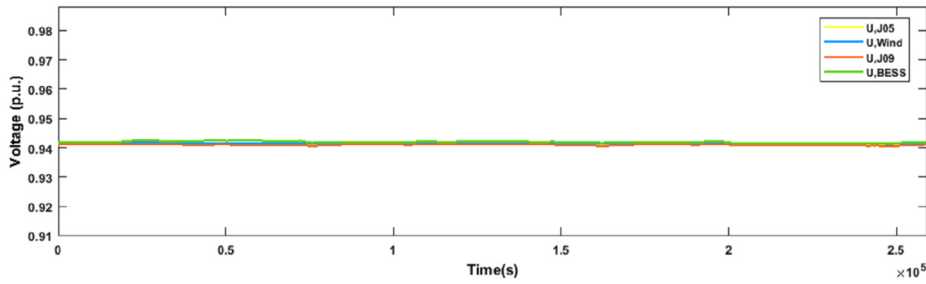


Fig. 13. MV bus voltages in SSG (Case 1 simulation results).

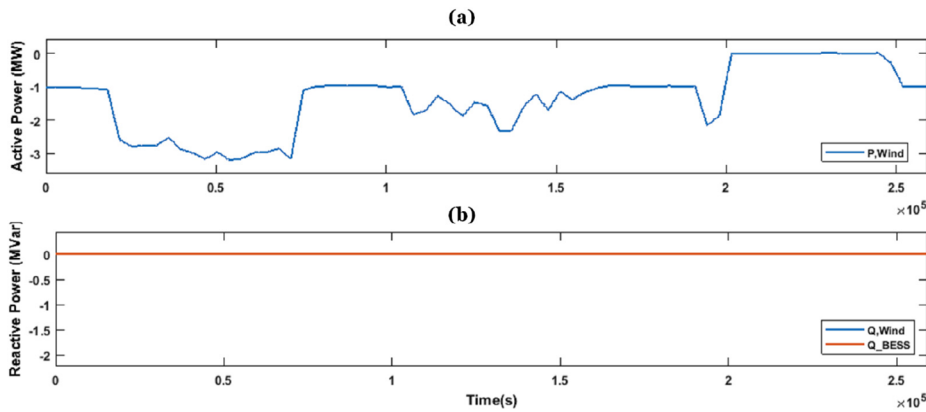


Fig. 14. (a) WTG power generation; (b) reactive power contribution from WTG and Li-ion BESS (Case 1 simulation results).

4.2. Case 2: active ANM scheme and new Li-ion BESS (at 0 cycles of operation)

The effect of proposed ANM scheme and the amount of power and energy a new Li-ion BESS (i.e. at 0 cycles of operation), can support the  $P_{BESS,REF}$  generated by Eq. (3). The QU-secondary control comes into effect along with the P-control to manage voltage regulation and complement wind power generation. Fig. 14(a) in previous case represents the active power generation of WTG, which is unchanged. Fig. 15 shows the amount of reactive power services offered by QU-control which is satisfied by  $Q_{Wind}$  alone. Quite much (closer to 1.5 MVar) reactive power feeding is required for voltage compensation, this is due to the fact that WTG is almost directly connected to the HV/MV substation MV bus (which makes it a very stiff connection point from voltage effect point of view). The QU-controller does not need reactive power services from Li-ion BESS in this case. Based on the QU-controller's operation, the voltages at various buses of MV distribution system are seen to improve (0.95 p.u. and above) and fall within the purview of conditions provided by grid codes as described in Fig. 16. Hence, proposed ANM scheme satisfies its first objective.

Fig. 17 represents the Li-ion BESS active power charge and discharge

characteristics. The blue line in in Fig. 17 corresponds to the overall available charge and discharge power ( $P_{BESS,REF}$ ) based on Eq. (3) and that of red line corresponds to the actual charge and discharge power ( $P_{BESS}$ ), dispatched to and from the Li-ion BESS. In this case, the Li-ion battery is considered as new system without any cycles of charge and discharge. Comparing  $P_{BESS,REF}$  and  $P_{BESS}$  it is evident that the P-control (which considers SOC and age as its input) works as desired by keeping the battery charge and discharge power within the maximum possible threshold. It can also be observed that the  $P_{BESS,REF}$  has lower power and lower DODs (i.e. the cycles in the middle of Fig. 6) and can be entirely satisfied by  $P_{BESS}$ .

Fig. 18(a) represents the SOC of Li-ion BESS which as committed, cycles between 10 % and 90 % SOC and Fig. 18(b) shows the total number of charge/discharge cycles accumulated in a period of 3 days. The major objective of this study was to validate the design and operation of secondary controllers (QU- and P-controllers), which allows enforcement of the ANM scheme which has now been verified for a new Li-ion BESS.

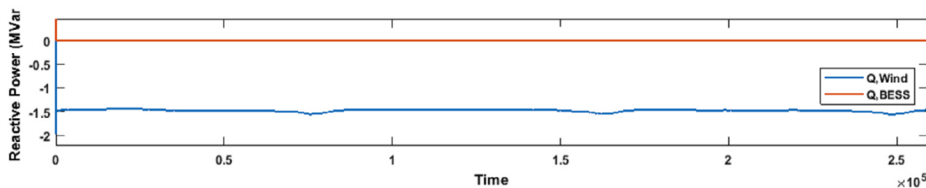


Fig. 15. Reactive power contribution from WTG and Li-ion BESS (Case 2 simulation results).

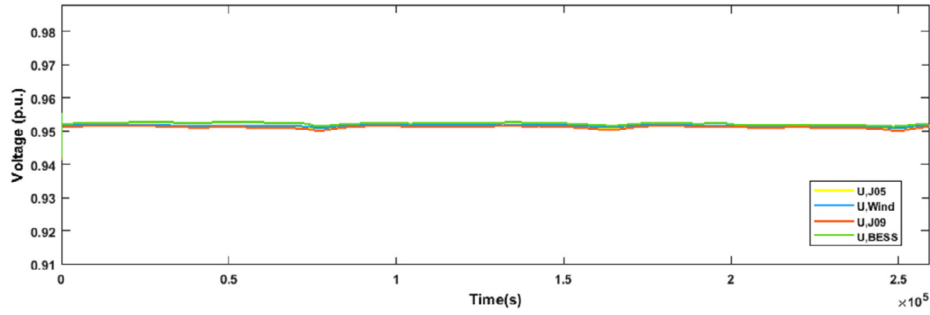


Fig. 16. MV bus voltages in SSG (Case 2 simulation results).

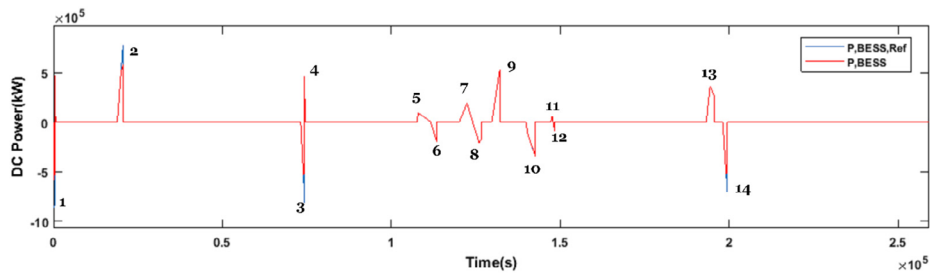


Fig. 17. Li-ion BESS active power reference and actual power dispatch for new cells (Case 2 simulation results).

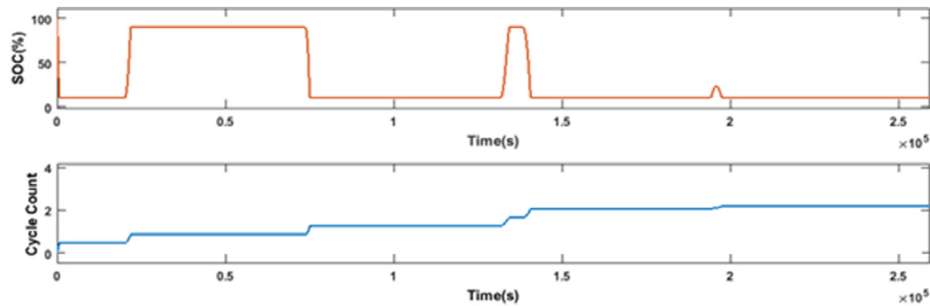


Fig. 18. (a) Li-ion BESS SOC and (b) Battery cycle count of operation (Case 2 simulation results)

4.3. Case 3: active ANM scheme and used Li-ion BESS (after 1200 cycles of operation)

Objective of this case to understand the impact of Li-ion BESS aging on its performance, particularly the peak load it can support. In this simulation case, the Li-ion BESS has been considered to have undergone considerable aging, i.e. about 1200 cycles of charge/discharge operations.

Fig. 19 shows the amount of reactive power services offered by  $QU$ -

control, which is satisfied by  $Q_{Wind}$  alone, even in this case with aged Li-ion BESS. The voltages in the MV distribution system are seen to be within the threshold values defined by grid codes as seen in Fig. 20. However, the active power characteristics which is based on the aging aware  $P$ -control of Li-ion BESS provides a different picture on actual active power discharge. Compared to Fig. 17, in Fig. 21 the actual peak active power of the Li-ion BESS has been modified based on the age related controller. The PP outputs are observed to be lesser in magnitude where the cycles are deep with higher DOD and  $P_{BESS,REF}$ . Table I

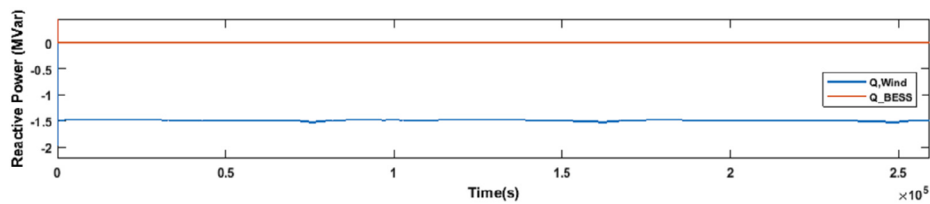


Fig. 19. Reactive power contribution of WTG and Li-ion BESS (Case 3 simulation results).

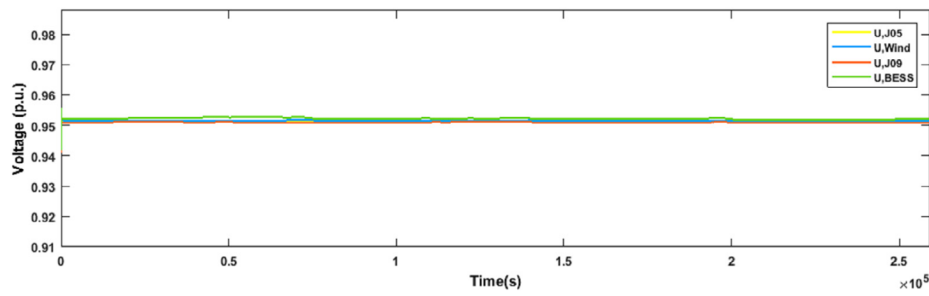


Fig. 20. MV bus voltages (Case 3 simulation results).

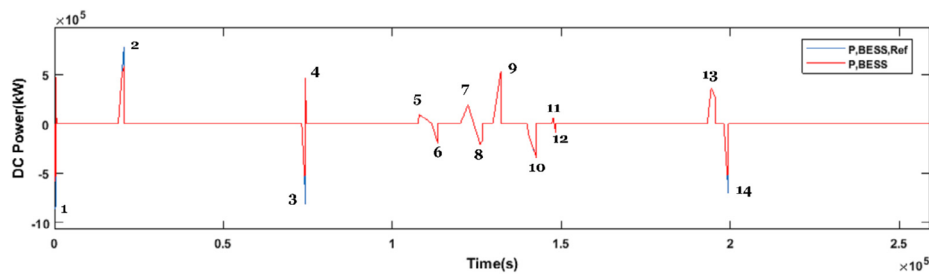


Fig. 21. Li-ion BESS active power reference and actual power dispatch for aged cells (Case 3 simulation results).

provides comparison in active power changes of Li-ion BESS, which shows that cycles 1,2,3 and 14 which has higher power levels compared to other pulses and  $P_{BESS,REF}$  are seen to have a dip in the PP dispatch. This is due to the  $P$ -control characteristics, which tends to lower PP of Li-ion BESS with aging (Table 1).

## 5. Conclusion

The application of Li-ion BESS in this work has been for active network management (ANM) of distribution grids and to improve renewable energy penetration and utilization in smart grids. The ANM scheme is designed to maintain the distribution system stable within the limits defined by the grid codes by tapping the flexibility services (both active and reactive power related flexibility services) offered by flexible energy sources.

However, the Li-ion battery tends to age with usage causing degradation in their performance characteristics that in turn lead to reduction in their PP charge/discharge capability. This change in PP provisioning of the Li-ion BESS needs to be captured in the secondary control layer of

the active network management scheme, as the power dispatch in this control layer are typically of higher DODs and power ratings compared to the primary control layer.

For that reason, an age (for Li-ion BESS) influenced adaptive  $P$ -control layer (secondary control layer) in the ANM has been proposed in this study, which considers the operational battery SOA (number of completed charge/discharge cycles) as input to the control system. The battery management system (within  $P$ -control layer), consists of an accurate second order equivalent circuit Li-ion battery model that generates accurate voltage, power and energy characteristics of the Li-ion battery cell, considering battery SOC and SOH as its affecting parameters. The BMS also hosted the PP calculation algorithm, which provides the PP reference of the battery cell at all instances of SOH. The overall objective of  $P$ -control layer has been to generate the Li-ion BESS active power reference which is within the threshold of battery charge/discharge PP capability, which is defined by its SOH and provided by PP calculation algorithm. Thereby, solving the problem of managing the battery charge/discharge operations always within the threshold of their peak active power performance.

Based on the simulation studies results, it can be noted that the designed EMS controllers acted as required to provide flexibilities to manage system voltages within the threshold defined by grid codes. Despite aging aware control of Li-ion BESS using  $P$ -controller of the EMS, it can be observed that the voltages were maintained within the threshold defined by grid codes by the  $QU$ -controller. It can also be observed that the cycles with higher power discharge and DOD showed the influence of battery aging by reduced power dispatch with aging and the cycles with lower power discharge and DODs had no impacts of battery aging on their power dispatch.

## 6. Future studies

Li-ion battery aging is an irreversible phenomenon which leads to permanent degradation of its performance parameters, i.e., its capacity and power dispatch characteristics in particular. These degradation parameters must be considered, especially while developing battery controllers and various other technical studies involving Li-ion batteries

Table 1

Li-ion BESS PP dispatch comparison.

Cycle number	Case 2: new Li-ion BESS active power dispatch (kW)	Case 3: aged Li-ion BESS active power dispatch (kW)
1	-631,4	-559,2
2	603,7	561,8
3	-556,4	-519,7
4	438,5	438,5
5	174,6	174,6
6	-282,7	-282,7
7	264,1	264,1
8	-310,4	-310,4
9	478,7	478,7
10	-345,9	-345,9
11	44,4	44,4
12	-52,1	-52,1
13	183,7	183,7
14	-537,1	-515,9

such as techno-economic analyses, battery sizing and determining their optimum location in the power system. Therefore, the future research directions are multi-fold in nature. The main ones are listed below:

1. Impact of battery aging shall be studied in detail by development of aging aware adaptive controllers in their secondary and tertiary control layers, for various applications that require higher power charging and discharging at higher DODs. The comparison between adaptive and non-adaptive  $P$ -control on the aging rate and safety aspects of Li-ion BESSs needs to be analysed experimentally, which is of interest for future research.
2. The size and location in the power grid of Li-ion BESS in a power system is highly influenced by its technical performance and aging characteristics [40–42]. Therefore, determination of optimal size and location of Li-ion BESS based on their performance characteristics, including its aging characteristics has been considered for future research.
3. Due to the changing PP characteristics of Li-ion BESSs due to aging, techno-economic analysis of Li-ion BESS participation has to include their aging characteristics and this forms another interest towards future studies, where scheduling of Li-ion BESSs shall drastically change with aging.

#### CRedit authorship contribution statement

**Chethan Parthasarathy:** Conceptualization, Methodology, Software, Validation, Formal analysis, Investigation, Writing – original draft, Visualization. **Hannu Laaksonen:** Writing – review & editing, Supervision, Project administration, Funding acquisition. **Eduardo Redondo-Iglesias:** Writing – review & editing, Methodology, Validation. **Serge Pelissier:** Writing – review & editing, Methodology, Validation.

#### Declaration of competing interest

The authors declare that they have no known competing financial interests or personal relationships that could have appeared to influence the work reported in this paper.

#### Data availability

The data that has been used is confidential.

#### References

- [1] Y. Yang, S. Bremner, C. Menictas, M. Kay, Battery energy storage system size determination in renewable energy systems: a review, *Renew. Sust. Energ. Rev.* 91 (March) (Aug. 2018) 109–125.
- [2] S. Bin Wali, et al., Battery storage systems integrated renewable energy sources: a biblio metric analysis towards future directions, *J. Energy Storage* 35 (November 2020) (2021) 102296.
- [3] O. Palizban, K. Kauhaniemi, J.M. Guerrero, Microgrids in active network management - part I: hierarchical control, energy storage, virtual power plants, and market participation, *Renew. Sust. Energ. Rev.* 36 (2014) 428–439.
- [4] O. Palizban, K. Kauhaniemi, J.M. Guerrero, Microgrids in active network management - part II: system operation, power quality and protection, *Renew. Sust. Energ. Rev.* 36 (2014) 440–451.
- [5] G. Rancilio, A. Rossi, C. Di Profio, M. Alborghetti, A. Galliani, M. Merlo, Grid-scale BESS for ancillary services provision: SoC restoration strategies, *Appl. Sci.* 10 (12) (2020) 1–18.
- [6] M. Mahesh, D.V. Bhaskar, T.N. Reddy, P. Sanjeevikumar, J.B. Holm-Nielsen, Evaluation of ancillary services in distributed grid using large-scale battery energy storage systems, *IET Renew. Power Gener.* 14 (19) (2020) 4216–4222.
- [7] C. Parthasarathy K. Sirviö H. Hafezi H. Laaksonen, “Modelling Battery Energy Storage Systems for Active Network Management – Coordinated Control Design and Validation,” *IET Renew. Power Gener.*, pp. 1–10.
- [8] D. Choi, et al., Li-ion battery technology for grid application, *J. Power Sources* 511 (July) (2021), 230419.
- [9] H.C. Hesse, M. Schimpfe, D. Kucevic, A. Jossen, Lithium-ion battery storage for the grid - a review of stationary battery storage system design tailored for applications in modern power grids vol. 10, no. 12, 2017.
- [10] L. Cai, N.F. Thornhill, S. Kuenzel, B.C. Pal, A test model of a power grid with battery energy storage and wide-area monitoring, *IEEE Trans. Power Syst.* 34 (1) (2019) 380–390.
- [11] W. Liu, Y. Xu, X. Feng, Y. Wang, Optimal fuzzy logic control of energy storage systems for V/f support in distribution networks considering battery degradation, *Int. J. Electr. Power Energy Syst.* 139 (July) (2021) 2022.
- [12] A.M. Shotorbani, B. Mohammadi-Ivatloo, L. Wang, S. Ghassem-Zadeh, S. H. Hosseini, Distributed secondary control of battery energy storage systems in a stand-alone microgrid, *IET Gener. Transm. Distrib.* 12 (17) (Sep. 2018) 3944–3953.
- [13] L. Zhang, et al., Improved cycle aging cost model for battery energy storage systems considering more accurate battery life degradation, *IEEE Access* 10 (2022) 297–307.
- [14] K. Liu, et al., Electrochemical modeling and parameterization towards control-oriented management of lithium-ion batteries, *Control. Eng. Pract.* 124 (Jul. 2022), 105176.
- [15] X. Jin, Aging-aware optimal charging strategy for lithium-ion batteries: considering aging status and electro-thermal-aging dynamics, *Electrochim. Acta* 407 (Mar. 2022), 139651.
- [16] Y.R. Lee, H.J. Kim, M.K. Kim, Optimal operation scheduling considering cycle aging of battery energy storage systems on stochastic unit commitments in microgrids, *Energies* 14 (2) (Jan. 2021) 470.
- [17] M. Abogaleela, K. Kopsidas, Battery energy storage degradation impact on network reliability and wind energy curtailments, in: 2019 IEEE Milan PowerTech 2019, PowerTech, 2019, pp. 1–6.
- [18] D. Kirli, A. Kiprakis, Techno-economic potential of battery energy storage systems in frequency response and balancing mechanism actions, *J. Eng.* 2020 (9) (2020) 774–782.
- [19] Y. Li, et al., Design of minimum cost degradation-conscious lithium-ion battery energy storage system to achieve renewable power dispatchability, *Appl. Energy* 260 (November 2019) (2020) 114282.
- [20] Y. Li, M. Vilathgamuwa, S.S. Choi, T.W. Farrell, N.T. Tran, J. Teague, Development of a degradation-conscious physics-based lithium-ion battery model for use in power system planning studies, *Appl. Energy* 248 (May) (2019) 512–525.
- [21] J.M. Reniers, G. Mulder, S. Ober-Blöbaum, D.A. Howey, Improving optimal control of grid-connected lithium-ion batteries through more accurate battery and degradation modelling, *J. Power Sources* 379 (January) (2018) 91–102.
- [22] A. Allahham, D. Greenwood, C. Patsios, P. Taylor, Adaptive receding horizon control for battery energy storage management with age-and-operation-dependent efficiency and degradation, *Electr. Power Syst. Res.* 209 (Aug. 2022), 107936.
- [23] D.J. Ryan, R. Razzaghi, H.D. Torresan, A. Karimi, B. Bahrani, Grid-supporting battery energy storage systems in islanded microgrids: a data-driven control approach, *IEEE Trans. Sustain. Energy* 12 (2) (Apr. 2021) 834–846.
- [24] R. Zhao, R.D. Lorenz, T.M. Jahns, Lithium-ion battery rate-of-degradation modeling for real-time battery degradation control during EV drive Cycle, in: 2018 IEEE Energy Convers. Congr. Expo. ECCE2018, Dec. 2018, pp. 2127–2134.
- [25] N. Tian, H. Fang, Y. Wang, Real-time optimal lithium-ion battery charging based on explicit model predictive control, *IEEE Trans. Ind. Informa.* 17 (2) (Feb. 2021) 1318–1330.
- [26] H. Laaksonen, Future-proof islanding detection schemes in Sundom smart grid, *Cired* 2017 (June) (2017) 12–15.
- [27] H. Laaksonen, C. Parthasarathy, H. Khajeh, M. Shafie-Khah, N. Hatzigiorgiou, Flexibility services provision by frequency-dependent control of on-load tap-changer and distributed energy resources, *IEEE Access* 9 (2021) 45587–45599.
- [28] C. Parthasarathy H. Laaksonen, “Control and Co-ordination of Flexibilities for Active Network Management in Smart Grids – Li-ion BESS Fast Charging Case.”.
- [29] J. Meng, G. Luo, M. Ricco, M. Swierczynski, D.-I. Stroe, R. Teodorescu, Overview of lithium-ion battery modeling methods for state-of-charge estimation in electrical vehicles, *Appl. Sci.* 8 (5) (2018) 659.
- [30] C. Parthasarathy, K. Sirviö, H. Hafezi, H. Laaksonen, Modelling battery energy storage systems for active network management—coordinated control design and validation, *IET Renew. Power Gener.* 15 (11) (Aug. 2021) 2426–2437.
- [31] G. Kucinskis, M. Bozorgchenani, M. Feinauer, M. Kasper, M. Wohlfahrt-Mehrens, T. Waldmann, Arrhenius plots for Li-ion battery ageing as a function of temperature, C-rate, and state of health – an experimental study, *J. Power Sources* 549 (September) (2022), 232129.
- [32] J. Teh, Uncertainty analysis of transmission line end-of-life failure model for bulk electric system reliability studies, *IEEE Trans. Reliab.* 67 (3) (2018) 1261–1268.
- [33] B. Xu, A. Oudalov, A. Ulbig, G. Andersson, D.S. Kirschen, Modeling of lithium-ion battery degradation for cell life assessment, *IEEE Trans. Smart Grid* 9 (2) (2018) 1131–1140.
- [34] R. Xiong, Y. Pan, W. Shen, H. Li, F. Sun, Lithium-ion battery aging mechanisms and diagnosis method for automotive applications: recent advances and perspectives, *Renew. Sust. Energ. Rev.* 131 (Oct. 2020), 110048.
- [35] X. Lai, et al., Critical review of life cycle assessment of lithium-ion batteries for electric vehicles: a lifespan perspective, *eTransportation* 12 (May 2022), 100169.
- [36] S. Nejad, D.T. Gladwin, D.A. Stone, A systematic review of lumped-parameter equivalent circuit models for real-time estimation of lithium-ion battery states, *J. Power Sources* 316 (2016) 183–196.
- [37] R. Arunachala, C. Parthasarathy, A. Jossen, J. Garche, Inhomogeneities in large format lithium ion cells: a study by battery modelling approach, *ECS Trans.* 73 (1) (2016) 201–212.
- [38] C. Parthasarathy, H. Hafezi, H. Laaksonen, Integration and control of lithium-ion BESSs for active network management in smart grids: Sundom smart grid backup feeding case, *Electr. Eng.* 104 (2) (Apr. 2022) 539–553.

*C. Parthasarathy et al.*

*Journal of Energy Storage 57 (2023) 106268*

- [39] IEEE Standard Association, IEEE Std. 1547-2018. Standard for Interconnection And Interoperability of Distributed Energy Resources With Associated Electric Power Systems Interfaces, 2018.
- [40] H. Alsharif, M. Jalili, K.N. Hasan, Power system frequency stability using optimal sizing and placement of battery energy storage system under uncertainty, *J. Energy Storage* 50 (April) (2022), 104610.
- [41] Y. Yang, S. Bremner, C. Menictas, M. Kay, Battery energy storage system size determination in renewable energy systems: a review, *Renew. Sust. Energ. Rev.* 91 (January) (2018) 109–125.
- [42] M.K. Metwaly, J. Teh, Optimum network ageing and battery sizing for improved wind penetration and reliability, *IEEE Access* 8 (2020) 118603–118611.



# Aging Characteristics Consideration in Adaptive Control Design of Grid-Scale Lithium-ion battery

Chethan Parthasarathy, Hannu Laaksonen  
Flexible Energy Resources  
School of Technology and Innovations University of Vaasa,  
Finland  
[chethan.parthasarathy@uwasa.fi](mailto:chethan.parthasarathy@uwasa.fi)

Ilari Alaperä  
Business Development Manager  
Fortum Spring  
Helsinki  
Finland

**Abstract**—Lithium-ion battery energy storage systems (Li-ion BESS) have been extensively used for frequency containment reserves for disturbances (FCR-D) and frequency containment reserves for normal operations (FCR-N) in Finland. Typically, for both these applications, active power-frequency ( $Pf$ )-droop curve defines the Li-ion BESS active power dispatch to the power grid. However, Li-ion BESS's performance is affected due to aging resulting in the reduction of its peak power capability and capacity degradation. These issues need to be considered when defining  $Pf$ -droop controller curves. Therefore, adaptive  $Pf$ -droop control methodology should be developed which considers battery aging characteristics. This will ensure Li-ion BESS to function within its safe operating margins. It also provides the possibility to automatically modify Li-ion BESS control settings and flexibility services provision capability based on battery performance and aging. In this paper, detailed analysis will be performed on the cycling of real-life Li-ion BESS which is installed and operated in Finland in order to understand the cycle aging process when they provide services to FCR-N markets. In addition, an enhanced, simple adaptive  $Pf$ -droop control curve has been proposed by considering the effect of Li-ion battery aging. Effectiveness and the impact of the proposed adaptive droop control curves will be validated by means of case studies

**Keywords**— Lithium-ion batteries; energy storage systems; adaptive droop control; battery aging;

## I. INTRODUCTION

Tackling climate change issues has led to rapidly increasing penetration of renewable energy sources (RES) in power systems. One of the major issues in RES integration arises from their intermittency and various ways to mitigate the variability forms a wide range of research topic. BESSs have shown immense capability to address challenges arising due to the RES intermittency in the medium and low voltage (MV and LV) electricity distribution systems, particularly their ability in tendering multiple flexibility / technical ancillary services such as voltage and frequency regulation, black start, load levelling and peak shaving [1].

Recently, Li-ion BESSs have become the forefront choice for utilization in land based grid support applications, by acting as a flexible energy resource (FER) which is capable of providing multiple flexibility services in the distribution system [2]. Most particularly, their appropriate role in short term frequency control applications. In order to enable smooth operation of BESSs in the distribution networks for FCR-N/FCR-D applications, well-co-ordinated automatic BESS controls have to be established in the form of active network management (ANM) schemes. ANM control schemes are typically used to manage voltage or thermal limits related congestion in the distribution network by

utilising existing FER, like BESS or RES, reactive and active power ( $Q$  and  $P$ ) control capabilities together with coordinated control of other options such as transformer on-load-tap-changers [3].

In order to extract FCR-N related services, typical active power-frequency ( $Pf$ )-droop based controllers (Fig.1) are often used for Li-ion BESS control [4]. Various types of droop controllers have been proposed in the existing literature considering Li-ion BESSs as a solution for system-wide frequency control as well as local distribution network voltage control. Decentralised adaptive droop control tracking the variable virtual resistance was utilised for the BESSs in [5], with the capability of managing bus voltage and load power dispatch keeping the BESS state of charge (SOC) in balance.

Dynamic SOC balance control strategy with an adaptive droop control relying on SOC of the ESSs was established in [6]. Adaptive droop controller for fuel cell-BESS hybrid energy storage system (ESS) was proposed in [7] to minimise the BESS utilisation for frequency support application. The proposed droop controller was for the hybrid ESS as a whole, considering the fuel cell as the primary source, which is complemented by the BESSs, which leads to the decreased cycling and increased lifetime of BESSs. In [8], variable/adaptive incremental cost-voltage droop controllers were proposed based in order to reduce the total battery degradation cost in islanded DC microgrids.

Performance of Li-ion BESSs are affected by various parameters such as depth of discharge, SOC, temperature and aging [9]. Further, performance degradation due to aging, mainly leads to change in battery capacity and their peak power capability. Changes in the peak power capability leads to reduced peak power outputs from Li-ion BESSs, which has not been considered previously in the available droop controller design based literature. Failure to do so might accelerate the overall aging process and may lead to fatality due to internal short circuits, especially when expected peak power can no longer be offered by the Li-ion BESSs, which shall happen particularly when the battery is nearing its end of life.

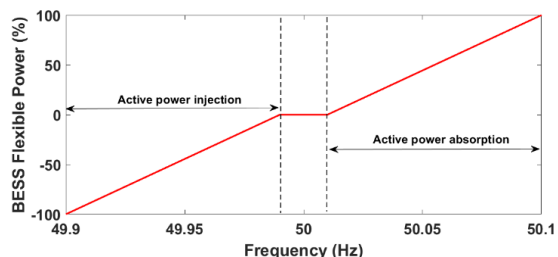


Fig 1. Typical  $pf$  droop curve for BESS participation in FCR-N market

One of the objectives of this study will be to analyse the impact of load requirements due to FCR-N services on the Li-ion BESS in Finland, mainly in terms understanding their cycling pattern that leads to battery degradation. Followed by proposing an adaptive *Pf*-droop curve, which enables tracking changes in their aging by including the peak power dispatch capability, by keeping power dispatch within its safe operating limits. Therefore, in this paper,

1. Field measurements of Li-ion BESS usage for FCR-N application are used to understand cycling depth and total number of cycles used by means of rainflow counting algorithm [10]
2. Aging model is based on the details provided by manufacturer's datasheet, which describes cycling degradation characteristics of the Li-ion battery at different depth of discharge (DODs)
3. Based on the cycling characteristics of Li-ion BESS in the field and peak power capability decrease due to aging in the battery cells, simple adaptive droop curves have been proposed for better utilisation of Li-ion BESSs for FCR-N and FCR-D applications and the impact such curves on Li-ion BESS operations are analysed

## II. BATTERY FIELD CYCLING ANALYSIS

Battery cell accelerated aging tests in the laboratory are generally performed at higher temperatures and full equivalent cycles of charging and discharging at different current rates in order to observe aging parameters such as internal resistance and capacity loss [11]. However, when utilised in the field, Li-ion BESSs have different depths of discharges at different cycling depths, typically most of the cycle being micro-cycles (very low DODs). In that case, it becomes difficult to predict the Li-ion BESS aging characteristics in the field. Fig. 2 represents the SOC variations of Li-ion BESSs installed in Finland, when utilised for FCR-N services. It can be observed that the cycling characteristics are highly uneven constituting mainly of micro-cycles with very low depths of discharges. Based on the literature, rainflow counting technique [12], which is mainly used in reliability analysis provides an accurate estimate of the overall number of cycles at different DODs, thereby providing an avenue to understand the amount of degradation a particular type of battery has undergone in the field usage.

Fig. 3 shows the results from the rainflow counting algorithms unpacking the information on the cycling characteristics shown in Fig 2. Therefore, from the results, information on total number of micro-cycles, their DODs and occurrences at which particular SOC's shall be gathered. Based on the observation of the results, it is evident that when Li-ion BESSs are utilised for FCR-N application very high

number of micro-cycles at low DODs are prevalent. Hence, tracking them is of utmost importance due to its contribution to battery aging.

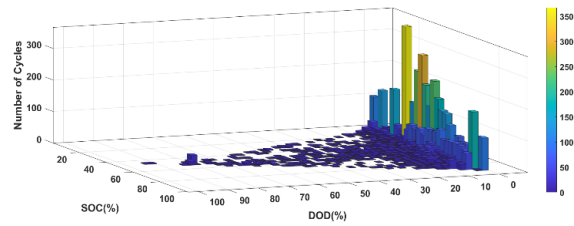


Fig 3. Rainflow counting results on field SOC characteristics

## III. BATTERY AGING CHARACTERISATION

Lithium-ion batteries suffer performance degradation due to aging caused by phenomena such as loss of active lithium ions and other active materials, growth of solid electrolyte interface (SEI) layer etc., which in turn are a result of calendric and cyclic aging [13], [14] of the battery cells. These aging processes are affected by battery operating conditions such as temperature, depth of discharge and the magnitude of charge/discharge current (C-rate).

The battery systems when utilised for grid applications are typically installed in an air-conditioning environment, which regulates ambient temperature at pre-defined levels. Hence, temperature as a factor for aging shall be considered constant in this study. However, the power/energy requirements from Li-ion BESSs for FCR-N operations do not follow a steady pattern and is highly variable based on multiple factors such as network parameters, RES intermittency etc. The range of power/energy requirements that Li-ion BESSs can support over a period of time shall vary based on their aging characteristics. Controlling the charge or discharge rate within its maximum allowed power/energy capability of Li-ion BESSs based on the aging of Li-ion batteries forms an important factor in their planning and utilisation, as they lead to efficient operations within the safe operating regions at all times.

Fig. 4 shows the aging characterisation of Li-ion BESSs from the manufacturer's datasheet utilised in Finland for FCR-N applications. Data from Fig.4 provides us with the number of cycles the battery can support at different DOD's (0 to 100%). The usable capacity ( $CAP_{BESS}$ ) is calculated from (1), which is just the difference between the battery capacity at beginning of its life ( $CAP_{BOL}$ ) and its end of life ( $CAP_{EOL}$ ). From both of these information, capacity lost per cycle at different DODs ( $CAP_{LOSS,DOD}$ ) can be calculated from (2). The cumulative loss of battery capacity ( $CAP_{LOSS,CUMULATIVE}$ ) when cycled in the field is caused due to different cycle depth. The information on total number of cycles at different DODs is obtained from the result of using rainflow-counting algorithm in previous section. Therefore,

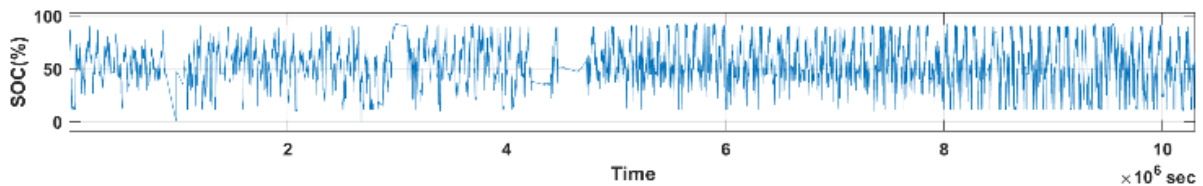


Fig 2. Measured real-life BESS SOC behaviour when utilised for FCR-N frequency control markets

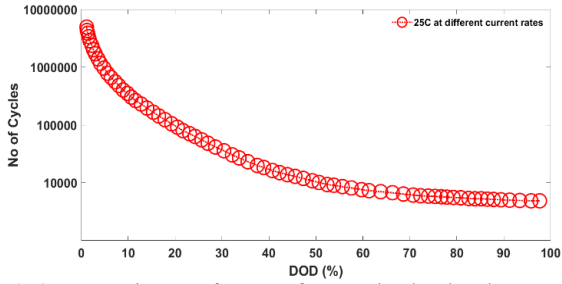


Fig 4. Battery aging curve from manufacturer's datasheet based on DoD

$CAP_{LOSS,CUMULATIVE}$  is calculated from (3) where  $N_{DODn}$  represents number of battery charge/discharge cycles at DOD,  $n$ . The remaining battery capacity is then calculated by (4). However, the parameter of interest for designing adaptive droop curves is the peak power capability ( $P_{PEAK}$ ) of the battery. State of health (SOH), which gives indication on the evolving  $P_{PEAK}$  of the Li-ion BESS is calculated by (5).  $P_{PEAK}$  is calculated by (6), where it's a function of  $P_{PEAK,BOL}$  corresponds to the Li-ion BESS active power peak during their beginning of life (BOL) and SOH.  $P_{PEAK,BOL}$  is obtained from manufacturer's datasheet. Both calculated  $P_{PEAK}$  and  $P_{PEAK,BOL}$  considered in this study corresponds to the peak power of the battery at 100% SOC. By this means, SOH shall form an input for the Li-ion BESS control loop design for their adaptive control considering aging characteristics. It has to be noted that the ( $P_{PEAK}$ ) at various instances of aging is not an electrochemical hard limit on the Li-ion BESSs, i.e. at SOH of 80%, the batteries are still capable of dispatching peak power at SOH 100%, however, this may accelerate aging to higher magnitudes and may pose significant safety challenges in the long run. Such challenges can be verified by further experimental studies alone.

#### IV. PROPOSED DROOP CURVE

Conventional droop control techniques help in managing the output power of an inverter based distributed energy resources (DERs) by local measurement of power system parameters such as current, voltage, frequency, etc. [15]. Based on these measurements, the output power (active and

reactive power,  $P$  and  $Q$ ) of DERs are dispatched by means of droop curves, as depicted in Fig. 1. It is very similar to the operation of conventional generators. Conventional droop curves are designed based on (7), where the required frequency,  $f$ , is a function of  $f_0$ , rated frequency of the DER, droop constant  $K_p$ , DER rated power  $P_0$  and DER power dispatch  $P$ . The value of  $K_p$  which decides the slope of the droop controller is as shown in (8), is a function of difference between desired and measured frequencies,  $\Delta f$  and maximum active power  $P_{max}$  of the DER. Li-ion BESS enables bi-directional power flow by means of charging and discharging characteristics. It has to be observed that the peak power ( $P_{PEAK}$ ) during both charging and discharging powers are affected due the capacity fade of battery systems with aging, i.e. their state of health (SOH). Hence, this property needs to be integrated in the droop controllers making them adaptive in nature. The slope of the adaptive droop controller will be facilitated by (8), which is a function of  $\Delta f$  and  $P_{PEAK}$  (affected by SOH).

The calculated value of  $P_{PEAK}$ , being a function of SOH, thereby provides the way to introduce Li-ion BESS aging

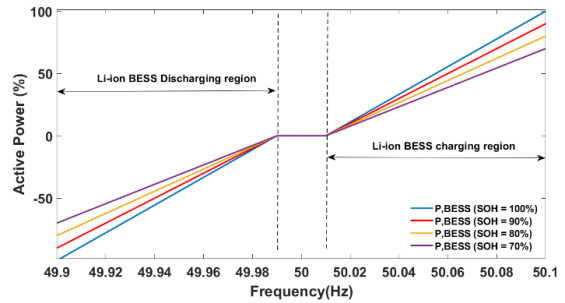


Fig 5. Proposed adaptive droop controller

Table I. Li-ion BESS Peak Power Calculations

SOH (%)	Peak Power (kW)
100	300
90	270
80	240
70	210

$$CAP_{BESS} = CAP_{BOL} - CAP_{EOL} \quad (1)$$

$$CAP_{LOSS,DOD} = \frac{CAP_{BESS}}{N_{CYC,DOD}} \quad (2)$$

$$CAP_{LOSS,CUMULATIVE} = \sum_{i=1}^n N_{DOD_i} * CAP_{LOSS,DOD_i} + N_{DOD_2} * CAP_{LOSS,DOD_2} + \dots + N_{DOD_n} * C_{LOSS,DOD_n} \quad (3)$$

$$CAP_{REM} = CAP_{BOL} - CAP_{LOSS,CUMULATIVE} \quad (4)$$

$$SOH = \frac{CAP_{REM}}{CAP_{BOL}} \quad (5)$$

$$P_{PEAK} = SOH * P_{PEAK,BOL} \quad (6)$$

$$f = f_0 + K_p(P_0 - P) \quad (7)$$

$$K_p = \frac{\Delta f}{P_{max}} \quad (8)$$

$$K_p = \frac{\Delta f}{P_{PEAK}} \quad (9)$$

characteristics to be included in the adaptive droop controller curve design for battery systems.  $P_{PEAK}$  of the Li-ion BESS at different SOH is represented in Table I, whose values are calculated based on (6). These values are then utilised to develop adaptive droop control mentioned in Fig. 5, providing inputs of changing peak power capability of the battery system. The proposed adaptive droop controller, whose droop curve slopes are dependent on equation (9), providing a range of power dispatch considering battery aging. Fig. 5 represents the droop curves at different SOH levels for both charging and discharging operations of the Li-ion BESS, whose peak power charge/discharge decreases with aging characteristics. Evolution of  $P_{PEAK}$  with aging has been represented in Fig. 5, thereby, embedding adaptive droop characteristics for Li-ion BESS control in order maintain the power dispatch within the allowable limits dictated by the battery's SOH at all times. Following section explains the design of controller for Li-ion BESS including the proposed droop curve.

### V. CASE STUDY

To understand the effectiveness and impact of the adaptive droop curves proposed in section V, case study is conducted on an installed Li-ion BESS in Finland. The specification of the battery system is shown in Table II, whose functionality includes  $Pf$ - control for FCR-N operation despite supporting other applications. Based on the data sheet information, the peak power supported by this battery system is about 300 kW in the BOL conditions. It is also stated that the EOL conditions are attained when its capacity is reduced by 30%, which provides the peak power calculation to be about 210

kW. Two sub-cases are further considered, where the first sub-case considers the Li-ion BESS which is at its BOL and the second sub-case depicts the operation of Li-ion BESS towards its EOF.

**Table II.** Lithium-ion Battery Characteristics

Nominal DC voltage	700 V
Peak Voltage	790 V
Cut-off Voltage	588 V
Nominal Power	~100 kW

#### A. Sub-case 1: Li-ion BESS at BOL

The characteristics of the installed Li-ion BESS is shown in Table II, which is designed for a continuous nominal power of 100 kW with peak support upto 300 kW (pulsed in nature). In this sub-case, the battery is considered at its BOL. One of the purposes of this Li-ion BESS is to provide FCR-N related services, i.e. to stabilize the grid frequency within the limitations specified by grid codes. The field measurements of the grid frequency for three months, i.e. Dec-2019 to Feb-2020 within the ranges mentioned in Table I is shown in Fig. 6. The active power dispatched by the Li-ion BESS in order to mitigate frequency fluctuation by means of providing FCR-N operations are shown in Fig. 7. They are based on the droop control curve depicted in blue in Fig. 5, which corresponds the BOL characteristics. It is evident that the range of frequency fluctuations has been predominantly between 49.9 Hz to 50.1 Hz and the active power dispatch in the Li-ion BESS has been upto the maximum of 300 kW, by means of  $Pf$ - droop curve shown in Fig. 1, whose 100% power corresponds to 300 kW. Therefore, the basic non-adaptive droop curve is able to support all the battery-

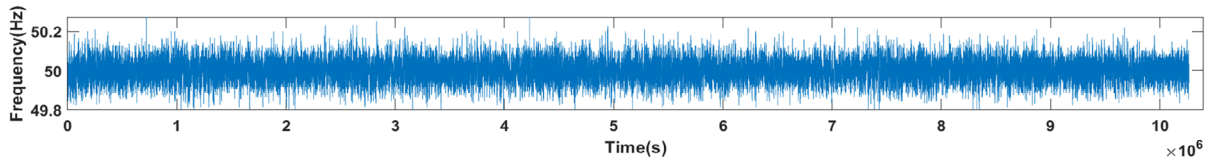


Fig 6. Power System Frequency

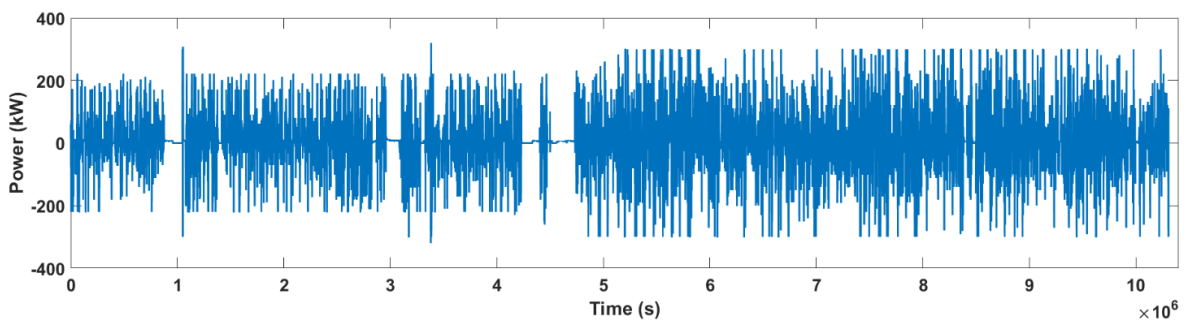


Fig 7. FCR-N supported by Li-ion BESS during BOL

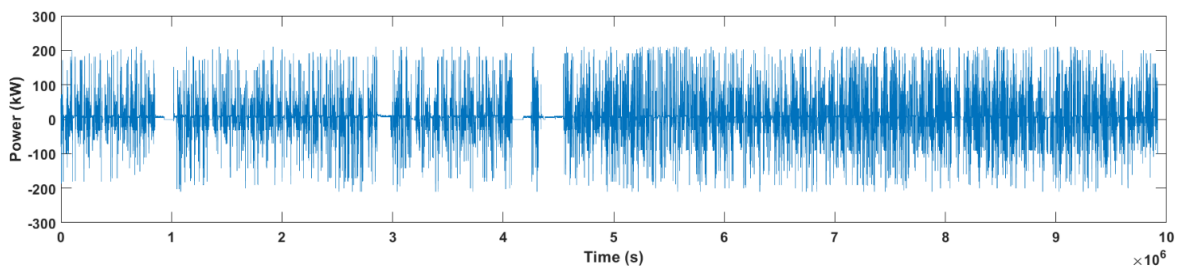


Fig 8. Li-ion BESS power dispatch for FCR-N during BOL

required operations at its BOL, which corresponds to the blue line in Fig. 5.

#### B. Sub-case 2: Li-ion BESS at EOL

Degradation of Li-ion BESSs is a serious concern, particularly when it will be utilized for FCR-N purposes, due to their mission profiles, which seek high power charge/discharge in a shorter span of time, evident from the field data characteristics. The SOH calculation of the Li-ion BESS due to its cycling, its relative capacity loss and subsequently the changes in their peak power capability has been explained in section III. Therefore, to avoid over charging/discharging and to maintain the Li-ion BESSs peak power discharge always within peak power capability at all times, an adaptive droop curves have been designed (section's IV and V). This sub-case has been performed to understand the impacts of the changing Li-ion BESS characteristics (predominantly its peak power characteristics) with respect to aging.

In the previous sub-case where new Li-ion BESS was utilized FCR-N application, it has been observed that the battery dispatch power reaches its peak limit of 300 kW (Fig. 7). During the Li-ion BESSs BOL all FCR-N loads were supported. In this sub-case, we consider the same Li-ion BESS towards its EOF, i.e. capacity of the battery has reduced by 30% of its initial value and that of its reduction in peak power characteristics.

However, based on the proposed SOH sensitive adaptive droop curves, it is evident that the peak power discharge is limited to about 210 kW for the installed Li-ion BESS system towards its EOF. The droop curve dictating Li-ion BESS power flow under these circumstances corresponds to violet colored line in Fig. 5. Hence, the frequency ranges supported for FCR-N operations by BESS towards its EOF, when the proposed adaptive curve is used, is as shown in Fig. 8. The corresponding Li-ion BESS charge/discharge power dispatch is shown in Fig. 9, whose characteristics are different, compared to the battery in its BOL. The charge/discharge power ranges more than 210 kW were not supported, thereby safeguarding the battery operations within their threshold operational limits. Further, it can be observed that the FCR-N operations seeking more than 210 kW power has not been entertained by the droop curve.

#### VI. CONCLUSION

Integrating battery-aging characteristics in the control and planning of Li-ion BESSs for grid applications improves overall utilisation of batteries and helps maintain their operations within the safe operating regions. Control of these Li-ion BESSs for FCR-N operation are generally defined by typical Pf- droop curves as in Fig. 1. However, the Li-ion battery degradation characteristics tend to reduce the peak power charge/discharge capability of the BESS. To address this issue, an adaptive droop curve has been proposed which modifies the Li-ion BESSs peak active power capability based on its SOH. The impact of such adaptive droop curves were analysed by means of case studies and it has been established that, as the battery ages, it is advised to omit certain range of FCR-N services (preferably high power charge/discharge operation) keeping the battery safety in check. Thereby, solving the problem of managing the battery charge/discharge operations always within the threshold of

their peak active power performance. In order to reduce the computational requirements of counting the cycles of battery usage by means of rainflow counting technique (section III), this task shall be performed periodically (say for e.g. 30 days interval) rather than in real time, as the battery degradation is a slow process and update its corresponding peak power characteristics in the battery inverter control settings.

#### VII. REFERENCES

- [1] G. Rancilio, A. Rossi, C. Di Profio, M. Alborghetti, A. Galliani, and M. Merlo, "Grid-scale BESS for ancillary services provision: SoC restoration strategies," *Appl. Sci.*, vol. 10, no. 12, pp. 1–18, 2020.
- [2] C. Parthasarathy, K. Sirviö, H. Hafezi, and H. Laaksonen, "Modelling Battery Energy Storage Systems for Active Network Management – Coordinated Control Design and Validation," *IET Renew. Power Gener.*, pp. 1–10.
- [3] C. Parthasarathy, H. Hafezi, and H. Laaksonen, "Integration and control of lithium-ion BESSs for active network management in smart grids: Sundom smart grid backup feeding case," *Electr. Eng.*, no. Lv, 2021.
- [4] B. Li *et al.*, "Distributed Control of Energy-Storage Systems for Voltage Regulation in Distribution Network with High PV Penetration," *2018 UKACC 12th Int. Conf. Control. Control 2018*, vol. 9, no. 4, pp. 169–173, 2018.
- [5] S. Wang, L. Lu, X. Han, M. Ouyang, and X. Feng, "Virtual-battery based droop control and energy storage system size optimization of a DC microgrid for electric vehicle fast charging station," *Appl. Energy*, vol. 259, no. November 2019, p. 114146, 2020.
- [6] K. Bi, W. Yang, D. Xu, and W. Yan, "Dynamic SOC Balance Strategy for Modular Energy Storage System Based on Adaptive Droop Control," *IEEE Access*, vol. 8, pp. 41418–41431, 2020.
- [7] M. H. Marzabali, M. Mazidi, and M. Mohiti, "An adaptive droop-based control strategy for fuel cell-battery hybrid energy storage system to support primary frequency in stand-alone microgrids," *J. Energy Storage*, vol. 27, no. September 2019, p. 101127, 2020.
- [8] J. O. Lee, Y. S. Kim, T. H. Kim, and S. Il Moon, "Novel Droop Control of Battery Energy Storage Systems Based on Battery Degradation Cost in Islanded DC Microgrids," *IEEE Access*, vol. 8, pp. 119337–119345, 2020.
- [9] H. C. Hesse, M. Schimpe, D. Kucevic, and A. Jossen, *Lithium-ion battery storage for the grid - A review of stationary battery storage system design tailored for applications in modern power grids*, vol. 10, no. 12, 2017.
- [10] D. I. Stroe, M. Swierczynski, A. I. Stroe, R. Laerke, P. C. Kjaer, and R. Teodorescu, "Degradation Behavior of Lithium-Ion Batteries Based on Lifetime Models and Field Measured Frequency Regulation Mission Profile," *IEEE Trans. Ind. Appl.*, vol. 52, no. 6, pp. 5009–5018, 2016.
- [11] M. Ghorbanzadeh, M. Astaneh, and F. Golzar, "Long-term degradation based analysis for lithium-ion batteries in off-grid wind-battery renewable energy systems," *Energy*, vol. 166, pp. 1194–1206, 2019.
- [12] M. Musallam and C. M. Johnson, "An efficient implementation of the rainflow counting algorithm for life consumption estimation," *IEEE Trans. Reliab.*, vol. 61, no. 4, pp. 978–986, 2012.
- [13] E. Sarasketa-Zabala, I. Gandiaga, E. Martinez-Laserna, L. M. Rodriguez-Martinez, and I. Villarreal, "Cycle ageing analysis of a LiFePO<sub>4</sub>/graphite cell with dynamic model validations: Towards realistic lifetime predictions," *J. Power Sources*, vol. 275, pp. 573–587, 2015.
- [14] M. Kassem, J. Bernard, R. Revel, S. P??lissier, F. Duclaud, and C. Delacourt, "Calendar aging of a graphite/LiFePO<sub>4</sub> cell," *J. Power Sources*, vol. 208, pp. 296–305, 2012.
- [15] I. Alaperä and T. Hakala, "25 th International Conference on Electricity Distribution BATTERY SYSTEM AS A SERVICE FOR A DISTRIBUTION SYSTEM OPERATOR 25 th International Conference on Electricity Distribution Madrid , 3-6 June 2019 Main design characteristics," no. June, pp. 3–6, 2019.

# Effects of Battery Aging on BESS Participation in Frequency Service Markets – Finnish Case Study

Hosna Khajeh<sup>1</sup>, Chethan Parthasarathy<sup>1</sup>, Hannu Laaksonen<sup>1</sup>

<sup>1</sup>School of Technology and Innovations, Flexible Energy Resources  
University of Vaasa  
65200 Vaasa, Finland

**Abstract**—Increasing share of intermittent inverter-based renewable power is being integrated into the power systems. This affects the power system dynamics and frequency stability. As a result, the systems need more resources that provide frequency control related technical services. In this regard, this paper proposes the participation of a Lithium-ion Battery Energy Storage System (Li-ion BESS) in providing frequency containment reserve for normal operation (FCR-N). The Li-ion BESS reacts to the frequency deviations from 0 to 0.1 Hz and -0.1 to 0 Hz in FCR-N operations. In addition, the paper presents a method to schedule the charging and discharging power of BESS while considering the effects of BESS cycling aging. In the simulation section, a 50 kWh BESS is supposed to react to the three-minute frequency changes and the corresponding outcome is estimated for three months. At the end, the paper assesses whether the cycling aging affects the BESS economic outcome when it provides FCR-N service.

**Index Terms**—BESS, frequency regulation, BESS aging, cycle counting, FCR.

## I. INTRODUCTION

A large share of variable weather-dependent, renewable inverter-based generation is being connected into power systems. This adversely affects the power system dynamic behavior and stability, especially frequency stability, during different events and disturbances. To resolve this issue, future power systems need to adopt new sources of flexibility that can provide frequency control services for the system. Recent studies have proposed the utilization of BESS for this purpose since they are capable of responding to frequency changes very fast due to their controllability and flexibility features [1], [2]. However, the participation of BESS in providing frequency services should be profitable for its owner. In other words, BESS participation should not impose additional costs on the BESS owner. Thus, a thorough techno-economic study needs to be conducted including battery aging costs for Li-ion BESS.

In the literature, there are works trying to schedule a BESS in a way to provide frequency services. For instance, [3] proposed the optimal operation of a Li-ion BESS if it participates in Nordic FCR markets. The work mostly concentrated on one-day scheduling of the BESS and the

battery aging effects were disregarded. Another thorough work conducted by [4] was to schedule a Li-iron phosphate battery to be in line with the regulation markets' needs and also proposed the simultaneous participation in energy markets. However, the type of services that the battery is scheduled for was not clearly specified.

TABLE I. COMPARISON OF OUR WORK WITH SOME EXISTING RESEARCH

Ref.	Service provision	Effects of cycling on BESS' capacity reduction	Medium-/long-term economic analyses
[5]	Spinning reserve	X	X
[6]	Not reserve service	X	X
[7]	Frequency control ancillary services	X	X
[8]	Primary frequency regulation	X	X
[9]	The type of reserve service was not specified	X	X
[10]	The type of reserve service was not specified	X	X
[11]	The type of reserve service was not specified	X	✓
This paper	FCR-N	✓	✓

Each market has its own characteristic and needs its own technical requirements. For instance, the BESS cannot provide some frequency regulation services with energy at the same time meaning that its total capacity should be reserved for the frequency regulation and thus it is not allowed to participate in energy-related markets. In addition, the study tried to consider BESS aging effects in 24 hours but the capacity degradation cannot be estimated thoroughly in a one-day interval. Another

daily analysis was conducted by [12] proposing the contribution of a BESS to the FCR as well as peak-shaving services. Again, cycling effects and the type of battery technology were not thoroughly considered. Study in [13] proposed a business model and regulatory frameworks considering the BESS as a service provider in Finland. The BESS technology includes a wide range of batteries such as lead, Li-ion, condenser and flow battery. The aging of the capacity was however disregarded in their analyses. Authors of [14] tried to schedule a vanadium redox BESS that provides frequency restoration reserves in a community environment and [15] proposed the provision of ancillary services by the household BESS without specifying the battery technology. Both studies did not take into account the effects of cycling on the BESS capacity. Although [16], [17] analyzed and schedule a Li-ion BESS based on its cycling aging effects, they do not consider these effects if the BESS provides frequency regulation services. Table I compares some other existing literature with the work of this paper in order to highlight the contribution of this research.

In this regard, this paper aims to conduct a three-month analysis to consider the effects of cycling aging if a Li-ion BESS participates in Nordic FCR-N provision. The contribution of the paper will be twofold:

- It proposes a method and strategy to schedule the charging and discharging power of a Li-ion BESS that can count the cycle simultaneously and estimate the capacity based on the cycles. Most of the existing research (such as [5] and [9]) modeled BESS cycling aging through the relationship between BESS life cycles and its depth of discharge. However, this paper considers the effects of BESS cycling on its capacity degradation.
- It conducts a three-month economic analysis and obtains the economic outcome of a 50 kWh Li-ion BESS that responds to the three-minute real measured frequencies and provides FCR-N. This outcome is calculated with and without cycling effects for comparison purposes.

The rest of the paper is organized as follows. Section II describes how a resource can provide the FCR-N service. Section III introduces the proposed method including cycle counting, capacity estimation, and Li-ion BESS scheduling. Section IV introduces the cases studies and implementation of the proposed scheduling methodology on a 50 kWh Li-ion BESS. Finally, Section V concludes the paper.

## II. BESS PARTICIPATION IN FCR-N MARKET

Frequency Containment Reserves (FCR) are deployed to regulate frequency continuously. This service is categorized into FCR for normal operation (FCR-N) and FCR for disturbance situations (FCR-D). FCR-D is responsible to control frequency when it falls below 49.9 to 49.5 Hz and when it goes above 50.1 to 50.5 Hz. The focus of this paper is on the FCR-N service which is designed for normal operation. FCR-N services should react to the frequency changes from 0 to 0.1 Hz and -0.1 to 0 Hz [18].

FCR-N is considered as a symmetrical service and market. This means that an FCR-N provider should be able to reserve

both upward and downward services at the same time. Thus, a BESS that has the capability to be charged and discharged, can be an FCR-N provider. The full reserve capacity of the FCR-N provider needs to be activated when the frequency goes below 49.9 Hz. Correspondingly, in cases where the frequency goes above 50.1 Hz, the resource should be fully activated with its 100 percent capacity. When the frequency level is within the range of 49.9 to 50.1 Hz, The activated capacity needs to be proportional to the magnitude of the frequency changes. In addition, when the frequency deviation happens, the reserve should be activated in less than 3 minutes and it should not be delayed on purpose [18].

When a BESS is an FCR-N provider and it reaches the maximum or minimum level of its state-of-charge (SOC), the service activation needs to be interrupted until the direction of the frequency changes. A balancing service provider is responsible for scheduling the charging and discharging level of the BESS. The recharging power, SOC management and forecasting as well as scheduling timetable of BESS can be a challenge when it provides FCR-N services.

A reserve provider receives two types of payment if it contributes to the FCR-N provision. Firstly, it receives a capacity payment for the amount of capacity that is reserved to respond to the frequency deviations. Secondly, it is paid if its upward flexible capacity is activated. When the upward capacity is activated, the provider injects power into the grid. On the other hand, when the downward capacity is activated, the flexible resource increases its consumption. Although the reserve provider is paid in case its upward capacity is activated, it should pay for its consumption based on the downward regulation prices when it is providing downward flexibility. However, it is worth mentioning that the prices of downward flexibility are always equal to or lower than those of the spot market [15]. This means that it is always more beneficial for a consumer to consume power based on downward regulation prices rather than spot market prices. Correspondingly, the prices of upward regulation are always equal to or higher than those of the spot market. Hence, it is more beneficial for a producer to provide upward flexibility and sells it into the reserve markets rather than the spot market [15].

A BESS can be deployed as an FCR-N provider. In this way, the BESS is charged whenever the frequency increases from 50 to 50.1 Hz meaning that the system needs downward flexibility. The BESS is discharged in cases where the frequency falls between 50 to 49.9 Hz. In these cases, the system requires upward flexibility. The charging/discharging power needs to be proportional to the frequency deviation. In addition, there should be a local measurement device to direct the BESS towards the right amount and direction of power. Thus, the BESS is managed according to the local frequency measurement.

## III. PROPOSED METHODOLOGY

This paper proposes the participation of a Li-ion BESS in providing FCR-N services. In this regard, we propose a linear optimization problem that schedules the BESS. However, in the process of BESS' scheduling, we need to determine the remaining capacity of the battery in each cycle. In addition, a

fast Li-ion BESS cycle counting method is needed as a first step to calculate the cycles.

A. Li-ion BESS Cycle Counting

Li-ion BESS cycle is counted by modifying the method proposed by [19].

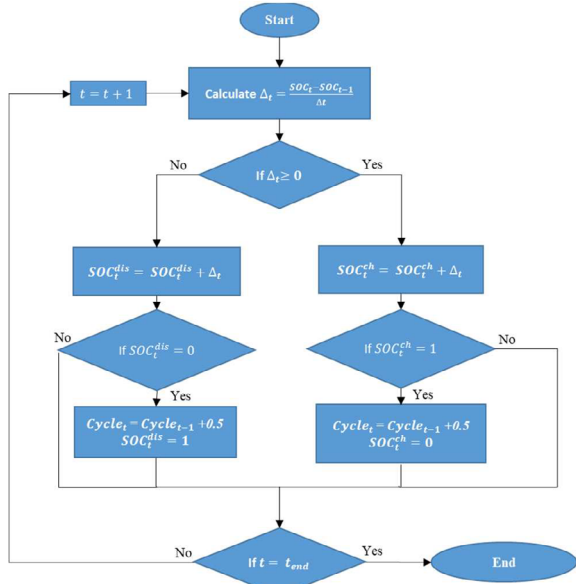


Figure 1. A flow chart representing BESS cycle counting

According to this method, the first step calculates the SOC change within the predefined time slot. If the SOC increases, it means that the Li-ion BESS was charging. Hence, it adds the SOC increase to the value of a variable denoted by  $SOC_t^{ch}$ . It should be noted that this variable is totally different from the BESS SOC at  $t$  denoted by  $SOC_t$ . The variable  $SOC_t^{ch}$  is just used to calculate the Li-ion BESS cycle. If  $SOC_t^{ch}$  reaches its maximum level, which is one, the cycle increases by 0.5 and  $SOC_t^{ch}$  is reset to one. Otherwise, the algorithm continues with the current cycle.

Correspondingly, if the SOC decreases during one time slot, the battery was discharging. Hence, the change is added to another variable denoted by  $SOC_t^{dis}$ . This variable is just utilized to calculate the cycle. If  $SOC_t^{dis}$  approaches its minimum level, zero, the cycle increases by 0.5 and  $SOC_t^{dis}$  is reset to zero. This algorithm ends when the BESS stops being charged and discharged. Fig. 1 summarizes the method adopted to calculate the Li-ion BESS cycle counting.

B. Li-ion BESS Capacity Estimation Considering BESS Cycling Aging

Li-ion BESS capacity decreases with the cycle (age) increase. Thus, Li-ion BESS capacity can be defined as a function of cycle while the cycles reflect the age of the battery. In order to obtain capacity-cycle function, we use the field data on a 50 kWh Li-ion BESS. The field data is based on measured capacities of a 50 kWh Li-ion BESS after passing some cycles. Then, a polynomial regression is deployed to obtain the

relationship between the Li-ion BESS capacity and the cycle. Finally, mean squared error (MSE) criteria is utilized to choose the best fitted function. Regarding our data, the best fitted function that models the Li-ion BESS capacity based on its charging/discharging cycle was a polynomial of degree 4. Fig. 2 depicts the curve fitted on the data. Fig. 2 illustrates the relationship between capacity and cycle for the studied BESS.

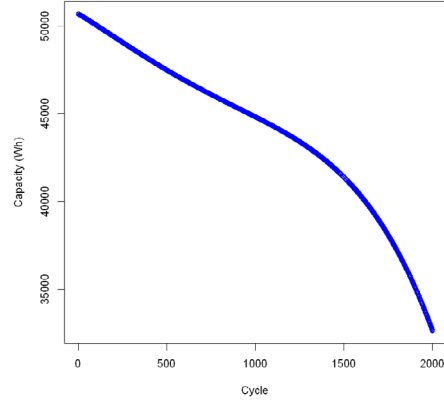


Figure 2. The curve representing studied Li-ion BESS capacity-cycle

As Fig. 2 states, the cycling of the BESS can affect its maximum capacity. For the case of 50 kWh of a Li-ion BESS, its maximum capacity falls to less than 35 kWh after 2000 cycles. Accordingly, it is necessary to consider the BESS cycling effects when the study aims to assess the Li-ion BESS long-term economic outcome.

C. Li-ion BESS Scheduling

BESS scheduling should be done according to the volume and direction of the frequency deviation. Moreover, the power of charging/discharging should not result in the Li-ion BESS SOC exceeding its predefined limits. Therefore, a scheduling problem can be developed with linear programming (LP) method. The problem is written separately for scheduling the charging and discharging power, as follows:

If  $FD_t \geq 0$  then the BESS is charging with  $P_t \geq 0$ :

$$\max P_t \tag{1}$$

Subject to:

$$0 \leq P_t \leq \frac{FD_t}{0.1} \times P^{max} \tag{2}$$

$$SOC_t = SOC_{t-1} + \frac{\eta_{ch} P_t}{Cap(Cycle_t)} \Delta t \tag{3}$$

$$SOC^{min} \leq SOC_t \leq SOC^{max} \tag{4}$$

If  $FD_t < 0$  then the BESS is discharging with  $P_t < 0$ :

$$\min P_t \tag{5}$$

Subject to:

$$\frac{FD_t}{0.1} \times P^{max} \leq P_t \leq 0 \tag{6}$$



$$SOC_t = SOC_{t-1} + \frac{P_t}{\eta_{dis} \times Cap(Cycle_t)} \Delta t \quad (7)$$

$$SOC^{min} \leq SOC_t \leq SOC^{max} \quad (8)$$

Where:

$$FD_t = freq_t - 50 \quad (9)$$

Where,  $SOC^{min}$  is the lowest allowable SOC while  $SOC^{max}$  indicates the higher limit defined for the SOC. Also,  $\eta_{ch}$  and  $\eta_{dis}$  denote Li-ion BESS charging and discharging efficiencies, respectively.  $Cap(Cycle_t)$  is the function that calculates the value of BESS maximum capacity based on the real-time cycle at  $t$  ( $Cap(Cycle_t)$ ). This function was determined in subsection B. The cycle is also counted using the method proposed in subsection A.

$P_t$  is the scheduled power determined by solving (1)-(8). If the frequency deviation at  $t$ , i.e.  $FD_t \geq 0$ , the BESS needs to provide downward flexibility by charging the BESS. Thus,  $P_t$  is also positive and the optimization problem (1)-(4) should be solved. Otherwise, if the frequency deviation is negative, the BESS should be discharged. The discharging power can be obtained by solving (5)-(8).

In the optimization problems,  $P^{max}$  is the absolute value of charging/discharging power. As previously stated, an FCR-N provider should be activated with the power that is proportional to the frequency deviation. Regarding FCR-N services, the ratio of the frequency deviation equals  $\frac{FD_t}{0.1}$ . This means that the charging power should be equal to or lower than  $\frac{FD_t}{0.1} \times P^{max}$  and the discharging power should be equal to or higher than  $\frac{FD_t}{0.1} \times P^{max}$ . If the BESS SOC does not limit the charging/discharging power, optimization problems (1-4) and (5-8) yield  $P_t = \frac{FD_t}{0.1} \times P^{max}$ . Otherwise, it gives us the highest absolute value of discharging/charging power that maintain the SOC within the permissible range.

#### IV. CASE STUDY

The proposed methodology has been tested on a 50 kWh Li-ion BESS. Table II illustrates the battery characteristics. Also, the frequency data from January 1<sup>st</sup> to 31<sup>st</sup> March, 2021, was extracted from ‘‘Fingrid Open Data on the Electricity Market and the Power System’’ [20]. Fingrid is the Finnish Transmission system operator (TSO).

TABLE II. BATTERY CHARACTERISTICS

Maximum Capacity for cycle =0 [kWh]	$P^{max}$ [kW]	$SOC^{min} / SOC^{max}$	$\eta_{ch} / \eta_{dis}$ [%]
50.69	100	0.05/0.95	90

R programming language was utilized to implement the methodology including data preprocessing, polynomial curve fitting, and solving the linear optimization problem. Fig. 3

explains the steps designed to schedule the charging and discharging power of the BESS as well as obtain the outcomes.

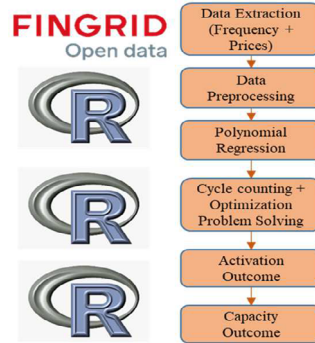
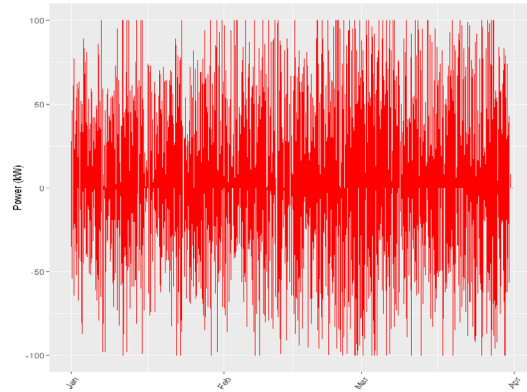
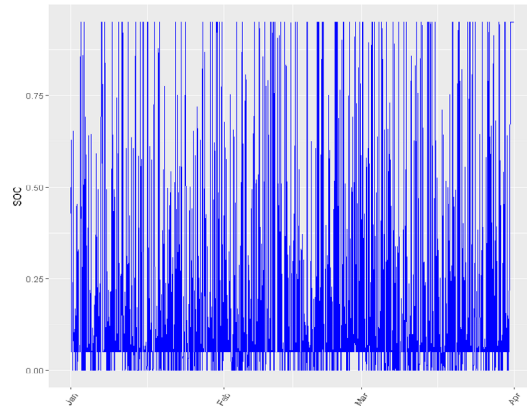


Figure 3. The steps to calculate the outcome of the BESS providing FCR-N



(a)



(b)

Figure 4. a) Charging/discharging power obtained after scheduling the BESS based on the frequency deviations. b) SOC variations after responding to the frequency changes

The charging/discharging power of the BESS was scheduled according to the proposed methodology. Fig. 4 (a) and Fig. 4 (b) indicate the charging power (negative values for

discharging and positive values for charging) as well as the BESS SOC variations. As the figure states, the BESS is continuously reacting to the frequency changes. The initial BESS SOC was considered 0.5.

#### A. Economic Analysis

This subsection analyzes the economic outcomes of the BESS participating in the FCR-N provision. As stated before, the BESS as an FCR-N provider has two resources of the outcome. It receives payment for the capacity it has reserved for providing FCR-N. In 2021, the capacity price for providing 1 kWh FCR-N was equal to 1.25 Cents [20]. The FCR-N is activated by charging and discharging the BESS. Regarding our case study, the BESS was being charged and paid the prices of downward regulations. It was being discharged and received the prices of upward regulations. Fig. 5 depicts the upward and downward regulation prices for the defined time period. The figure proves the fact that the prices of upward regulation are always equal to or higher than those of downward regulation.

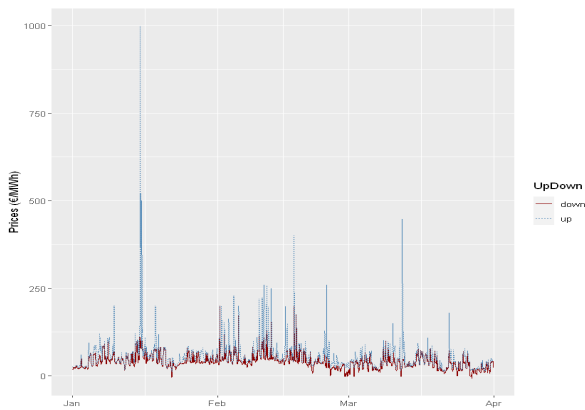


Figure 5. Upward and downward regulation prices during January to March 2021

The BESS makes profits by receiving the capacity payment and the upward activation payment. However, it should pay according to the downward prices for its charging power. The total activation outcome and the capacity outcome have been calculated for the BESS regarding the three-month period. The results are written in Table III.

TABLE III. RESULTS OBTAINED AFTER SCHEDULING THE BESS BASED ON THE PROPOSED METHOD

Capacity Outcome (cent)	Activation Outcome (cent)	The Number of Cycles	Total Outcome (cent)	Final SOC
134812.5	-16955.199	234	117857.3	0.95

The table shows a negative activation outcome which means that in total, the system needed more downward flexibility than upward one. Hence, the BESS should pay approximately € 169. On the other hand, the BESS receives a rather high payment equaling € 1348 for reserving its capacity for the FCR-N service. In total, the BESS is paid nearly € 1178 for its three-month participation in providing the FCR-N service.

#### B. Effect of BESS Cycling Aging

In our simulation results, we have considered the effects of BESS cycling aging in the process of BESS scheduling. In this subsection, we create another case where the cycling effects are disregarded. In this way, BESS capacity has a constant value and is not a function of the cycle. Accordingly, the charging/discharging power is scheduled and the outcomes are calculated. In order to analyze the effect of cycling in an economic way, we propose an indicator that calculates the total outcome for each cycle. The indicator is denoted by TOPC (Total Outcome per Cycle). This indicator is calculated for the BESS with and without BESS cycling effects. The results are shown in Table VI. The table states that aging decreases the BESS profits by 6.06 Cent in each cycle.

TABLE IV. TOPC INDICATOR WITH AND WITHOUT CYCLING EFFECTS

	With BESS cycling effects	Without BESS cycling effects
TOPC [Cent/kWh]	503.66	509.72

#### V. CONCLUSIONS

Renewable-based power systems require more flexible energy resources participating in the provision of frequency regulation services. In this regard, BESS is a very potential resource that can provide different types of technical ancillary (i.e. flexibility) services. FCR-N market needs a symmetrical flexibility service provision. This paper focused on the provision of the FCR-N service by a Li-ion BESS which had the ability to be charged and discharged, and was capable of being a FCR-N provider. Further, this paper discussed the participation of a Li-ion BESS in providing FCR-N, taking into account the effects BESS cycling aging, particularly on their degradation effects on battery capacity.

The paper proposed a methodology that schedules the BESS in a way to be proportional to frequency deviations. The charging/discharging power was based on frequency deviations' direction and volume. In addition, the methodology includes the effects of Li-ion BESS cycling on its capacity. Finally, the proposed method was implemented on a 50 kWh Li-ion BESS. The BESS was scheduled according to the real frequencies measured for three months and the economic outcomes were discussed. Also, the results demonstrate that aging can decrease the BESS profits by 6.06 Cent in each cycle.

#### ACKNOWLEDGEMENT

The work of Hosna Khajeh was supported by Ella and Georg Ehrnrooth Foundation in Finland.

#### REFERENCES

- [1] E. Pusceddu, B. Zakeri, and G. Castagneto Gisse, "Synergies between energy arbitrage and fast frequency response for battery energy storage systems," *Applied Energy*, vol. 283, p. 116274, Feb. 2021, doi: 10.1016/j.apenergy.2020.116274.
- [2] H. Alsharif, M. Jalili, and K. N. Hasan, "A Comparative Analysis of Centralised vs. Distributed Battery Energy Storage System in Providing Frequency Regulation," in *2021 IEEE PES Innovative Smart Grid Technologies - Asia (ISGT Asia)*, Brisbane, Australia, Dec. 2021, pp. 1–5. doi: 10.1109/ISGTAsia49270.2021.9715576.

- [3] P. Hasanpor Divshali and C. Evens, "Optimum Operation of Battery Storage System in Frequency Containment Reserves Markets," *IEEE Transactions on Smart Grid*, vol. 11, no. 6, pp. 4906–4915, Nov. 2020, doi: 10.1109/TSG.2020.2997924.
- [4] C. Wu, X. Lin, Q. Sui, Z. Wang, Z. Feng, and Z. Li, "Two-stage self-scheduling of battery swapping station in day-ahead energy and frequency regulation markets," *Applied Energy*, vol. 283, p. 116285, Feb. 2021, doi: 10.1016/j.apenergy.2020.116285.
- [5] N. Padmanabhan, M. Ahmed, and K. Bhattacharya, "Battery Energy Storage Systems in Energy and Reserve Markets," *IEEE Transactions on Power Systems*, vol. 35, no. 1, pp. 215–226, Jan. 2020, doi: 10.1109/TPWRS.2019.2936131.
- [6] W. Lee, M. Chae, and D. Won, "Optimal Scheduling of Energy Storage System Considering Life-Cycle Degradation Cost Using Reinforcement Learning," *Energies*, vol. 15, no. 8, p. 2795, Apr. 2022, doi: 10.3390/en15082795.
- [7] E. Bayborodina, M. Negnevitsky, E. Franklin, and A. Washusen, "Grid-Scale Battery Energy Storage Operation in Australian Electricity Spot and Contingency Reserve Markets," *Energies*, vol. 14, no. 23, p. 8069, Dec. 2021, doi: 10.3390/en14238069.
- [8] X. Wang, L. Ying, K. Wen, and S. Lu, "Bi-level non-convex joint optimization model of energy storage in energy and primary frequency regulation markets," *International Journal of Electrical Power & Energy Systems*, vol. 134, p. 107408, Jan. 2022, doi: 10.1016/j.ijepes.2021.107408.
- [9] A. Gupta, S. R. Vaishya, M. Gupta, and A. R. Abhyankar, "Participation of Battery Energy Storage Technologies in Co-Optimized Energy and Reserve Markets," in *2020 21st National Power Systems Conference (NPSC)*, Gandhinagar, India, Dec. 2020, pp. 1–6. doi: 10.1109/NPSC49263.2020.9331865.
- [10] L. Wei, L. Gong, J. Zhang, Y. Guo, X. Shen, and J. Shi, "Joint Bidding Strategy of Large-Scale Battery Storage Company in Energy, Reserve and Regulation Markets," in *2021 IEEE/IAS Industrial and Commercial Power System Asia (I&CPS Asia)*, Chengdu, China, Jul. 2021, pp. 355–359. doi: 10.1109/ICPSAsia52756.2021.9621608.
- [11] M. Khojasteh, P. Faria, and Z. Vale, "Energy-constrained model for scheduling of battery storage systems in joint energy and ancillary service markets based on the energy throughput concept," *International Journal of Electrical Power & Energy Systems*, vol. 133, p. 107213, Dec. 2021, doi: 10.1016/j.ijepes.2021.107213.
- [12] H. Shafique, L. B. Tjernberg, D.-E. Archer, and S. Wingstedt, "Energy Management System (EMS) of Battery Energy Storage System (BESS) – Providing Ancillary Services," in *2021 IEEE Madrid PowerTech*, Madrid, Spain, Jun. 2021, pp. 1–6. doi: 10.1109/PowerTech46648.2021.9494781.
- [13] A. Ramos, M. Tuovinen, and M. Ala-Juusela, "Battery Energy Storage System (BESS) as a service in Finland: Business model and regulatory challenges," *Journal of Energy Storage*, vol. 40, p. 102720, Aug. 2021, doi: 10.1016/j.est.2021.102720.
- [14] H. Firoozi, H. Khajeh, and H. Laaksonen, "Optimized Operation of Local Energy Community Providing Frequency Restoration Reserve," *IEEE Access*, vol. 8, pp. 180558–180575, 2020, doi: 10.1109/ACCESS.2020.3027710.
- [15] H. Khajeh, H. Firoozi, and H. Laaksonen, "Flexibility Potential of a Smart Home to Provide TSO-DSO-level Services," *Electric Power Systems Research*, vol. 205, p. 107767, Apr. 2022, doi: 10.1016/j.epsr.2021.107767.
- [16] L. Zhang *et al.*, "Improved Cycle Aging Cost Model for Battery Energy Storage Systems Considering More Accurate Battery Life Degradation," *IEEE Access*, vol. 10, pp. 297–307, 2022, doi: 10.1109/ACCESS.2021.3139075.
- [17] Y.-R. Lee, H.-J. Kim, and M.-K. Kim, "Optimal Operation Scheduling Considering Cycle Aging of Battery Energy Storage Systems on Stochastic Unit Commitments in Microgrids," *Energies*, vol. 14, no. 2, p. 470, Jan. 2021, doi: 10.3390/en14020470.
- [18] Fingrid, "The technical requirements and the prequalification process of Frequency Containment Reserves (FCR)," no. January, p. 17, 2019.
- [19] B. Gundogdu and D. T. Gladwin, "A Fast Battery Cycle Counting Method for Grid-Tied Battery Energy Storage System Subjected to Microcycles," in *2018 International Electrical Engineering Congress (iEECON)*, Krabi, Thailand, Mar. 2018, pp. 1–4. doi: 10.1109/IEECON.2018.8712263.
- [20] Fingrid, "Open data on the electricity market and the power system." [Online]. Available: <https://data.fingrid.fi/en/>